LEVEL II

2

28th DEFENSE CONFERENCE ON NONDESTRUCTIVE TESTING (28th)

27-29 NOVEMBER 1979.

(11) 27 Nov 79

(12) 296

AD A097214

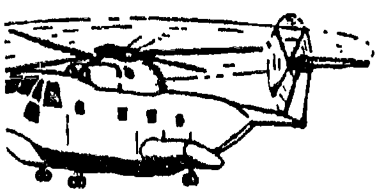

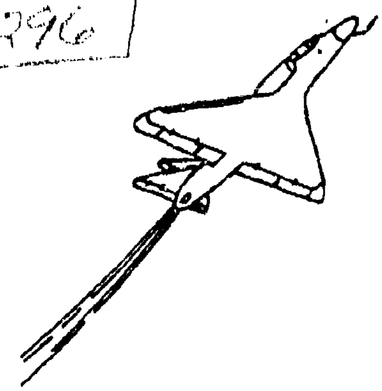

NAVAL AIR REWORK FACILITY
PENSACOLA

HOST:

NAVAL AIR REWORK FACILITY
NAVAL AIR STATION
PENSACOLA, FLORIDA 32508

S/C 393602

81 3 30 030

FOREWORD

The 28th Defense Conference on Nondestructive Testing was held 27-29 November 1979 at Pensacola Beach, Florida, with 192 persons in attendnace. The attendees represented various Department of Defense activities and were assembled to hear technical papers that explained new techniques or that described present problems in the field of nondestructive testing.

Sincere thanks are extended to RADM Louis R. Sarosdy (USN), Assistant Commander for Logistics/Fleet Support, Naval Air Systems Command for his keynote address "Nondestructive Inspection in the Naval Air Systems Command." Thanks also to Captain Joseph J. Walter (USN), Commanding Officer, Naval Air Rework Facility Pensacola for his support.

Thanks to Mr. Lou Brown, Mayor Pro-Tem of Pensacola for welcoming the attendees to the Pensacola area.

Thanks to Richard McSwain, Clifford Smith and Betty Lurton for their assistance to the Host Chairman. And finally to the Steering Committee members under the leadership of Ed Matzkanin.

E. F. NICOSIA, Host Chairman
NAVAIR Engineering Support Office
NAVAL AIR REWORK FACILITY
Pensacola, Florida 32508

CONTENTS

PURPOSE OF DEFENSE CONFERENCE ON NONDESTRUCTIVE TESTING

SCOPE

To provide a forum for nondestructive testing and inspection personnel of Department of Defense Agencies.

OBJECTIVES

1. To interchange information, pertaining to nondestructive testing methods and applications, among attendees and their respective Defense Department establishments.

2. To present technical problems, submitted by the various agencies, to the assembled nondestructive testing specialists and technicians so that they, utilizing their knowledge, skills and experience. may advance potential solutions.

3. To encourage uniform practices in the application of nondestructive testing methods.

4. To provide the opportunity to establish personnal contact with similarly employed specialists of other agencies and thus provide attendees with continuously available resources of additional knowledge and experience.

PARTICIPATION AND BY-LAWS

1. PARTICIPATION

Attendance shall be restricted to include only active military personnel and Defense Department civilian employees concerned with nondestructive testing. inspection, or evaluation. In addition, the Steering Committee may invite attendance by representatives of other U.S. Government agencies and their "captive laboratories".

2. OFFICERS

A Steering Committee, elected by the conferees, shall plan and conduct the Conference. The Steering Committee shall be composed of not less than four, nor more than eight members, providing equal representation of the Army, Navy and Air Force plus and Executive/Treasurer, a Chairman and a Host Representative.

A. Steering Committee Members

Steering Committee members shall be elected for a two-year term of office. The Steering Committee shall be a rotating group with one half of its members retiring each year. The retiring members shall be replaced by elected members from the same service.

(1) During the second Steering Committee Meeting, the Steering Committee Chairman shall appoint a nominating committee to develop a panel of nominees (two from each service) for the election

to be held at the Conference. This Committee shall be chaired by the Executive Secretary and shall include one representative from each service. It shall be the responsibility of this Committee, through the Chairman, to solicit prospective nominees and then correspond with their agencies to delineate the Steering Committee members responsibilities and to assess the degree of support which their agencies will provide. The panel of nominees so developed shall be announced to the Conferees and the first opportunity and in addition, floor nominations shall be invited.

(2) All Conferees shall be eligible to vote for each of the prospective memberships. In the event that a tie develops, a vote shall be taken among the existing Steering Committee to decide the electee. If a second tie develops the Steering Committee shall decide the electee.

(3) In the event a member can no longer serve on the Steering Committee, the Chairman should appoint a member from the same service to serve until the next regular Defense Conference. The next Conference shall formally elect a person from the same service as the resigned member to serve any remaining tenure. A Steering Committee member so elected shall be eligible for the Chairmanship at the end of the original two-year term.

B. Steering Committee Chairman

The Steering Committee Chairman shall be elected, as detailed below, during a conference and shall serve as Steering Committee Chairman until the end of the next conference (usually one year).

(1) At the second Steering Committee Meeting, the senior members of the Steering Committee shall state their position with regard to their intention to run for Steering Committee Chairman. After the second meeting, the existing Steering Committee Chairman shall address a letter to the Commands of the prospective Steering Committee Chairman requesting offical statements as to their willingness to support the interested candidates.

(2) The Steering Committee Chairman shall be elected from among the supported, out-going members of the Steering Committee after conference election of the new Steering Committee members. All members of the Steering Committee, including newly elected members, shall participate in discussions regarding the new Steering Committee Chairman, however, only senior and junior members actually in attendance, shall vote. In the event of a tie vote, the existing Steering Committee Chairman shall cast the deciding vote.

(3) In the event that no senior Steering Committee member is able to obtain support as a candidate for Chairman, the Steering Committee shall consider the following as candidates and in the order stated: junior Steering Committee members, Ad Hoc committeemen, former chairmen. If a junior member is elected, then the runner-up to the new member from the same service shall be declared as a one-year member of the Steering Committee, and the runner-up shall be an automatic [illegible]date for the Steering Committee the following year.

(4) In the event that the Steering Committee Chairman cannot fulfill his responsibilities, the Executive Secretary/Treasurer shall convene a meeting of the Steering Committee and any Ad Hoc Committees. A new Steering Committee Chairman shall be elected from among any of the senior Steering Committee members and the Ad Hoc Committee members volunteering for this service. A senior member so elected should be replaced as stated in 2A (3).

(5) If the Steering Committee Chairman changes service, and can obtain support from his new activity, he shall continue as Steering Committee Chairman. If he cannot obtain support, he shall be declared unable to fulfill his duties and paragraph 2B (4) shall apply.

C. <u>Executive Secretary/Treasurer</u>

An employee of the Army Materials and Mechanics Research Center shall serve as a permanent, non-voting member of the Steering Committee as the Executive Secretary/Treasurer. The Executive Secretary/Treasurer shall assist the Chairman by:

(1) Recording and providing timely copies of minutes of all Steering Committee Meetings.

(2) Initiate correspondence as directed by the Steering Committee Chairman.

(3) Providing information regarding the continuity of the Conference and Steering Committee Meetings.

(4) Maintaining Conference records, including finances.

(5) Maintaining address files of conferees.

(6) Chairing the Nominating Committee as detailed in paragraph 2A (1).

(7) Assuming the responsibility for determining in the upcoming Conference is being planned in a timely manner. To accomplish this, he shall poll the Steering Committee and, if a majority of the members determine the the Chairman is not fulfilling his duties, then the Executive Secretary/Treasurer shall apply paragraph 2B (4).

3. <u>AD HOC COMMITTEES/TASK GROUPS</u>

The Chairman may appoint any Ad Hoc committees or task groups deemed necessary to perform special tasks for him and the Steering Committee. Committees/Task Groups shall only function for, and report to the Chairman who appoints them. It is recommended that past chairman be utilized for this function because of their familiarity with the Conference format and for the experience and continuity they can bring to the Steering Committee.

4. HOST AGENCY

Each year the Conference will be hosted by one of the following three Department of Defense Agencies in the following sequence: Army, Navy and Air Force. A representative of the Host Agency shall participate as a non-voting member of the Steering Committee.

5. STEERING COMMITTEE QUORUM

A Steering Committee quorum shall exist and shall be empowered to carry on Steering Committee business if at least one representative of each service and the Chairman are present. Ad Hoc Committee members and officially delegated substitute representatives may be utilized to constitute a quorum during times of restricted participation by the elected Steering Committee members.

LOCATIONS AND DATES OF PREVIOUS CONFERENCES

Conference	Date	Location
Organizational Meeting	3-4 Oct 51	Watertown Arsenal, Watertown, Massachusetts
2nd	23-24 Jan 52	Frankford Arsenal, Philadelphia, Pennsylvania
3rd	19-20 Nov 52	U.S. Naval Gun Factory, Washington, D.C.
4th	17-18 Mar 54	Army Research and Development Laboratory
5th	16-17 Mar 55	Naval Ordnance Plant, Indianapolis, Indiana
6th	9-10 Apr 56	Detroit Arsenal, Centerline, Michigan
7th	19-20 Feb 57	U.S. Naval Ordnance Test Station, China Lake, California
8th	4-5 Dec 57	SAAMA, Kelly Air Force Base, Texas
9th	15-16 Oct 58	Army Ballistics Missile Agency, Redstone Arsenal, Alabama
10th	6-7 Oct 59	Naval Air Material Center, Philadelphia, Pennsylvania
11th	13-15 Sep 60	OCAMA, Tinker Air Force Base, Oklahoma
12th	28-30 Aug 61	Army Natick Laboratories, Natick, Massachusetts
13th	25-27 Sep 62	Naval Ammunition Depot, Concord, California
14th	25-27 Aug 64	Robbins Air Force Base, Georgia
15th	4-6 Oct 66	U.S. Army Materials Research Agency, Watertown, Massachusetts
16th	26-28 Sep 67	U.S. Naval Ordnance Laboratory, White Oak, Maryland
17th	18-20 Sep 68	USAF-ATC, Randolph AFB, San Antonio, Texas
18th	29-31 Oct 69	Defense Contract Administration Services Region, San Francisco, California
19th	4-6 Nov 70	U.S. Army Mobility Equipment Command, St. Louis, Missouri

20th	10-12 Nov 71	Naval Air Rework Facility, Jacksonivlle, Florida
21st	31 Oct-2 Nov 72	San Antonio Air Material Area, San Antonio, Texas
22nd	13-15 Oct 73	Defense Contract Administration Services Region--Dallas, Houston, Texas
23rd	4-6 Sep 74	U.S. Army Logistic Control Office, Presidio, San Francisco, California
24th	10-13 Nov 75	Naval Air Rework Facility, San Diego, California
25th	31 Aug-2 Sep 76	Army Materials and Mechanics Research Center, Boston, Massachusetts
26th	15-17 Nov 77	62nd Military Airlift Wing (MAC) McChord AFB, Seattle, Washington
27th	24-26 Oct 79	U.S. Army Proving Ground, Yuma, Arizona

28TH DEFENSE CONFERENCE ON NONDESTRUCTIVE TESTING

Steering Committee

Ed Matzkanin, Chairman
Physical Test Section, STEYP-MLS
Yuma Proving Ground
Yuma, AZ 85364
899-6745/465/702

Charles P. Merhib, Exec. Secretary
NDE Branch, AMMRC
Watertown, MA 02172
955-3343/552

Eli F. Nicosia, Host Chairman
Naval Air Rework Facility Code 341
Naval Air Station
Pensacola, FL 32508
922-3551

Navy Members

John Mittleman
Naval Coastal Systems Center
Panama City, FL 32407
436-4388

Ken W. Fizer
NESO-341 NARF
Naval Air Station
Norfolk, VA 23511
690-8811

Air Force Members

CMSgt John F. Dorgan
60 FMS/MAFF Stop 30
Travis Air Force Base, CA 94535
837-3369

Joe O'Neil
438 MAW/MAFF
McGuire Air Force Base, NJ 08641

Army Members

Robert L. Huddleston
STEAP-MT-G
Aberdeen Proving Ground, MD 21005
283-3409

Thomas J. Pojeta
Army Aviation R&D Cmd
P.O. Box 209
St. Louis, MO 63166
693-0733

DSA Guest Representatives

Wilmont Tidd
DCASR, Atlanta
DCRA-QT
Marietta, GA 30060
679-9244

29TH DEFENSE CONFERENCE ON NONDESTRUCTIVE TESTING

Steering Committee

Joe O'Neill, Chairman
438 MAW/MAFF
McGuire Air Force Base, NJ 08641
440-3271

Charles P. Merhib, Exec. Secretary
NDE Branch, AMMRC
Watertown, MA 02172
955-3343/552

Host Chairman

Navy Members

John Mittleman
Naval Coastal Systems Center
Panama City, FL 32407
436-4388

Ken W. Fizer
NESO-341 NARF
Naval Air Station
Norfolk, VA 23511
690-8811

Air Force Members

CMS. R. Muthart
Hq. San Antonio AFLC/MMEW
Kelly AFB Texas 78241

Army Members

John T. Conroy
HQ, U.S. Army Aviation R&D Command
P.O. Box 209
St. Louis, MO 63166
698-2513

Mark Weinberg
ARRADCOM
ATTN: DRDAR-QAR-I, Bldg. 62
Dover, NJ 07801

DSA Guest Representative

INTRODUCTION

FOLKS, WELCOME TO THE 28TH DEPARTMENT OF DEFENSE CONFERENCE ON NONDESTRUCTIVE TESTING. I'VE DELIBERATELY USED THIS LESS FORMAL GREETING AS AN INDICATION THAT THIS CONFERENCE IS INTENDED TO BE A FRIENDLY GET-TOGETHER OF PEOPLE WITH LIKE INTERESTS - NONDESTRUCTIVE TESTING.

BY USING THE LESS FORMAL APPROACH, I FEEL WE CAN BETTER COMMUNICATE WITH EACH OTHER TO FURTHER THE ART OF NONDESTRUCTIVE TESTING. WE CAN SHARE WITH EACH OTHER OUR EXPERIENCES SO THAT WE LEARN TOGETHER WITH LESS TRIAL AND ERROR AND CONSEQUENTLY LESS COST TO OUR EMPLOYER, THE DOD, AND TO OURSELVES AS TAXPAYERS. IN PARTICULAR, PLEASE DO NOT BE BASHFUL IF YOU HAVE ANY IDEAS THAT MIGHT HELP OUT DURING THE PROBLEM-SOLVING SESSIONS. IN MANY CASES IN THE PAST, EVEN FAR OUT, SEEMINGLY ABSTRACT SUGGESTIONS HAVE TRIGGERED IDEAS THAT CONTRIBUTED TO THE SOLUTION OF A PROBLEM. WE ALL WORK FOR THE SAME DEPARTMENT OF DEFENSE. LET'S ALL CONTRIBUTE WHEREVER WE CAN TO HELP OUR FELLOW NDTer AND MAKE THIS ANOTHER FRUITFUL AND WORTHWHILE CONFERENCE.

IT IS MY PLEASURE AT THIS TIME TO INTRODUCE THE NAVAIR ENGINEERING SUPPORT OFFICER OF THE NAVAL AIR REWORK FACILITY, COMMANDER JACK HOOD.

ED MATZKANIN, CHAIRMAN
STEYP-MLS-P
U.S. ARMY YUMA PROVING GROUND
YUMA, ARIZONA 85364

CAPTAIN JOSEPH J. WALTER, USN
COMMANDING OFFICER
NAVAL AIR REWORK FACILITY
PENSACOLA, FLORIDA

HOST

JOSEPH J. WALTER

CAPTAIN, USN

Captain Joseph J. Walter graduated from the U.S. Naval Academy in 1955, and was designated a naval aviator in March 1957. He was promoted to his current rank in November 1975.

Captain Walter holds a master's degree in aeronautical engineering from Princeton University, a BSAE degree from the U.S. Naval Postgraduate School, a BS degree from the U.S. Naval Academy and a master's degree in management from the Fuehrungs Akademie der Bunderwehr in Hamburg, Germany.

His career has involved operational service in four naval aircraft squadrons deployed aboard the USS FORRESTAL, USS SARATOGA and USS INDEPENDENCE. Captain Walter also qualified as a command pilot in the Luftwaffe, flying a variety of European designed fixed wing aircraft and helicopters. Engineering designation led to shore assignments as the Naval Plant Representative at McDonnell Douglas Corporation in St. Louis, Missouri, where he administered and monitored various government programs such as the F-4 Phantom II, NASA Sky Lab and the Navy Harpoon Missile. He also participated in the design and early development phase of the USAF F-15 EAGLE. Captain Walter served briefly as the USN/USMC deputy program manager for the now cancelled U.S. Army Heavy Lift Helicopter. Subsequently he served in the Naval Air Systems Command as assistant project manager, responsible for engineering design and development of the F-14 program.

Captain Walter is the seventh Commanding Officer of the Naval Air Rework Facility. He reported to Pensacola from Norfolk, Virginia, where he served as Air Material and Engineering Officer for the U.S. Naval Air Force, Atlantic Fleet and was responsible for the material readiness and combat capability of more than 1700 U.S. Navy and U.S. Marine Corps aircraft and helicopters.

RADM LOUIS R. SAROSDY
ASSISTANT COMMANDER FOR LOGISTICS/FLEET SUPPORT
NAVAL AIR SYSTEMS COMMAND
WASHINGTON, D.C.

KEYNOTE SPEAKER

LOUIS R. SAROSDY

RADM, USN

RADM Louis R. Sarosdy assumed duties as Assistant Commander for Logistics/Fleet Support, Naval Air Systems Command, on 1 September 1978. He reported to the Command from assignment as Assistant Chief of Staff (Material) on the Staff of Commander, Naval Air Force, U.S. Atlantic Fleet.

A native of Pittsburgh, Pennsylvania, RADM Sarosdy was graduated from the U.S. Naval Academy in June 1951. He completed flight training in December 1952, earning his Naval Aviator designation. A three year tour with Fighter Squadron 171 followed, including deployed duty aboard the aircraft carriers USS WASP and USS CORAL SEA. In addition, he served a two-year tour as Primary Flight Instructor at Pensacola.

He was graduated from California Institute of Technology at Pasadena, California, in June 1960, earning the degree of Aeronautical Engineer (AeE). Subsequent fleet tours included assignments with VF-142 at NAS Miramar and VF-132 at NAS Cecil Field. Deployments during those tours were made in the USS KITTY HAWK and USS CONSTELLATION.

In 1962, RADM Sarosdy reported to Naval Air Station, North Island assigned to the Deputy Commander, Operational Test and Evaluation Force as the Assistant Air Warfare Officer.

He attended the Armed Forces Staff College in December 1964. Assignment with the Naval Air Systems Command followed. He was assigned as Project Coordinator for the TF30 engine designed to power the A-7, F-111 and the F-14 aircraft. This tour represented his first duty as an Aeronautical Engineering Duty Officer.

RADM Sarosdy served later tours at Commander Fleet Air, Western Pacific, Atsugi, Japan as Air Material Officer and Naval Plant Branch Representative, Pratt and Whitney Aircraft Research and Development Center, West Palm Beach, Florida, before assignment to Commander Naval Air Force, U.S. Atlantic Fleet in 1972. He later commanded the Naval Air Rework Facility at NAS North Island, San Diego, California, the largest of six such Facilities; and from 1976 until 1977, served with the Naval Air Systems Command as the Depot Management Division Director.

KEYNOTE ADDRESS

NONDESTRUCTIVE INSPECTION IN THE NAVAL AIR SYSTEMS COMMAND

The Naval Air Systems Command faces problems today that simply were not in existence twenty years ago. These problems have resulted from changes in our economic condition and advances in technology that require greater engineering responsibility. The problem areas may be catagorized as inflation, material shortage, manpower shortage, safety and reliability, and product complexity. A major solution to these problems has been found in nondestructive inspection. The most significant impact of nondestructive inspection on the Naval Fleet has been in the evaluation of components and airframes of deployed aircraft. Inspection methods based on visual, penetrant, magnetic particle, eddy current, ultrasonic, and radiographic techniques have been used as required to determine the condition of a component. This has been done to assure structural integrity without destroying the part being inspected; and hopefully without dismantling the aircraft.

This morning we will focus on the problem areas we face from the perspective of the Naval Air Systems Command, examine ways that nondestructive inspection can solve these problems, and give some specific examples based on the work of Naval Air Rework Facility, Pensacola. Pensacola has had considerable experience in inspecting Navy helicopters, an aircraft type that depends heavily on nondestructive inspection for continued operation. Keep in mind that each of the six Naval Air Rework Facilities face identical type problems and could offer similar examples.

INFLATION

Inflation affects each of us today individually and collectively. Inflation has caused the Naval Air Systems Command and other Department of Defense agencies to expend considerable effort to minimize cost. A significant way of achieving this goal has been in the extension of aircraft service life. The Navy H-2 and H-3 helicopters are prime examples: they are now expected to provide service to the year 2000 and beyond. This means at least a 40 year service life for the aircraft.

The basic problem encountered with extended lives has been occurence of fatigue failures. The loads and severe environment under which Naval aircraft operate cause many structural materials to become susceptible to fatigue. Parts which have had no previous history of fatigue failures suddenly develop fatigue cracks. This is a constant problem. We have found that nondestructive inspection will provide some protection against the negative effects of service life extension and in so doing; will attack inflation. Usefulness is found both for aircraft undergoing rework and for aircraft in the field. Previously, aircraft rework has required complete dissassembly to verify that given components were suitable for continued use.

In recent years aircraft rework has grown to depend on nondestructive inspection to provide needed information on the quality of component parts. It has also been used to eliminate dissassembly where possible and still provide needed information on the structural integrity of a component. This approach to aircraft inspection provides the margin of safety needed to operate an aircraft for extended periods between rework and to provide needed life extension for improved economy. Field inspections may become necessary between rework phases to detect the presence of material degradation by cracking or corrosion. The Navy maintains capability to develop suitable inspections to keep its aircraft flying.

A recent example of how this is done was the inspection of the H-2 main rotor blade. It was discovered that the H-2 blade was developing corrosion beneath a joint in the erosion guard. A nondestructive inspection technique based on eddy-sonics was developed. It allowed the blades to be field inspected and field repaired as required. The combined field inspection and repair kept the H-2 aircraft on an active status and saved a tremendous amount of money. The procedure kept the blades in use and prevented the corrosive attack from completely destroying the blades. Nondestructive inspection has become a primary tool to allow us to continue to safely operate our aircraft under the adverse condition of extended lives and aging parts and components.

MATERIAL SHORTAGE

Material shortage also plagues the Naval Air Systems Command. Aircraft structural members and components at times need replacement. Even when money is available to acquire the needed replacement parts, they're not always obtainable. We have found ourselves in an economic period in which materials are becoming scarce and many vendors are not interested in producing small quantities of parts. Coupled with this is the lead time in acquiring new parts; many forgings today require a lead time of 18 to 36 months for acquisition. One solution to the acquisition problem has been to backrob needed parts from other aircraft. This however, leads to additional problems later. The only viable solution to the problem has been in the use of nondestructive inspection to periodically verify the structural integrity of aircraft components while waiting for new parts to become available.

There are several current examples of this situation. The A-4 tail pipe adaptor has been failing prematurely at a seam weld. The lead time on replacement parts was totally unacceptable. We have been forced to rely on nondestructive inspection at the depot level to ensure the continued quality of the part. The H-1 main rotor blade is another example of material shortage problems. The 540 series blade was originally designed for a life of 2200 hours. Because of the onset of material failure, the life was reduced to 1100 hours. Continued failures led to the reduction of operational life to 550 hours.

In conjunction with the reduction in life and to solve the problem of lack of availability of replacement blades, nondestructive inspection was initiated to keep the blades in service until replacements could be obtained.

The T-2 nose landing gear is a third example of replacement part availability problems. The nose landing gear was originally designed with insufficient wall thickness. This landing gear was later redesigned to provide greater fatigue strength by increasing the wall thickness. Because of the lead times involved in acquiring the redesigned gear, an ultrasonic inspection technique was developed to detect fatigue cracks. The inspection continues on a periodic basis and detects the onset of fatigue cracking, preventing a catastrophic accident.

MANPOWER SHORTAGE

Manpower shortage has also developed into a problem for the Naval Air Systems Command. The loss of many qualified maintenance personnel in recent years has led to problems in field maintenance of aircraft. Nondestructive inspection has been forced to provide ability for inspection without dissassembly. This has been beneficial in that it has reduced overall maintenance costs. A prime example has been the H-53 flight control rods. The rods existed in two different configurations, hollow and solid. It was determined from field experience that one configuration led to excessive harmonic rations and possible failure. In order to remove the defective control rods from service, each rod was to be removed from the rotor head, weighed to determine type, and only the proper rods reinstalled. As an alternative, a nondestructive inspection technique was developed to classify the type rods and reduce the maintenance impact. The technique was submitted to the fleet for inspection of the control rod with the rod in place. This reduced the possibility of maintenance error, saved time in the overall maintenance process, and still accomplished the basic objective.

AIRCRAFT SAFETY AND RELIABILITY

The Naval Air Systems Command is keenly interested in aircraft safety and reliability. Again the age of many Naval aircraft increases the odds of incurring safety problems or of developing an unsatisfactory reliability condition. Nondestructive inspection has come to the aid of the Naval Air Systems Command by ensuring the ability of a part to perform its particular function. Inspection has always been critical but in recent times has been heavily depended upon to ensure the safety of an aircraft and its crew. Two examples follow.

The H-3 main rotor blade spindle has experienced fatigue cracks in both the lug area and in the shank. Catastrophic accidents have resulted from both type failures.

The lug failure led to the development of an ultrasonic inspection technique to determine the onset of fatigue cracking. Navy personnel have performed the inspection on a periodic basis with no dissassembly required, ensuring the reliability of the rotor head spindle lugs to perform their designed function.

The shank failure also led to the development of an ultrasonic inspection technique. However, some dissassembly was required to gain access to the spindle shank for inspection. It was determined that the best approach to the problem would be the deployment of a depot level field team consisting of NDI technicians and mechanics who specialized in rotor head rework. This approach was in lieu of removal of the rotor head from the aircraft, shipment of the rotor head to the nearest depot for complete dissassembly and inspection, and reassembly with return of the rotor head to the aircraft. This would have had a phenomenally adverse effect on fleet readiness and would have incurred great expense to the government. An ultrasonic inspection technique was developed which required the design and manufacture of a special fixture to guarantee a quality field inspection. The inspection technicians were trained, and field teams were deployed to aircraft locations around the world within a 2 week period. The total inspection effort was successfully accomplished. The flight safety of the H-3 aircraft has depended on these two inspections.

The H-46 helicopter also depends on similar on-going inspections to assure the continued reliability of the forward and aft main rotor shafts. A periodic inspection of each shaft is performed by Navy personnel to detect the development of fatigue cracks in threaded areas and high stress locations. The techniques also utilize special tooling designed for the particular application.

COMPLEXITY

Structures complexity is another problem area for the Navy. This is found both in the new materials that are beginning to see use in Naval aircraft and in finding solutions to the continually worsening problem of corrosion. Advanced composite materials entering service on Naval aircraft are usually epoxy matrix composites with either glass, graphite, or other fiber reinforcement. These materials don't obey the general laws of engineering fracture mechanics and also don't respond to the usual approaches to nondestructive inspection. Two Navy aircraft currently under development with extensive composite material application are the F-18 and the AV-8B. Each has composite structures. A planned maintenance requirement for the F-18 is a periodic ultrasonic inspection of the entire wing section. Six hours of inspection time are currently being programmed to perform this inspection. This requirement is considered to be unreasonable. The development of a computerized ultrasonic testing system to reduce the inspection time required and to improve reliability should provide the solution to this problem. Development is also taking place in the area of infrared imaging to scan large sections of composite materials to obtain an overview of possible delaminations. Ultrasonic imaging may also prove to be valid technique for composite material inspection.

Corrosion detection continues to be a major problem in Naval aircraft with corrosion occuring in airframe members, skins, rotor blades, and numerous other locations. The T-39 has been a source of great difficulty in corrosion control. The aircraft after many years of service began to develop an extensive amount of hidden corrosion between the skin and airframe. The only technique available for the detection of this corrosion was partial or total deskinning. Since the T-39 aircraft relies on the skin as a load bearing member, the complete skin removal process required extensive fixturing to maintain alignment of the airframe. Corrosion detection and repair of corrosion damage for the T-39 was an extremely costly task. Two inspection techniques for corrosion detection were evaluated: low frequency eddy current and neutron radiography.

Low frequency eddy current using state of the art equipment was investigated and found to be capable of detecting hidden corrosion in many cases. A review of the work was presented at the 26th DOD conference on NDI and at the Airline Transport Association meeting the same year. Other DOD Activities as well as commercial aircraft corporations have followed the Navy's lead in this inspection technique. Development of the low frequency eddy current technique to detect hidden corrosion also led to applications in the detection of second member cracking beneath aircraft skins on the T-39 and detection of exfoliation corrosion of wing skin panels. As new and more sophisticated eddy current equipment becomes available to the Navy, advanced solutions to the corrosion detection problem are expected.

Neutron radiography was also investigated for application to the T-39 corrosion detection problem. It has been shown to be highly useful in detection of hidden corrosion and of hidden cracking because of its sensitivity to corrosion product. The complexity of the aircraft setup and fixturing at that time prohibited its use on the T-39 fuselage.

However, Naval Air Rework Facility, North Island has had tremendous success in the use of neutron radiography. Particularly important has been their experience in detecting corrosion in the E-2C aircraft wing structure. In conjunction with the IRT Corporation, they were able to inspect the entire wing, tank skin for the presence of corrosion without disassembly. This was done at a considerable savings in man-hours over the alternate inspection technique. More recently, the development of an on-off portable neutron radiography system by Vought Corporation under AMMRC funding is highly promising and should make neutron radiography a widely used inspection technique.

THE FUTURE

This leads us to the question of where are we going in nondestructive inspection. The future is bright. The Navy is investigating ways of making nondestructive inspection more practical by reducing problems associated with routine inspections.

Radiography is a prime example. An investigation is currently underway to develop a suitable collimation technique for performing X-ray radiography on board ship. Presently radiography requires clearing a large area of ship work space to perform radiographic inspections. The development of suitable collimation should make on-board radiography less of a nuisance. Another advance in radiography that is beginning to be realized is real-time imaging. Computerized image processing is making real-time imaging a viable technique. Some of the advances in neutron-radiography have already been discussed. We have high hopes in this area.

Advances in ultrasonics are being made in computer-aided inspection and testing. This was related to the F-18 and AV-8B composite wing structure. Ultrasonic imaging is also receiving considerable interest. The development of laser generated ultrasonics should be a real advantage because no couplant is needed between the transducer and the part being inspected, thus making ultrasonics imaging more feasible.

Eddy current inspection is seeing advancement in equipment design, based on developments in electronic circuitry and computer technology. Low frequency eddy current and multi-frequency eddy current are two areas of special interest.

Acoustic emission for in-flight monitoring of crack and corrosion detection continues to provide hope for improved aircraft systems reliability. Design of portable and dependable systems should make this a major technique also.

The Naval Air Systems Command and the Department of Defense as a whole are tasked to conserve assets, to provide adequate safety, and to maximize usage of existing hardware. Nondestructive inspection is one of our primary tools in accomplishing this objective. Yet we must continually keep in mind the need to maintain simplicity in technique, equipment, and operation, in order to minimize operator impact and to provide required structural information free from operator subjectivity.

My challenge to you is to use this 28th Department of Defense Nondestructive Conference to further this worthy goal.

THIS PAGE INTENTIONALLY BLANK

INSPECTION FOR CRITICAL MECHANICAL PROPERTIES OF ADVANCED COMPOSITE STRUCTURES

Frederick H. Immen
Chief, Advanced Systems Research Office
US Army Research and Technology Laboratories (AVRADCOM)
Ames Research Center
Moffett Field, CA 94035
AUTOVON 359-5581

ABSTRACT

Advanced composite construction has become standard engineering practice on the most modern of US Army helicopters. Resin matrix fibrous composites of epoxy and combinations of glass, graphite, and Kevlar are used to fabricate production main and tail rotor blades, and elements of the airframe structure. The components are fatigue critical primary structure which require constant surveillance of structural integrity during their life cycle from initial design until final retirement or replacement.

The usual fatigue degradation of composite structure entails a loss of shear transfer strength through the resin. The resin provides the shear path for load transfer from an adjacent faying surface through the matrix and shear transfer from the matrix to the individual fiber. A lack of capacity in adhesion or cohesion will degrade the strength of the component and lead to premature failure.

Current NDT techniques for composites in industry are offshoots of metal NDT techniques and rely primarily on ultrasonics or coin tap to detect complete lack of shear strength in the form of voids or debonds at difficult-to-define levels in the component. Although this gives a gross indication of component quality, and can be compared to a standard, it falls short of adequacy.

It has been found that resin shear strengths can vary considerably from the standard laboratory value during manufacture and in service for many reasons; e.g., improper storage of constituents, poor cleanliness during fabrication, and exposure to severe environmental extremes.

The quality engineer requires a nondestructive inspection device which will define the shear strength of the resin in the absence of a gross and obvious debond to ensure continued structural integrity. The inspection device should be able to quantitatively define a property of the resin which can be directly related to shear strength at various levels within the component. It should define the strength at various adhesive faying surfaces with different materials and the cohesive strength of the resin itself.

Problem No. 1

INSPECTION FOR CRITICAL MECHANICAL PROPERTIES OF ADVANCED COMPOSITE STRUCTURES

Frederick H. Immen
Chief, Advanced Systems Research Office
US Army Research and Technology Laboratories (AVRADCOM)
Ames Research Center
Moffett Field, CA 94035
AUTOVON 359 5581

PROBLEM SUMMARY

Advanced composite construction has become standard engineering practice on the most modern of US Army helicopters. Resin matrix fibrous composites of epoxy and combinations of glass, graphite, and Kevlar are used to fabricate production main and tail rotor blades, and elements of the airframe structure. The components are fatigue critical primary structure which require constant surveillance of structural integrity during their life cycle from initial design until final retirement or replacement.

The usual fatigue degradation of composite structure entails a loss of shear transfer strength through the resin. The resin provides the shear path for load transfer from an adjacent faying surface through the matrix and shear transfer from the matrix to the individual fiber. A lack of capacity in adhesion or cohesion will degrade the strength of the component and lead to premature failure.

Current NDT techniques for composites in industry are offshoots of metal NDT techniques and rely primarily on ultrasonics or coin tap to detect complete lack of shear strength in the form of voids or debonds at difficult-to-define levels in the component. Although this gives a gross indication of component quality, and can be compared to a standard, it falls short of adequacy.

It has been found that resin shear strengths can vary considerably from the standard laboratory value during manufacture and in service for many reasons: e.g., improper storage of constituents, poor cleanliness during fabrication, and exposure to severe environmental extremes.

The quality engineer requires a nondestructive inspection device which will define the shear strength of the resin in the absence of a gross and obvious debond to ensure continued structural integrity. The inspection device should be able to quantitatively define a property of the resin which can be directly related to shear strength at various levels within the component. It should define the strength at various adhesive faying surfaces with different materials and the cohesive strength of the resin itself.

MECHANICAL REQUIREMENTS ON THE MATRIX

The material requirements on the matrix of a composite are among the most complex and demanding in all of materials science (1). We will be concerned here only with the mechanical stress and deformation requirements. First, the single-ply of unidirectional composite material will be considered, then the multi-ply laminate, and finally a complete structure.

The role of the matrix under longitudinal tension or compression stress is far from simple (2). Under tension the primary function of the matrix is to maintain the effective load carrying capability of fibers after they have broken at their weakest points. To do this the matrix material in the vicinity of each broken fiber must redistribute the load that was originally in the broken fiber to the adjacent fibers as gently as possible in order not to cause breaks in the adjacent fibers. At the same time the matrix must reload the broken fiber so that it resumes its tensile function a short distance away from the break. The principal mechanism whereby the matrix accomplishes these roles are by shear stress transfer from one fiber/matrix interface to another. Without this capability large composite components containing long reinforcing fibers would have little or no strength because most high strength fibers are extremely flaw-sensitive and contain so many flaws that longer lengths have relatively low strengths. Thus, large composite parts would have much lower strengths than small parts, to the extent that the material would be much less useful.

The role of the matrix in longitudinal compression is more evident. Were it not for the stabilizing effect of the matrix it would not be possible for a composite to develop any practical compression properties. The ultimate compression strength is usually dictated by matrix shear stiffness retention at lower compression strain states and fiber/matrix interfacial bond integrity. Both of these mechanisms resist shear crimping, the dominant compression failure mode of most unidirectional composites (See Figure 1).

Under transverse tension, compression or shear it is commonly known that the fiber, matrix and interface must all share a weakest-link role in the composite strength function. The load carrying requirements are more or less equal for all three. In fact, the presence of stiff fibers aggravate the matrix/interface conditions by introducing stress risers and embrittling constraints on the matrix deformations (See Figure 2). The first one of these elements to fail precipitates transverse cracking of the composite which if not catastrophic is usually undesirable.

Matrix stiffness and fiber/matrix bond strength also play a dominant role in the composite toughness and impact resistance. The energies required to fracture brittle fibers are generally low. The primary energy absorption mechanism in unidirectional composite failure is fiber/matrix debonding and subsequent interfacial sliding friction losses (3).

The creep response of most composites are dominated by the matrix creep characteristics. Most fiber reinforcements show little or no creep response. However, when the matrix relaxes a redistribution of loads takes place within the composite that manifests itself as composite creep (4). Much the same is true of long term thermal stability of composites.

The matrix also controls the creep rupture characteristics of composites. The matrix localizes the effect of prematurely broken fibers just as it does in the static tension case. This is also true of longitudinal tensile fatigue behavior. Longitudinal compression fatigue behavior has also been observed to consist of the gradual breakdown of the matrix stabilizing influence on the load carrying fibers leading to progressive local buckling of fibers near flaws and delaminations (5).

There are several additional mechanical requirements on the matrix material that are introduced when the unidirectional composite is fabricated into a multi-directionally reinforced laminate. Most of these have been grouped under the heading of interlaminar edge effects. These are analagous to the end effects in a bending beam, i.e., simple beam theory only applies in regions away from concentrated loads and ends. Lamination theory has similar restrictions. The stresses in a laminate near free edges, cutouts and concentrated or line loads require more detailed calculations. These stresses generally tax the matrix strength capabilities to a much greater extent than lamination theory predicts. These high matrix stresses were ignored until some data became available to show they did indeed have a gross effect on coupon fatigue life (6). The precise magnitude of these stresses is not known since they have yet to be subjected to micromechanical analysis, but their general nature is understood and their influence on static laminate properties has been demonstrated. The interlaminar stresses generally take the form of high combined shear and normal stresses between the plies, either close to or at the edges of a test specimen or component, which cause local delamination of the laminate which can propagate with repeated loading or reduce the static strength, residual strength or useful lifetime. Laminates may also be subject to a similar type of damage around fastener holes although a small amount of fastener clamping pressure may effectively suppress the tensile interlaminar stress components, which are generally regarded as the worst offenders.

The presence of local hard points, joints and concentrated loads invariably place additional requirements on the matrix material by virtue of the fact that abrupt structural discontinuities almost always lead to three-dimensional stress distributions that are difficult to counter with composite construction where the reinforcement is essentially two dimensional. This results in higher demands on the matrix from loads in directions which are unreinforced. Load transfer in bonded joints generally follows a path from fiber to matrix to adhesive to matrix to fiber, traversing all the material interfaces as well, with strength determined by the weakest link in the load path. This is one of the reasons for past problems with bonded joint reliability. A single quality control problem with a matrix or adhesive material or with any of the interface preparations will seriously degrade the bonded joint integrity. This is a reason for the continuing popularity of less efficient mechanically fastened composite joints (7). Bolted joints are somewhat insensitive to interface problems but still depend on matrix bearing strength in the immediate vicinity of the bolt holes. Substandard or improperly cured resin areas could lead to premature elongation of fastener holes and attendant joint fatigue problems.

Concentrated load introduction, with the exception of wrap around joints, generally involves the same matrix strength dependencies as bonded or bolted joints. Wrap around fittings (See Figure 3) appear to be a highly efficient alternative to bolted or bonded joints and they often are; however, there are also problems associated with these designs. These are usually related to proper resin content and fiber tension control. The designs do involve matrix shear and bearing stresses but the associated failure modes are probably not catastrophic types.

Existant field and shop repair techniques are usually matrix property dependent in much the same way as bonded or mechanical joints.

MATRIX STRENGTH DEGRADATION

Matrix property degradation can occur in a number of ways. The initial way is through incorrect, substandard, improperly stored, overage or adulterated matrix materials and (or) catalysts. Mistakes at this level usually can be detected in material acceptance testing and corrected. Examples of these problems reaching component fabrication stages are rare. At the materials processing level matrix properties can be degraded by overaging, improper resin content, adulteration, high void content, improper viscosity control and wetting characteristics, improper bleeding, loss of curing pressure, nonuniform heating during cure, high exotherm, loss of vacuum, incorrect sizing agent, etc. Most of these mistakes can be detected by test tabs on the laminated parts. In manufacturing or assembly there is a danger of matrix property degradation by overheating during bonding cycles, improper bonding surface preparation, improper adhesive selection, and incorrect bondline thickness control. If proof testing is used there is the possibility of matrix crazing, cracking or debonding under proof loading. In storage prior to use there is a danger of contamination, overheating, high humidity and attack by fungus or organisms; all of which can degrade matrix properties.

In service, all the environmental factors can contribute in some way to matrix property degradation. This can range from prolonged UV radiation to improper cleansing agent damage (8).

PROBLEM DEFINITION

It can be seen from the above that the matrix of a composite component is a structural member serving a function much the same as a sheet of aluminum, a shear pin or a rivet would do in conventional metal structure. A fundamental difference is that the matrix is fabricated and its structural strength and durability is established as the component is created. This is analogous to delivering a carload of aluminum ore to Boeing and asking them to build a 747. Many process and quality controls are truncated in the case of composite design and fabrication. From this, the need for more stringent composite NDT methods becomes obvious.

By considering the principal physical and mechanical characteristics of importance to maintaining structural continuity in the composite and the major causes of strength degradation in the composite in its life cycle, it may be possible to measure properties of the material nondestructively which will define strength directly or deductively. Because the matrix plays such a fundamental role in the composite structural integrity and is most subject to degradation in its lifetime, it requires special NDT methods to measure its strength and primarily shear strength. The means of meeting this challenge, the author leaves to the NDT specialist.

REFERENCES

(1) Proceedings of the Society of the Plastics Industry, Reinforced Plastics/Composites Institute, Annual Conferences.

(2) R.M. Jones: Mechanics of Composite Materials, Mc Graw-Hill Book Co., New York, N.Y., 1975.

(3) P.W.R. Beaumont: Fracture Mechanisms in Fibrous Composites, Interim Reports on AFOSR Project F08671-78-00988.

(4) R.L. Foye: Creep Analysis of Laminates, Proceedings of ASTM Composite Reliability Conference, Las Vegas, Nevada, April 1974.

(5) S.C. Kunz & P.W.R. Beaumont: Microcrack Growth in Graphite Fiber Epoxy Resin Systems During Compressive Fatigue, ASTM-STP569, Dec. 1973.

(6) R.L. Foye & D.J. Baker: Design of Orthotropic Laminates, AIAA/ASME 11th SDM Conference, Denver, Colorado, April 1970.

(7) Engineering Design Handbook-Joining of Advanced Composites, U.S. Army Material Development and Readiness Command Pamphlet DARCOMP-706-316, March 1979.

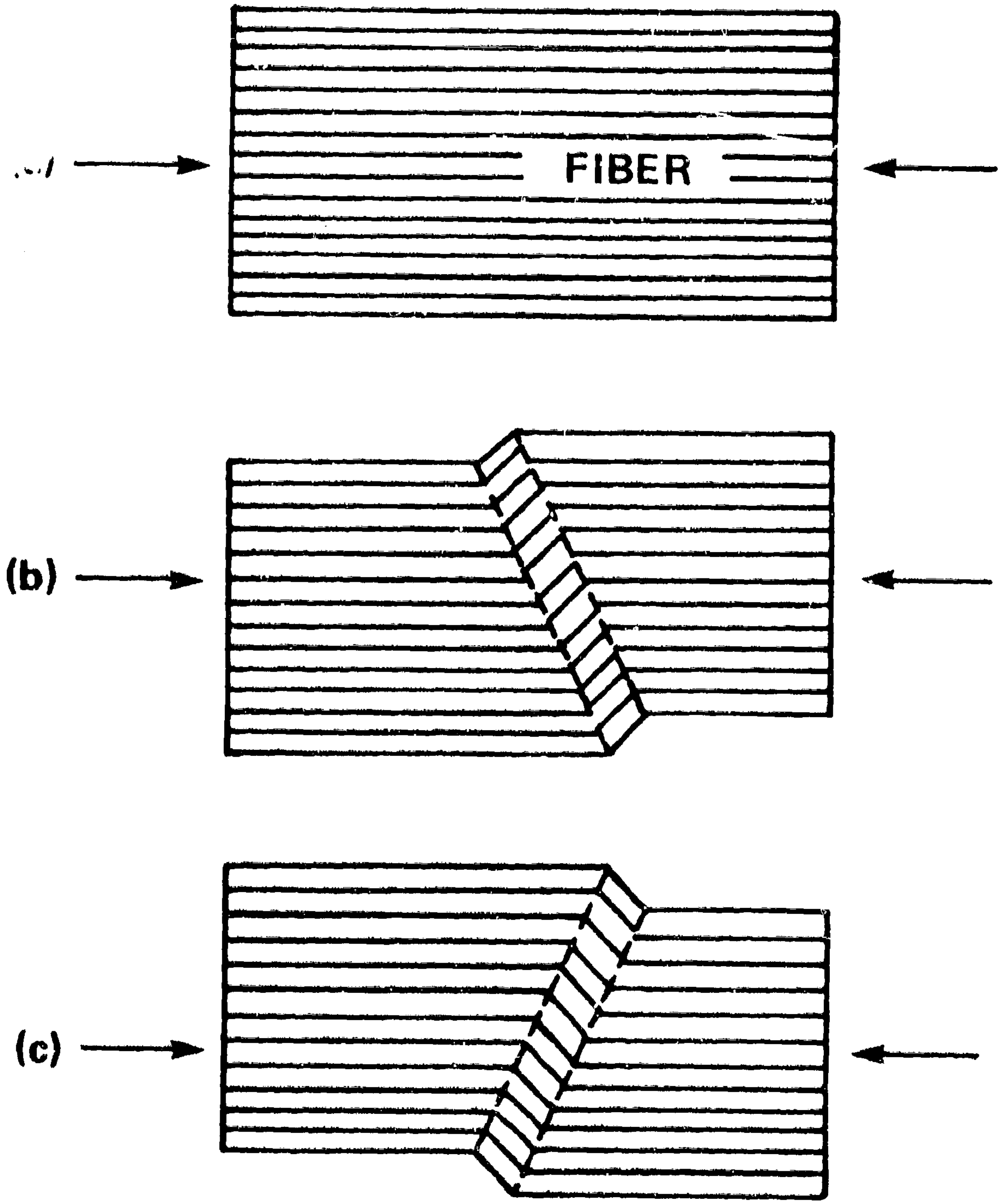

Figure 1. Shear Crimping Mode of Compression Failure

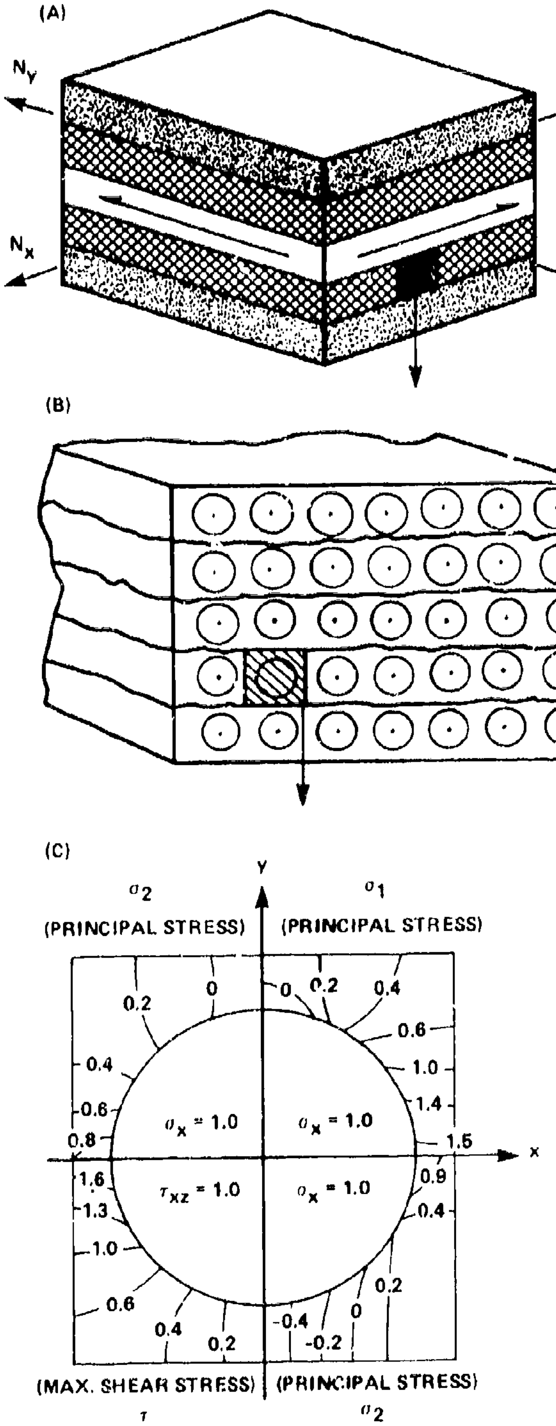

Figure 2. Stresses in the Matrix

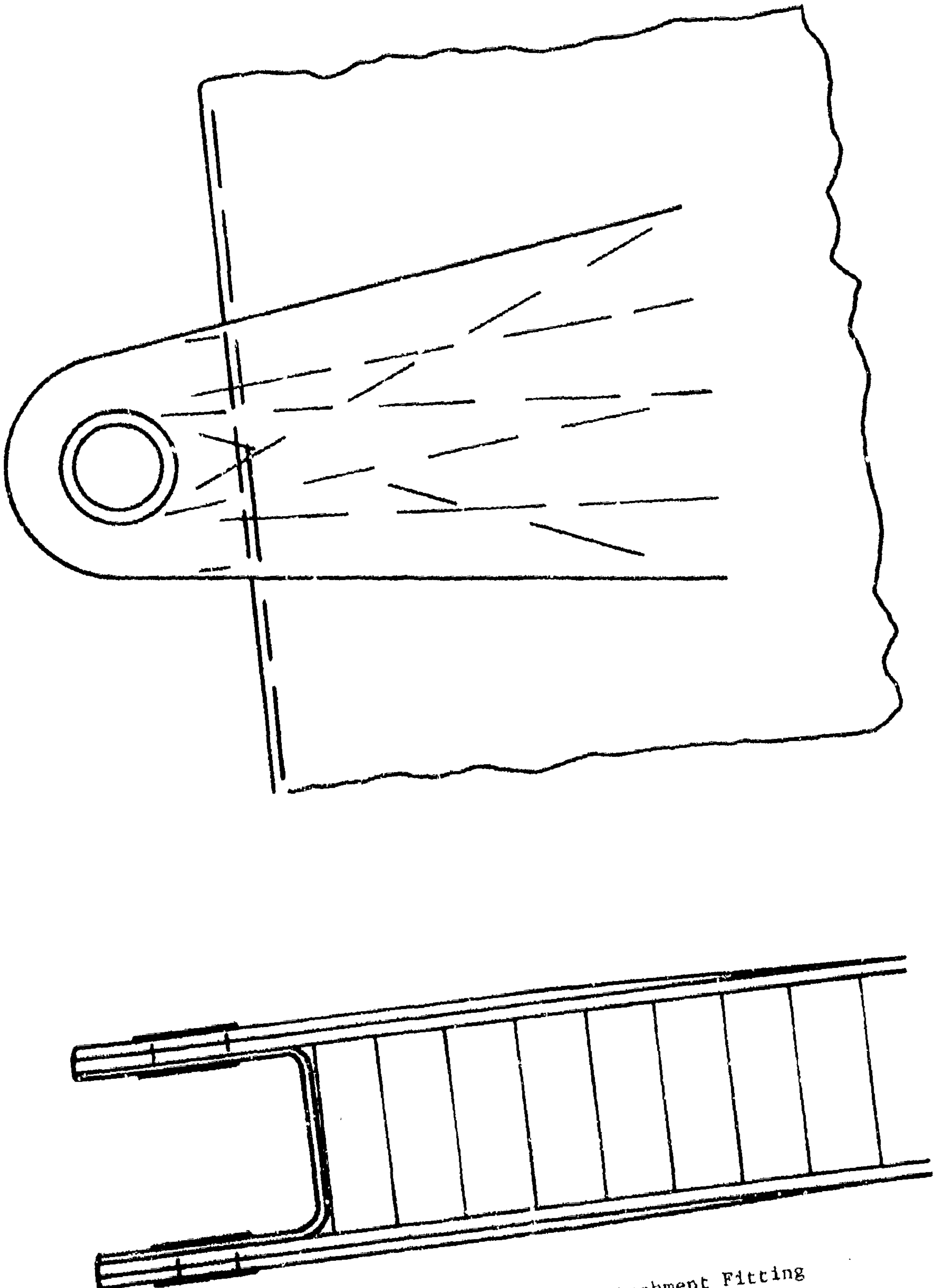

Figure 3. Wrap-Around Lug Attachment Fitting

REPORT ON PROBLEM NO. 1

28th NDT CONFERENCE

PROBLEM: Inspection for Critical Mechanical Properties of Advance Composite Structures

PRESENTED BY: Mr. Frederick H. Immen

AFFILIATION: U.S. Army Aviation R&D Command, Research & Technology Laboratories, AMES Research Center, Moffett Field, CA

PROBLEM COORDINATOR: Mr. John T. Conroy

AFFILIATION: U.S. Army Aviation R&D Command, Directorate for Product Assurance, St. Louis, MO

BRIEF REVIEW OF PROBLEM: Current NDT techniques for composites are off shoots of metals NDT techniques and rely primarily on ultra-sonics or coin-tapping to detect complete lack of shear strength in the form of voids or debonds at difficult to define levels in components. More work needs to be done to provide an NDT device to define the shear strength of composite structures for aircraft.

PROPOSED SOLUTIONS:

A. Electro-Magnetic Excitation (EME)
Suggester: Bill Bennett, Jr.
Suggestion: Kaman Services in Colorado has developed the EME technique to study the properties and presence of defects in silicon-nitrate turbine blades. The technique could be used to study:

Bulk Modules
Logrithmic Decramant
Internal Friction

Industrial Contact: Dr. Donald Sachs

B. Harmonic (Flaw) Detector
Suggester: E. Fritz
Suggestion: Shurtronics has acoustic device which incorporates a transducer head that can be modified to accommodate raised curved surfaces such as aircraft ra domes.

C. Acoustic Flaw Detector
Suggester: Gwynn McConnell
Suggestion: Inspection Instrumentation, Ltd. In UK has device similar to item described in B (above), but considered to give better results.

D. Ultrasonic Detector
Suggester: Gwynn McConnell
Suggestion: British aerospace industry is using an ultrasonic measurement device with considerable success to locate voids/debonds in graphite-epoxy structural panels in transport aircraft.

E. Ultrasonics
Suggester: Gwynn McConnell
Suggestion: NADE has investigated the use of Ultrasonics to map the fillet areas of bonded joint between fibre glass skins and Nomex cores on rotar blades. They have worked in the 7.5MHz range with the AeroTec 3/4 inch focused transducer. (A single chart scan). The current work was provided for inspection. The work has not progressed to the point where structural properties are predictable at this point. The technique appears highly satisfactory for visualization of the bond, or absence of the bond, at the skin to core interface. Additional work is planned with the objective of eventually being able to predict bonded strength as a function of adhesive fillet properties.

F. X-Ray Defraction
Suggester: D. Farmer
Suggestion: The current joint services work in X-ray Detection investigation of various structural materials may have potential application to aircraft composite structures. This work also involves the Electric Power Institute. It is being coordinated by The Denver Research Institute.

G. N-Ray
Suggester: Bill Bennett, Jr.
Suggestion: The use of the portable equipment described by Dr. Antel of AMMRC should be considered a potential too (since it has abilities to detect various elements that we normally present in composite materials).

H. Speckle Interfarometry
Suggesters: Terry Vandiver/Bill Bennett, Jr.
Suggestion: The papers on Surface and Subsurface Investigations using laser and acoustic processes we considered to have potential and should be investigated for this problem. See paper numbers 12 and 15 for additional details in these processes.

RECOMMENDED SOLUTION: The problem is generic to a wide range of composite structure applications. No immediate solution is available. Most of the suggested solutions warrant further investigation.

DEVELOP AN NDT TECHNIQUE TO INSPECT THE QUALITY OF THE BONDED INTERFACE OF TITANIUM AND BRASS

Alfred H. Davidoff
USA ARRADCOM
DRDAR-QAN-I
Dover, New Jersey 07801
Autovon 880-2830

PROBLEM ABSTRACT

We have a requirement to develop a valid technique to nondestructively inspect the quality of the bonding of a brass rotating band to the titanium rocket motor body for the XM785 projectile development program. A technique is being developed to bond the interface by a diffusion process which will provide approximately the shear strength of the brass. This is required to assure the proper function of the rotating band with a failure rate of less than one in one thousand. Therefore, 100% inspection is considered necessary. In order to assure proper function of the rotating band it is believed that more than an intimate contact of the brass to the Ti is necessary.

Several NDT techniques have been considered to solve this problem but none have been proven successful as yet to determine the strength of the bond. An attempt is being made to use ultrasonic C scan by through transmission. However, this does not appear to yield enough information to predict the strength of the interface bond.

The need to predict by NDT the quality of the bond interface of Ti/Brass is established by the reliability requirement, cost of the hardware and undesirability of relying on the control of manufacturing process alone.

PROBLEM OUTLINE

Product

The problem is associated with the rocket motor for the 155MM (XM785) projectile for the M109 Howitzer system.

Quality Characteristic

The inspection characteristic we are attempting to evaluate is the mechanical strength of the bond between the rotating band and the rocket motor body. A defective bond which allows the rotating band to break loose in the gun tube or in flight could affect the flight characteristics or become a safety hazard.

Problem No. 2

Specification Requirements

A specific numerical value has not been developed for the quality of the bond since the item is in the early stages of development. However, it will be defined either in terms of strength or how large an area of the mating surface is bonded. This criteria must assure us that the rotating band will not separate in any area. The inspection must be performed on 100% of the rocket motors nondestructively.

Materials

The forged rocket motor body is a 662 Titanium alloy (MIL-T-46038) which has a groove .025 in. deep machined to accept the rotating band. The rotating band is cut from brass tubing of 10% Zn with an internal diameter of 6.340 in. and a 6.812 inch outside diameter.

Process of Manufacture

The two parts are bonded by diffusion using a Hot Isostatic Pressure (HIP) furnace. While the final process is still being developed it can presently be described as follows:

(1) The rotating band and Titanium body are both completely cleaned through separate processes designed to free them of all contaminants.
(2) The rotating band is slipped in position over the rocket motor body and pressed in place in a tire setter. The pressure is applied evenly around the circumference.
(3) A Titanium sleeve is placed over the band/body assembly with a tight fit over the band and EB welded to the body at the ends. The assembly is helium leak tested and sealed.
(4) The diffusion bonding is accomplished in an autoclave by means of the HIP process. Eight bodies and one test ring are placed in the furnace at once and the heat brought up to 1200°F and maintained for one hour. A pressure of 15,000psi is applied around the sleeve during the temperature cycle.
(5) After cooling the sleeve is machined away and the assembly is ready for inspection.
(6) After inspection the assembly is machined to the final configuration.

Production Rate

The items will be produced at a low production rate and will require 100% inspection.

Present Inspection Method

During the R&D phase the rocket motor body is being inspected with ultrasonics C scan using through transmission, 5m Hz transducer. Several samples which appeared to be defective on the C scan were treepanned - that is, a sample was cut out and a shear test performed; these test samples have verified the ultrasonic "C" scan for intimate contact but have not necessarily indicated that there was diffusion.

At the present time eight bodies are HIPed at the same time with a test ring which consists of a Ti ring and a brass rotating band which are assembled with the same interface dimensions at the same time as the motor bodies.

Previous rotating band to shell or rocket motor assemblies were different materials and different processes but were successfully inspected with ultrasonics. We have not proven that ultrasonics will provide sufficient information to assure the strength of bond of the XM785 Projectile.

PROBLEM #2

PROBLEM: Need to develop an NDI technique to inspect the quality of the bonded interface of titanium and brass.

PRESENTED BY: Alfred H. Davidoff

AFFILIATION: DRDAR-QAN-1, ARRADCOM
Dover, NJ 07801
201-328-2830

PROBLEM COORDINATOR: Gary J. Hood

AFFILIATION: 47FMS/MAFF
Larghlin AFB, Tx 78840
512-298-5268 732-5268

BRIEF REVIEW OF PROBLEM: 100% inspection is considered necessary of the brass rotating band on the titanium rocket motor body of the XM785 projectile. Improper firing, mis-tracking, etc. could result. Knowing the mechanical shear strength of the bond is imperative.

SOLUTIONS PROPOSED: There is no such thing as a "sticky bond". You either have bond or you don't. You may have two faying surfaces that are in very intimate contact. If the gap is in the order of a few thousand angstroms or less, longitudinal waves will be transmitted across it, but normal incidence shear waves will be reflected from a much narrower gap. C-scans using shear waves can be accomplished by the use of non-contact electromagnetic transducers (EMAT's).

RECOMMENDED SOLUTION: If samples can be provided, the following named individuals would be interested in attempting this approach to the problem. They are negotiating for EMATs.

Stephen D. Hart
Code 8431
Naval Research Lab
Washington, DC 20375
202-767-3613/3094
AV 297-3613/3094

Dr. J. Smith
NDE Branch, AMMRC
Watertown, MA 02122
AV 923-3333

DETECTION AND MEASUREMENT OF CRACKS ORIGINATING AT CORNERS OF A SLOT

Bruce B. Brown
U.S. Army Armament Research and Development Command
Benet Weapons Laboratory
Watervliet, NY 12189
Autovon 974-4249

ABSTRACT

A problem exists in autofrettaged cannon barrels in detecting and measuring cracks at exterior stress concentrators. With the exterior residual tensile stress of autofrettage, ultimate fatigue failure can be caused by cracks originating in external features such as recoil slide slots and keyways. Since these cracks originate along slot fillets with longitudinal tool marks and do not appreciably open up before failure, they are difficult to detect and recognize as cracks by conventional NDT means. A detection and measurement method is needed to allow barrel condemnation prior to catastrophic failure.

Laboratory usage of magnetic particle and dye penetrant techniques have been only partially effective since the fillet corners and tool marks tend to obscure real cracks. Ultrasonic scans by angle probes have so far not been effective probably due to nonradial crack growth. To be effective, a technique should be usable by field and depot inspectors and not confined to laboratory specialists.

1. INTRODUCTION

The fatigue test laboratory of the Benet Weapons Laboratory is concerned with not only establishing safe fatigue lives for cannon components but evaluating methods to prevent fatigue failure. In the examples shown safe operating lives have been or are being established. However, backup NDT methods are of great concern to screen cannon components for impending fatigue problems irregardless of gun crew record keeping on rounds fired and charge levels.

The hydrostatic cyclic fatigue testing we do allows rapid accumulation of fatigue cycles under controlled laboratory conditions. Attendent to the fatigue testing we perform NDT inspections to detect crack initiation and measure crack growth through the component. The problem presented is one whose solution has eluded our conventional NDT methods but we feel is worthy of efforts to solve in that its solution would be applicable both for laboratory and field usage.

2. PROBLEM

Most modern cannon barrels are of autofrettaged construction whereby a residual stress, compressive at the bore and tensile at the outside surface, is imposed during manufacture. The general effect of this is to provide a lighter and longer lived barrel. Because of the residual tensile stress on the O.D. and the additional tensile firing stresses it is possible to experience fatigue failure from various stress concentrators on the outside surface. Due to the tensile field with added cyclic tensile operating stresses and the geometry of the stress concentrators, these cracks are often long and shallow and obscured through most of their lives and result in failure with only slight radial growth.

We have consistently good results in detecting and measuring bore originating cracks using ultrasonics. However, some cases of external cracking have presented problems so far not satisfactorily handled by 'conventional' NDT techniques.

A specific example is the 155 mm M185 cannon barrel. This barrel contains a 66 inch long, 1 inch wide, and 0.4 inch deep key way on the outside surface in the high pressure, high stress region. Figures 1 and 2 show this slot.

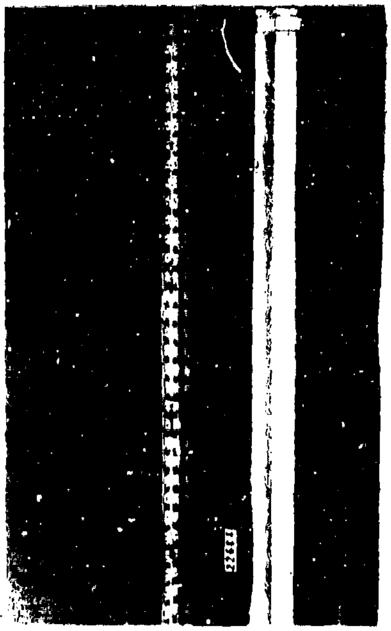

Figure 1. Barrel with Slot

Figure 2. Cross Section of Slot

This slot serves to prevent barrel rotation in the recoil mechanism. The mode of failure is the generation of several small fatigue cracks along the fillet of this keyway which grow longitudinally, with very little growth in depth, linking up into a major crack which when approximately 12 inches long, results in rapid failure with the crack depth at failure in the order of 1/4 inch. Figures 3, 4, and 5 show the fatigue failure.

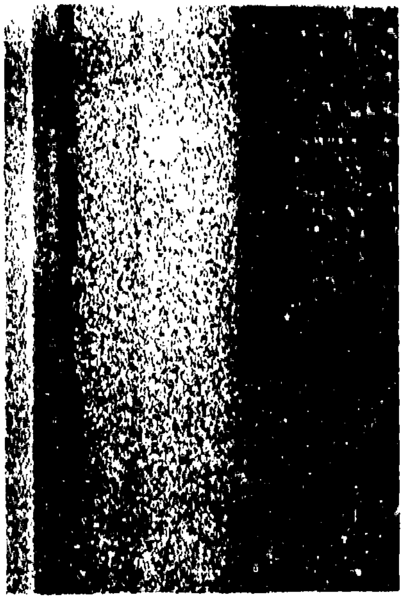

Figure 3. Dye Penetrant Indications

Figure 4. Failure Crack

Figure 5. Fracture Surface

Present laboratory use of ultrasonics, magnetic particle and dye penetrant have been only marginally useful. The detection and measurement problem stem from the following:

(1) The fillets of the slot are reasonably sharp and contain longitudinal tool marks.

(2) The cracks never attain much depth and at failure are 1/8 - 1/4 inch deep.

(3) The cracks propagate along the fillets but do not open up sufficiently to be identifiable by eye except immediately prior to barrel failure.

The hoped for solution to this problem would be an easily applied technique operable by normal barrel inspectors, perhaps calibrated to a go - no go mode. The inspection process would be applied at specific round life intervals and also to screen barrels with questionable firing histories. We have hopes that an electrical measurement technique, eddy currents, or surface wave ultrasonics might be applicable.

3. FURTHER APPLICATIONS

Beyond this problem with the 155 mm barrel similar problems exist with slots on other cannon barrels (i.e., 8" M201). Beyond the slot cracking problem other types of exterior stress concentrators cause initiation of fatigue failures and are worthy of attention for NDT applications. The sectored threads in some barrels are crack initiators due to the edge present at the side of the sectors. Figure 6 shows this feature.

Figure 6. Thread Sector Crack Initiation

On some barrels locking holes recessed into the barrel exterior are the source of fatigue failure as shown in Figure 7.

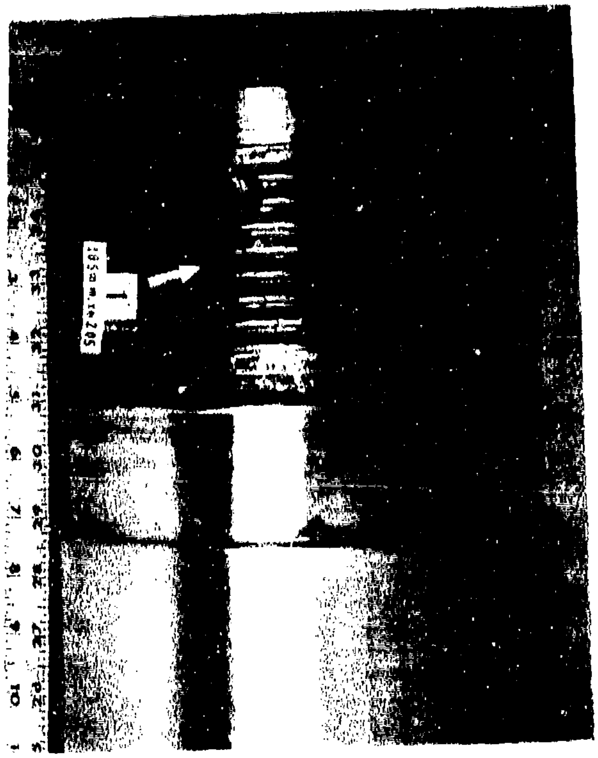

Figure 7. Locking Hole Crack Initiation

4. PROBLEM OUTLINE

(1) Name of Product: Barrel, 155 mm Howitzer M185.

(2) Characteristic to be Measured: Fatigue cracks at fillet of slot.

(3) Limits to be Evaluated: Detection with depth of 1/16 to 1/8 inch and measurement of length: 1 to 12 inches.

(4) Material: Gun steel, 170,000 yield strength.

(5) Processing: Heat treated forging with residual stresses due to autofrettaging. Tensile stress in area of concern.

(6) Geometry: See Figure 2.

(7) Quantity of Items: 1000+

(8) NDT Methods Presently Used: (1) Magnetic Particle: Hard to differentiate tool marks and fillet from crack; (2) Dye Penetrant: Same; (3) Ultrasonics: Due to small depth involved, geometry of inspection area and random radial crack path, we have had only marginal results.

(9) Equipment Limitations: A portable, easily applied and interpreted method would be ideal for depot use. A more complex system would still be of interest but might be limited to laboratory and proving ground use.

(10) Previous Submissions: None to our knowledge.

PROBLEM NO. 3

REPORT ON PROBLEMS FROM THE FLOOR

28TH NDT CONFERENCE

PROBLEM: "Detection and Measurement of Cracks Originating at Corners of a Slot"

PRESENTED BY: Bruce B. Brown
Large Caliber Weapon System Lab
Watervliet, NY

PROBLEM COORDINATOR: Ronald L. Frailer
Material Testing Directorate
Aberdeen Proving Ground, MD

BRIEF REVIEW OF PROBLEM: The M185 gun tube is currently being fired at higher than original design tube pressures to support the newer Higher velocity projectiles. This increased pressure combined with residual tensile stresses in the gun tube created by the autofrettage process is causing cracks to develop in the recoil slots and keyways. Efforts to detect cracking by magnetic particle testing have been hampered because the milling of a sharpe radius in the slots and tool marks cause false crack indications. An inspection technique is needed that can replace the magnetic particle inspection method or verify cracking when magnetic particle indications are seen.

SOLUTIONS PROPOSED: Several possible solutions have been proposed. One possible solution is to use an eddy current probe specially designed to fit into the slot, to detect and measure the depth of the cracks that originate along slot fillets. Eddy current techniques have been successful in detecting cracks and measuring crack depth in bolt holes and in other tight quarters. Some laboratory work will be needed to determine the coil geometry but an instrument can be developed that will be easy to use under field conditions.

A second suggested solution is to measure the electrical resistance across the recoil slot using a four-wire measuring device that is currently on the market. This instrument is capable of measuring crack depth and with preparation of test samples could be calibrated to make estimates of crack length and depth. The instrument can be used in the field to verify the indications of cracking after a magnetic particle examination of the slot.

Another possible solution is to partially fill the tube with oil and place a fixturing device in the bore holding an ultrasonic transducer that would be directed at the recoil slot. The gain would be set very high to detect a reflection from the edge of the crack. This is a technique that has worked in other items similar in geometry to gun tubes.

Another solution is to construct a holding device that would be positioned over the recoil slot and hold two ultrasonic transducers position so that one would transmit a pulse to just below and parallel to the bottom of the slot and the other transducer would be positioned on the other side of the slot to receive the pulse. Thus a thorough transmission inspection would be performed of the area just below the recoil slot.

Also suggested was the possibility of placing a small surface-wave transducer in the slot to detect cracking at the corners.

In addition to the suggestions concerning detection of the cracks, it was also suggested that gun tubes that do not show any indication of cracking be shotpeened to provide compression stresses at the surface which would retard the onset of fatigue cracking.

RECOMMENDED SOLUTION: All of the proposed solutions seem feasible and should have a high probability of being successful in solving this problem. Because of the ease of testing and simplicity of implementing the eddy current suggestion it is being recommended as the possible solution to be tried first. Off the shelf instrumentation is available and construction of a special probe can be done by the equipment manufacturer in very little time and at a very small additional cost. Some effort will have to be made to collect a number of representative samples of slots with magnetic particle indications that have and do not have actual cracks in them. These samples will be necessary to design and verify the performance of the eddy current probes.

It is also recommended that the suggestion to shotpeen the recoil slots in the field before getting indication of cracking be considered as a method to retard crack initiation.

Nondestructive Test Method for the Determination of Aircraft Arrestment Hook Point, Metallized Hard Face Process Coating Thickness Hard Face Coating Adherence, and Base Metal Cleanliness prior to Coating Process

Submitter: Michael J. Hromoko
General Engineer
Naval Air Engineering Center
Quality Assurance Office
Code 99114
Lakehurst, NJ 08733
Autovon 624-2213
Commercial (201) 323-2213

Presenter: Robert Fegan
Code 915F
Naval Air Engineering Center
Lakehurst, NJ 08733
Autovon 624-2595
Commercial (201) 323-2213

ABSTRACT

An adequate scientific method to determine thermo spray metallized hard face coating material thickness and adherence characteristics is unavailable at the present time. Recent problems involving inconsistent material thickness and poor material adherence following application of metallized coatings have developed with a current Navy aircraft hookpoint contract vendor. It has become evident that an accurate and rapid inspection method is needed to evaluate hardware prior to and following thermo spray material application.

Specific areas of attention include: base metal surface analysis for degree of cleanliness, metallized coating thickness uniformity of and actual coating thickness measurements on irregularly contoured surfaces, detection of voids between base metal and material coating following thermo spray and fusion process, and an adequate means of determination that total coating material adherence is accomplished. Lack of total adhesion presents the possibility of coating material separation from hookpoint during aircraft flight deck pendant impact, thereby creating FOD hazards to engines.

Problem No. 4

Nondestructive Test Method for the Determination of Aircraft Arrestment Hook Point, Metallized Hard Face Process Coating Thickness, Hard Face Coating Adherence, and Base Metal Surface Cleanliness prior to Coating Process.

Submitter: Michael J. Hromoko
General Engineer
Naval Air Engineering Center
Quality Assurance Office
Code 99114
Lakehurst, NJ 08733
Autovon 624-2213
Commercial (201) 323-2213

Presenter: Robert Fegan
Code 915F
Naval Air Engineering Center
Lakehurst, NJ 08733
Autovon 624-2595
Commercial (201) 323-2595

Summary: Discovery of Problem

Recent problems involving the application of a metallized hard face coating on Navy aircraft arrestment hookpoints has identified several serious process quality control deficiencies. The almost 100% material rejection rate of a new Navy aircraft hookpoint vendor has made it evident that an accurate and rapid scientific method is needed to evaluate hardware being processed via the current metalizing thermo spray method. Also, an adequate method to nondestructively test for certain process characteristics/conditions is not currently available.

Problem to be Investigated

The three specific NDT areas involved in this presentation are:

(1) Base metal surface analysis for degree of cleanliness.
(2) Measurement, metalized coating thickness uniformity of an actual coating thickness on irregularly contoured surfaces.
(3) Detection of voids between base metal and material coating following thermo spray and fusion process/ adequate means of determination that total coating material adherence is accomplished.

Discussion: Metallized Hardface Process

Hard facing is the practice of protecting metal parts from wearing quickly by fusing a layer of wear resistant material over the parent metal. This is generally performed on worn parts to replace metal lost through wear and new parts when wear is anticipated. The Navy's application of hard face coating of Aircraft Arresting Hook Points has greatly increased the useful life-span of these parts, since a part protected with a properly applied coating will last many times as long as it would unprotected. Basically, this means fewer new replacement parts, less labor required to re-install parts and Aircraft with less down time. The term hard-facing or metallizing, as it is sometimes called, is a type of flame spraying process where the hard face coating substance is continuously melted in an oxygen-fuel-gas flame and atomized by a compressed air blast which carries the metal particles to the previously prepared surface. For proper adhesion, the need for a clean surface is imperative! No oils (Hydrocarbons) or other contaminants can be present in order to assure a complete bond. Continuing, the individual particles mesh to produce a coating of the sprayed metal.

The metal hard face coating operation is applied by hand, thereby limiting the accuracy of coating thickness uniformity to the "trained" eye and reflexes of the operator. Coating thickness uniformity and duplication is practically impossible in this application, but tolerances are furnished to provide acceptance ranges of coating thickness. However, even with generous tolerances the required coating thickness may not be obtained 100% of the time within prescribed tolerances. Following the flame spraying process the treated part is heated in a controlled atmosphere furnace or hand torch to a temperature of approximately 1900°F. The previous mechanical bond now becomes a fused or welded bond. This resulting fused chromium boride surface will withstand corrosion and abrasion up to 25 times longer than hardened steel.

Finally, since total adhesion of the metallized hard coat material to the base metal is required, a method/measuring instrument to determine voids between the hard coat substance and base metal is necessary. Less than total adherence will produce a substantial increase in failure rates and possibly create sharp cutting surfaces, should hard face coating fail at time of Aircraft Hook Point/ship deck pendant impact. Lack of total adhesion also presents the possibility of coating material separation from the hookpoint during aircraft arrestment, thereby creating FOD hazards to aircraft engines.

Quality Characteristics: Measurement/Evaluation

(1) Measurement of Metallized hardface coating thickness: Since the hardface coating application is performed by hand the uniform coating thickness requirement is not being met. Success of uniform coating, within tolerances, determines useful life of part. Range of measurement capability must be 0-0.100 inches (minimum).
(2) Detection of non-adherence of hardface coating on base metal surface: Detection of voids/separation between the two materials must be accomplished. Any separation must be detected and is cause for rejection.
(3) Detection method for non-cleanliness of base metal surfaces prior to hardfacing: Any oils or contaminants will inhibit a total adherence between the base metal surface and metallized coating.

Present Inspection Methods

The present inspection methods regarding the 3 areas of concern are:

(1) Metallized coating thickness.

The coating is measured at one point by a dial indicator at the top of hook point rope groove. Any other like physical multipoint measurement would be cumbersome and prohibitively time consuming. A rapid and suitable (able to adjust to irregularly contoured surfaces) instrument or tool is mandatory.

(2) Cleanliness - Visual. Visual inspection has proven to be unsatisfactory.

(3) Adherence/Voids/Coating Separation.

This method employs the use of a high temperature torch. The flame is passed over the hard face fused coating, heating the surface to approx. 300-400°F. Any large area of non adherence, voids or coating separation from the base metal appears as a "hot spot" (red glowing area) and is cause for rejection. Extreme care must be taken with this inspection method as not to damage an acceptable coating with excessive heat. Another, more precise method than torch flame testing is desired at the present.

Type of NDT Equipment Desired

Prefer hand portable units with self contained power supplies.

PROBLEM #4

PROBLEM: Nondestructive Test Method for the Determination of Aircraft Arresting Hook Point, Metallized Hard Face Process Coating Thickness, Hard Face Coating Adherence, and Base Metal Surface Cleanliness Prior to Coating Process

PRESENTED BY: Robert J. Fegan

AFFILIATION: Naval Air Engineering Center, Code 912A1
Lakehurst, New Jersey 08733

PROBLEM COORDINATOR: Robert D. Wyckoff

AFFILIATION: Naval Air Rework Facility
NAVAIR Engineering Support Office, Code 341
NAS, Norfolk, Virginia 23511

BRIEF REVIEW OF THE PROBLEM: An adequate scientific method to determine plasma spray metallized hard face coating material thickness and adherence characteristics is unavailable at the present time. Specific areas of interest include:

1. base metal surface analysis for degree of cleanliness;

2. determination of coating material adherence;

3. metallized coating thickness uniformity and actual coating thickness measurements on irregularly contoured surfaces; and

4. detection of voids between base metal and material coating following plasma spray and fusion process.

CONTRIBUTING MEMBERS:

1. H. W. Bennett, Jr.
STEWS-TE-AE
WSMR, NM 88002

2. K. W. Fizer
NESO Code 341
NARF, NAS Norfolk, Va 23511

3. Gilberto Leos
Corpus Christi Army Depot (Attn: SDSCC-QLE)
NAS Corpus Christi, Tx 78419

PROBLEM #4
(Contd)

4. R. D. Santangelo
NARF Code 341
NAS Jacksonville, Fl 32216

5. H. G. Simpson
NESO Code 341
NARF, MCAS Cherry Point, NC 28533

6. M. H. Weinberg
CDR US Army ARRADCOM, Attn: DRDAR-QAR-1
Bldg. 62, Dover, NJ 07801

SOLUTIONS PROPOSED AND RECOMMENDED:

1. Base Metal Surface Cleanliness:

The following procedures were proposed to assure adequate cleanliness characteristics of the base metal substrate:

(a) Complete and uniform grinding or machining of the base metal surface.

(b) Vapor degreasing with baths that have been adequately checked to assure that hydrochloric acid has not been formed by combination of dissociated chlorinated hydrocarbons and water.

(c) Grit blasting using "dry air", oil free dry air, or nitrogen and employing grit such as Metcolite C which leaves little or no dust remaining. In addition, it was suggested that the grit for blasting be used in small quantities for ease of purging and replacement in the event of contamination.

(d) No subsequent vapor degreasing operation as this can only lead to detrimental effects during torch fusion and heat treatments.

(e) Employment of a surface electrical resistance technique to indicate the presence of any remaining surface contamination.

(f) Immediate plasma spraying after grit blasting and electrical resistance measurements.

2. Coating Material Adherence:

(a) Run flat plate coupons simultaneously with the hook point during spraying operations. Perform 90° bend test or plunge test, etc. on the coupons to determine the as-sprayed adhesion. Good adherence in the as-sprayed condition should help to guarantee good adherence following torch fusion and subsequent heat treatment.

(b) Perform adherence tests employing infared technology or thermal imaging testing to better identify areas of poor quality bond.

3. Metallized Coating Thickness and Thickness Uniformity:

The following techniques were proposed for determining coating thickness:

(a) Employ conventional eddy current devices with a suitably designed probe to measure thickness of the coating over the entire cable grove contour in a systematic pattern.

(b) Employ a three dimensional cordax measuring system picking up on a single reference point before and after applying the coating. The entire contour coating thickness could be easily determined with this method.

(c) Beta back scatter techniques employing equipment such as a Beta Scope TC-2000 for thickness determinations.

4. Detection of Voids Between Base Metal and Material Coating:

It was felt that if the above precautions and test methods were employed and correct plasma and flame spray procedures followed, little problem with voids or separation should be encountered. However, several methods were suggested for void detection.

(a) Eddy sonics using equipment such as Shurtronics Bond Tester if a probe of the correct size could be manufactured.

(b) Ultrasonics

(c) Acoustic emission signature analysis.

INSPECTION OF ROCKET PROPELLED TRACK TEST VEHICLES

J. D. Bush
6585th Test Group/TKEE
Holloman AFB, NM, 88330
Autovon 349-2689

ABSTRACT

Inspection of rocket propelled track test vehicles (sleds) at Holloman Air Force Base is a continued problem. Approximately 300 sleds of various types and sizes are maintained in the operational inventory. The sleds serve as propulsion or payload carriers for testing many different systems and components on the track. Typical of these systems are missile guidance systems, aircraft crew escape systems and aerodynamic decelerator systems. Most of the sleds are rigid frame or monocoque structures. Welded steel tubing and plates, welded aluminum plates and bonded honeycomb panels make up the majority of the structural elements. Many limited access areas, complex joints and inaccessible areas exist in the structures. Present inspection techniques (ie., dye penetrant, magnaflux, ultrasonics and x-ray) are inadequate. New or improved inspection methods are needed which will more adequately guarantee the integrity of sled structures.

BACKGROUND

The Test Track Division of the 6585th Test Group at Holloman AFB maintains an inventory of over 300 operational Track Test Vehicles. These specially designed vehicles, also known as "Sleds", vary in size from small monorail vehicles, which weigh less than 100 pounds each, to large dual rail vehicles, which weigh over 30,000 pounds each. Shape of the sleds varies from box type configurations, with very high aerodynamic drag characteristics, to sleek, low drag configurations which are aerodynamically tailored to operate in the supersonic and hypersonic speed regimes. Some sleds are designed to serve only as "Test Item" or "Payload" carriers. Others are designed to serve only as propulsion units to "Push" the payload carriers down the track. Still others are designed as independent vehicles and incorporate propulsion and payload on a single sled. The sleds are restrained to the track rails in the vertical and lateral directions by specially designed structural attachments called "Slippers". The sleds are propelled along the track rails by solid or liquid fuel rocket motors.

Problem No. 5

Several different structural concepts are used in design and construction of the sleds. The liquid fuel rocket sleds, for example, are made up of pressure vessels mounted to box type slipper beams. The pressure vessels are welded cylindrical tanks. The pressurized gas tanks are fabricated from steel; the fuel and oxidizer tanks are fabricated from aluminum. The steel tanks are designed for an operating pressure of 3000 PSI. The aluminum tanks are designed for an operating pressure of 700 PSI. The Slipper Beams are formed of welded steel plates and support the tanks on the track. The solid fuel rocket sleds are typically rigid space frame structures formed from welded steel tubular members. The frame structure is supported on the track by box type slipper beams which are formed of welded steel plates. Most of the payload carrier sleds are lightweight monocoque, semi-monocoque or honeycomb type structures, and are also supported on the track by box type slipper beams.

The Holloman sleds are utilized in support of various government agencies and private industry to conduct research, developmental and qualification tests on many different types of systems and components. The sled speed, acceleration, and other environmental factors can be closely controlled during a test mission. This makes the sled an ideal vehicle for simulating operational design parameters of many systems and components. Aircraft ejection seats, ICBM guidance systems, crew escape capsules, airfoils, parachutes, aerodynamic decelerators, nose cones, warheads and fuses are examples of systems which have been, or are being sled tested on the Holloman Track.

THE PROBLEM

The sleds, because of the wide variety of test applications, are required to operate under very severe performance and vibrational environments. Speeds up to 7000 feet per second have been achieved. Downtrack acceleration levels of over 30 g's are common for dual rail sleds. For monorail sleds acceleration levels of 100 g's are common. Lateral and vertical vibration levels, induced to the sled by the track rails and aerodynamic buffeting often exceed 25 g's. These operational conditions subject the active sleds to very severe steady state and dynamic loadings which fluctuate throughout a given track run. These loadings have caused structural damage in the form of cracks in welds, material delamination, rivet failures, bolt failures and bond separation. Sleds are designed for a life cycle of 100 runs. However, some of the sleds which were fabricated as early as 1958 have exceeded their design life.

The sleds also suffer damage from meteorological environmental factors. Approximately 20% of the sleds see active service during a typical one year period. The remaining sleds, because of limited availability of facilities, are kept in open storage areas. While in these "Parking" areas, the sleds are subject to moisture accumulation, wide variations in temperatures, blowing sand, high winds and other conditions which are conducive to corrosion and other types of material deterioration and damage.

Because of the severe operational and storage environments, sleds are inspected prior to each dynamic track test in an effort to verify their structural integrity. The inspection methods currently used are Dye Penetrant, Magnaflux, X-Ray and Ultrasonics. The large number of complex structural joints, areas of limited access and inaccessible areas makes reliable verification of structural integrity, by these methods, a continuing problem. An example of a major problem area is the internal baffle structure used in the fuel and oxidizer tanks of the liquid fuel rocket sleds. These aluminum baffle structures are welded in place as the tanks are assembled. The only access to the welds is through three line/tank flange fittings, each of which is approximately two inches in diameter. Inspection of the baffle welds through these small openings is very difficult and reliability of inspection results is low. A crack in certain areas of the baffle-weld, will not prevent the sled from operating. It can, however, decrease the usable thrust time of the engine and may precipitate a premature malfunction shutdown. Another example of a major problem area is the internal weld joints of the box type slipper beams. Access to these joints is at best, very limited and inspection is difficult. Several structural failures or near failures have resulted from undetected flaws in these areas.

SUMMARY

The current NDI methods used for inspection of rocket sleds have proved to be unsatisfactory in some cases. While the methods have been used successfully to detect most of the structural flaws and damaged areas have been repaired before failures occurred, some defects have gone undetected and catastrophic failures have occurred. Expensive hardware and test data have been lost because of these failures. A new or improved inspection technique, which will more reliably guarantee the quality of sled structures, is needed.

PROBLEM #5

PROBLEM: Inspection of Rocket Propelled Track Test Vehicles

PRESENTED BY: J. D. Busch

AFFILIATION: 585th Test Group/TKEE
Holloman AFB, NM

PROBLEM COORDINATOR: MSGT Ed Holland, USMC

AFFILIATION: COMFAIRWESTPAC Staff
Box 3
FPO Seattle, WA 98767
(NAF Atsugi, Japan)

BRIEF REVIEW OF PROBLEM:

Item A - Failure of Sled Slippers resulting in complete disintegration of Sled.

Item B - Cracks in Motor Baffles causing loss of power resulting in unsuccessful test.

Item C - Thrust fluctuation of Rocket Motor.

Item D - Inspection of Cluster Welds of tubes to plates.

SOLUTIONS PROPOSED:

Item A - (1) Determine load and stress area using strain gages.

(2) Magnetic suspension system on rails.

(3) Ultrasonic inspect from inside the weld attach point of slipper structure to ring.

(4) Change weld process from stick electrode to wire metal inert gas.

(5) Block off back of slipper carrier frame, fill with brine to act as heat sink.

(6) Inspect slipper using magnetic rubber.

PROBLEM #5 (Continued)

Item B - (1) Ultrasonic inspect baffle weld from outside.

(2) Check weld integrity using metallic/non-metallic bond/ debond tester.

(3) Cut access panels for direct contact inspection.

Item C - (1) Radiographic inspect motors and look for cracks, porosity or any other irregularities in solid fuel.

Item D - (1) Use water washable fluorescent penetrant.

(2) Magnetic particle inspect using probes.

(3) Magnetic particle inspect using wrap-around coil.

<u>RECOMMENDED SOLUTION</u>:

Item A - (1) Ultrasonic inspect from inside, the weld attach of slipper structure to ring. Allow no discontinuities.

(2) Block off back of slipper frame, fill with brine (needed) only for one-time high speed run).

(3) Change weld process from stick electrode to wire metal inert gas.

Item B - (1) Ultrasonic inspect baffle weld from outside.

Item C - (1) Radiographic solid fuel for cracks and porosities.

Item D - (1) Inspect with water washable fluorescent penetrant.

NONDESTRUCTIVE TEST OF SHROUDED, SHACKLE, HIGH SECURITY PADLOCK

Morris L. Budnick

Chief, Tentage & Organizational Equipment Branch (DRDNA-USO)
Shelters Engineering Division
Aero-Mechanical Engineering Laboratory
U.S. Army Natick Research and Development Command
Natick, MA 01760
Commercial: (617) 653-1000, Extensions: 2692/2517
Autovon: 955-2692/2517

ABSTRACT

The current forced entry test of the Shrouded Shackle, High Security Padlock, detailed in paragraph 4.4.11, Specification MIL-P-43607, is destructive, nonduplicative, and subjective. Also, the method and equipment used in the conduct of the test are not the types normally associated with effective and economical test techniques. The padlock conforms to the forced entry requirement if it is resistant to forced entry attempts for not less than seven minutes. Briefly, the test technician uses a combination of brute force, temperature, torque, and cutting devices to determine if the padlock conforms to the specification requirement. The fact that the test is nonduplicative and that the sequence and duration of applying the various elements of the test are discretionary with the test technician are major deficiencies. Another major consideration in the conduct of the test is that it is intended to duplicate the forced entry attempts which will be used to defeat the padlock. One approach being considered is to develop a fixture for holding a lock assembled to a hasp and to subject the assembly to impact and torque loads. How to evaluate nondestructively the capability of the lock to withstand the effects of temperature and various cutting tools is still unanswered.

Problem No. 6

NONDESTRUCTIVE FORCED ENTRY TEST OF SHROUDED SHACKLE, KEY OPERATED, HIGH SECURITY PADLOCK

Morris L. Budnick

Chief, Tentage & Organizational Equipment Branch (DRDNA-USO)
Shelters Engineering Division
Aero-Mechanical Engineering Laboratory
U.S. Army Natick Research and Development Command
Natick, MA 01760
Commercial: (617) 653-1000, Extensions: 2692/2517
Autovon: 955-2692/2517

The forced entry test of the Shrouded Shackle, Key Operated, High Security Padlock, paragraph 4.4.11, Specification MIL-P-43607 is a problem test for a number of reasons. Specifically, it is destructive and cost intensive, and cannot be duplicated for each test sample item. Another consideration which complicates is that the test is an attempt to duplicate what might be done to defeat the lock. Briefly stated, the test technician uses brute force, temperature, and cutting edges in the conduct of the test. It is recognized that none of these are normally associated with objective and effective test techniques. Another problem is that the test technician is free to determine what tools he uses, the order of the various test phases, and the duration of each phase.

The test is specified in paragraph 4.4.11, Specification MIL-D-43607D, dated 30 June 1976 and reads as follows:

"4.4.11 Forced entry test. Unless otherwise specified (see 6.2), this test shall be performed by the US Army Natick Research and Development Command, Natick, MA 01760. Any style hasp specified in MIL-H-43905 shall be secured to a solid upright member in a manner that will withstand the forces of this test. The padlock shall then be locked to the hasp. Any combination of the following tools, not exceeding 10 pounds and with restrictions noted, shall be used in an attempt to defeat the padlock:

a. Bolt-cutters shall be hand powered and shall not exceed 24-inches in length.

b. Saws and drills shall be other than power driven.

c. Heating equipment shall be limited to single tank torches.

d. Hammer weight shall not exceed 3 pounds.

e. Torquing levers shall not exceed 18 inches.

f. Chisels, jimmys, and wrecking bars not exceeding 18 inches.

Defeat of the padlock in less than the specified 7-minutes test time for the type II padlock shall constitute failure of this test."

Unquestionably, a review of the details of the forced entry test raises some question. Specifically, if one of the considerations of the test is to duplicate what will be done in an attempt to defeat the padlock, why the restrictions noted in paragraph 4.4.11? Any individual whose primary concern is to defeat the lock in the shortest possible time will use those tools he believes will defeat the padlock without consideration to size, weight, or power. The seven minute maximum time was selected as the maximum unobserved time which will be available between guard rounds. What effect does the condition of the tools have on the results of the test? What effect does the order of the various phases have on the results? How does the test technician divide up the test time of seven minutes? What constitutes failure? These are only a few of the questions which will develop from an in depth review of the test in paragraph 4.4.11 of the specification. The major concern is the development of a test which is nondestructive, less labor intensive, can be duplicated, and objective.

One approach being considered in the development of a nondestructive test is the use of a test fixture for both the impact and torque phases. The fixture would be designed to hold the padlock hasp assembly in the normal use configuration. The padlock would be subject to a number of impact and torque loads within a specified time in a mechanical press. The padlock fails the impact and torque phases if the shackle separates from the padlock or if there is any visible evidence of a crack in either the shackle or the padlock body.

Two approaches are being considered in an attempt to negate the need for the temperature and cutting edge phases. The first is to conduct a computed design analysis of the padlock and hasp configuration to determine if an assembly configuration can be attained which will not expose the areas of the shackle to the various cutting edges. The second is to develop materials which by themselves will withstand the effects of temperature and cutting edges. The need for the temperature and cutting edges phases could be eliminated through an inprocess inspection of the materials for the shackle and padlock body. It is possible that both the configuration and materials must be closely monitored to obtain the required quality. Some consideration is being given to combining the torque and impact tests with a minimum of selective destructive tests. The criteria to be used in selecting the destructive tests are: (1) the probabilities are high that the techniques will be used by individuals attempting to defeat the padlock, and (2) there is a fifty percent chance that the technique will result in failure.

To assure that the results from the above tests are objective, the specifics for each test would be detailed to the extent that each sample would be tested in an essentially identical manner.

It is recognized that this problem is not the type of problem normally considered under nondestructive test equipment and methods. However, it is presented with the expectation that some research is being done which could solve this problem.

PROBLEM #7

P OBLEM: Nondestructive Test of Shrouded, Shackle, High Security Padlock

PRESENTED BY: Morris L. Budnick

AFFILIATION: Chief, Tentage & Organization Equipment Branch (DRDNA-USO)
Shelters Engineering Division
Aero-Mechanical Engineering Laboratory
U.S. Army Natick Research and Development Command
Natick, MA 01760
Commercial: (617)653-1000, Ext. 2692/2517
Autovon: 955-2692/2517

PROBLEM COORDINATOR: Chief Petty Officer Wallace T. "Tabe" Levin

AFFILIATION: Commander, Fleet Air Med. Material Division for
Aircraft Maintenance NDI Coordinator
COMFAIRMED Box 2, Naples Italy
FPO New York, NY 09521
Autovon: 625-4633/34/35/36

BRIEF REVIEW OF PROBLEM: The current force .try test of the Shrouded Shackle, High Security Padlock, detailed in paragraph 4.4.11, Specification MIL-P-43607, is destructive, nonduplicative, and subjective. Also, the method and equipment used in the conduct of the test are not the types normally associated with effective and economical test techniques. The padlock conforms to the forced entry requirement if it is resistant to forced entry attempts for not less than seven minutes. Briefly, the test technician uses a combination of brute force, temperature, torque, and cutting devices to determine if the padlock conforms to the specification requirement. The fact that the test is nonduplicative and that the sequence and duration of applying the various elements of the test are discretionaly with the test technician are major deficiencies. Another major consideration is the conduct of the test is that it is intended to duplicate the forced entry attempts which will be used to defeat the padlock. One approach being considered is to develop a fixture for holding a lock assembled to a hasp and to subject the assembly to impact and torque loads. How to evaluate nondestructively the capability of the lock to withstand the effects of temperature and various cutting tools is still answered. Test requirements are ambigious with no set, calibratable test; therefore, none of the tests are repeatable.

SOLUTIONS PROPOSED: Change specification showing design of padlock, state body and shackle material-hardness. Require test procedures be performed with equipment that is calibrated to provide a consistant and reliable test assuring a consistant product quality.

PROBLEM #7 (Continued)

RECOMMENDED SOLUTIONS: Screen other Federal agencys for specifications that are currently in effect. If specification is in effect the desired product is, more than likely, already in production.

QUALIFICATION AND CERTIFICATION OF NDT PERSONNEL

Patrick C. McEleney
Army Materials and Mechanics Research Center
DRXMR-MI
Watertown, MA 02172
AUTOVON: 955-3444
Commerical: 617/923-3444

ABSTRACT

A review of the multiplicity of documents and practices in qualification and certification of NDT personnel is presented. Suggestions are advanced with the aim of elimination of duplication of coverage and to bring about a considerable reduction of the number of documents addressing this subject. Documents considered will include Government NDT personnel certification documents and those from the private sector and technical societies. Other areas requiring certification such as equipment and laboratories will be addressed.

The opinions and conclusions expressed in this paper are of the author and not necessarily of the Army.

Many of the documents and practices in qualification and certification of NDT personnel will be reviewed. Some suggestions are advanced with aim of elimination of duplication of coverage and to bring about a considerable reduction of the number of documents addressing this subject. Documents considered will include government NDT personnel certification documents and those from the private sector and technical societies. Other areas requiring certification such as equipment and laboratories are addressed.

First and foremost, in the review of NDT personnel certification documents is the Recommended Practice SNT-TC-1A. SNT-TC-1A provides a format that industry (employers) can follow in writing procedures for the qualification and certification of personnel which meets the needs and requirements unique to each segment of industry.

This document is referenced in the documents cited.

REFERENCE DOCUMENTS

MIL-STD-410D	ASNT SNT-TC-1A and Supplements
MIL-STD-00410C (MR)	DARCOM Regulation 702-22
MIL-STD-1263 (MR)	ASME Codes
MIL-STD-271 (Portions)	AWS B3.0-41
MIL-STD-453 (Portions)	NMAB 252, 337
MIL-I-8950 (Portions)	STP 624
MIL-R-11470 (Portions)	NAVSHIPS 250-1500-1
MIL-S-11356E (Appendix C)	MIL-I-6870D

Scope of SNT-TC-1A

1. Scope

1.1 It is recognized that the effectiveness of nondestructive applications depends upon the capabilities of the persons who are responsible for, and carry out, nondestructive testing (NDT). This Recommended Practice has been prepared to establish guidelines for the qualification and certification of nondestructive testing personnel whose specific jobs require appropriate knowledge of the technical principles underlying the nondestructive tests they perform, witness, monitor, or evaluate.

1.2 This document provides guidelines for the establishmnet of a qualification and certification program.

1.3 These guidelines have been developed by the American Society for Nondestructive Testing to aid employers in recognizing the essential factors to be considered in qualifying employees engaged in any of the test methods listed in Par. 3.

1.4 It is recognized that these guidelines may not be appropriate for certain applications. In developing his written practice as required by Par. 5, the employer shall review the detailed recommendations presented herein, and shall modify them as necessary to meet his particular needs.

1.2 This document provides guidelines for the establishment of a qualification and certification program. The employer establishes the program.

Note 1.4 Recommendation can be modified by employer to meet particular needs.

The first 1.2 would encourage a proliferation of qualification and certification documents. Each employer would have its own documentation.

1.4 Would give the employer the latitude to develop a written practice after reviewing recommendations of SNT-TC-1A to meet his particular needs and modify document recommendations as required.

A written practice (certification procedure) based on SNT-TC-1A with reasonable deviations should be the goal of an employer building a certification program.

As Robert A. Baker noted in his recent presentation at the National Fall Conference of Nondestructive Testing, SNT-TC-1A has one outstanding philosophy; Be reasonable and only one requirement - Prepare a written procedure.

In the foreword first paragraph we read:

FOREWORD

MIL-STD-410D specifies the qualification and certification requirements for nondestructive testing personnel performing eddy current, liquid penetrant, magnetic particle, radiographic and ultrasonic test methods.

The scope of MIL-STD-410D states:

1. Scope

1.1 This standard establishes the minimum requirements for the training, qualifying, examining and certifying of nondestructive inspection personnel for the inspection of materials and parts by the eddy current, liquid penetrant, magnetic particle, radiographic, and ultrasonic test methods.

Notice 1 to this STD - specifies 4.3.1 Recertification (non-Air Force Personnel) and 4.3.3 Recertification (Air Force Personnel only).

4.3 Recertification

4.3.1 Recertification (non-Air Force Personnel). Level I, Level I Special, and Level II personnel must be requalified and certified as specified in 3.9 at intervals not to exceed three years The certification records shall be revised to show proof of requalification and recertification.

4.3.2 Personnel may be re-examined and have their certification extended or revoked any time at the discretion of the employer.

4.3.3 Recertification (Air Force Personnel only). Level I, Level I Special and Level II personnel must be requalified and certified as specified in 3.9 at intervals not to exceed three years. In addition, at intervals, not to exceed one year, these personnel must successfully demonstrate that they meet Practical requirements given in 3.9.6 and either 3.10.1.3 or 3.10.2.3.

Certification is revokable at any time and cannot be granted to those personnel that fulfill the General and Specific requirements, but fail to meet the Practical requirements. Only upon the yearly successful completion of the Practical requirements can full certification be granted.

In 3, General Requirements, we see only mention of prime contractor, subcontractor and outside agency.

3. General Requirements

3.1 Written Requirements. Each prime contractor, subcontractor and outside agency performing the specified nondestructive testing inspections shall establish a written practice for the control and administration of NDT personnel training, qualification, examination and certification in accordance with the requirements of this standard.

3.1.1 Standard Compliance. The prime contractor shall be responsible for assuring the subcontractor and outside agency's personnel qualification and certification programs comply with this standard.

3.1.2 Qualification to Standard. Inspection personnel of the prime contractor. subcontractor and outside agency shall be trained, examined, qualified and certified in accordance with this standard before conducting the specified NDT inspection.

3.2 Qualification/Certification. The subcontractor or outside agency shall be responsible for maintaining and making available to the prime contractor a copy of the nondestructive inspection personnel qualification and certification program.

3.3 Qualification/Certification Approval. The prime contractor shall review and approve when necessary, the subcontractor or outside agency nondestructive inspection personnel qualification and certification program.

A proposed MIL-STD-410E in the foreword first two paragraphs we read:

FOREWORD

MIL-STD-410E specifies the minimum qualification and certification requirements for nondestructive testing personnel performing eddy current, liquid penetrant, magnetic particle, radiographic and ultrasonic test methods.

This revision incorporated requirements for application to maintenance and small contractors supplying replacement of parts, materials and components in addition to prime contractors supplying major systems.

The first paragraph is similar to 410D. The second paragraph refers to application in maintenance and small contractors supplying replacement of parts, material and components in addition to prime contractors supplying major systems.

This would appear to mean that these applications (maintenance and small contractors) are not accommodated under MIL-STD-410D or SNT-TC-1A, or on the other hand, that the latter documents (or at least MIL-STD-410D) is/are geared only to prime contractors.

In 3.2 of this document we read:

3.2 Qualification to Standard. All prime contractor, subcontractor, and/or outside agency personnel who can affect the accuracy of any NDT test shall be trained, examined, and certified in accordance with this standard before conducting their specified NDT duties.

The area of application must be clearly defined.

This document has many changes from 410D. We note a requirement of outside agencies used by the prime contractor or subcontractor to perform NDT services or to prepare and administer a qualification program in regard to specific experience.

3.4.2 Specific Experience. The outside agency personnel performing the NDT service or preparing and administering the qualification program must be knowledgeable of the procedures, codes, and specifications utilized by the contracting agency and/or the design engineers to assure that the program or inspection service conforms to applicable requirements. He must either have experience or become familiar with the engineering requirements in the specific industry for which he is performing the service. For example: aerospace, materials producer, ordnance, shipyards, pipeline or building construction, etc. Evidence of experience and/or familiarization program shall be documented and placed in the records (para 3.5)

Here evidence of experience and/or familiarization program in the specific industry for which the applicant is performing the service is required.

Proceeding, we review another significant document; DARCOM Regulation 702-22, dated 26 October 1976. This is being revised currently.

The purpose and scope are as follows:

1. Purpose. This regulation establishes the minimum requirements for training, examining, qualifying and certifying DARCOM personnel for competence at appropriate levels in Nondestructive Testing and Inspection (NDTI) methods applied for testing and inspection of an item or material. The following NDTI methods are included within the purview of this regulation: eddy current, liquid penetrant, magnetic particle, radiography and ultrasonics. DARCOM personnel who are responsible for the performance of any NDTI task contained in paragraph 4.a will be identifed and certified in accordance with this regulation. The requirements of this regulation may not be applied to procedures for the appointment, promotion, reassignment, or demotion of civilian employees.

2. Scope. This regulation applies to Headquarters DARCOM, DARCOM major subordinate commands and centers including their subordinate installations and activities; Project Managers (PM) reporting directly to DARCOM; central laboratories that have a procurement mission for DARCOM items; and depots involved in surveillance and reconditioning of DARCOM material.

The area of application is rather well defined. Further along we note in Appendix C.

2. Outside Agency

At the option of the installation/activity, an outside agency may be engaged to provide qualification training and examination services. The program developed will be reviewed by the administering activity prior to implementation. In such instances, the responsibiltiy for certification will still be retained by the installation/activity.

a. Where an outside agency is utilized to prepare and/or conduct the total qualification and certification program or specific portions thereof, the outside agency personnel so engaged will be Level III in the method of concern. These Level III personnel will be knowledgeable of the procedures, standards and specifications utilized by the contracting installation/activity to assure that the program conforms to specific installation/activity requirements. Their qualifications should be related to experience in the specific field for which they are preparing the program. For example: aerospace, nuclear, material producer, testing laboratory, etc. If they lack experience in the contracting installation/activity's field, the following rules apply:

(1) They will review all pertinent procedures, specifications and standards.

They will spend sufficient time at the contracting agency's nondestructive test facility to familiarize themselves with pertinent products test techniques, facilities, equipment and training programs.

Here again, specific examinations are required. This is employer's responsibility. If we take over this requirement, we should also be responsible for certification of the personnel.

One final group of documents will be briefly considered. "The Canadian vernment Specification Board" documents such as 48-GP-4M Radiographic 48-GP-7M Ultrasonic and 48-GP-8M Magnetic Particle.

Unlike other documents, they have a Central Certifying Agency, the Dept. of Energy, Mines and Resources is the neutral Certifying Agency responsible for the organization and conduct of the Certification Program. They also provide for examination by the employer in the specific application for which an individual is employed.

Earlier documents had certification in many special categories - Light Alloy Castings + Forgings Welds + Weldments Heavy Metal Castings + Forgings Aircraft Structures - however, this was not found workable - it would spawn a plethora of additions to the standard and cause it to become unwieldly and difficult to control. The responsibilities for the examination and certification of these items was not possible because of the additional staffing demands it would make. All special categories were deleted except for aircraft structure. Employers have the responsibility for the qualifying of personnel on specific products and procedures.

Currently, they are implementing Canadian Forces Specification D-12-020-001/SI such that all NDT within the scope of the specification shall be subject of surveillance. This means they can enter and assess NDT facilities, techniques and personnel at any time, thereby assessing product person and technique satisfaction.

Summarying - the area of applicability of the document should be specified so that it can be readily understood. In these documents it is the responsibility of the employer to apply whatever specific examination requirements he deems necessary before the employer certifies the individual. Where military or DoD personnel are being certified, the government is the employer and separate consideration from that imposed on prime contractors, subcontractors and outside agencies is required.

Definitions

The next area I would like to discuss is definition of terms. In looking over a few documents I compiled the following list:

DARCOM Reg 702-22	MIL-STD-410D
Level I	Qualification
Level II	Qualified
Level III	Certification
Administering Activity	Certifier
Administering Liaison	Certifying Agency
Certification	Prime Contractor
Certifier	Subcontractor
Certifying Agency	Outside Agency

DARCOM Reg 702-22

Experience
NDT Examiner
Outside Agency
Qualification
Reviewing Activity

MIL-STD-410D

NDT Examiner
Contracting Agency
Experience
Employer

Draft MIL-STD-310E

Qualification
Qualified
Certification
Certifier
Certifying Agency
Prime Contractor
Subcontractor
Outside Agency
NDT Instructor/Examiner
Contracting Agency
Experience
On-the-Job Training
Employer

SNT-TC-1A

Qualification
Certification
Certifying Agency
Recommended Practice
Employer
Training

DEFINITION OF "CERTIFICATION"

MIL-STD-410D

Certification means written testimony of qualification.

Draft MIL-STD-410E

Certification. Written testimony of qualification by the employer.

ASNT SNT-TC-1A

Certification. Written testimony of qualification.

DARCOM REG 702-22

Certification. Written testimony of training and qualification.

We note similarities in all definitions but some changes made in #2 and #4.

Reviewing the October 1979 revision of SNT-TC-1A Part E in Section 6.4 we read certification means holding a certificate. In 6.2, certified here means applicant has met the guidelines of SNT-TC-1A paragraph 8.5.3(a) General Examination and 8.5.3(c) Practical Examination - no mention of 8.5.3(b) Specific Examination - yet the applicant is certified.

6. Certification

6.1 The ASNT Level III Certification is a certification that the records of an individual indicate attainment of the qualifications required to satisfy the provisions of paragraphs 3 and 4 of this document; that the individual has successfully passed the Basic and one or more Methods examinations in accordance with paragraph 5; that the individual agrees to abide by the Code of Ethics for Level III Nondestructive Testing Personnel Certified by ASNT.

6.2 Individuals certified to Level III in any NDT method by ASNT are considered to have met the guidelines of SNT-TC-1A, paragraphs 8.5.3(a) (General Examination) and 8.5.3(c) (Practical Examination), June 1975 edition.

6.3 Individuals eligible for Certification as Level III by ASNT will be notified of eligibility by ASNT. Such notification shall be considered as evidence that an individual has met the requirements for eligibility to take ASNT examinations and has successfully passed the examinations indicated on the notification.

6.4 Individuals eligible for Certification will be Certified by ASNT as NDT Level III upon written request for a Certificate and payment of the appropriate fee as required in paragraph 7.4. Only holders of such Certificates may use the term, "Certified by ASNT," or otherwise infer such Certification by ASNT.

In ASTM STP 624 in F. C. Berry's article on SNT-TC-1A he quotes an article by former President of ASNT C. E. Lautzenheiser and published in the May 1976 issue of Material Evaluation.

Certification in accordance with the guidelines of SNT-TC-1A indicates that an employer has made a review of the individual's qualifications and has accepted the responsibility for the Level III activity of the person within the employer's organization. It is very important to note that the word "Certification" indicates a record of achievement and/or qualification, in one case, and an acceptance of responsibility by management in the other case. Also, even though an employer uses ASNT services he can and probably will apply a specific examination requirement to insure that the Level III person is technically competent in the employer's specific requirements. The major criticisms that have been leveled against SNT-TC-1A are that the requirements for a Level III individual are not definitive and that the individual can be certified without examination.

Efforts were made to clarify the situation in ASNT. In a letter from the chairman of the Technical Council E. Pade to the Secreatry of ASNT Aman we read where these efforts were frustrated by action of the Board of ASNT.

4. The Board would not consider revising the PTCC description substituting the term "ASNT Examinations" for "ASNT Certification" and "ASNT Revalidation" for "ASNT Certification." It is my personal feeling that present literature is misleading in that it at least implies that ASNT is in the certification business.

This term can thereby have two definitions in the same document.

Another key term is "qualification" and it too is defined in a variety of ways in each document reviewed.

DEFINITION OF "QUALIFICATION"

MIL-STD-410D

Qualification means compliance with the requirements of this standard. The ability of personnel to meet the minimum requirements for a specific level of capability.

DRAFT MIL-STD-410E

Qualification. The ability to comply with the requirements of this standard.

ASNT SNT-TC-1A

Qualification. Skill, training, and experience required for personnel to properly perform the duties of a specific job.

DARCOM REG 702-22

Qualification. The ability of personnel to meet the requirements for a specific level of capability in compliance with the requirements of this regulation.

MIL-STD-00453 (UASF)

Qualification. The ability of personnel to meet the minimum requirements for a specified level of capability.

One other item we might note. Level III will mean different things to differert employers. One cannot reasonably expect it to be otherwise. However, if we take a look at ASNT-TC-1A, Part E revision, October 1979, we see in 1.3 and the asterisked section at the end that an NDT Level III has to perform functions that include several of the listed capabilities and responsibilities.

1. Introduction

1.1 Each applicant for Certification by ASNT as NDT Level III must meet all requirements as set forth herein.

1.2 It is the applicant's responsibility to properly fill out and process to conclusion all documentation required to support claims and statements appearing on the application form.

1.3 Certification of NDT personnel by ASNT applies to individuals who perform functions that include several of the following capabilities and responsibilities.

"An NDT Level III individual shall be capable of, and responsible for, establishing techniques; interpreting codes, standards and specifications; and designating the particular test method and technique to be used. He shall be responsible for the complete NDT operation he is qualified for and assigned to, and shall be capable of evaluating results in terms of existing codes, standards and specifications. He shall have sufficient practical background in applicable materials, fabrication, and/or product technology to establish techniques and to assist the design engineer in establishing acceptance criteria where none are otherwise available. It is desirable that he have general familiarity with other commonly used NDT methods. He shall be responsible for the training and examination of NDT Level I and Level II personnel for certification."

This might indicate that Level III can mean different qualifications within a single employer. Certainly different levels of competency are indicated.

It seems in these days when terms such as inspection, testing and examination have been given very precise meanings in legal actions that less attention can be given in defining terms in this area. Is there really a need for this situation? It is difficult to come to solutions to problems when agreement cannot be reached in terminology.

One final point, certification of personnel is a significant item in upgrading nondestructive evaluation of materials. The effectiveness of nondestructive applications depends upon the capabilities of the persons who are responsible for, and carry out, nondestructive testing. Other actions are required before a meaningful personnel certification program can be implemented.

First, qualification of equipment is needed. I have witnessed instances where the personnel would probably pass any Level III examinations, yet a quick survey of the equipment indicated problems. The response from different systems was quite variable. As control documents were not specified, and most personnel were only involved with one system, this condition was not remedied. No assurance could be advanced that any unit met the minimum requirements other than the equipment appeared to be working satsifactorily. Minimum requirements of the equipment must be determined and equipment should be standardized or controlled.

A second area that should be qualified is the nondestructive testing agency. An ASTM document is available, E543, for determining the qualification of nondestructive testing agencies. This recommended practice establishes minimum requirements for agencies performing nondestructive testing.

Qualification of personnel, qualification of equipment, qualification of the organization doing the inspection or testing do not guarantee a 100% solution to the problem of upgrading of nondestructive evaluation of materials. However, they do guarantee a significant advance in that direction.

The qualified personnel must be working in a qualified nondestructive testing agency; this includes independent, public or in-house agencies. The qualified agency's responsibilities and duties are detailed in ASTM E-543, "Recommended Practice for Determining the Qualification of Nondestructive Testing Agencies."

4. Responsibilities and Duties

4.1 A nondestructive inspection and testing agency's capabilities should include, but not be limited to, one or more of the following test methods: magnetic particle, penetrant, radiographic/fluoroscopic, ultrasonic, eddy current, and leak testing.

4.2 It is the responsibility of the agency to ensure that:

4.2.1 It performs only inspection or tests for which it is adequately equipped and staffed.

4.2.2 Its employees perform only inspection and tests for which they are adequately qualified.

4.2.3 Its equipment is calibrated and personnel are certified in accordance with applicable specifications.

4.2.4 All equipment is properly maintained.

4.2.5 It informs the authority of any discrepancy by such factors as surface finish, form, shape, or procedure.

4.3 The following duties are those usually performed by the agency:

4.3.1 To perform all testing and inspection operations in accordance with specified standards or quality control criteria or both. (The necessary documents shall be furnished by the authority, the agency, or both, as specified in the applicable purchase agreements.) The agency should call to the attention of the authority at once any irregularity or deficiency noted in the documents.

4.3.2 To submit promptly to the authority formal reports of all tests and inspections that indicate compliance or noncompliance of the material with 4.3.1. The agency should be prepared to substantiate test results when required.

4.4 The agency may, in accordance with an agreement with the authority, report only compliance or noncompliance with the applicable specifications or control documents. The authority reserves the right for disposition of noncomplying material.

4.5 The authority may, at its discretion, inspect the procedures, equipment, and personnel program of the agency.

Each agency should have a written procedure manual. This is detailed in Seciton 11 of ASTM E-543.

LABORATORY PROCEDURE MANUAL

11. Minimum Requirements

11.1 Each agency shall have prepared a written Laboratory Procedures Manual for the type of work for which the agency is contracted. The manual shall contain, as a minimum requirement, sections in accordance with 11.2 through 11.6. The sections shall be of sufficient detail to provide complete guidance for their use by the agency's personnel.

11.2 Process Control (Operations Procedures) - This section shall contain the information necessary to control the various activities necessary for the testing of materials. Items covered shall include receiving and preparing test material, identification and marking, inspection procedures and specifications to use, reports, and return of test material.

11.3 Personnel Qualification - The requirements, procedures for training, certification, and recertification for each level of qualification, and the maintenance of personnel records shall be covered in this section. As required by Section 5 of this recommended practice, SNT-TC-1A shall be used as the basis for the development of 11.3.

11.4 Equipment Maintenance and Calibration - This section shall contain all of the following:

11.4.1 Inventory Listing - All available equipment shall be listed with the following information noted:

11.4.1.1 Name of the manufacturer.

11.4.1.2 Equipment model and serial number.

11.4.1.3 Characteristics subject to calibration.

11.4.1.4 Range of operation and range of calibration.

11.4.1.5 Reference to recognized standardization procedures acceptable to the authority, if applicable.

11.4.1.6 Frequency of calibration.

11.4.1.7 Allowable tolerances or maximum sensitivity.

11.4.1.8 Source of verification.

11.4.2 Calibration - Each instrument or machine, when calibration is required, shall have either a calibration sticker affixed, or record of certification on file, containing the following:

11.4.2.1 Instrument calibrated.

11.4.2.2 Serial No.

11.4.2.3 Calibration date.

11.4.2.4 Calibration next due.

11.4.2.5 Name of individual who performed last calibration.

If calibration is not required, a sticker stating no calibration is necessary shall be affixed, or a record shall be on file to this effect.

11.4.3 The equipment shall be calibrated against currently certified standards calibrated by accepted government or industrial agencies (or shall indicate that it is calibrated as used, or that no calibration is necessary) at least at the following specific intervals in accordance with a written procedure which shall also specify who is to calibrate each equipment type:

11.4.3.1 Magnetic Particle

a. Timer and Ammeter - Check every 90 days, unless subjected to electrical repair or inadvertently damaged, at which time calibration is required prior to use.

b. Black Lights - Maintain a minimum level of intensity, as specified by the agency.

c. Suspension Concentration Test - Check prior to use or daily, whichever is less restrictive.

11.4.3.2 Penetrant

a. Penetrants and Emulsifiers - Check monthly for contamination.

b. Dryers - Check monthly for thermostat accuracy.

c. Black Lights - Maintain a minimum level of intensity, as specified by the agency.

11.4.3.3 Radiographic - Calibrate densitometers prior to each use, utilizing calibrated film strips.

11.4.3.4 Ultrasonic - The authority shall approve the required calibration intervals.

11.4.3.5 Written records of the results of the checks and calibrations are to be maintained at a central location. The above checks are minimum and do not relieve the responsibility of constantly checking and immediately repairing any item which may affect test results. A history of the repairs, modification, or substitutions shall be maintained.

11.5 Equipment Operation and Technique File

11.5.1 Each type of equipment in use shall have a complete manual which contains all information necessary to operate and maintain the equipment in accordance with applicable codes and specifications. The manual shall include the maintenance procedures and schedules for each type of equipment and the calibration schedule of each type of equipment.

11.5.2 A technique file should be maintained for each type of equipment. It should be available for the guidance of the technician. The manual shall include:

11.5.2.1 Summary of inspection procedure.

11.5.2.2 Step-by-step preparation of material for inspection.

11.5.2.3 Defect calibration standard, if applicable.

11.5.2.4 Control of essential variables, such as the time required for each test step (if applicable).

11.5.2.5 What indications should appear at each step.

11.5.2.6 Test indications and their evaluations.

11.5.2.7 Recording of test results.

11.6 Records and Documentation

11.6.1 Records - All applicable records pertaining to 11.2 through 11.5 shall be maintained in a central file and in other accessible files as necessary, and should be available for examination by the authority.

11.6.2 The internal process forms or job record forms shall be filed with the written report to the authority and become a part of the permanent record. They should include the following minimum information:

11.6.2.1 Order and reference numbers.

11.6.2.2 Specification.

11.6.2.3 Type of inspection or test and procedure identification.

11.6.2.4 Serial or part numbers, alloy numbers, heat and lot numbers, as applicable.

11.6.2.5 Special instructions from the customer.

11.6.2.6 Customer's (authority's) name.

11.6.2.7 Results of the examination.

11.6.3 All applicable internal reports should be signed by the technician performing the work and by Level II or Level III personnel. A procedure for auditing of reports by Level III personnel must be included.

11.6.4 Personnel qualification records should be developed in accordance with 5.2 and be available in an active file as long as employment continues. When personnel leave the agency, the records may be transferred to an inactive file but should not be discarded for a period of 5 years or as otherwise specified.

11.6.5 Specification File - The company should maintain an orderly file containing all codes, specifications, and amendments under which it is performing work. The company does not have to possess codes and specifications for which it has no use.

Each of the areas covered in this manual represents minimum requirements and each area is essential and must be considered to have a meaningful personnel certification program. I could speak at length supporting this part of the program, but because of time limitations, will only suggest these vital elements. These areas are intimately related and cannot stand alone to improve the reliability of DoD nondestructive evaluation of materials.

Much time and energy have been spent in developing the documents we have reviewed in this presentation. With the experience gained in these efforts, more meaningful specifications and standards can be developed in personnel certification and related areas for DoD use in upgrading the quality and reliability of NDT materials.

UNDERWATER NONDESTRUCTIVE EXAMINATION OF SHIP HULLS

John Mittleman
Naval Coastal Systems Center
Code 715
Panama City, FL 32407
904-234-4388, Autovon 436-4388

ABSTRACT

Developments in underwater nondestructive examination (NDE) have grown, in the past fiscal year, to include stereophotography, magnetic particle inspection, ultrasonic thickness gauging and flaw detection. Research and development in these areas, conducted at NCSC under NAVSEA sponsorship, has led to systems which are substantially independent of the diver's skill and experience. This paper concentrates on actual field examinations of U.S. Navy ships which have been conducted within the past year.

INTRODUCTION

At the 27th DoD Conference on Nondestructive Testing the author of this paper presented a paper on Underwater Ultrasonic Inspections. This paper dealt largely with the prototype equipment and techniques that had been developed at the Naval Coastal Systems Center (NCSC) during FY 78, but was centered around the philosophic idea that even the best of underwater inspectors will be unable to perform as well as he could in a shirt-sleeve atmosphere. This, compounded by the fact that most Navy divers are not highly skilled in NDT makes it imperative that R&D minimize the diver's effect on test results.

Hardware which conforms to this philosophy has been developed at NCSC and permits underwater stereophotographic, ultrasonic and magnetic particle inspections to be performed by a team composed of Navy divers and trained NDT technicians. Test results are, to varying extents, independent of the diver's skill, motivation and environmentally produced problems. Both stereophotography and ultrasonic thickness gauging are virtually unaffected by these factors, while ultrasonic flaw detection and magnetic particle inspections currently require some cooperation from a diver who has had some training.

Stereophotography, magnetic particle inspection and ultrasonic thickness gauging were used on 12 ships during FY 79, using divers with absolutely no prior training in most cases. In the case of thickness gauging, close cooperation with PERA CSS has led to procedures designed to produce data compatible with existing Thin Hull Survey requirements. In all cases, the results of these underwater inspections have been delivered in a form useful to managers, engineers, and planners. Because the hardware systems have been designed to produce hard copy results for topside personnel, the normally low level of confidence that managers, engineers, and planners tend to have in results obtained by divers has been raised substantially. These white collar personnel, armed with data in which they can believe, can avoid costs by planning overhaul work in advance or by avoiding some dry dockings altogether. The possibilities are numerous, but the fundamental issue remains unchanged: with accurate and timely information money can be saved.

In the following sections, each technique that has been used in the field will be described, and examples of the results will be presented.

STEREOPHOTOGRAPHY

Principles

Stereophotography, a means of producing three dimensional photographic images, requires that two photographs of the same object be taken from somewhat different camera positions. If elevation measurements are to be made, it is preferable that the camera positions be carefully controlled and that such things as lighting and object distance be held constant. Once all this is done we have color, three-dimensional documentation to turn over to the decision makers and engineers, and they may be looking for answers to questions like:

- o how deep are the corrosion pits?
- o how bad is the barnacle growth?
- o is the paint peeling? (how many of the layers?)
- o is that "crack" the diver saw really a crack!?
- o when this ship is docked, do we have to sandblast to bare metal? or will sweep blasting or water jets do it?
- o did the divers do a good job on this underwater repair?
- o did the hull cleaning contractors damage the paint?
- o are all those mussels and oysters on the rudder the kind that are good to eat?
- o do the zincs need replacing? . . . et cetera.

How nice it would be to give any diver in the Navy a camera, push him overboard, and have a roll of high quality prints come back. But (with notable exceptions) most divers take pictures that are out of focus or poorly lit (in clear water) or all of the above plus worthless due to backscatter (in the low-to-zero visibility that we have in almost every Navy harbor). With one exception, the stage is now set for a description of the Stereo Camera Assembly developed at NCSC to overcome these difficulties (posed by the men and environments we work with), and to produce those high quality photographs that the engineers and decision-makers lust after. The exception, a common theme throughout this paper, is that anything used underwater will be flooded, lost or taken home (if it's shiny), or broken, if possible. Thus, that which is used by divers should be relatively indestructible and certainly inexpensive.

Technically speaking, the first obstacle to overcome is lack of visibility, the second, lack of skill in photography, and the third, the axiomatic impossibility of making anything sailor-proof. We did our best despite these overwhelming odds, and it all springs from a solution to the first problem. Lack of visibility usually means that in Navy harbors, with a good light, the diver can see at least 6 inches. Enough, at any rate to find areas of the hull that require documentation. Now, reviewing the list of questions which the recipients of this underwater photography might pose, we see that the important ways in which a ship's hull deteriorates are small scale phenomena (generally less than a few inches across). Therefore, a clear plastic box, filled with clear water and placed in between the ship's hull and the camera would solve the visibility problem without sacrificing engineering information since even a small field of view is adequate. And now the icing: with such an arrangement (Figure 1) the camera (fitted with a close-up attachment) is always the same distance from the hull. Therefore the focus, shutter speed, aperture and strobe output will always be the same. Why not engrave them on the side of the clear water box? In solving the visibility problem, the occurrence of poorly lit and out-of-focus pictures drops dramatically, and the diver's responsibilities are reduced to slapping the assembly up against the hull and clicking the shutter. In fact, a properly designed apparatus leaves no room for the diver's fingers to accidently hit any of the preset knobs. Finally, to obtain stereo pairs, the camera is set on the tray which can be moved from a left position to a right position behind the clear water box. Theoretically all stereo pairs taken with this apparatus should have the same camera spacing and object distances, so that one elevation calibration should do for all the pairs. In practice the clear water box may move a little between exposures and ruin this calibration, but if a small object of known dimensions is included in each pair, elevations are easily calibrated, and are measurable to within about 1/50 of an inch.

Practice

In early 1979 NCSC, in cooperation with the Charleston Naval Shipyard (CNSY) divers, performed a photographic survey of a submarine hull. This survey was requested by the Submarine Type Desk Repair Officer, and was a test to see if there was any value in performing such an inspection prior to a scheduled dry docking. Approximately 10 rolls of film were shot, mostly as stereo pairs. The location of each exposure was determined beforehand, and in such a way as to generate a reasonably unbiased impression of the hull's condition, although extra photos were taken in areas where serious damage was found. To position the diver, lines were passed around the hull at predetermined frames, and these lines were marked at 10-foot intervals. The diver exposed a stereo pair at each marker on the line and at places in between where noteworthy conditions existed; a frame-by-frame log was kept so that the developed pictures could be identified.

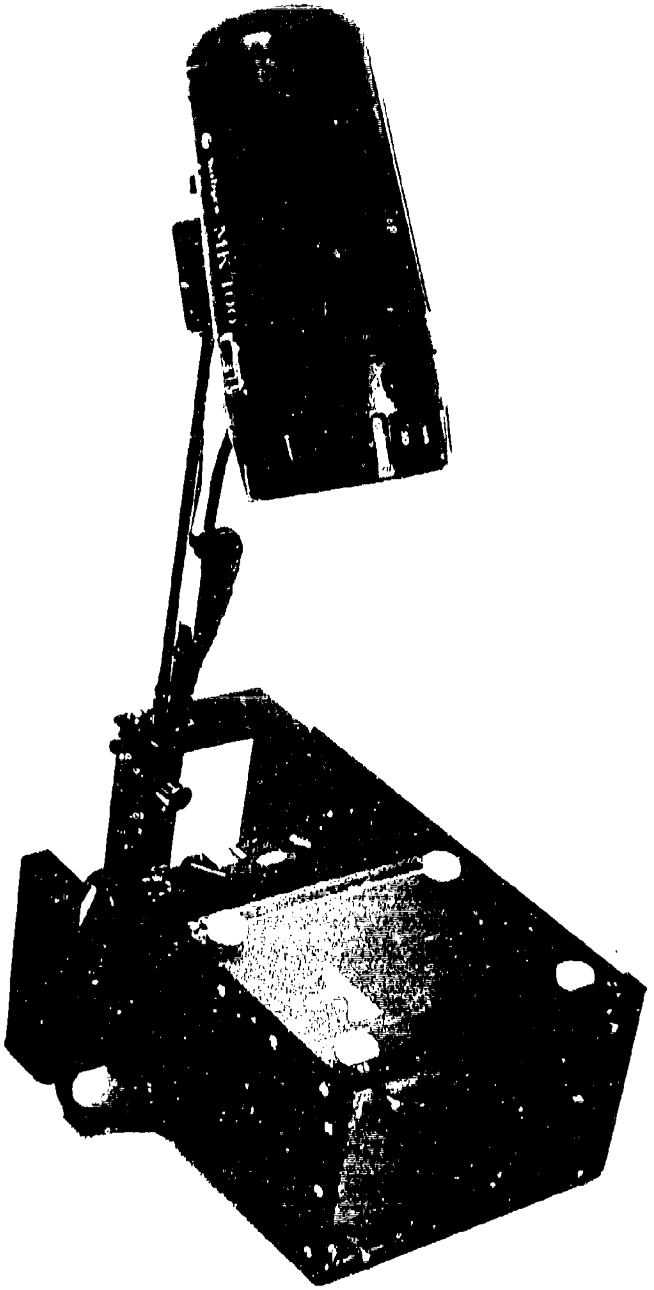

FIGURE 1. STEREOPHOTOGRAPHIC ASSEMBLY

After the survey was completed and an informal briefing given to the Type Desk, the prints were received and the process of mounting them as stereo pairs was begun. At this point a number of shipyard planners and engineers started showing up at the diving locker to see the pictures. Not only were they surprised to see such clear photography come from the muddy Cooper River, but also they spontaneously started planning on the basis of the photography. Areas requiring sandblasting to bare metal were identified, as were those where a sweep blast or water jet blast would be sufficient. In one general area of the hull severe pitting was found and documented in three dimensions by the photography. The engineers were able to assess the damage and decide which pits would require clad welding and which would not. In all, the information was found to be comparable to that which would normally be produced by a surveyor once the ship was in dry dock; had this ship not been scheduled for dry docking anyway, the photos (and not the diver's say-so) would have clearly supported the (somewhat costly) decision to dry dock the ship for repairs.

Stereophotography has also been applied to two ships which had cracks below the waterline. In one case, the cracking was in the vicinity of the weld joining the bilge keel to the hull of a guided missile cruiser. Although this inspection relied primarily on magnetic particles (to determine the true extent of cracking), stereophotography and a photo mosaic of the crack were used to document conditions before and after the underwater repair was made. This photography provided the ship with records that there was indeed a problem requiring immediate attention (and a commitment of funds), and that the repair made by CNSY divers was done well. In fact, this ship was scheduled to make a voyage to the Mediterranean just days after the repair, and a dry docking would have severely affected the ships operating schedule. Even if this had not been the case, the cost differential between a few days of diving services and a dry docking is tremendous. But without credible underwater inspection the more expensive route would have to have been chosen.

The second case in which a cracked hull was documented took place in San Diego, in the spring of 1979. The destroyer involved was about 35 years old, and had developed an athwartship crack in the hull plating between the flat keel and the bilge keel, about amidships. This crack had already been "fixed" by repairs made inside the hull. These repair procedures included three arresting holes, gouging and filling the crack and welding in a doubler plate over the cracked area. A thorough underwater inspection was requested by SUPSHIPS who had reason to believe that the repairs were inadequate. NCSC, supported by divers from the USS PRAIRIE (a destroyer tender), responded with stereophotography, magnetic particle inspection and ultrasonic inspection. Of these techniques, the photography produced the most substantial evidence that indeed, the repair was not adequate. Clearly visible on a photo mosiac of the "repaired" crack are

- the arresting holes, none of which intercept the crack ends
- numerous unarrested branches of the crack
- lack of filler weld penetration over all but a very small percentage of the length of the crack.

Additionally, ultrasonic inspection showed extensive laminations in the hull plate and several other critically thin areas of plate in the vicinity of the crack. SUPSHIP's feelings that the repair was inadequate were documented, and on the basis of this inspection, the ship was taken out of service a few months before it was scheduled for decommissioning. Note that if credible inspection results had not been available, the obvious political pressure to keep the ship active may have prevailed, and (in light of the inspection results) the risk of a serious mishap would have been quite high.

Stereophotography has also been used as an adjunct to ultrasonic Thin Hull Surveys on several occasions, both to document the condition of the hull's paint system and to supplement the ultrasonic readings at locations where external pitting was significant.

Stereophotography has been made feasible by the development of a simple clear water box. With the hardware developed at NCSC it is possible for any Navy diver to consistently produce high quality photographs of underwater hull conditions. Already, on the basis of such photography, important maintenance and repair decisions have been made, and at the same time, the value of underwater inspections has been more fully appreciated by managers, engineers, and planners. Stereophotography was, for the underwater inspection R&D at NCSC somewhat of a springboard; for some reason, everyone from admirals to seamen seem to think 3-D pictures are great, and this generated support for other NDE investigations.

ULTRASONICS

Principles

Underwater ultrasonics should, in principle, be extremely easy to do since immersion techniques are used routinely around the world. Steel in a marine environment is, however, substantially different from steel on the receiving docks. Ultrasonically, the former steel presents an inhospitable entry surface except at the tops of small bumps and the bottoms of small pits. These problems, as well as the general philosophy behind our approach to underwater ultrasonics were discussed at the 27th DoD Conference on NDT and will be summarized (rather than detailed) in this paper.

Basically, the problems all boil down to the impossibility of trying to replace a trained UT specialist with a relatively untrained diver who is usually working in low visibility, encumbered by thick gloves, and floating freely, at the mercy of currents and non-neutral buoyancy.

This diver does, on the other hand, have totally unrestricted access to the hull, and if it were possible to take a good reading quickly (almost on-the-fly), and without worrying about gain settings etc., then the fact of unrestricted access would really pay off. The diver's counterpart aboard ship would have to pump the bilges, gas-free the tanks, and crawl into some really tight places to get the same readings.

The advent of powerful computers that fit into a suitcase made this whole problem tractable. With a computer assisted system, taking a thousand readings (rather than one manual reading) is no problem. Odds are very much in favor of catching numerous good (ultrasonically coupled) readings under such conditions, and the diver's job is reduced to simply rubbing a transducer around rather indiscriminately for a few seconds while the computer does the work. Of course there's more to it than that; while the diver needs no special UT background, the man sitting at the topside end of the transducer cable must control the ultrasonic machine and type "bookkeeping" information into the computer as well. At least, however, he is working in a shirt-sleeve atmosphere. This approach effectively separates the functions of transducer manipulation from data acquisition, reduction and interpretation, and by storing raw and reduced information on magnetic tape, this approach provides hard copy records that can be scrutinized later by engineers responsible for judging the ship's structural integrity. The computer's role in underwater ultrasonic thickness gauging is diagrammed in Figure 2 which is a flow chart of the most recent version of our software. In discussing this flow chart reference will be made to Figures 3 and 4 which are, respectively, the raw data acquired by the computer, and a frequency distribution plotted from those thicknesses. The flow chart starts with a few questions to the operator, one of which asks if he needs instructions; this instruction set (which is retrieved from magnetic tape) is intended to refresh the memory of an operator who has been trained but has not run the program in a while. Specifically, it covers how to plug the computer, the analog-to-digital (A-D) converter and the ultrasonic machines together, how to calibrate the A-D converter and how to respond to questions the computer might ask during the course of operations. Bookkeeping information is requested at this time, to identify the magnetic tape, the ship, etc.

Calibration follows the input of the basic situation information. Since calibrating the entire system (the ultrasonic machine, A-D converter and computer, together) proceeds along virtually the same lines as thickness measurements (once the calibration is complete) we will describe the various computer subroutines at this point instead of later. But before describing the subroutines, a very detailed description of the diver's part in calibration: he holds a step block in one hand and rubs the transducer up and down the back of the step block (the smooth side) until 1000 readings have been acquired (about 7 seconds). Meanwhile, the computer branches to:

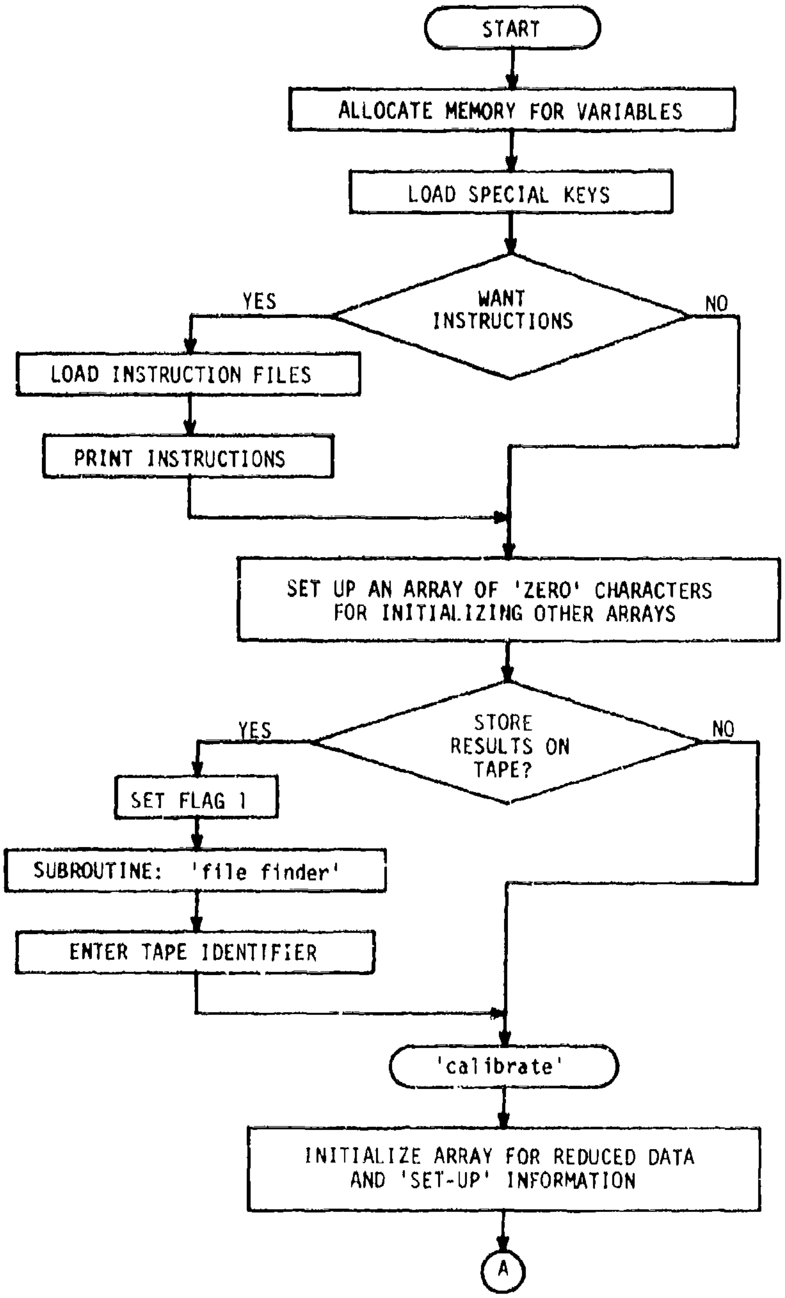

FIGURE 2. FLOW CHART OF A COMPUTER PROGRAM TO ASSIST IN THICKNESS GAUGING
(Sheet 1 of 5)

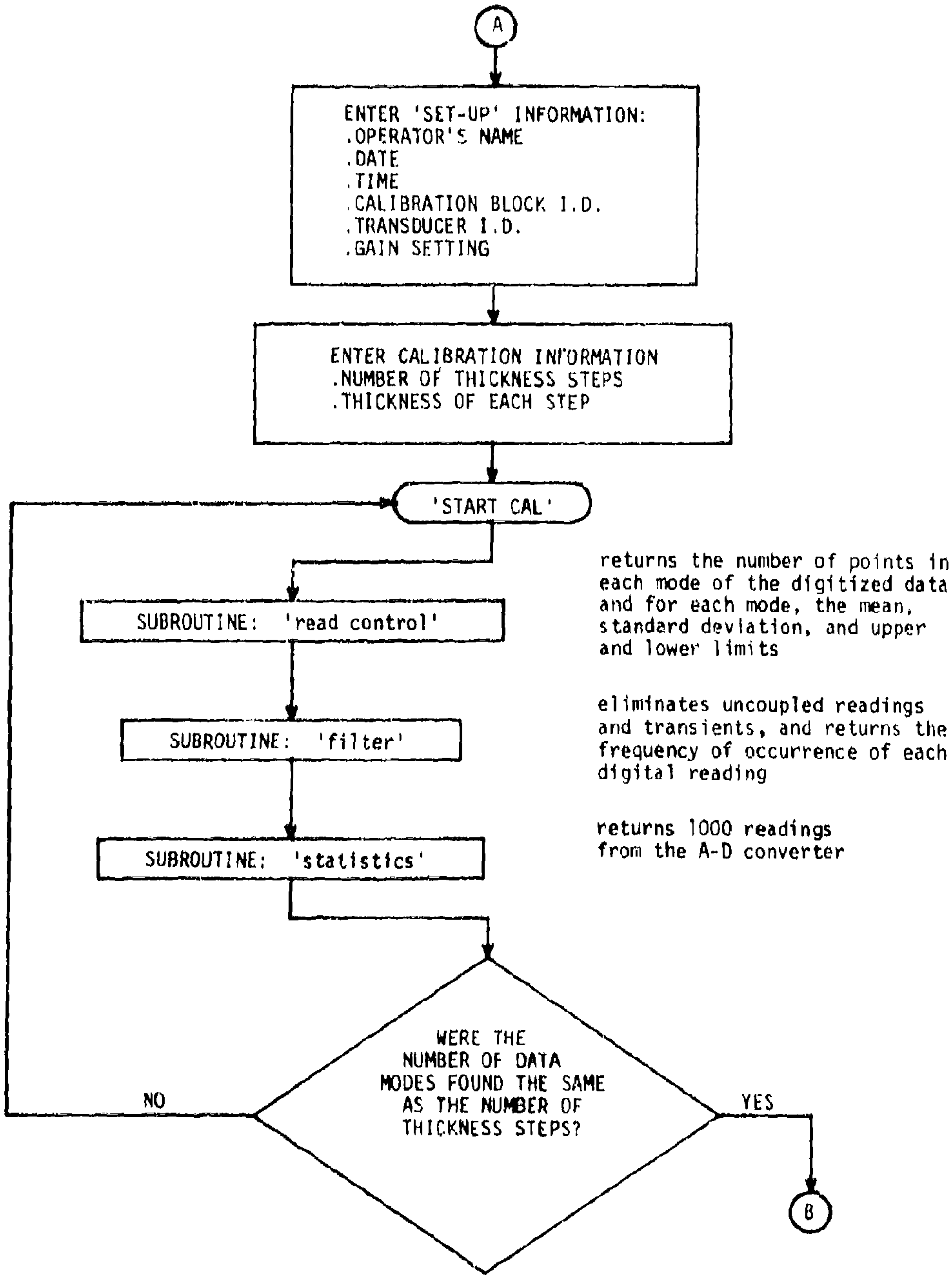

FIGURE 2.
(Sheet 2 of 5)

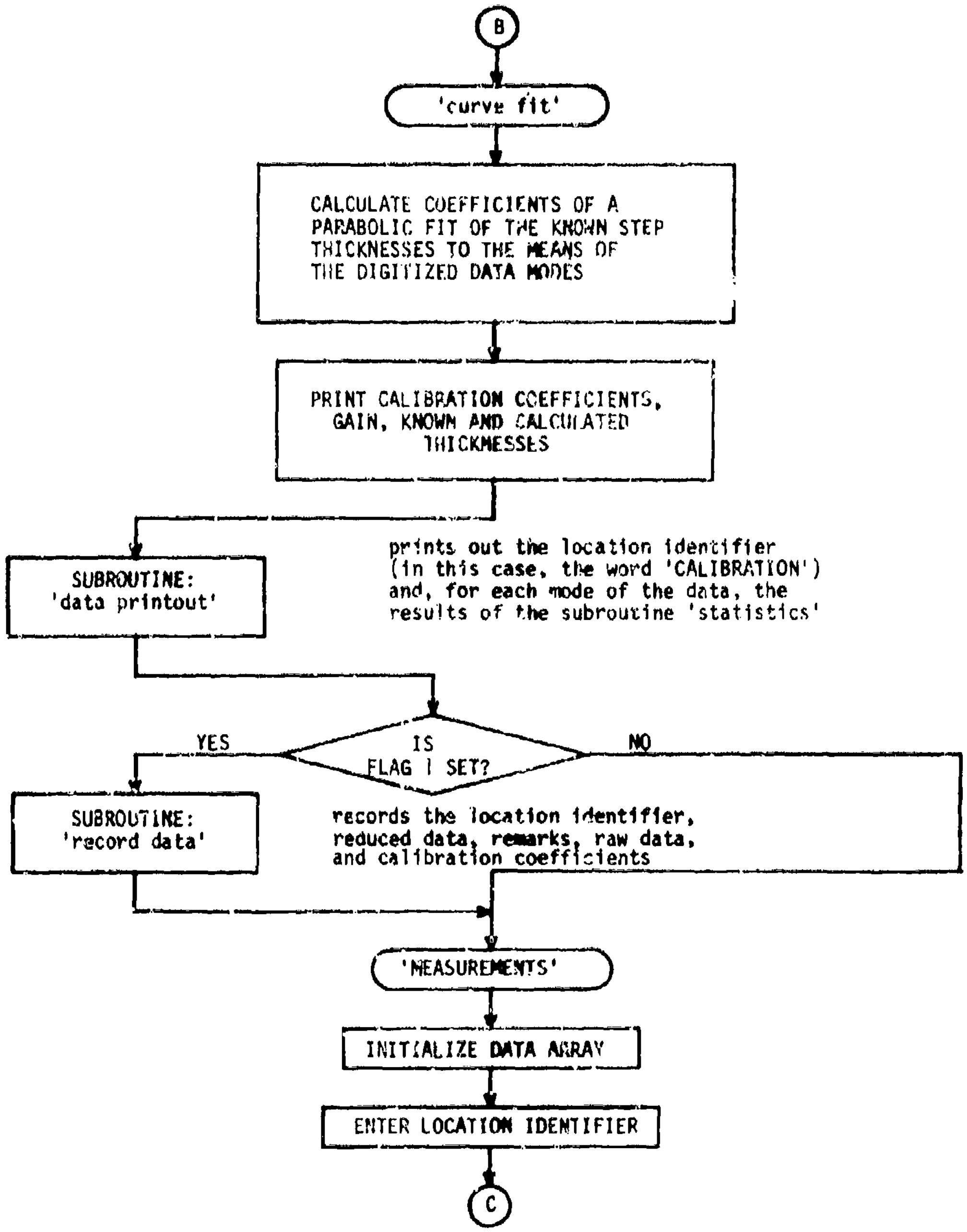

FIGURE 2.
(Sheet 3 of 5)

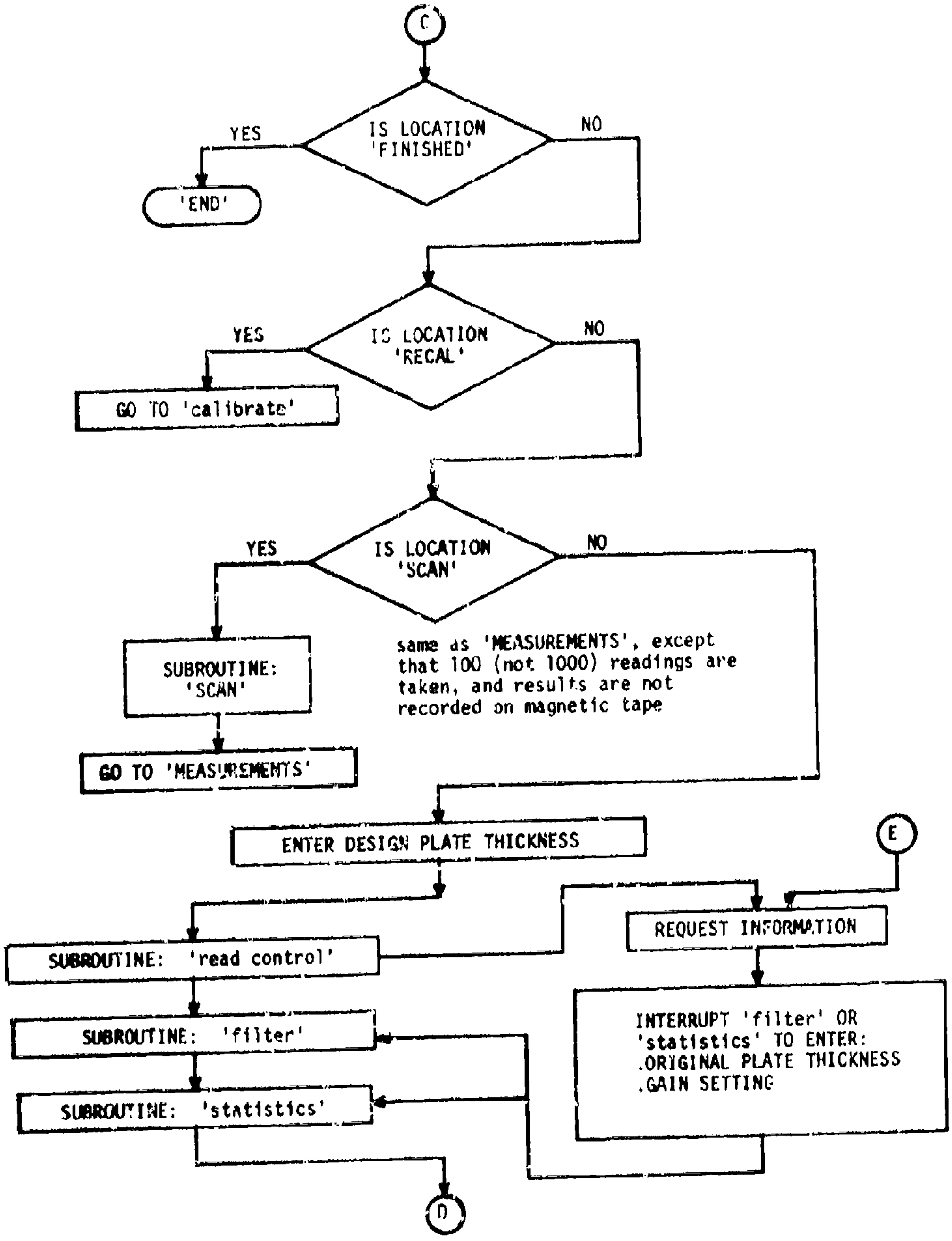

FIGURE 2.
(Sheet 4 of 5)

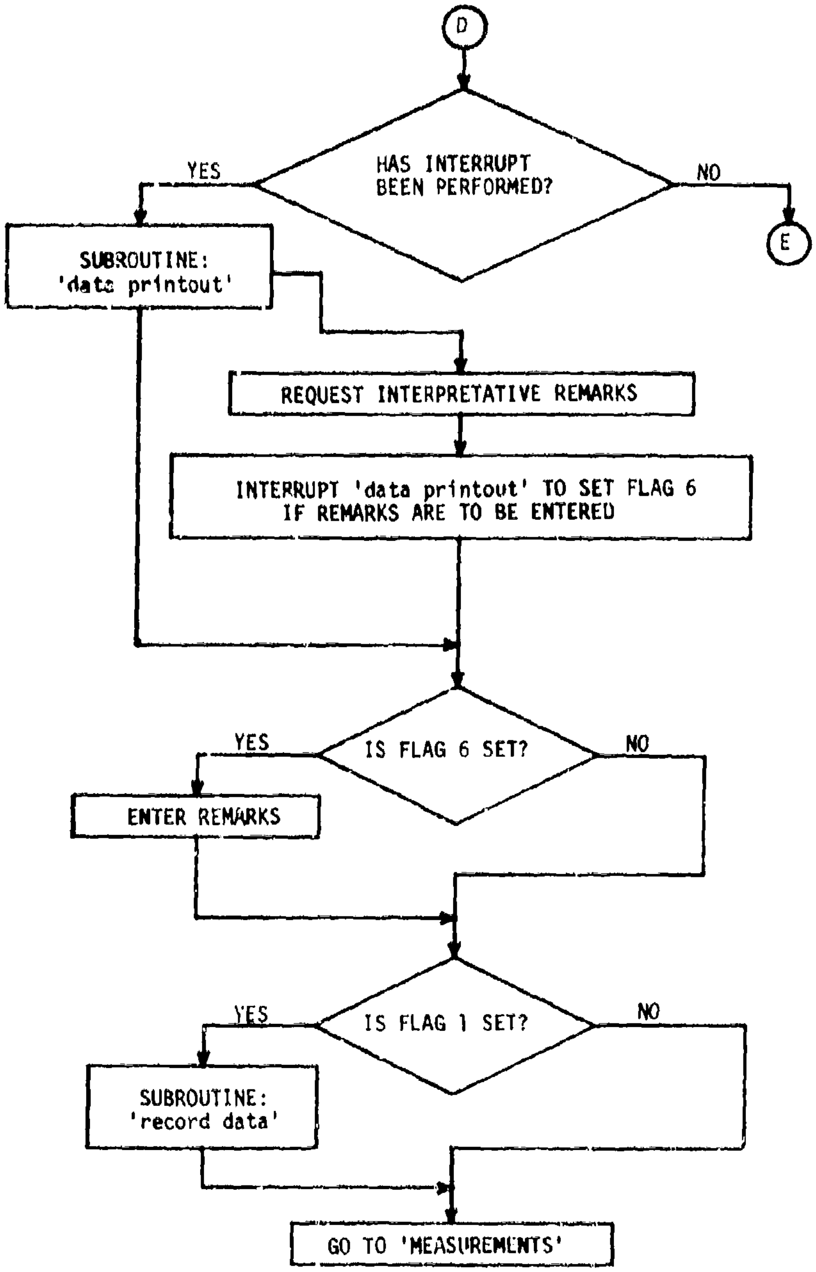

FIGURE 2.
(Sheet 5 of 5)

- o a subroutine called "read control" which interrogates the analog-to-ditital converter 1000 times and stores these digitized voltage readings (readings pbtained by this subroutine are shown in Figure 3)
- o a subroutine called "filter" which eliminates from the 1000 data the ultrasonically uncoupled readings and the electrical transients which occur before and after them. This subroutine returns a frequency distribution of the remaining data (Figure 4)
- o a subroutine called "statistics" which separates distinct "thickness" modes and calculates for each, the number of readings contained in each mode, the mean digitized voltage, the standard deviation of each such mode, and the maximum and minimum digitized voltage associated with each mode.

At this point calibration differs from thickness measuring. For calibration, the computer matches each mode of the digitized voltages with step thicknesses previously entered by the operator, and the computer calculates coefficients for a parabolic fit of digitized voltages to physically measured step thicknesses. For subsequent measurements on hull plate, these coefficients are used to calculate thickness (and its associated statistics) from digitized voltages. Also, during actual measurements the computer solicits remarks concerning the original plate thickness, current gain setting and interpretations of the screen. When all is said and done, in less than one minute (during which the diver rubs the transducer around the hull or calibration block), the computer has collected, reduced, printed out and stored thickness information based on 1000 individual readings. Is that better than a simple point reading taken by the diver equipped with a digital thickness gauge? We, and users such as PERA (Planning and Engineering for Repairs and Alterations) feel it is.

Features of this underwater ultrasonic system which make it attractive include:

(1) The involvement of qualified NDT personnel who can interpret and remark on the screen presentation
(2) The presence of a computer (psychologically this seems to make results more credible)
(3) The engineering usefulness of the data which comes from taking a large number of samples at each location
(4) The very minor effect the diver has on the data
(5) The use of immersion transducers which perform much better than contact transducers on corroded steel
(6) The minimal requirements for preparation (no deballasting or pumping tanks, etc.) and freedom of access to all parts of the underwater hull
(7) The timeliness of final reports, which are computer generated, and are usually sufficient to specify hull plate repair requirements in detail
(8) The minimal interference of underwater surveys with operating schedules. Often these surveys are scheduled around waterborne hull cleanings.

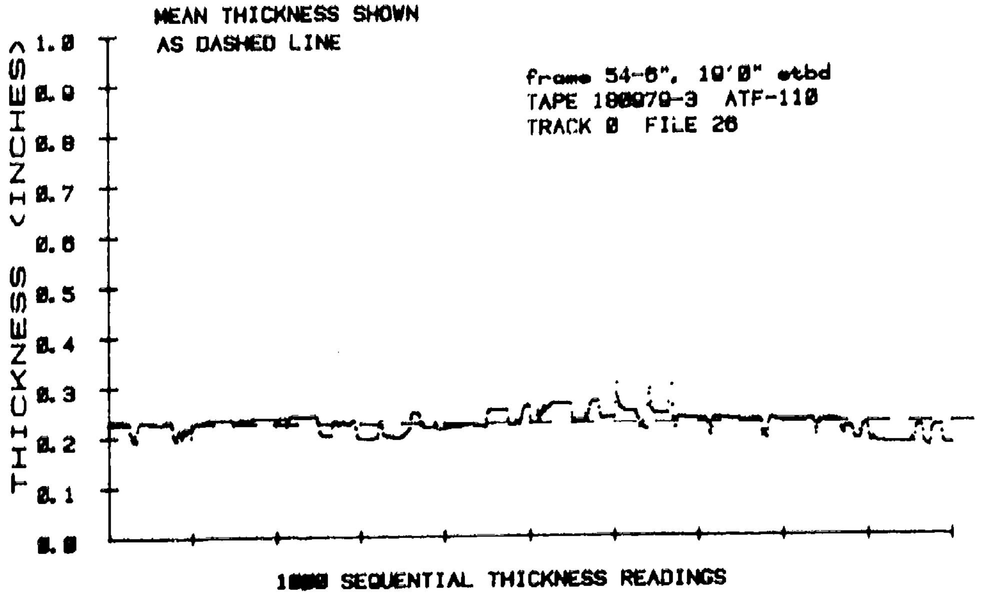

FIGURE 3. 1000 SEQUENTIAL THICKNESS READINGS

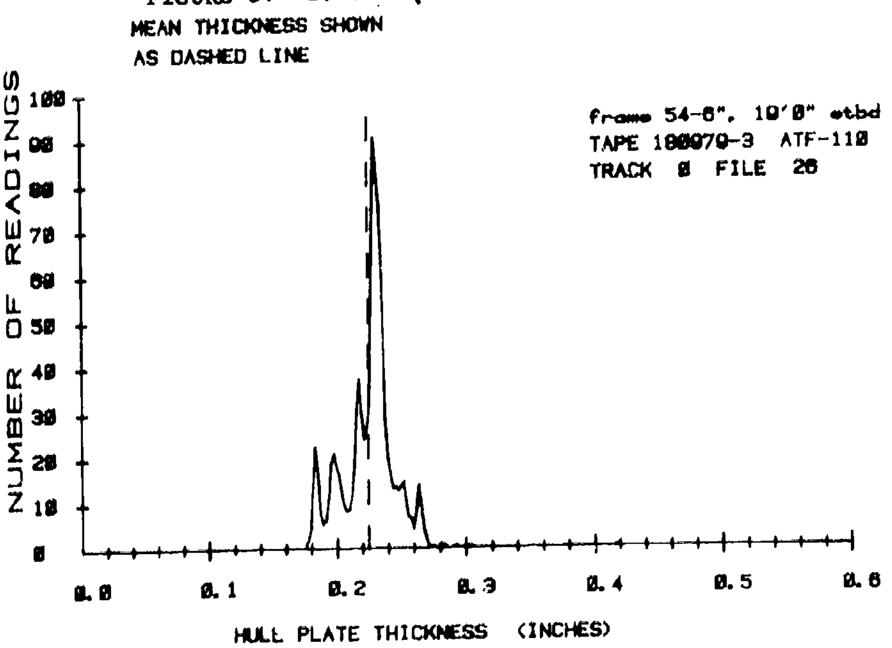

FIGURE 4. FREQUENCY DISTRIBUTION OF THICKNESS DATA IN FIGURE 3

Practice

Starting in the last month of 1978 the prototype hardware for underwater ultrasonic thickness surveys, and progressive modifications to the hardware/software system, have been exercised in the field to determine whether or not such systems could eventually be turned over to Fleet activities. In this year of field work, eleven thickness surveys have been performed: three barges, two destroyers, one cutter, three ocean going tugs and two salvage ships. In each case, local diving talent has been coordinated with NCSC and NAVSEA representatives to perform the survey. Results have been extremely good, and empirically it seems that the divers' "learning curve" gets above 90 percent within one day. In fact, the biggest obstacle to taking readings at the computer's maximum rate (a little more than 1 reading per minute) is the diver's ability to locate himself properly under the ship. To ease this problem, lines are run under the ship from port to starboard, at the frames where readings are required. These lines are marked every 2½ feet either side of the keel and should, theoretically, enable the diver to position himself quite accurately. Sarcasm ("theoretically") is not introduced out of malice, but rather, to point out how terribly important it is to divest the diver of responsibility for everything except breathing (the only activity in which he has a vested interest). We look forward to the day when navigation/positioning systems suitable for use under flat-bottomed ships become available and can be tied into our survey system.

As far as the ultrasonic testing aspects of the field operations go, there really isn't much to say except that the laboratory developments (basically the software flow-charted in Figure 2) have survived intact, in the field. On thin or pitted material we tend to use focused transducers, whereas on reasonably smooth steel, straight beam transducers work quite well. Referring to the very first sentence of the section on Principles we have indeed found that the UT part of the job is easy to do (in most cases). When trouble does arise (due primarily to severe external pitting), stereophotography complements the ultrasonics and the job goes smoothly anyway. Figure 5 is a replica (typewritten only because the computer's blue thermal printing reproduces poorly) of one page from a typical Thin Hull Survey. Note that the 10th line from the bottom corresponds to the raw and partially reduced data shown in Figures 2 and 3. In addition to a page of data (similar to Figure 5) for each frame of the ship that has been inspected, we normally forward to the funding agency a shell plate expansion on which thicknesses and percent deviation from design thicknesses are indicated, a written commentary describing thinned areas, and some photography (often stereo) to document pitting and the paint system's condition.

Interestingly enough, quite a lot of information concerning paint thickness can be obtained from the ultrasonic readings. Suppose, for instance, that thickness readings were taken on a brand new plate, and that these readings included the paint's contribution; i.e., the first

USS QUAPAW ATF-110

PROBLEM AREAS NEAR FRAME 54

LOCATION	DESIGN THICKNESS	MEAN	MAX	MIN	PERCENT THINNED
frame 54-12", 19'0" stbd	0.406	0.231	0.25[illegible]	0.224	43
frame 54-12", 19'0" stbd	0.406	0.282	0.284	0.278	31
frame 54-12", 19'0" stbd	0.406	0.207	0.232	0.197	49
frame 54-12", 18'10" stbd	0.406	0.233	0.260	0.210	43
frame 54-12", 18'8" stbd	0.406	0.265	0.284	0.232	35
frame 54-12", 18'6" stbd	0.406	0.273	0.290	0.246	33
frame 54-12", 18'2" stbd	0.406	0.374	0.378	0.372	8
frame 54-24", 19'0" stbd	0.406	0.414	0.428	0.384	-2
frame 54-22", 19'0" stbd	0.406	0.395	0.404	0.384	3
frame 54-22", 19'0" stbd	0.406	0.329	0.352	0.314	19
frame 54-20", 19'0" stbd	0.406	0.273	0.284	0.252	33
frame 54-20", 19'0" stbd	0.406	0.223	0.234	0.212	45
frame 54-20", 19'0" stbd	0.406	0.198	0.205	0.177	51
frame 54-18", 19'0" stbd	0.406	0.218	0.224	0.207	46
frame 54-18", 19'0" stbd	0.406	0.179	0.201	0.177	56
frame 54-16", 19'0" stbd	0.406	0.260	0.262	0.260	36
frame 54-14", 19'0" stbd	0.406	0.267	0.292	0.242	34
frame 54-12", 19'0" stbd	0.406	0.197	0.234	0.187	51
frame 54-10", 19'0" stbd	0.406	0.213	0.252	0.171	48
frame 54-8", 19'0" stbd	0.406	0.209	0.244	0.181	49
frame 54-6", 19'0" stbd	0.406	0.225	0.270	0.177	45
frame 54-4", 19'0" stbd	0.406	0.281	0.314	0.246	31
frame 54-2", 19'0" stbd	0.406	0.327	0.382	0.282	19
frame 54-0", 19'0" stbd	0.406	0.393	0.402	0.354	3
frame 54", 19'0" stbd (bare)	0.406	0.365	0.402	0.312	10
frame 54", 19'0" stbd (bare)	0.406	0.357	0.370	0.334	12
frame 54", 19'0" stbd (bare)	0.406	0.386	0.396	0.382	5
frame 54", 19'0" stbd (bare)	0.406	0.364	0.392	0.332	10
frame 54", 19'0" stbd (bare)	0.406	0.354	0.360	0.342	13
frame 54", 19'0" stbd (bare)	0.406	0.386	0.388	0.382	5

FIGURE 5. SAMPLE HULL THICKNESS SURVEY REPORT PAGE

front surface return to the first backwall echo was used to gauge thickness. One would expect the plate to contribute a reasonably constant amount (its thickness), and the paint to contribute some amount whose average (at any particular site) would be distributed normally about the mean of all average paint thickness contributions. By subtracting the nominal plate thickness out of all readings, and looking only at the excess thickness, we should obtain that normal curve. Unfortunately, the steel might be corroded on a real (not brand new) ship, and this would bias the curve toward lower values. On the other hand, it would not affect the upper portion, since the plate can't get thicker with age. It should then be feasible to fit a normal distribution to the upper half of the distribution of excess thicknesses and obtain some information on paint thickness. A small sample of the paint, measured physically and in situ, with a sharply focused transducer, will establish its sound velocity, and permit these excess thickness readings to be related to true paint thickness. Figure 6 (the histogram) shows such a distribution on one ship, and confirms the hypothesis that the upper half fits a normal distribution (the smooth curve), while the lower half is biased, presumably by plate corrosion. This same approach was tried on a second ship (Figure 7) with spectacular results; not one, but two modes of excess thickness were observed, and the upper portions of each mode were fit well by a curve which was the sum of two normal distributions, Divers confirmed and photographed peeling paint over a significant portion of the ship; the lower mode reflects the primer and anticorrosive layers only while the upper mode includes the antifouling layer as well. As interesting as this information is, however, unless we have a specific requirement to document paint thickness, or unless the steel is so badly corroded that multiple backwall echoes are not available, we usually measure thickness between the first and second backwall echoes, thereby virtually eliminating the effect of the paint system.

Very little data exists to confirm the accuracy of our underwater thickness gauging results since waterborne ships seem unwilling to destructively test their hull to satisfy our R&D requirements. However, on one of our first jobs, a floating crane, the results of our underwater survey were confirmed in dry dock, by direct physical measurement on plate removed from the hull. Figure 8 shows the distribution of thickness obtained ultrasonically (10 repetitions of 1000 points are shown) and the mean, maximum, and minimum of measurements taken with a cone-tipped micrometer are indicated above the distributions. The correlation is quite good. In quite another set of instances we have almost always been able to find interior scaling where, from the outside, the ultrasonic readings show severely thinned plate or multiple modes in the distribution of the thicknesses. Figure 9 shows a chunk of scaling plate lifted by hand from the inside of a salvage ship's hull. This kind of evidence often makes "believers" out of the ship's officers!

Ultrasonics can be done by divers, if their only responsibility is to hold the transducer. This philosophy (separating the transducer manipulation from all other phases of data acquisition, reduction and storage) has worked well in conjunction with the computer's ability to

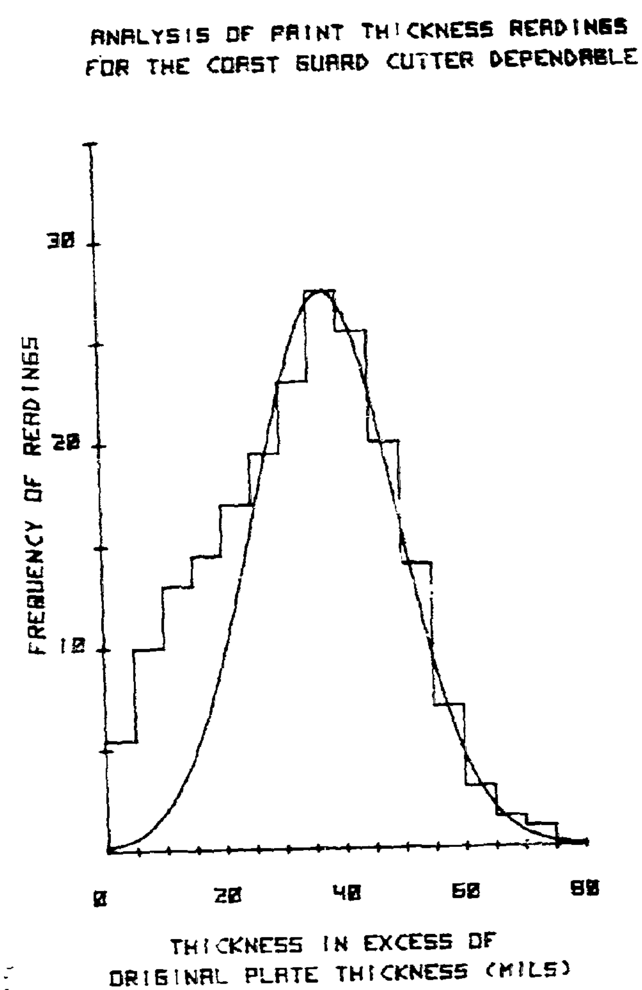

FIGURE 6. DISTRIBUTION OF THICKNESSES ATTRIBUTABLE TO AN INTACT PAINT SYSTEM

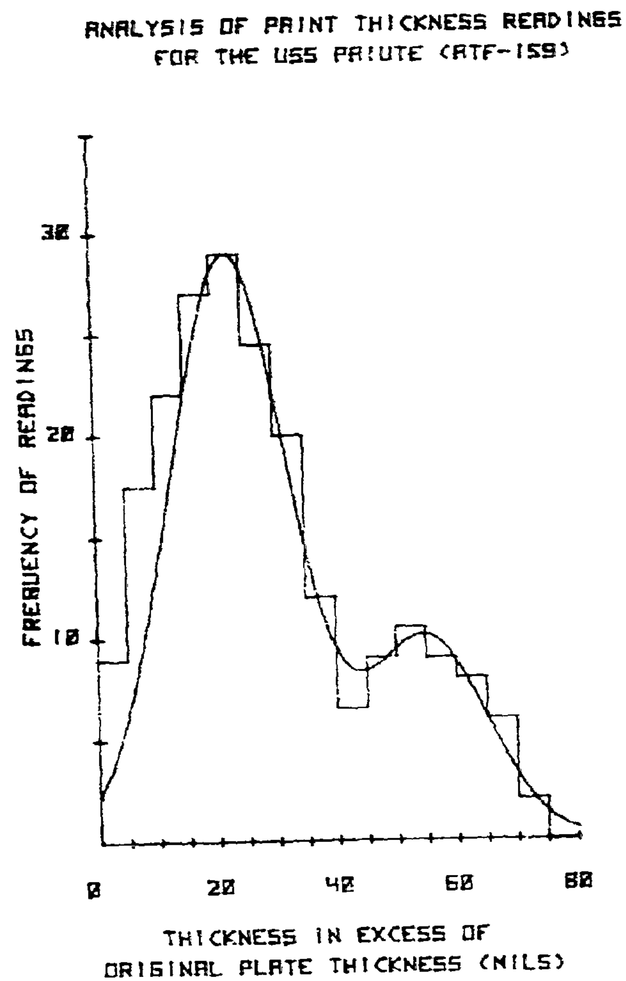

FIGURE 7. DISTRIBUTION OF THICKNESSES ATTRIBUTABLE TO A PEELING PAINT SYSTEM

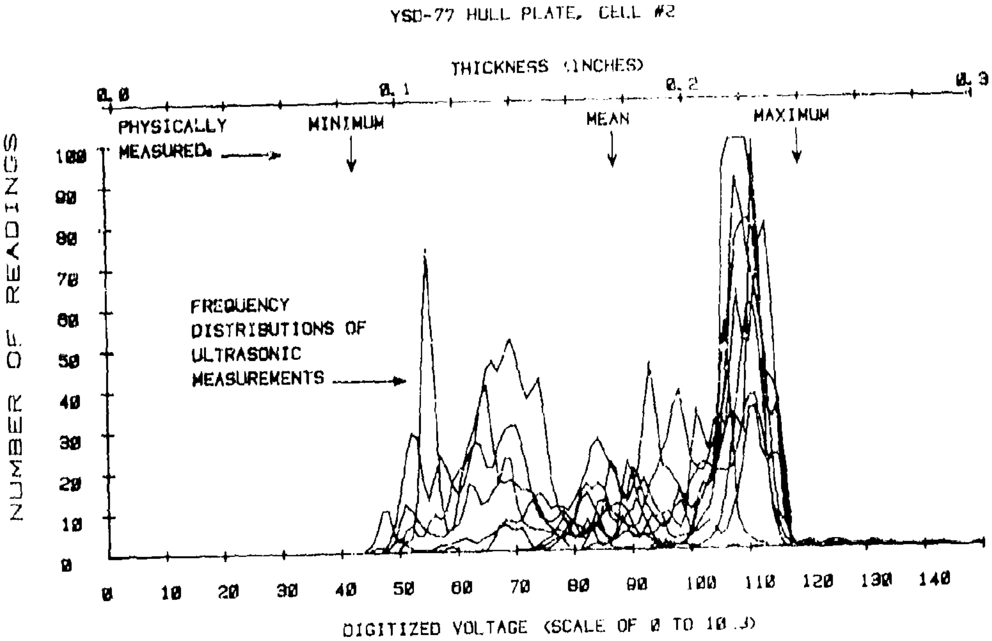

FIGURE 8. COMPARISON OF ULTRASONIC AND PHYSICAL THICKNESS MEASUREMENTS

FIGURE 9. PRODUCT OF INTERIOR SCALING CORROSION DISCOVERED BY EXTERNAL (UNDERWATER) THICKNESS GAUGING

acquire massive amounts of data in lieu of requiring artful manipulation. These concepts show promise for automated transducer platforms and for ultrasonic flaw detection. Both areas are currently being developed at NCSC.

MAGNETIC PARTICLE AND ELECTROMAGNETIC FLAW DETECTION

Principles

Underwater magnetic particle examinations have been performed successfully in the North Sea for several years now, using relatively standard techniques and equipment. Domestic progress in this field has, however, been relatively slow, perhaps because domestic requirements for inspection of offshore structures lag European requirements by several years. In any case, the feasibility of performing underwater MT had already been demonstrated when NCSC became involved in underwater ship hull inspection R&D. Unfortunately, the direct application of topside MT techniques to the underwater environment misses the primary goal of our development effort since (1) a fair amount of manual skill is required of the diver and (2) hard copy results are not normally produced. Thus, immunity from the diver's shortcomings and overall credibility are difficult to establish using conventional MT techniques. Nonetheless we chose to pursue the avenues followed in the North Sea, hoping that improvements would be possible and that insight could be gained.

Early investigations centered around the choice of a magnetic particle carrier, and the choice of a means of magnetization. In the former area, consideration was given to magnetic rubber, fluorescent particles (suspended in water) and magnetic "paint." Magnetic rubber performed marginally better than the fluorescent particles, and with the uncured rubber sealed in plastic pouches, was quite immune to dissipation by currents. Also, it produced hard copy results which could be brought topside to a qualified MT inspector. On the other hand, the pouches often prevented good contact over weld crowns, and in cold water, the rubber took "forever" to cure. While neither of these problems are insurmountable, the effort it would take to overcome them did not appear justified since the fluorescent particles performed nearly as well and were much easier to use. (Magnetic "paint" showed very little promise and was dropped quite early in the investigations.) Fluorescent magnetic particles, already in use in the North Sea, are applied by the diver who squirts them out of a small squeeze bottle, and the excess particles are fanned away gently. To assist the diver in setting up and reviewing his results, NCSC developed a combination (white or ultraviolet) light which is converted by simply swinging an ultraviolet filter in front of the mercury vapor bulb. Then, to produce "hard copy" records, a strip of putty tape is pressed over the area of interest; the particles stick to the putty, and the putty also forms to the metal's contours. Thus, an inspection record, complete with the local topography is produced and can be judged by a qualified inspector. By indexing the putty tape's position relative to the hull (with a grease pencil), the tape can be used as a template for locating arresting holes that may have to be drilled. Whereas this technique has been used successfully on two Navy ships, it still lacks the kind of immunity from the diver that we desire.

The second area of investigation (sources of magnetic flux) involved consideration of permanent magnets, a dc yoke, an ac (half wave) yoke, and current prods. Actually, the prods were never really considered since the prospect of having 1000 amps floating around underwater seemed to pose safety problems so severe that even the most failsafe hardware could not be made diver-proof (a step above sailor-proof). Permanent magnets, though safe, performed significantly worse than either electromagnet and were dropped quite early. Finally, the dc yoke we investigated did not have articulated arms and thus proved difficult to use on all but the simplest geometries. This left the ac yoke which proved easier to use and a better performer than any other candidate. Its only noteworthy shortcoming lay in its relatively low holding power, and to this end we are currently developing an articulated yoke which uses a larger dc component than we currently have.

Very quickly then, using a combination of commercially available equipment and in-house developments, we acquired a system capable not only of producing good MT results but also lethal dosages of electricity. A major effort, still on-going, is devoted to providing acceptable protection against electroshock. This has involved, as a start, using sensitive ground fault interrupt circuitry, isolation transformers, braided external ground conductors, metallic shields encasing all underwater electrical components, and the elimination of all switches from the ac yoke. Though the prototype system appears safe, it has not yet been approved for use in the Fleet, and we have yet to coax a volunteer into intentionally cutting a power cable or breaking a mercury vapor bulb underwater.

The other major R&D effort (aside from diver safety) revolves around alternative methods of performing electromagnetic flaw detection. Eddy current techniques have been found to work underwater but suffer the same sensitivity to extraneous metal properties as they do above water. Another technique which is receiving more attention uses Hall effect transducers to measure flux leakage near cracks. Though we haven't any underwater experience with this technique yet, it seems to be fully compatible with the basic goal of diver-independence, and appears to have at least as much sensitivity as fluorescent particles. Preliminary work shows that field strength measurements across a crack will be roughly like those shown in Figure 10. Since the Hall effect transducer produces an electrical signal, it can be read at high speed by a computer, allowing much the same approach as has proven successful in underwater ultrasonic

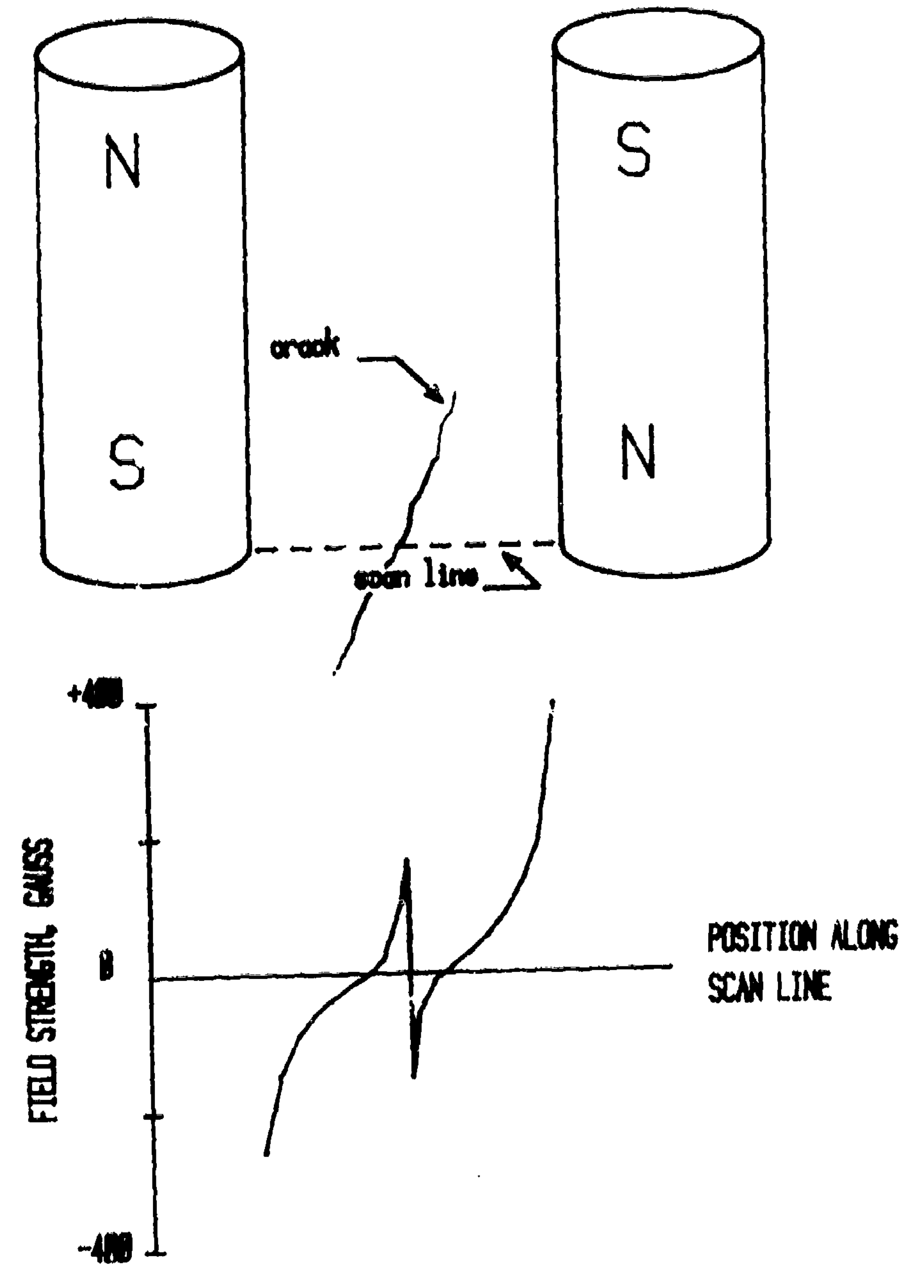

FIGURE 10. HALL EFFECT FLUX LEAKAGE MEASUREMENTS

thickness gauging. We look forward to getting this concept to the field testing stage.

Practice

NCSC has supported two underwater magnetic particle inspections, both of which were also discussed in "Stereophotography, Practice" earlier in this paper. In both cases, the ac yoke and fluorescent particles were used, bringing the particles topside on putty tape. Figure 11 shows one strip of putty (from the destroyer) illuminated

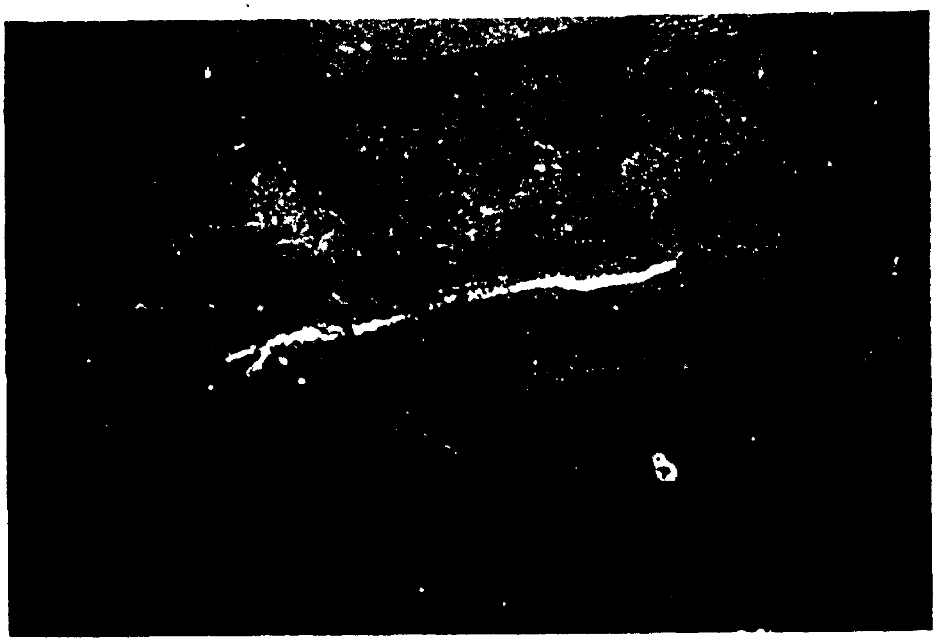

FIGURE 11. PUTTY TAPE RECORD OF AN UNDERWATER MAGNETIC PARTICLE INSPECTION

with UV light. Not only is the crack end visible, but also, the impressions left by two arresting holes, neither of which actually arrests the crack. This information, combined with photographic and ultrasonic documentation, allowed a major decision (early decommissioning) to be made with minimal risk to both the decision makers and the sailors assigned to the ship.

In the second example, involving a crack along the cruiser's bilge keel, magnetic particle inspection was used to fully define the extent of cracking, and to accurately position arresting holes which were drilled prior to making repairs. This effort coordinated shipyard engineers and MT inspectors, shipyard divers, and NCSC personnel. It saved the ship a dry docking and permitted operational schedules to be met. However successful this, and the previously described underwater magnetic particle inspections were, they did demonstrate to NCSC engineers that further R&D is required in order to end up with a system that requires minimal skill underwater.

SUMMARY

Between the 27th and 28th DoD Conferences on NDT significant field experience has been gained in underwater ship hull inspections. Twelve ships have been inspected, using stereophotography, magnetic particles and ultrasonics in various combinations. Results of these surveys have apparently been suitable to managers and engineers since some rather major decisions have been made on the basis of them. Though the hardware and techniques for underwater NDE are still under development at NCSC, their value in the field has already been demonstrated, and activities requiring inspection results while still waterborne are expressing support and encouragement. Future work will concentrate on new methods for flaw detection and on passing this year's prototype developments over to the Fleet.

MICROENCAPSULATED PENETRANTS, A NEW APPRAOCH TO PENETRANT INSPECTION

Albert Olevitch
Air Force Materials Laboratory
Attn: AFML/MXE
Wright-Patterson AFB, OH 45433
Autovon 785-3691

ABSTRACT

This paper describes the work demonstrating a new penetrant material and process, microencapsulated penetrants. The micro-encapsulation of an ultra violet fluorescent solution results in what appears to the eye as a powder. The individual microcapsules can be made to be as small as two microns diameter and are easily deformable. Thus this "dry penetrant" can be sprayed and mechanically forced instantly into cracks even smaller in width than the diameter of the microcapsules. Any excess microcapsules not in the crack are loosely held on the surface of the part and can be readily removed mechanically or by water rinse.

The above concept has been conclusively demonstrated. Zyglo 30 a standard liquid penetrant was microencapsulated to produce particles of a 2-5 microns diameter. Crack standards representing the highest sensitivity range were employed and the tests showed that this new penetrant form can successfully find the cracks. A large number of tests on real parts representing difficult problems such as welds, porous castings, hard to wet titanium, very shallow cracks were successfully tested. The paper also will describe a current contractual effort to further demonstrate the process, determine its shortcomings and economics and conduct a production line inspection demonstration.

MICROENCAPSULATED PENETRANTS, A NEW PENETRANT FORM AND PROCESS

Albert Olevitch
Air Force Materials Laboratory
Systems Support Division
Wright-Patterson AFB, Ohio 45433
Autovon 785-3691

INTRODUCTION

Penetrant inspection is the most widely used NDI technique in the Air Force. The process involves immersion of a part in a liquid which fluoresces under ultra violet light. After a period of immersion, which can be of 10 minutes duration or longer, the part is removed. The excess penetrant on the surface is removed by water washing or, in the case of the high sensitivity penetrant, by emulsification to achieve water solubility, and then water washed and dried. After drying, a developer is applied and the part is viewed under ultra violet and any cracks or defect seen as a yellow green fluorescing area.

This process has certain disadvantages such as the following:

a. Time critical steps are involved. For example a part must be inspected within a specific time after developer is applied. Time limitations exist in the emulsification procedure.

b. The time to process a part is long.

c. The various reactants used are not interchangeable between penetrant manufacturers products.

d. Difficult to wet or porous surfaces like those of castings are problems. On porous surface sometimes it is virtually impossible to get rid of background fluorescence due to the continuous bleeding of the penetrant from the pores of the surfaces even after repeated washing.

e. Contamination of emulsifier with penetrant on the surfaces of part results in periodic discarding of the contaminated emulsifier solution.

f. The fact that liquid penetrant works by physio-chemical process results in formulations of differing degrees of detectability. Hence one finds that the specification establishes numerous types or classes as to sensitivity.

g. Very shallow defects pose problems because the penetrant can be readily removed if overwashed.

The new concept, microencapsulated penetrants, was conceived because it had the potential to eliminate many of the difficulties enumerated above. Microencapsulation, a well established technique or process used in the drug and agricultural, and carbonless paper industries, can be used to contain U.V. fluorescent solutions in the form of small plastic spheres of a desired diameter. In this form these spheres could be made as small as 2 microns in diameter. Since these spheres were deformable we reasoned that one could spray them t some pressure entering as small a crack or defect as necessary without rupturing. If so then we had a way of getting U.V. fluorescent material into a small defect instantly and hopefully with minimal and easily removable background.

PREPARATION OF MICROENCAPSULATED PENETRANT

The product which was microencapsulated was a group VI, MIL-I-25125 penetrant, Zyglo 30 made by Magnaflux. This penetrant was arbitrarily selected because it is a qualified product. Any fluorescent solution of sufficient brightness could have been used. In other words the solution to be microencapsulated does not have to be formulated to be a liquid penetrant.

In most of our work we worked with microencapsulated Zyglo 30 of a 2-5 micron size diameter. The microencapsulation was done by Capsulated Systems, Inc. of Yellow Springs, Ohio. We have had success also with 8-10 micron diameter product. However this discussion will center on the 2-5 micron size microcapsules.

DETERMINATION OF SENSITIVITY

To determine sensitivity the encapsulated product was sprayed onto a number of crack standards. These crack standards were of two types: The Monsanto crack standard (cracked chrome plating) and fatigue crack standards of the type being used in qualification tests of Spec MIL-C-25135. Both types represented the highest sensitivity classification.

DISCUSSION OF PROCESS

The spraying was done with commercial paint type spray guns at various pressures. We believe that 60 psi pressure is a good one to use. The excess material on the surfaces was removed, in some cases, mechanically by vacuum assisted brushing. In some cases fairly good results were obtained by this method and in other cases results were mediocre or poor. We intend to pursue de-staticizing the encapsulated penetrant, because the main reason for the particles clinging to the surface is static charge attraction. Through de-staticizing we hope that we can reduce the amount of background on the part sufficiently that one can inspect the part immediately after spraying the micro-encapsulated penetrant onto the parts. In all cases a brief rinse of water with a little bit of household detergent was very successful even on porous surfaces such as those of castings. The detergent water rinse does not dissolve the capsules on the surfaces, but removes these by the de-staticizing effect of the detergent and the physical action of the water moving over the surface. The micro-capsules of penetrant in the wash water could be removed by filtering and drying and then reused. Also during spray application of the microcapsules, the excess oversprayed material could be recovered and reused.

After removal of the capsules on the surfaces the part is dried. Then it can be inspected with a U.V. light. In some cases conventional developer is beneficial. In our work we employed Metal-Check D-70 developer with excellent results.

The time required in our laboratory to inspect already cleaned parts such as turbine blades was about two minutes. This period of time was required for spraying the penetrant product, removing the background, wiping the part dry, applying developer, and inspecting under an ultraviolet light.

INSPECTION OF PARTS

During the course of this work we had the opportunity to inspect a number of engine parts using the 2-5 micron diameter penetrant. These were "real world" parts furnished by the General Electric Company, Evendale, Ohio and contained certain types of difficult defects. A titanium part which had hard to wet surfaces was inspected and the defects were found without any difficulty. Welded areas were inspected without any problems. Casting with the porous surfaces which presented the "bleed back" problem were readily inspected with the microencapsulated penetrant. A part with an extremely shallow crack was successfully inspected. Particular attempts were made to remove the microcapsules from the very shallow crack using vigorous brushing under a continuous strong water flow from a faucet. The capsules could not be washed out of this very shallow crack. Conventional liquid penetrant could not match this performance. A number of turbine blades with very fine cracks in the root end and at other locations were also successfully inspected. Every one of the parts furnished by G.E. were successfully inspected.

HEAT ASSISTED PENETRANT INSPECTION

Microencapsulated penetrants have interesting possibilities for expanded use of heat assisted penetrant inspection. In a recent paper, Heat Assisted Fluorescent Penetrant Inspection by A. G. Sherwin and W. O. Holden, given at the 1979 Spring Conference of the ASNT, it was noted that heating of parts opens up tight cracks. Thus one can, in effect, increase the sensitivity of penetrants by applying penetrant to heated parts. This paper points out that there are temperature restrictions in specifications which limit the allowable temperatures of parts. These temperature limitations are imposed because certain components of liquid penetrants evaporate too rapidly and also because fluorescence can be adversely effected by heat. The authors report successful results in operating at higher temperatures using penetrants containing high boiling point solvents.

Microencapsulated penetrants offer interesting advantages in heat assisted inspection. The fluorescent solution need not be formulated with high boiling point solvents or carriers. The microcapsule prevents or minimizes evaporation under extreme temperatures. In an informal communication Capsulated Systems, Inc. reported that microencapsulated toluene was kept above its boiling point for a year with only about an 8% loss by weight. In one experiment in our laboratory we observed continued good fluorescence from microencapsulated penetrant after one half hour at 300°F. At 400°F we detected significant vapors in the oven. This brief test suggests that conventionally formulated fluorescent solution will be usable at temperatures possibly up to 300°F if microencapsulated. Another favorable point is that the microencapsulated penetrant inspection process is of much shorter duration than the liquid penetrant process. Thus the time of exposure to high temperatures is quite short.

At the end of this paper figures are attached which include those of the parts, furnished by General Electric, Evendale, Ohio, with the microencapsulated penetrant flaw indications. Figure 1 shows a scanning electron microscope view of an agglomerate, 50 microns in diameter, of many 2 to 5 micron diameter capsules. These separate when sprayed onto surfaces. Figures 2, 3 and 4 show respectively the Group VIb (1/2 micron wide) crack standard, the liquid penetrant indication in this crack standard, and the microencapsulated penetrant in the same crack standard. It can be seen that the indications by these two penetrant forms are equivalent. The rest of the figures are sufficiently identified and no further description is required.

CURRENT STATUS

The AFML has issued a contract with General Electric, Evendale, Ohio to further evaluate this new penetrant. The overall objective of this contract is to evaluate this technique in a manufacturing environment, investigate possible improvement, develop a first cut at cost of inspection and of the defect detection efficiency.

The contractor will confirm the sensitivity of the penetrant, investigate spraying variables (varying pressures and distances), look into techniques for recovery of overspray, investigate other fluorescent solutions for encapsulation, conduct a simulated productive line inspection of a large number of parts using liquid penetrants and microencapsulated penetrants and establish the cost of inspection with encapsulated penetrant. This contract started in June 79 and will be completed in 15 months.

Attached are photos of some of the important aspects of this work. This paper has presented an abbreviated story of the work done and detailed discussions have been avoided. A full description of our work is reported in AFML TR-79-4027 which is available through normal distribution channels.

SUMMARY OF ANTICIPATED ADVANTAGES OF MICROENCAPSULATED PENETRANTS

a. Process simplicity
b. Automatable due to simplicity and rapidity of process
c. Works well on porous or hard to wet surfaces
d. Does not readily wash out of shallow cracks
e. Works on hot surfaces
f. Reduced problems with waste disposal
g. Simplified supply and logistics - no emulsifiers, one class of penetrant

Figure 1. Scanning Electron Microscope Photograph (Courtesy Hughes Aircraft Co) of a micro-capsule agglomerate at 4200X. Note individual capsules separate easily on impact at surface to be inspected.

Figure 2. View of Crack, Group VIB
Crack Standard ([illegible]X)

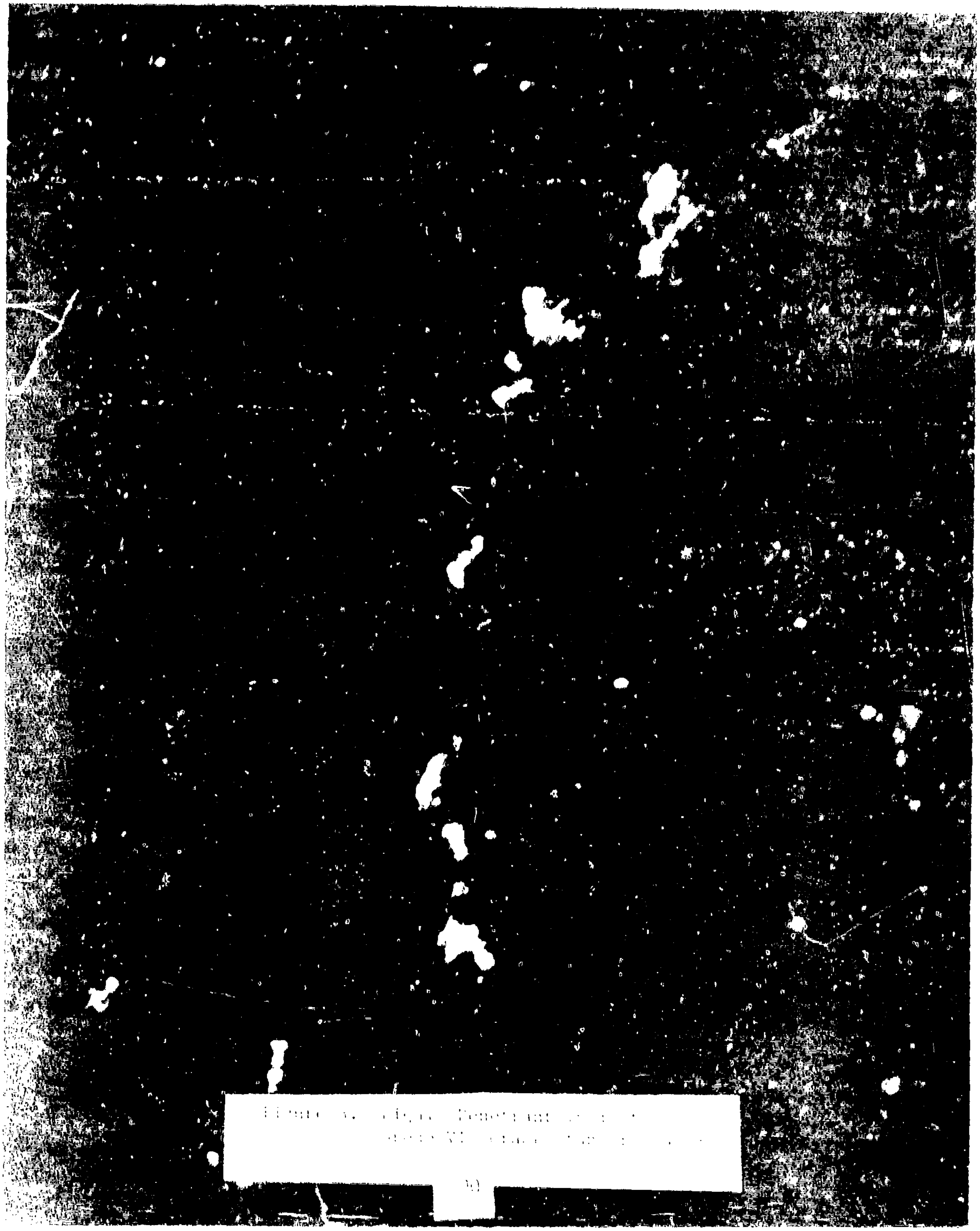

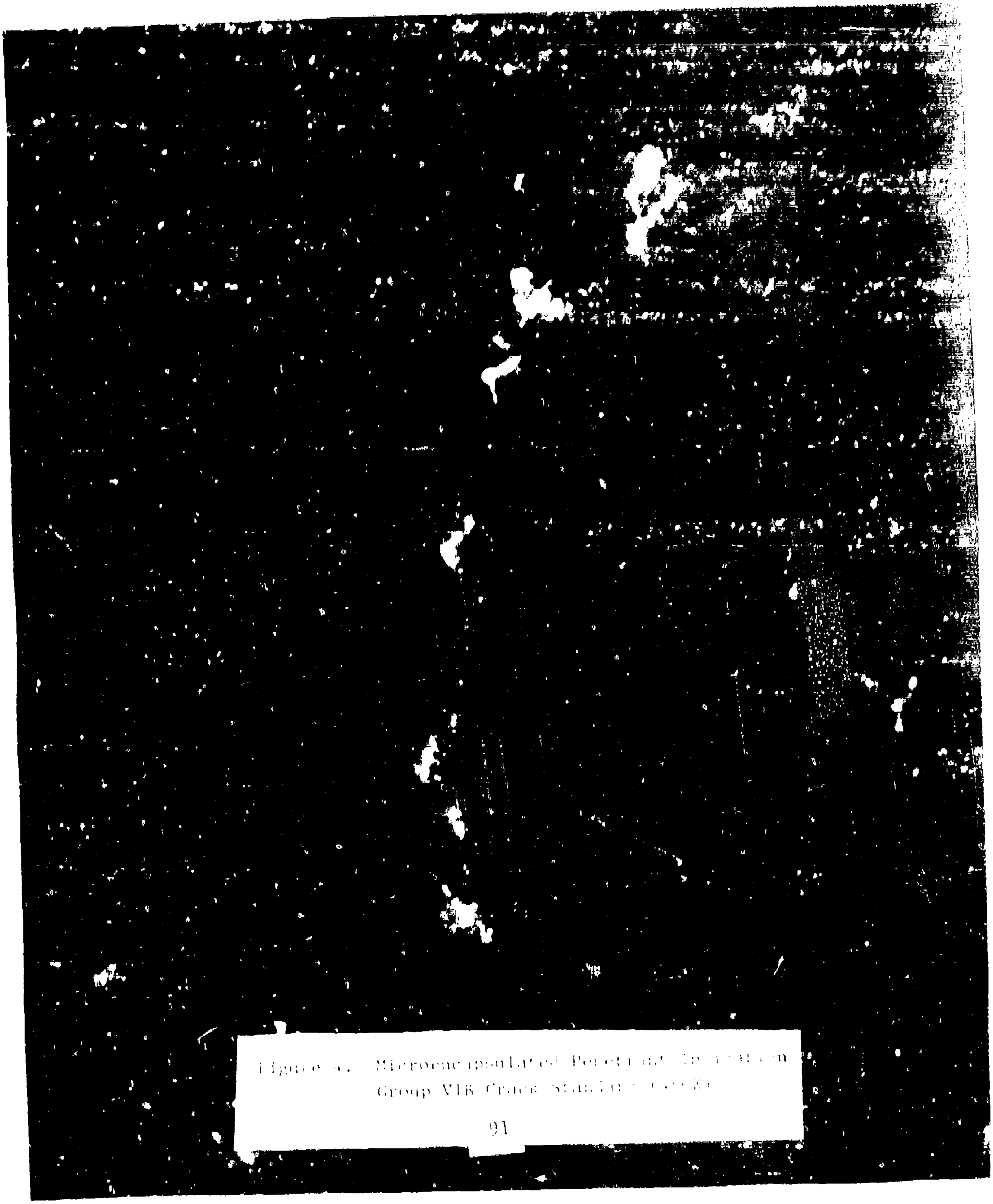

Figure [illegible]. Microencapsulated Penetrant [illegible]
Group VIB Crack Standard [illegible]

Figure 5. Fatigue Crack Standards for Group VIA and B Penetrants

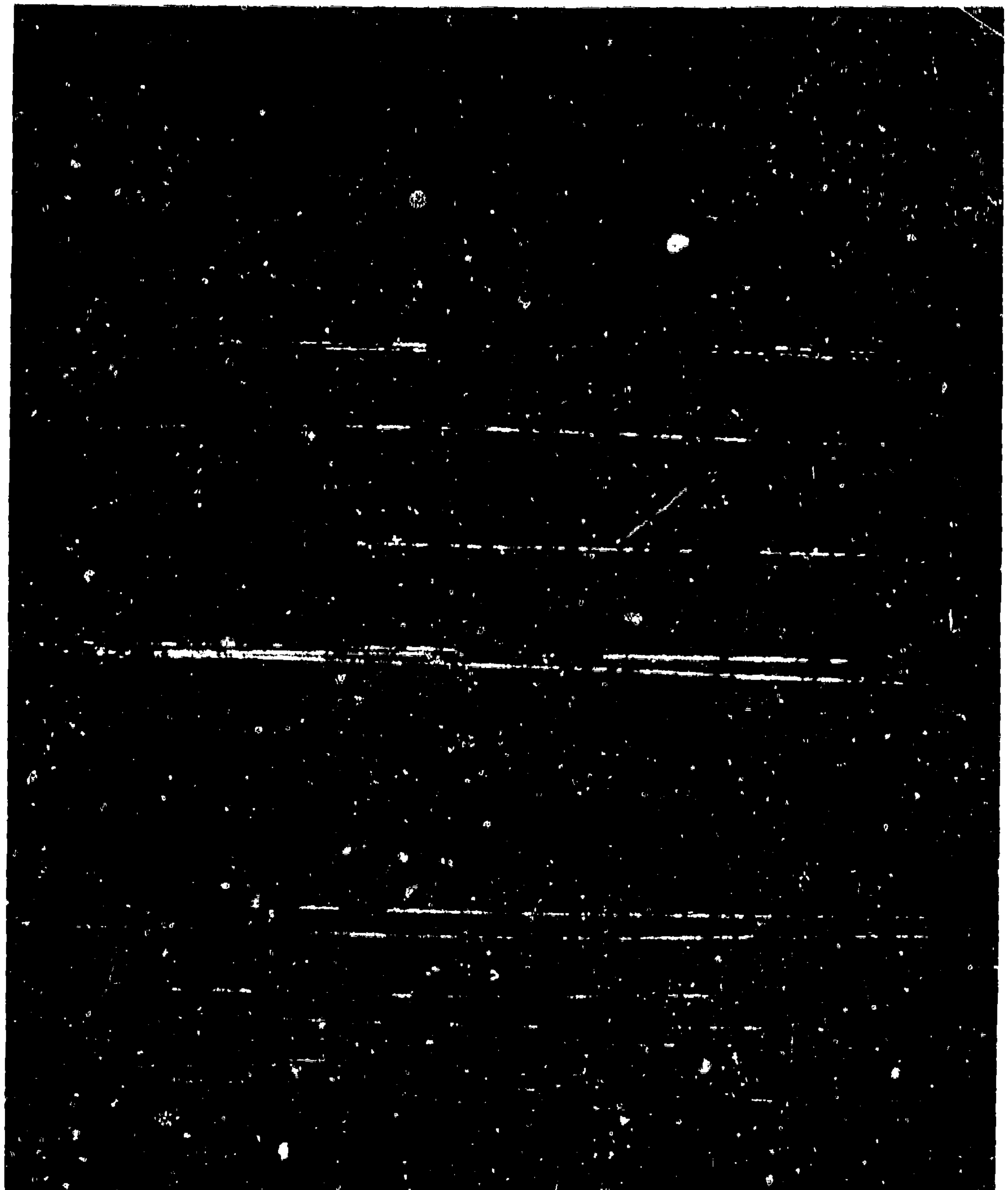

Figure 6. Fluorescent indications of Cracks on Monsanto Tram Crack Standard After Removal of Excess Capsules by Detergent-Water Rinse

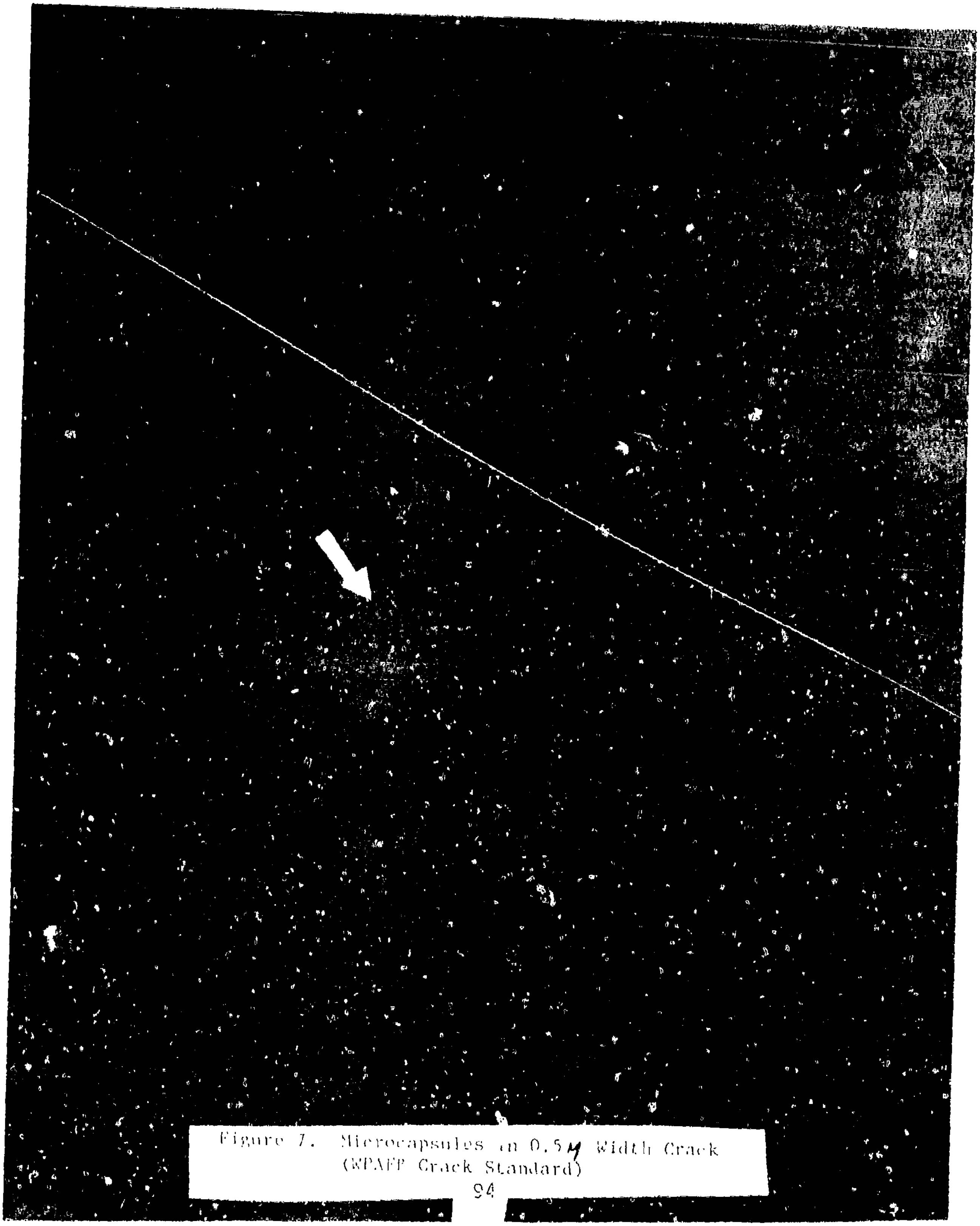

Figure 7. Microcapsules in 0.5μ Width Crack
(WPAFF Crack Standard)

Figure 8. Defect in Porous Casting

Figure [illegible]. Porosity Defects in Weld

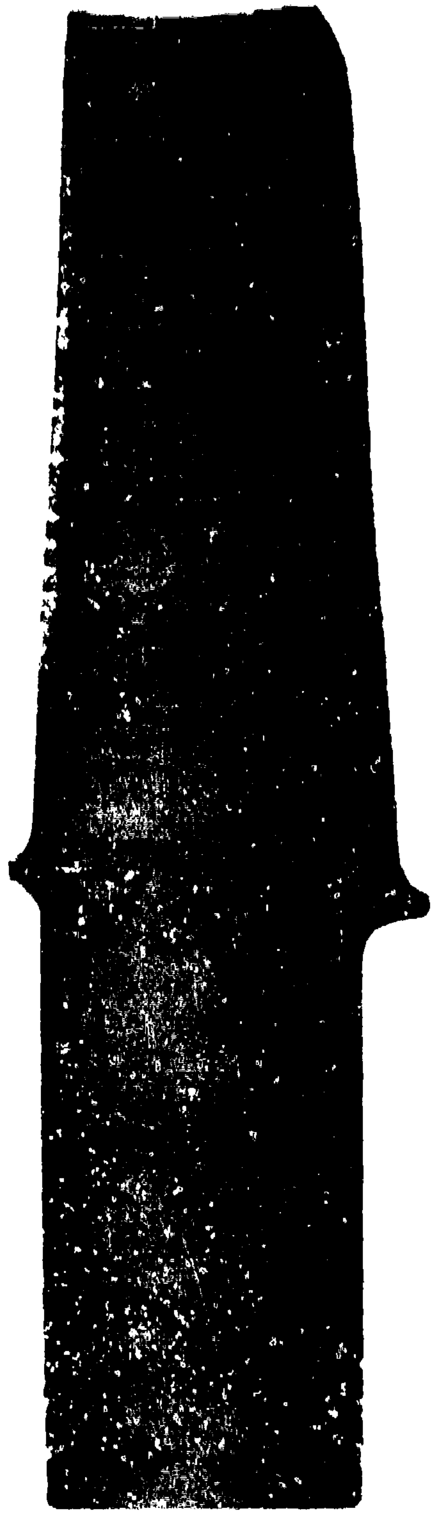

Figure 10. Defects in Edges of Turbine Blades

NONDESTRUCTIVE INSPECTION OF ARTILLERY SHELL

Mark H. Weinberg
US Army Armament Research & Development Command
ATTN: DRDAR-QAR-I
Dover, New Jersey 07801
Autovon 880-2550

ABSTRACT

Increasing use of thin-walled, highly stressed, high strength and low elongation steels for production of artillery projectile shells makes imperative more reliable and stringent inspection methods. This paper will describe the approach being used in designing the modern testing procedures.

First a stress map of the entire shell is derived. Yield strength and plane strain fracture toughness values are measured and critical crack sizes calculated. Next, determinations are made regarding the NDT methods to be applied. Typically, a combination of hydrostatic and ultrasonic testing are employed, inspecting the entire shell. Eddy current testing may be used for particular locations. Design of standards, relationship of the machined notches to critical crack sizes and the interrelationship between the notch length and the ultrasonic beam are discussed.

Problems encountered and some solutions adopted will be described.

All the basic engineering work was done and decisions were made in-house at ARRADCOM, with contributions from Frankford Arsenal (prior) and the Army Materials and Mechanics Research Center.

NON-DESTRUCTIVE INSPECTION OF ARTILLERY SHELL

Mark H. Weinberg
Product Assurance Directorate
DRDAR-QAR-I
Dover, New Jersey 07801
Autovon 880-328-2550

(1) This paper is limited to a discussion of the nondestructive inspection of artillery projectile metal shell for material integrity. (Parenthetical numbers, underlined, refer to figures which follow the text).

(2) Changes which are well under way in the field of armaments impose increasing burdens on the test and inspection community. The problems involve a wide range of disciplines: tightened tolerances require more sophisticated mechanical, pneumatic, electronic and optical gaging techniques; higher production rates require automated inspection means; complex electronic fuzing devices need computer-controlled inspection processes; and the use of high-strength, brittle artillery projectile shell subject to higher-than-before stresses indicate that concomitant nondestructive inspection techniques are needed to assure material soundness.

(3) By way of background, a brief historical review is in order. In the early part of this century, artillery shell were produced by forging with excess metal on all sides, then machining all surfaces, inside and out. Inspection was visual. The machining process in itself removed defects and the relatively smooth, clean surfaces existing after machining facilitated visual detection of defects. With the evolving political situation in 1938, it became evident that faster, more efficient production methods would be required. New forging procedures, involving either upset forming or pierce and draw techniques, allowed production of shell interiors to near final size so that as-forged interior cavities could be used in the finished product. Visual inspection remained the primary inspection means. Frankford Arsenal personnel established a library of shell illustrating various types and degrees of interior cavity defects and conducted training of inspectors who were then active in contractor's plants, performing in-process inspections, from 1941 through World War II.

In 1943 magnetic particle testing of hardened steel armor-piercing projectiles (the 90mm, M318 and 76mm, M339) was introduced as an acceptance means on a 100% basis. Additionally, dye penetrant was used for inspection of non-magnetic material.

Not until 1960 was there a full, integrated nondestructive test plan for a projectile item, the 81mm pearlitic malleable cast iron mortar shell, M362A1. This was inspected 100% by magnetic particle testing at each of three stages in production, including the final machined condition. An automatic ultrasonic shear wave inspection, circumferentially directed to look for essentially longitudinal defects, scanned the entire side wall of the projectile body, and an internal hydrostatic pressure was applied to assure adequate physical strength. Both of these latter were also applied to every shell.

In 1969, Francis I. Baratta of the Army Materials and Mechanics Research Center, Watertown, MA, published AMMRC TN69-05, Fracture Mechanics Approach to the Design of Projectiles." This was the first discussion of such applications. In 1976, two reports were published at Frankford Arsenal: "Fracture Mechanics Study of 105mm M1 and 8 in. M106 Projectile" by Joseph H. Mulherin, Carl M. Carman and Paul D. Flynn, and "Fracture Mechanics Study on 155mm M107 Projectile made from Isothermally Transformed HF-1 Steel" by Joseph H. Mulherin, William B. Steward and John D. Corrie. The era of modern, quantified - defect inspections was upon us. Since then similar studies have been made of a number of other shell; the procedure is an essential design and testing element.

(4) In determining the degree of inspection to be applied, the following elements must be considered:

a. The configuration of the item, taking cognizance of all aspects of shape: wall thickness, tapers, steps, threads, stress concentration points.

b. The environments in which the item must function: launch stresses, twist ratios and operational temperature extremes.

c. Fracture mechanics studies provide essential data on which to base acceptance/rejection criteria.

d. The interface between the shell interior and the high explosive (H.E.) fill must be assessed, considering the potentially critical nature of sharp projections into the cavity or circumferentially oriented tears which could be filled with H.E. and pinched by set-back forces during firing, possibly initiating a premature explosion in the bore of the gun.

(5) ARRADCOM has adopted the following philosophy:

> "Develop an inspection plan that has the highest reliability of preventing critical defects from reaching the stockpile by eliminating human interpretation and utilizing the most effective state-of-the-art inspection techniques."

(6) Illustrative of the changes which were noted at the opening of this discussion are the examples shown in this figure. Note that in each caliber there is a trend to higher strength material with lower elongation. These trends are imposed by the needs for greater range and lethality as required by the troops in the field.

(7) Greater stresses are imposed on the shell by the increasingly hostile environment to which they are subjected: increasing gun pressures, shell accelerations, travel in the gun tube and twist ratios (from one turn in 25 calibers of length to 1 in 20).

(8) The application of fracture mechanics to shell design and inspection has added a new dimension. Until such information was available, the objective of shell inspections was to eliminate all defects. However, the methods used - visual, dye penetrant and magnetic particle - all were dependent on the visual acuity and continual alertness of the inspector. Studies have shown such methods, under ideal conditions, to be on the order of 85% effective. Additionally, these techniques do not allow of quantification of the indications.

Utilization of fracture mechanics procedures enables definition of critical crack sizes throughout the projectile body. Armed with such knowledge, it becomes incumbent upon the quality community to assure that no shell containing cracks of critical or larger size reach the stockpile and field for use. Thus the inspection equipment design engineer must select the inspection technique or techiques which have the capability to automatically detect and quantify the defects of interest. By using an adequate safety factor in the inspection process, one can assure the integrity of accepted shell. The design of the equipment should include fail-safe provisions so that either the operation will be stopped or all inspected product will be rejected in the event of equipment or power failure. In other words, the reliability of the equipment operation must be very high. Thus the new procedures lead to more reliable inspections and safer projectiles in the field.

(9) The procedures for designing an inspection are illustrated with the body of the 155mm projectile, XM795, as an example. A stress map of the projectile body is constructed by inserting strain-gage measurements and calculations of stresses from firings and rough handling tests into computer programs for finite element analysis. These take into account shape factors of the shell, including stress risers, and basic material properties such as the modulus of elasticity.

(10) Experimental determinations are made of the material yield strength and plane strain fracture toughness. The primary method for measuring K_{1c} utilizes either a "compact tension" or a "bend bar" specimen per ASTM E399-72. For incorporation into a technical data package (TDP) of a requirement to monitor material toughness, the simpler precracked Charpy specimen is subjected to the slow bend to failure method. Results from the latter are quite satisfactory for the monitoring function.

(11) Four crack models are predicated: internal corner, edge, through-the-thickness and surface. The latter is the most prevalent; a ratio of length to depth of ten, minimum, is taken as conservatively representative of that condition usually seen in natural cracks. Actual production cracks generally are much longer; the resultant difference in calculated depth of a critical crack is insignificant.

(12) The values of applied stress, σ; yield strength, σ_{ys}; K_{IC}, plane strain fracture toughness and E, modulus of elasticity, are used in these equations to calculate the critical surface crack size at each point of the shell.

(13) The equations for the other crack models are considerably less complex. After all needed calculations are completed, a critical crack map can be drawn.

(14) Here one can see the most critical locations and, indeed, the requirements over the entire shell body. Note that in some areas the critical crack is through the wall.

(15) Next, the cracks which will be eliminated by applying a hydraulic pressure test, or hydrotest, are calculated. The pressure level is taken at that which will cause a stress not greater than 75% of the yield strength of the material at any point. The distributions for the XM795 shell are shown in these sketches.

(16) Finally, it has been taken as a matter of policy that through-the-wall cracks will not be tolerated. The minimum acceptable quality level has been rather arbitrarily taken as the smaller of 1/4 the wall thickness or 4.0mm minimum or, circumferentially, 2.5mm minimum aft of the largest interior diameter. The latter is controlled more closely because of the concern that interior circumferentially oriented tears might trap high explosive which could, on firing, pinch and initiate an in-bore premature explosion.

(17) This next chart puts all the previous information together. The areas requiring inspection for critical flaw size, shown with section-lining, are inspected by ultrasonics. Those areas which are satisfactorily covered by hydrostatic pressure testing (where the crack size screened by the hydrotest is equal to or smaller than the critical crack size or the minimum acceptable quality level, as appropriate) are shown by the crosshatching. The solid colored areas are those in which the controlling analysis is the minimum acceptable quality level; these areas are also inspected ultrasonically. In practice, it is normal to extend the ultrasonic inspection to cover all areas of the projectile; all areas of the side walls are generally scanned by at least two transducers looking both circumferentially, for longitudinally oriented

cracks, and longitudinally, for circumferentially oriented cracks. This redundant inspection provides added assurance of a high outgoing quality and experience has shown that the overall scrap rate is not adversely affected.

In another case, involving the 155mm M549 warhead, which is not too much different from this shell, an eddy current inspection for cracks is added to the first 3/4 inch of the nose outside diameter. This is done because the NDT must be performed after nose I.D. threading has been completed; thus the ultrasonic test is significantly degraded, since a 45° shear wave inspection is used.

(18) Some discussion of ultrasonic inspection standard design is in order, since this has been an area of major concern, involving significant problems. The limited amount of available data for artillery shell, relating U/T signals from machined notches or grooves to signals from natural cracks indicates that a worst-case ratio of one to four exists. That is, for a critical crack of depth a, the U/T standard notch should be a/4 deep. The original design chosen for the notch was a "thumbnail" shape, essentially equivalent to the semi-elliptical shape of the fracture mechanics studies. The depth was taken at a/4 and, since the length to depth ratio of ten was a minimum value, the notch length was taken at 20(a/4), or 5a, to make manufacturing easier (anticipating use of a saw or grinding wheel). The resulting notch area, in combination with an ultrasonic beam (applied by the contractor) on the order of 1-1/2 inches long, produced a system excessively sensitive to long, shallow discontinuities, such as draw marks, which are found in as-forged surfaces. The approach has been modified to make the notch (or a continuous, 360° groove for circumferentially oriented defects) a minimum of 10a long, with depth constant at a/4. In all cases the sound-reflecting side walls are held closely perpendicular to the surface which they intersect.

(19) It has been found to be equally essential to control the ultrasonic beam width at each inspection point. The relationship of beam width to notch length, taking into account the existence of a spiral scan for longitudinal cracks, is shown. The beam cannot exceed the notch length less the scan pitch. This assures a correct sensitivity setting.

(20) Production of standard notches has presented some significant problems. Original designs of the thumbnail notches called for widths of .008 inch with depths ranging from .010 to .040 and corner radii of .001" maximum. Initially, only one shop was found with the capability to produce such notches and the cost was extremely high, on the order of $250.00 per notch. Inquiries were made, concerning the effect of larger radii on the reflected

signal. Several industry experts as well as the National Bureau of Standards were contacted. It was the unanimous opinion that increasing the radius to .002" or .003" would have virtually no effect; however, no one had any data to support the opinion. Nonetheless, in order to broaden the production base for standards, the width was increased to .025" ± .005" and the radius to the greater of .0035" or 0.1 x depth. The wider slot facilitated making casts of the slot which can be inspected on an optical comparator. Using electric discharge machining (EDM), a first-class precision machine shop with modern equipment can reliably meet these requirements.

(21) Experience to date in applying sophisticated automatic nondestructive inspections to ammunition metal parts indicates the essentiality of conducting a thorough application study before implementing the NDT into production. Such a study must include assembly of sufficient equipment to inspect a statistically significant number of shell to demonstrate the problems which are likely to be encountered and to make the changes necessary to avoid those problems in production inspection.

A final requirement is the ultimate assessment of what the inspection system really does. This reliability study will involve shell rejected at the established production reject level and at several steps of greater sensitivity, perhaps 10, 25 and 50 percent greater than normal. Such rejects, after careful nondestructive characterization, must be sectioned to reveal the actual depth of the natural cracks. Thus the correlation between the ultrasonic or eddy current signals from machined standard notches or grooves and the signals from natural cracks can be established. In this manner, the reliability of the equipment to detect and remove from production material containing critical cracks will be determined. A program to do this for the 155mm M549 warhead body has been under way since the beginning of November 1979. A final report on this work is expected by January 1980.

(22) The effects of such work are far-reaching. As more intensive inspection is applied to the product, the producer is pressured to improve his processes in order to reduce scrap rates; ultimately the result is safer ammunition supplied to U.S. Army defense forces.

US ARMY ARMAMENT RESEARCH AND
DEVELOPMENT COMMAND
DOVER, NEW JERSEY

PRODUCT ASSURANCE DIRECTORATE

FIGURE 1

NEW TEST & INSPECTION BURDENS

- TIGHTER TOLERANCES
- HIGHER PRODUCTION RATES
  - AUTOMATED PRODUCTION
- COMPLEX ELECTRONIC DEVICES
- HIGH-STRENGTH, BRITTLE STEELS IN AMMUNITION

FIGURE 2

HISTORICAL BACKGROUND

- PRE–1939. VISUAL INSPECTION OF FULLY MACHINED SHELL
- 1939. INTRODUCTION OF AS-FORGED CAVITIES, DEVELOPMENT OF VISUAL STANDARDS
- 1943. MAGNETIC PARTICLE TESTING, ARMOR PIERCING PROJECTILES
- 1960. APPLICATION OF 100% TESTING
  - MAGNETIC PARTICLE
  - ULTRASONIC
  - HYDROSTATIC
- 1969. FRACTURE MECHANICS STUDY ON PROJECTILES PUBLISHED
- 1976. CRITICAL CRACK SIZES APPLIED TO SHELL DESIGN

FIGURE 3

ITEM REQUIREMENTS

- CONFIGURATION
- SYSTEM ENVIRONMENTS
- FRACTURE MECHANICS
- H/E PROJECTILE INTERFACE

FIGURE 4

STATEMENT OF PHILOSOPHY

- DEVELOP AN INSPECTION PLAN THAT HAS THE HIGHEST RELIABILITY OF PREVENTING CRITICAL DEFECTS FROM REACHING THE STOCKPILE BY ELIMINATING HUMAN INTERPRETATION AND UTILIZING THE MOST EFFECTIVE STATE-OF-THE-ART INSPECTION TECHNIQUES.

FIGURE 5

MATERIAL CHARACTERISTICS
ARTILLERY PROJECTILE METAL PARTS

CALIBER	MODEL	PERIOD	MATERIAL	Y.S. (KSI MIN)	ELONG (% MIN)
105MM	M1	1917-DATE	AISI 1012 AISI 1018 AISI 1045	65	15
	M548 RAP	1965-1972	AISI 52100 AISI 4340	135	5
155MM	M107	1925-DATE	AISI 1050	65	15
	M549	1965-DATE	HF-1	135	4
	XM795	1977-DATE	HF-1	120	4
8 INCH	M106	1965-DATE	AISI 1040	70	12
	XM650	1977-DATE	HF-1	125	4

FIGURE 6

LAUNCH ENVIRONMENT FOR ARTILLERY PROJECTILES

CALIBER	PROJ	CHARGE	MAX CHAMBER PRESSURE (KSI)	ACCEL (1000 Gs)	CANNON	TRAVEL IN TUBE (M)	TWIST
105MM	M1	M67	45.0	17.6	M2A1/A2	2.07	20
	M1	XM200	56.1	22.0	XM205	2.79	20
155MM	M107	M4A1	42.0	10.9	M1/A1	3.07	25
	M549, XM795	M203	60.3	15.5	M185, M199	5.08	20
8 INCH (203MM)	M106	M2	48.1	10.6	M2A2	4.26	25
	XM650	XM188	48.5	11.2	M201	6.93	20

FIGURE 7

QUANTIFICATION OF CRITICAL DEFECTS

- PRE-FRACTURE MECHANICS
  - NO DEFECTS ACCEPTED
- POST-FRACTURE MECHANICS
  - CRITICAL DEFECT QUANTITATIVELY DEFINED

FIGURE 8

155MM XM795 SHELL BODY FIRING TENSILE STRESSES (KSI)

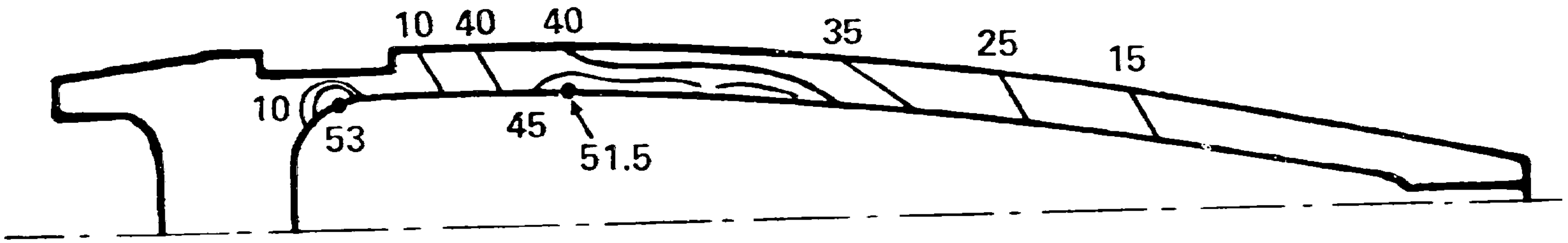

MATERIAL – HF1 STEEL
YIELD STRENGTH – 120

STRESS DIRECTION	HOOP	AXIAL
CHAMBER PRESSURE	60.3	6.2
ACCELERATION (G'S)	15,550	1,753

FIGURE 9

TEST SPECIMENS

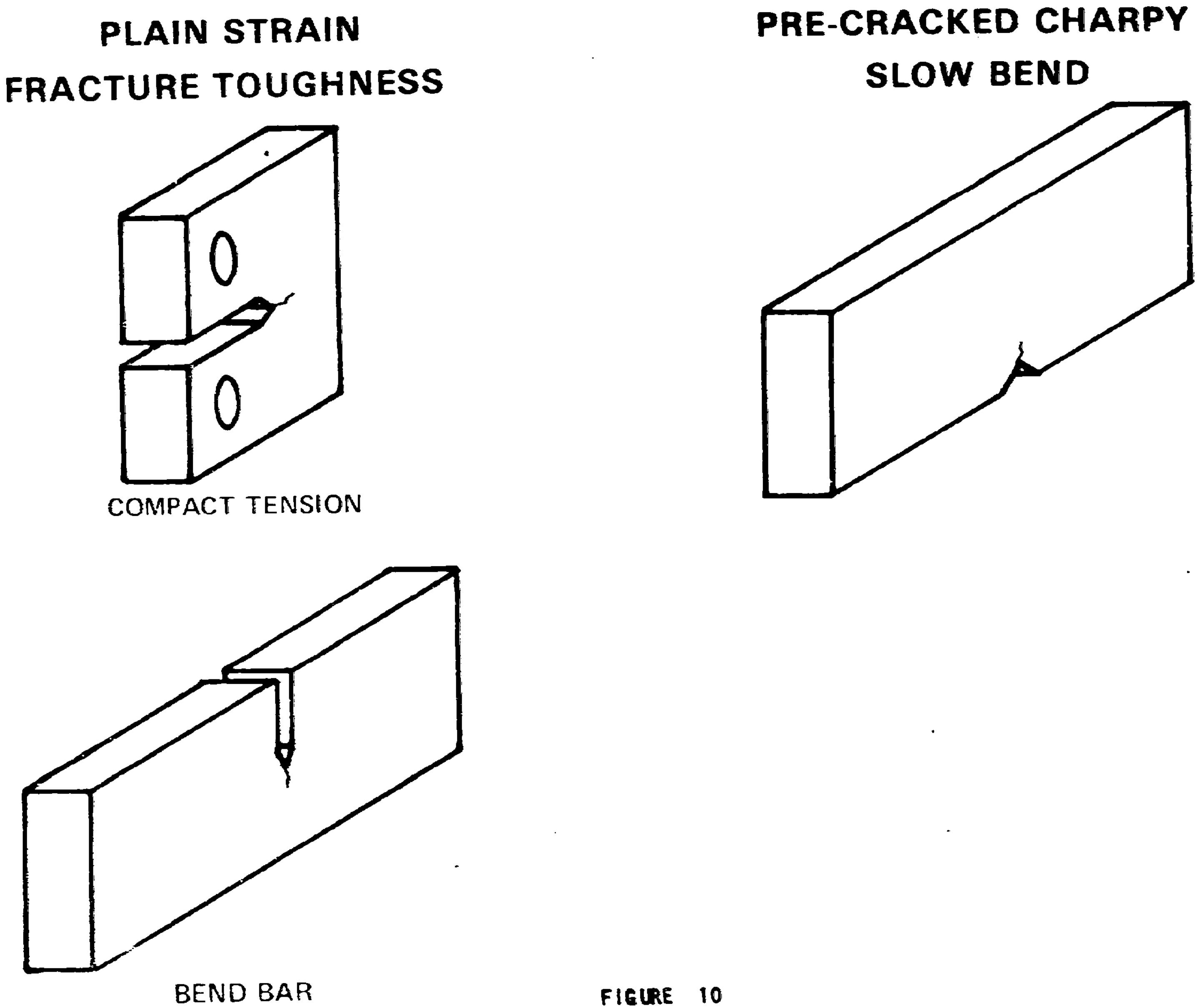

FIGURE 10

CRACK MODELS

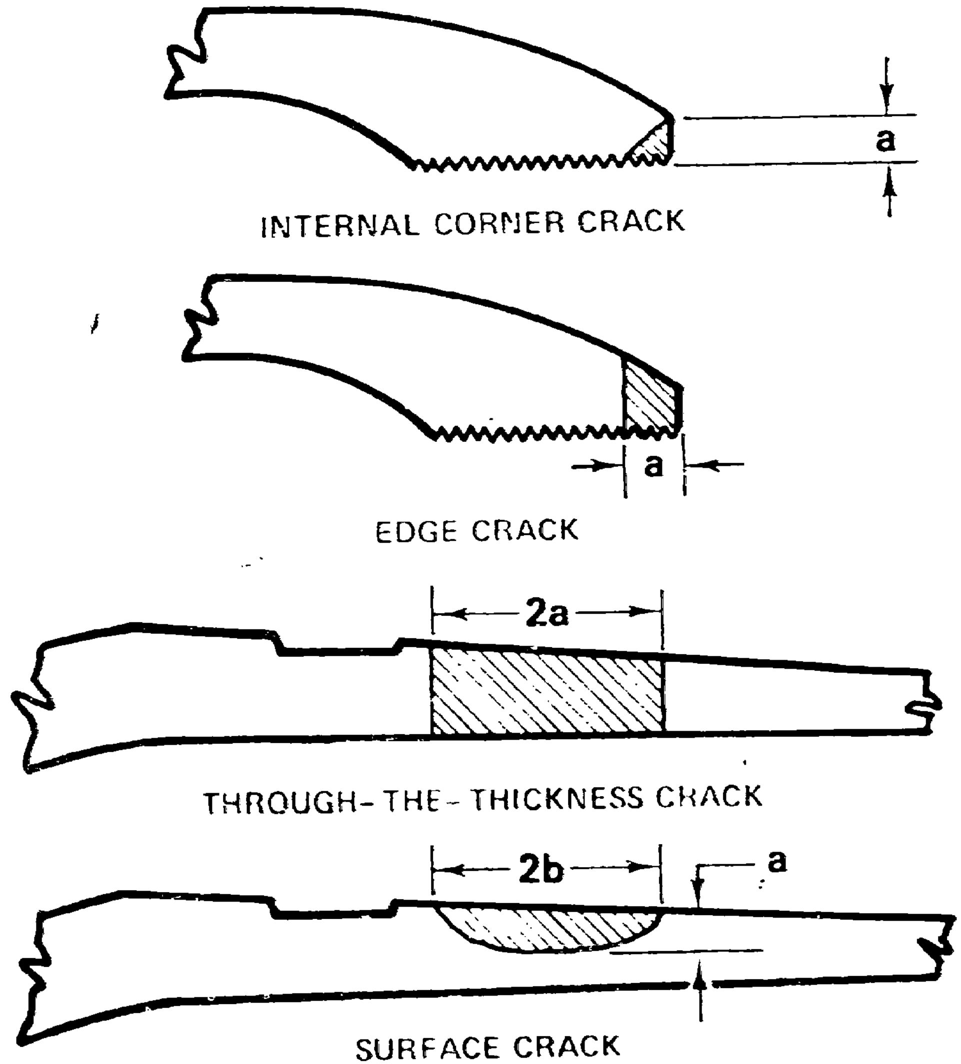

FIGURE 11

CRITICAL SURFACE CRACK SIZE

$$a_c = \frac{1}{\pi} \; {}^{-1}\tan \left[\frac{Q}{(1.1)^2} \left(\frac{K_{Ic}}{\sigma} \right)^2 \right]$$

Q = FLAW SHAPE PARAMETER
K_{IC} = PLANE STRAIN FRACTURE TOUGHNESS
σ = TENSILE STRESS NORMAL TO CRACK PLANE

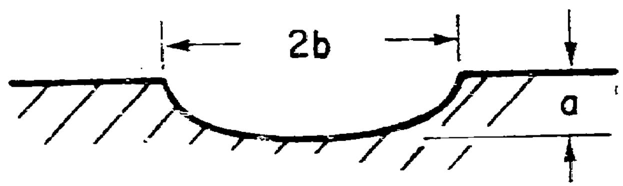

$$\frac{a}{2b} = 0.1$$

$$Q = E_k^2 - 0.212 \left(\frac{\sigma}{\sigma_{ys}} \right)^2$$

$$E_k = \int_0^{\frac{\pi}{2}} \left[1 - \frac{b^2 - a^2}{b^2} \sin^2 \theta \right] d\theta$$

(Q VS $\frac{\sigma}{\sigma_{ys}}$ AVAILABLE: TIFFANY-LORENTZ CHART)

FIGURE 12

CRITICAL CRACK SIZE

- THRU-THE-THICKNESS CRACK

$$a_c = \frac{1}{\pi}\left(\frac{K_{IC}}{\sigma}\right)^2 \left[1 - \frac{1}{2}\left(\frac{\sigma}{\sigma_{ys}}\right)^2\right]$$

- EDGE CRACK

$$a_c = \frac{1}{\pi}\left(\frac{K_{IC}}{1.1\,\sigma}\right)^2$$

- SEMI-CIRCULAR CORNER CRACK

$$a_c = \pi\left(\frac{K_{IC}}{2.56\,\sigma}\right)^2$$

FIGURE 13

XM795 PROJECTILE

CRITICAL CRACK DEPTHS (MM)

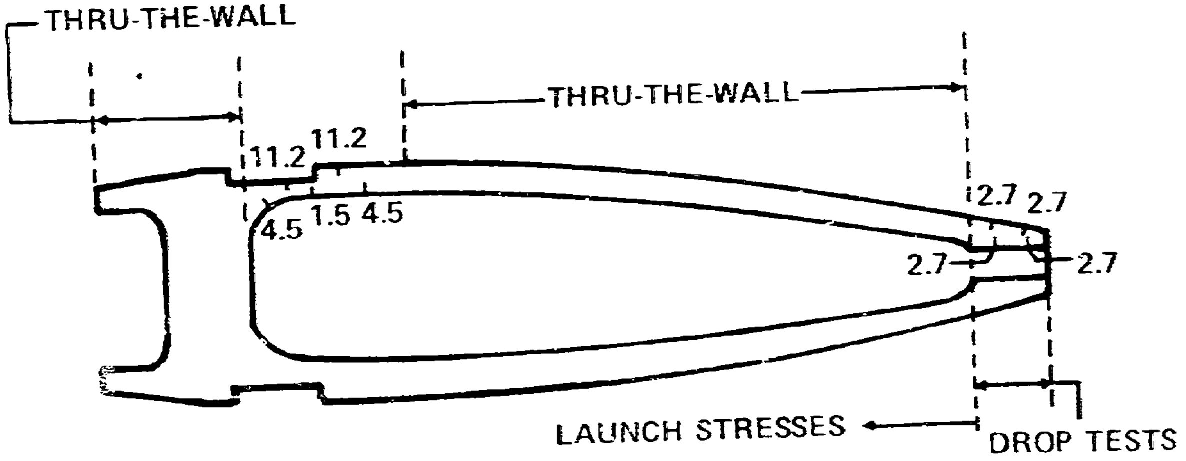

CIRCUMFERENTIAL CRACKS

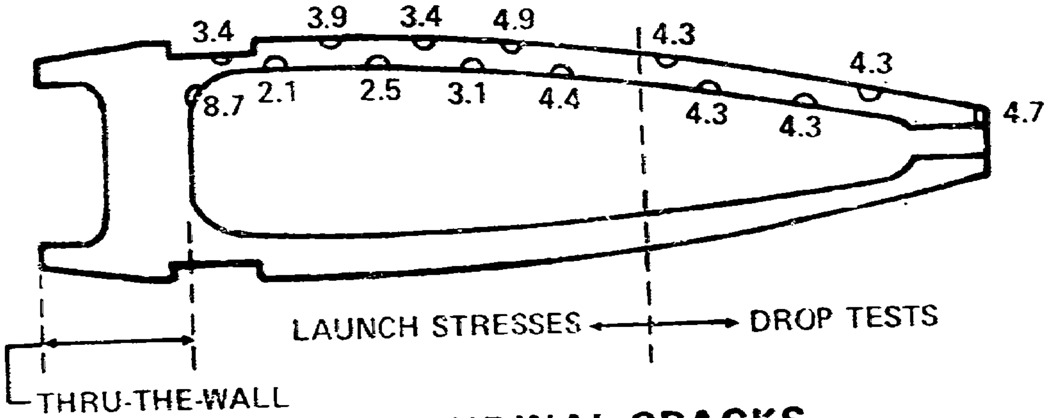

FIGURE 14

LONGITUDINAL CRACKS

XM795 PROJECTILE

HYDROTEST DETECTABLE CRACKS (MM)

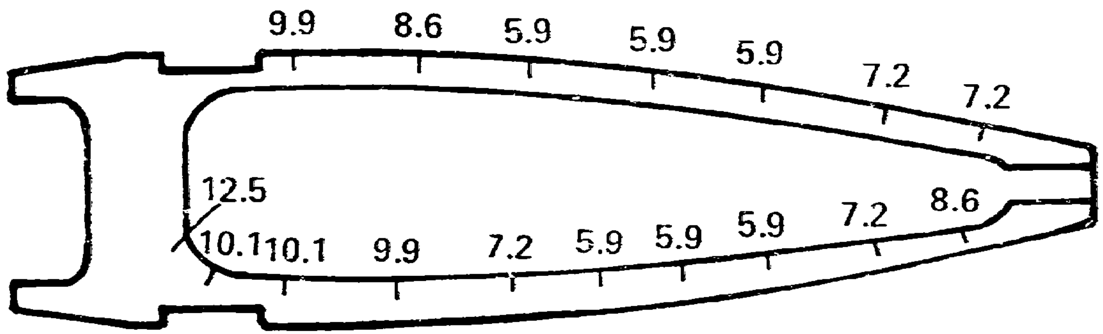

CIRCUMFERENTIAL CRACKS

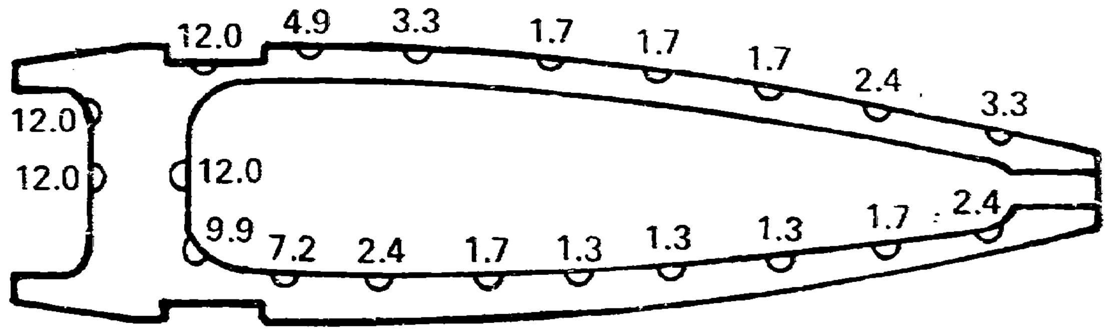

LONGITUDINAL CRACKS

FIGURE 15

XM795 PROJECTILE

MINIMUM ACCEPTABLE QUALITY LEVEL (MM)

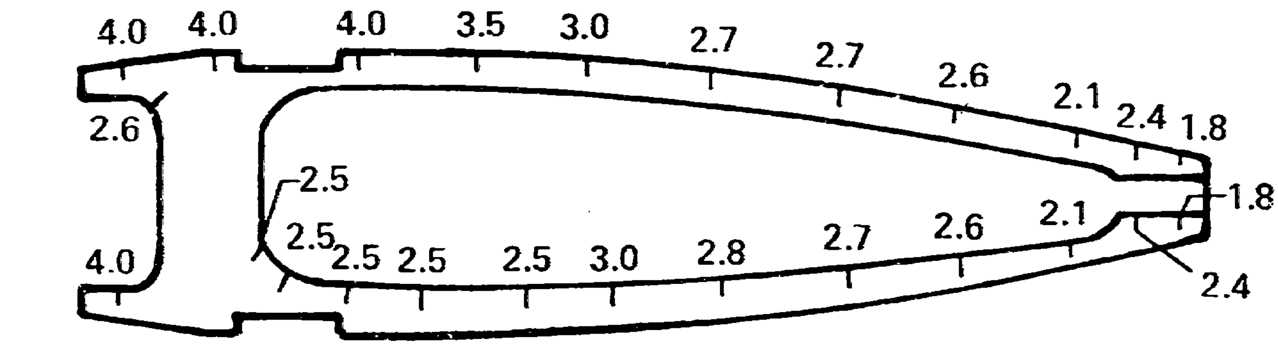

CIRCUMFERENTIAL CRACKS

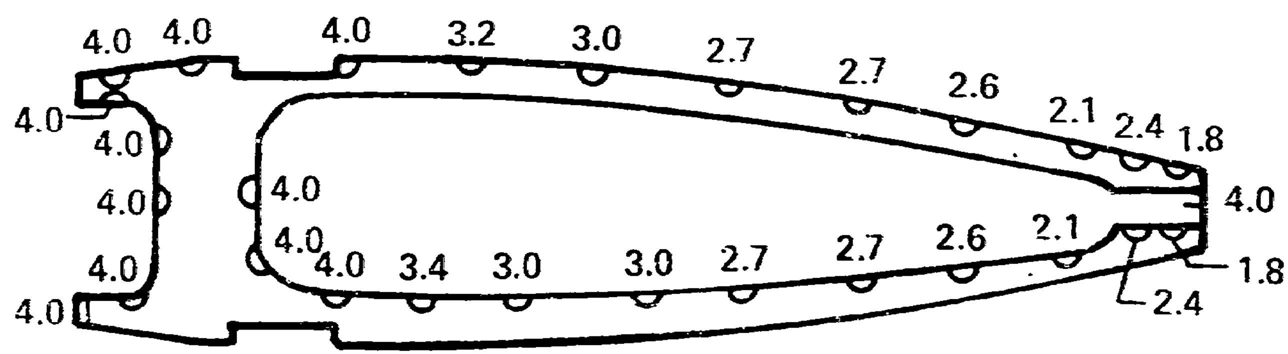

LONGITUDINAL CRACKS

FIGURE 16

ANALYSIS OF XM795 SHELL

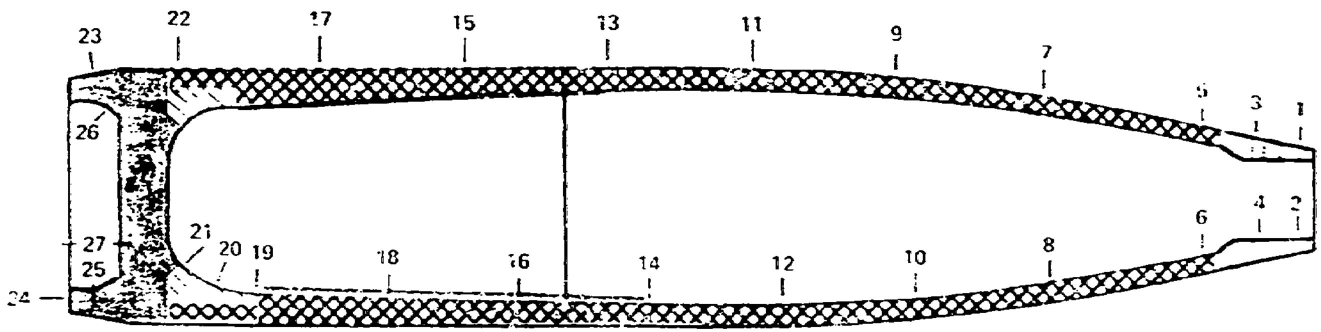

CIRCUMFERENTIAL LOCATIONS

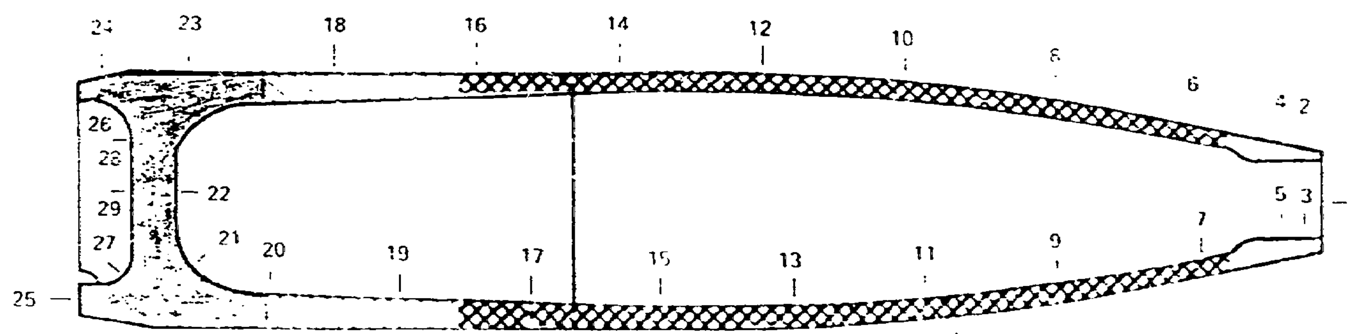

LONGITUDINAL LOCATIONS

CONTROLLING FACTOR	(TEST METHOD)	LEGEND
MINIMUM ACCEPTABLE QUALITY LEVEL	(ULTRASONIC)	Q_I
HYDROSTATIC PROFILE	(HYDRO)	H
CRITICAL FLAW SIZE	(ULTRASONIC)	C

FIGURE 17

ULTRASONIC STANDARD NOTCH DESIGN

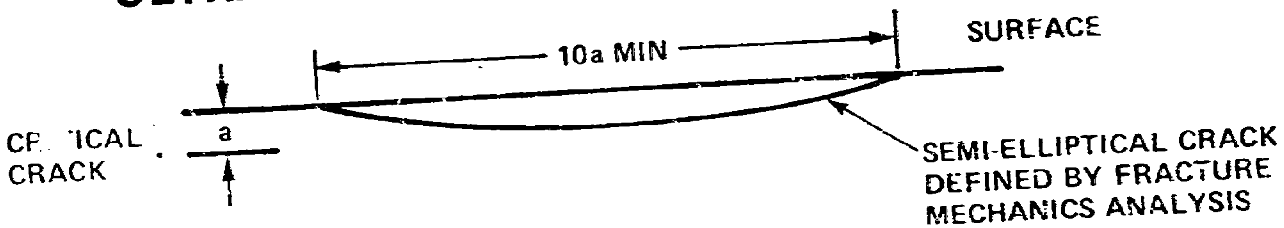

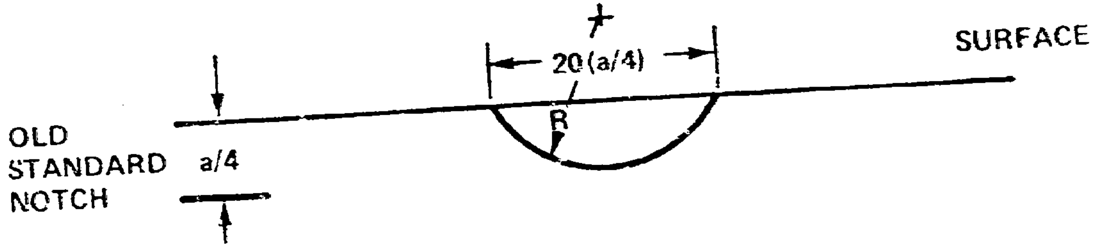

NOTE: THE a/4 IS BASED ON DATA SHOWING THAT THIS RATIO IS NEEDED TO ASSURE THAT NO NATURAL CRACK EXCEEDING THE CRITICAL SIZE WILL BE ACCEPTED BY ULTRASONIC INSPECTION

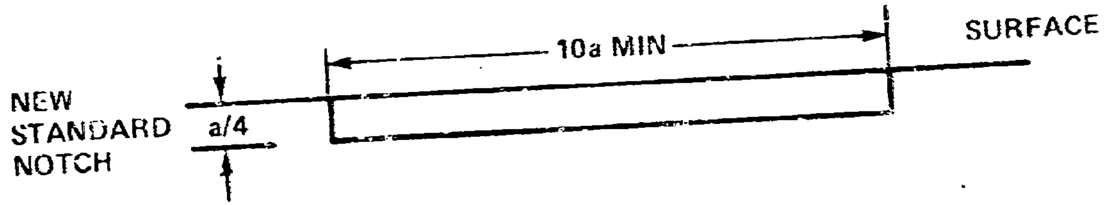

NOTE: THE PRIOR DETERMINATION TO USE A "THUMBNAIL" TYPE MACHINED NOTCH WAS AN UNWARRANTED EXTENSION FROM EARLIER DATA AND EXCESSIVELY STRINGENT

FIGURE 18

BEAM WIDTH DETERMINATION

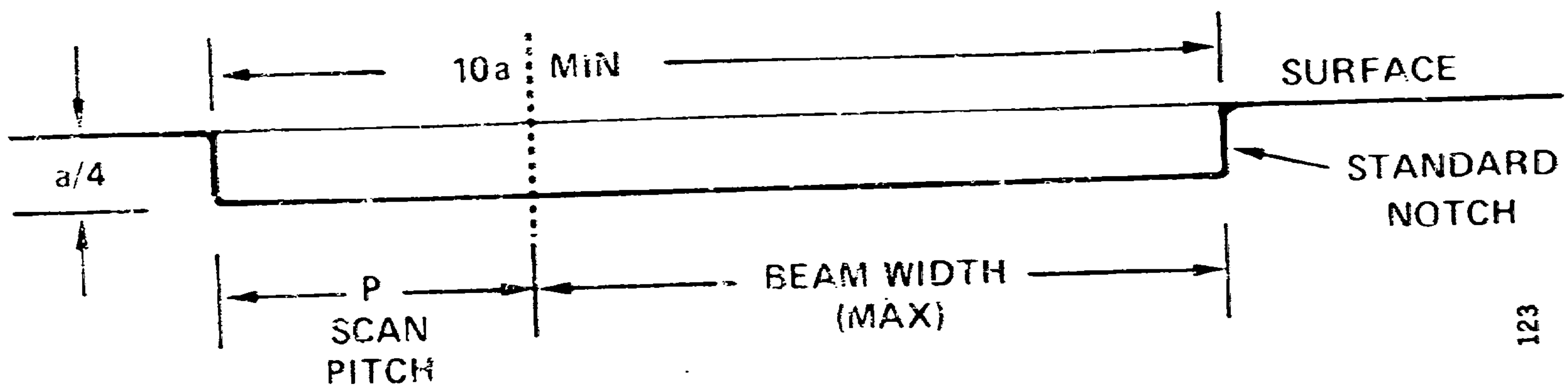

NOTE:

- THIS RELATIONSHIP IS ESSENTIAL TO ASSURE THAT A CRITICAL CRACK "a" DEEP AND A MINIMUM OF 10a LONG WILL BE REJECTED
- IT MAY RESULT IN REJECTING CRACKS "a" DEEP AND LESS THAN 10a LONG BUT OCCURRENCE OF SUCH CRACKS IS CONSIDERED TO BE OF EXTREMELY LOW LIKELIHOOD

FIGURE 19

ULTRASONIC TEST STANDARD NOTCH CROSS-SECTION

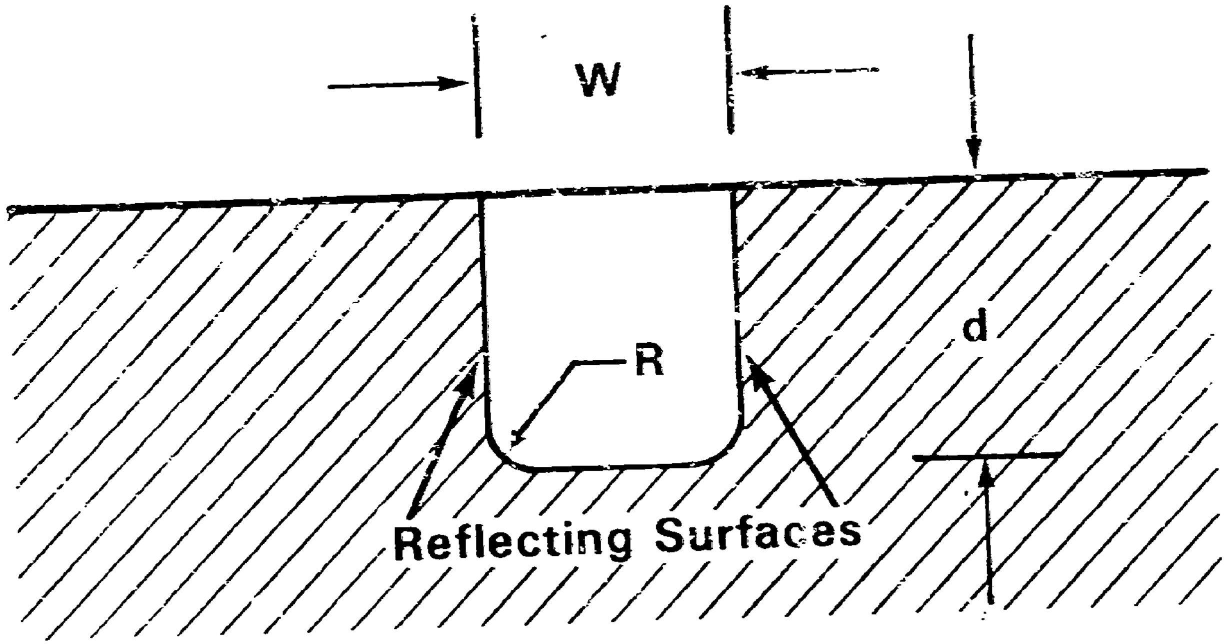

FIGURE 20

REQUIREMENTS FOR PRODUCTION NDT

- IN-DEPTH APPLICATION STUDY
- RELIABILITY STUDY

FIGURE 22

MORE INTENSIVE INSPECTION

↓

PRESSURE ON PRODUCER
FOR
BETTER QUALITY

↓

SAFER AMMUNITION
IN THE FIELD

FIGURE 23

"ACOUSTICAL SPECKLE INTERFEROMETRY"

John A. Schaeffel, Jr.
US Army Missile Command
GE&MS Directorate
Redstone Arsenal AL 35809
Phone 205-876-5692
Autovon 746-5692

ABSTRACT

If a continuous or pulsed wave of ultrasound is transmitted toward an object an echo will emanate from it. When the echo has a random spatial variation in relation to the object's geometry the variation is defined as acoustical speckle. If the object is deformed under an arbitrary set of loads the acoustical speckle will deform in a prescribed manner. An analysis is presented for utilizing acoustical speckle to determine interior and surface displacements of objects. Both pulse-echo and continuous wave scanning are treated in the analysis.

LIST OF SYMBOLS

Symbol	Definition
A_i	Wave amplitude
A_{iL}	Incident longitudinal wave amplitude
A_{rL}	Reflected longitudinal wave amplitude
C_{iL}	Media i longitudinal wave propagation velocity.

C_{is}	Media i shear wave propagation velocity
D	Distance from the liquid-solid interface to the acoustical reflecting-scattering layer
D_i	Distances over which acoustical waves are propagated
h_i	Distance for locating a receiver transducer
S_i	Wave amplitude energy ratio
Z_{iJ}	Acoustical impedance of media i for wave type J
α, β, ϵ	Angles
ρ_i	Density of media i

INTRODUCTION

Laser speckle interferometry is a relatively new and useful optical technique for examining the surface deformation of a body when subjected to an arbitrary load condition [1]. It has been widely applied to a variety of NDT problems with considerable success. The main drawback to using laser speckle interferometry appears to be that it is limited to measuring only the surface components of displacements in opaque bodies. For structures which have internal deformation or surface deformation inaccessible to an optical solution a requirment is dictated for another measurement technique.

Ultrasound has many analogies to light. Not only does it contain phase and amplitude information but unlike light it may be propagated into many optically opaque structures. If the surface of an object is insonified with ultrasound, structural irregularities in the object reflect and transmit the ultrasound. Due to the random arbitrary nature of an object's acoustical wave scattering structure, the structural irregularities both surface and subsurface act as an acoustical signature of the objects internal structure. For many objects the signature is spatially unique. If an object is displaced under some loading condition the acoustical signature shifts with the deformation. By examining the amount of shift in the signature, the surface or internal deformation of the structure may be predicted.

THEORY

Two possible configurations for mapping the acoustical echo from insonified bodies was investigated for use in acoustical speckle interferometry [2]. Figure 1 illustrates the two methods. In the pulse-echo mode, a pulse of ultrasound is sent from the transducer to the structure under investigation. When the ultrasonic pulse reaches the interface between the acoustical couplant and the structure a portion of the acoustical energy is reflected from the interface and the rest is transmitted into the structure. If substructure anomalies exist in the form of crystalline grain structure or inclusions, then they scatter the ultrasound and a reflected echo may be detected. In operation, the pulse-echo transducer is scanned over the structure in some region of interest. The echo return originating from some region in the structure is digitized as a function of space. The structure is then displaced under load and the echo return is again digitized. Using numerical correlation the amount of displacement is predicted between the loaded and unloaded conditions.

In contrast to pulse-echo scanning, continuous mode scanning utilizes separate transmitter and receiver transducers. By properly orienting the receiver transducer, the echo return from some level at or below the surface is recorded. The relative position of the two transducers remains fixed as the pair are scanned across the surface of the test object. As with pulse-echo scanning a mapping of the acoustical scattering medium in the structure is made before and after loading takes place. Numerical correlation of the two signals is then used to determine the amount of deformation between the two load conditions. The depth below or at the surface of an object where an acoustical echo originates in pulse-echo scanning is given by:

$$D = (t_s - t_1)\,\frac{C_{2L}}{2}$$

where,

D = depth below the object surface

t_1 = time at which a surface acoustical echo reflection is detected

t_s = time at which the echo from the region below the surface at D is detected

C_{2L} = longitudinal wave propagation velocity in the object

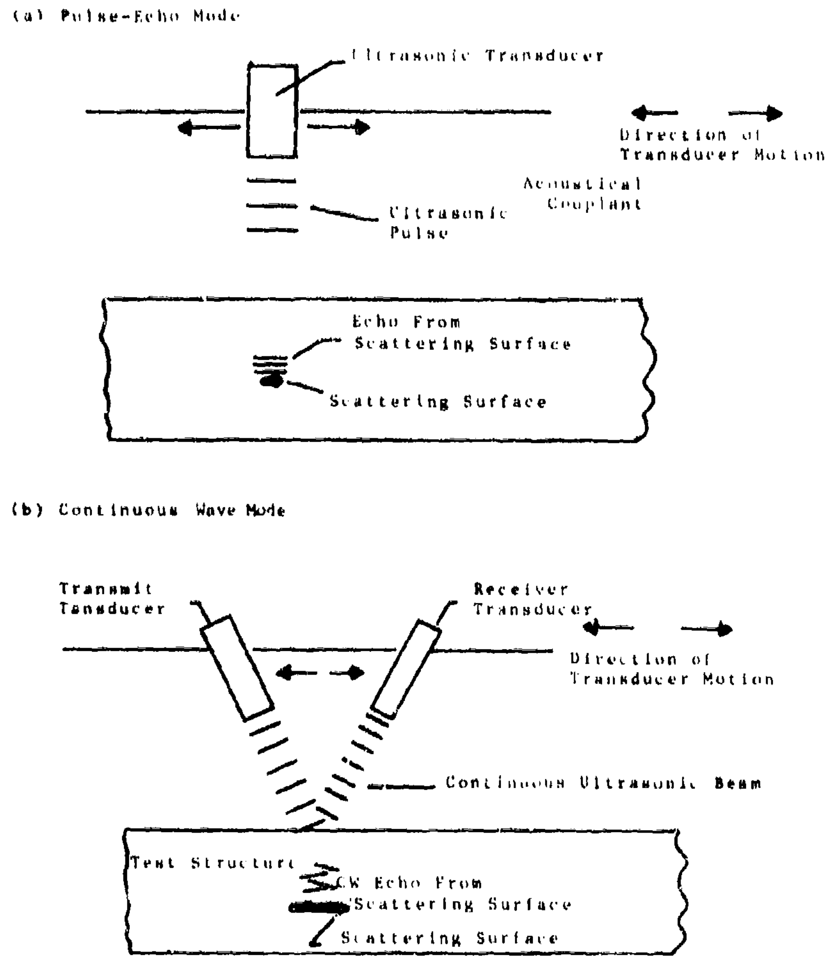

Figure 1. Geometry For Producing Acoustical Speckle Interferograms.

Continuous wave scanning does not require any time measurement but does depend on the orientation of the receiver and transmitter transducers to determine the depth D from which an echo is received. Figure 2 shows a sound-ray diagram of the wave propagation process. An ultrasonic wave of amplitude A_1 propagates along path D_1 and undergoes mode conversion at the solid-liquid interface into a shear wave of amplitude A_2, a longitudinal wave of amplitude A_5 and a reflected longitudinal wave of amplitude A_8. The transmitted ultrasonic waves transverse a thickness D of the solid to a reflecting-scattering layer. This layer for the purpose of the analysis is assumed to convert any incoming wave into either a pure shear or pure longitudinal wave which it reflects without energy loss back into the solid. Four possible waves result from this action: (1) a reflected shear wave A_3, (2) a reflected longitudinal wave A_4, (3) a reflected shear wave A_6, (4) a reflected longitudinal wave A_7. Each of these waves propagate to the solid-liquid interface and undergo mode conversion into waves of amplitudes A_9, A_{10}, A_{11}, and A_{12}. An analysis of the wave propagation process was performed [2] and the A_5 wave amplitude was found to be the most significant. For this case:

$$\sin\beta = \frac{C_{2S}}{C_{1L}} \sin\alpha$$

$$\sin\varepsilon = \frac{C_{2L}}{C_{1L}} \sin\alpha$$

$$D_2 = D_3 = D_6 = \frac{D}{\cos\beta}$$

$$D_4 = D_5 = D_7 = \frac{D}{\cos\varepsilon}$$

$$h_{12} = 2D_5 \sin\varepsilon \cos\alpha$$

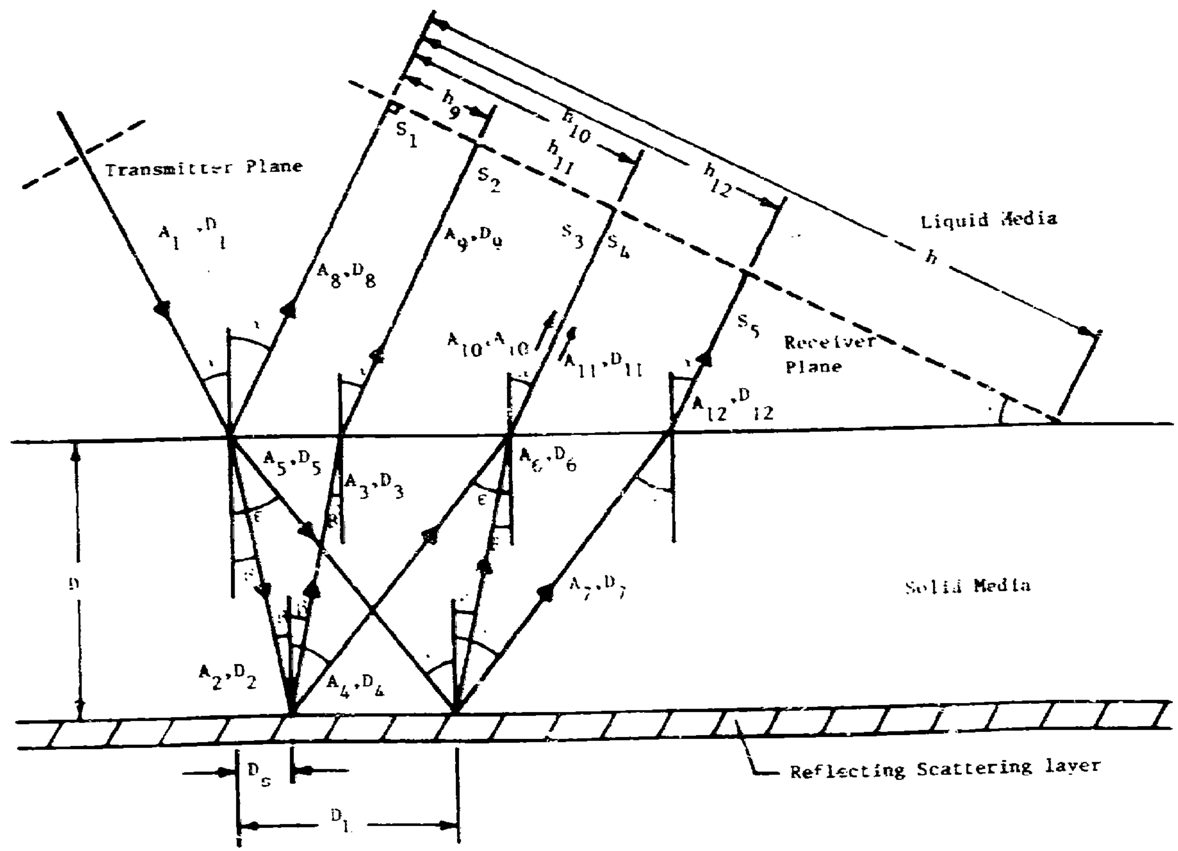

Figure 2. Ultrasound Wave Propagation In An LSL Interface.

The acoustical impedances are:

$$z_{1\ell} = \frac{\rho_1 \; C_{1L}}{\cos\alpha}$$

$$z_{2\ell} = \frac{\rho_2 \; C_{2L}}{\cos\varepsilon}$$

$$z_{2S} = \frac{\rho_2 \; C_{2S}}{\cos\beta}$$

The ratio of the received energy to the transmitted energy at the h_{12} position was found to be very dominant and is called the S_5 energy ratio.

$$\frac{A_7}{A_1} = \frac{\rho_1}{\rho_2} \, \frac{2z_{2\ell} \cos 2\beta}{z_{2\ell} \cos^2 2\beta + z_{2S} \sin^2 2\beta + z_{1\ell}}$$

$$\frac{A_{rL}}{A_{1L}} = \frac{z_{1\ell} + z_{2S} \sin^2 2\beta - z_{2\ell} \cos^2 2\beta}{z_{1\ell} + z_{2S} \sin^2 2\beta + z_{2\ell} \cos^2 2\beta}$$

$$\frac{A_{12}}{A_7} = \left\{\frac{\cos\varepsilon}{\cos\alpha \, \cos^2 2\beta}\right\} \left\{1 - \frac{A_{rL}}{A_{1L}}\right\} \frac{C_{1L}}{C_{2L}}$$

$$S_5^{*} = \frac{A_{12}}{A_7} \, \frac{A_7}{A_1} \, ,$$

$$S_5 = S_5^{*} \; S_5^{*}$$

Consider a transducer pair scanning over a solid as shown in Figure 3 from $X = X'$ to $X = X' + X''$. In general, the A_5 wave amplitude detected by the receiver will be a random variation of X. This variation is referred to as <u>acoustical speckle</u>. When the transducer pair crosses an inclusion located at $X = X'''$ a perturbation in the receiver echo signal occurs due to ultrasonic wave scattering. This effect is shown in graph (a). Now let the solid be displaced an amount ΔX and the transducer pair are again scanned as before. The perturbation will now occur at $X''' + \Delta X$ as shown in graph (b) of Figure 3. If the two signals shown in graphs (a) and (b) are cross correlated then ΔX may be determined.

Let a scan of the solid in a reference configuration be made from X' to $X' + X''$. N data points are sampled during the scan where $A_5(1) = A_5(X')$ and $A_5(N) = A_5(X' + X'')$. The increment between scan points is:

$$\Delta N = \frac{x''}{(N-1)}$$

Now the solid is displaced a distance

$$\Delta X = -r\Delta N$$

where r is an integer 0, 1, 2, ...
The solid is now scanned $M < N$ times from $X_a = X'$ to X_b, where:

$$X_b = (M-1)\Delta N$$

The new amplitude variation after specimen displacement is A_5' and $0 \leq r \leq N-M$. The least squares discrete correlation function is

$$C_D''(L) = \sum_{i=1}^{M} [\, A_5'(i) - A_5(i+L) \,]^2$$

$$0 \leq L \leq N - M$$

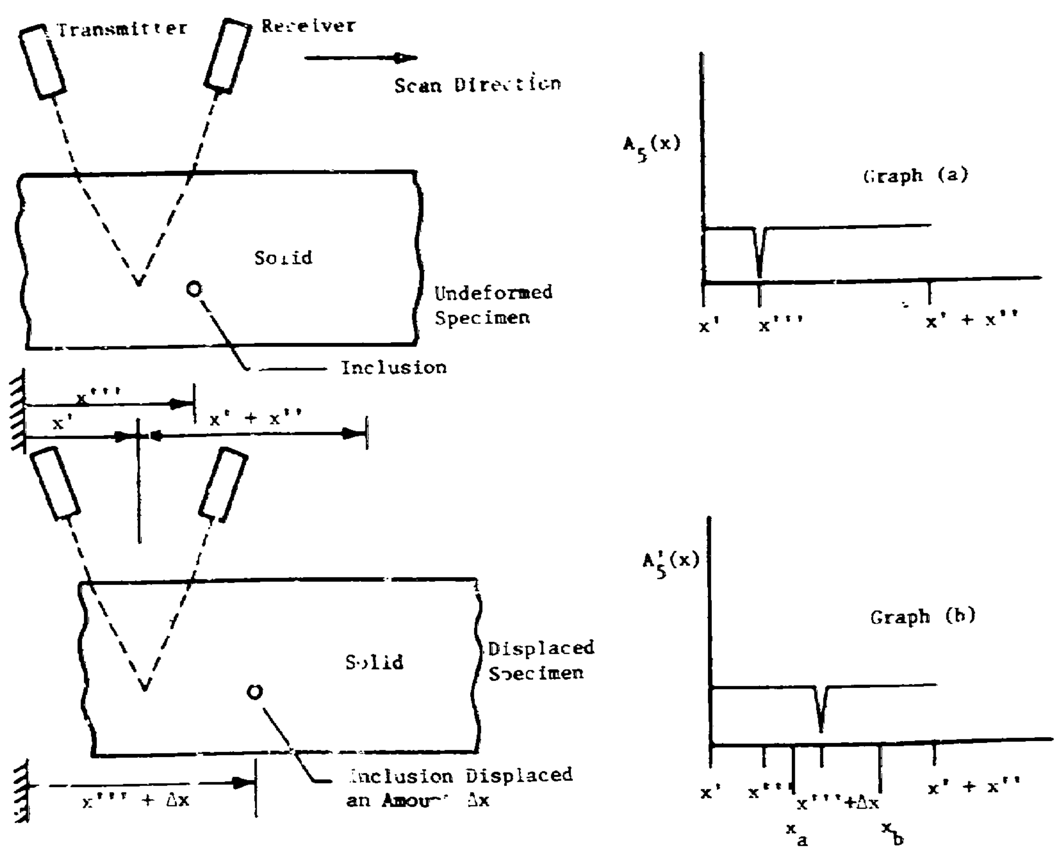

Figure 3. The A_5 Return Echo from an Undeformed and Deformed Solid Scattering Layer.

CD" will have a minima for L=r. If r is not an integer value for the displacement then the equation will interpolate to the nearest integer value. Therefore, displacements of $\pm\ \Delta N$, the sampling interval, can be measured.

RESULTS AND CONCLUSIONS

Many tests were performed to verify the theory and are presented in extensive detail in Reference [2]. Tests were conducted in both the pulse-echo and continuous wave modes using such materials as aluminum, slip-cast-fused silica and plexiglas. The theory was verified for both surface and subsurface deformation and is presented in much greater detail in the reference.

Figure 4 illustrates the results of measuring the displacement of a 51.56 X 22.35 X 11.43 mm plexiglas sample which was translated various distances. The surface of the sample was cut using a band-saw and served as an acoustical rough scattering surface for ultrasound. In the test the sample was scanned in the pulse-echo mode for X" = 2.54 mm using .0254 mm increments between scan points. The specimen was then displaced various distances and a second scan of 1.27 mm in .0254 mm increments was made. The two signals were then cross correlated and the results are shown in Figure 4.

Figure 5 shows the same specimen when the first scan length was 5.08 mm with .0508 mm scan increments and the second scan length was 2.54 mm with the same scan increment. This test was used to verify that the technique could predict displacements to within one scan increment. It should be noted that when the actual displacement was an integer multiple of the scan increment, the cross-correlation predicted displacement was exactly correct. However, when the actual displacement was not an integer multiple of the scan increment, the predicted displacement was rounded off to the nearest integer scan increment multiple by the correlation function.

The system hardware used to produce these results was not described in this paper for brevity but is documented in Reference [2]. The systems developed were found to be very accurate and could detect displacements to within $\pm$ .0254 mm. Pulse-echo acoustical interferometry was found to be sensitive to three dimensional motion while continuous wave acoustical interferometry was mainly sensitive to motion in the plane of the transducer pair. The technique was found to be a very reliable method of measuring both surface and subsurface deformation. Work is in progress to extend acoustical speckle interferometry to complex structural geometries and scattering-reflecting media.

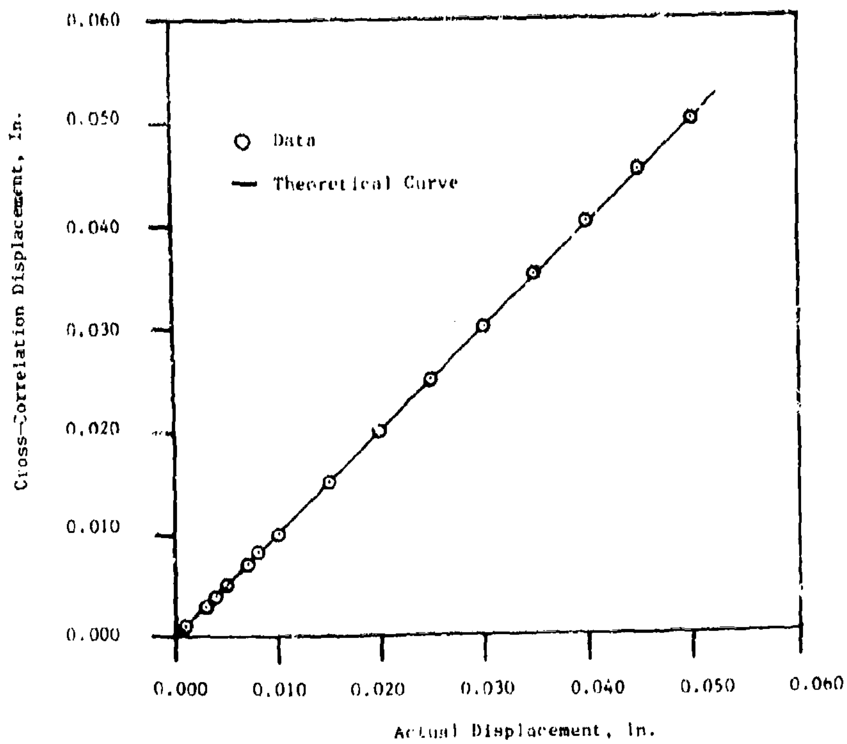

Figure 4. Displacement of a Plexiglas Specimen Determined By Pulse-echo Acoustical Speckle Interferometry.

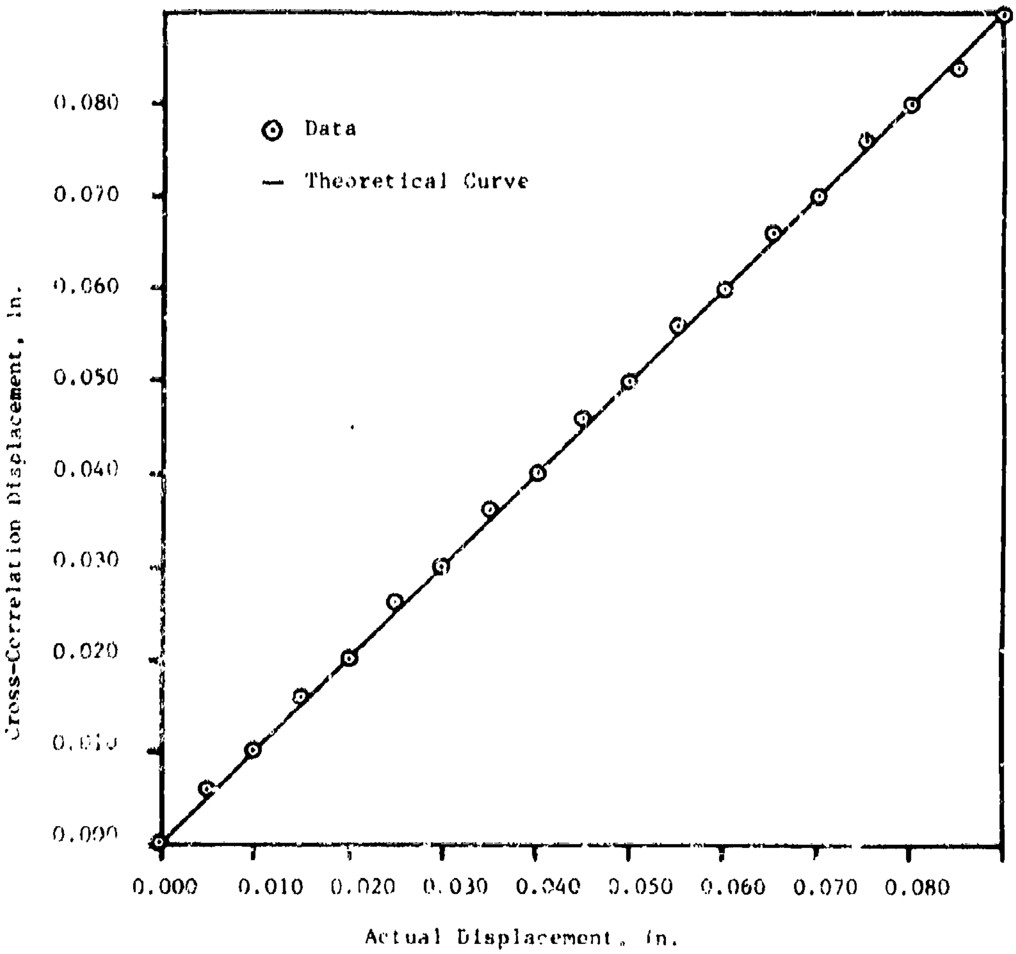

Figure 5. Numerical Round-Off Effects of the Correlation Function.

REFERENCES

1. Archbold, E., Burch, J.M., Ennos, A.E., Recording of Inplane Surface Displacement by Double Exposure Speckle Photography, Optica Acta, Vol. 17, No. 12, 1970, Pg. 883-898.

2. Schaeffel, J. A., "Acoustical Speckle Interferometry," US Army Missile Research and Development Command, Redstone Arsenal, Alabama 35809, March 1979, Technical Report T-79-39.

ULTRASONIC TIRE INSPECTION
FIELD EVALUATION RESULTS

Robert J. Watts
USATARADCOM
Product Assurance Directorate
Warren, Michigan 48090
Autovon 273-2849

ABSTRACT

This paper presents the program justification, background, and field results for the Product Assurance Directorate, TARADCOM, effort to evaluate a commercially available ultrasonic tire inspection equipment, the tire degradation monitor (TDM). Results from independent evaluations at Red River Army Depot (RRAD) and Yuma Proving Grounds (YPG) support ultrasonic tire inspection's potential for monitoring and controlling retread tire quality and for estimating the expected retread tire life. Details and analyses of data from the RRAD TDM evaluation verify a direct correlation between TDM measurements and the visual tire spreader inspection determination of a tire's unsuitability for retreading. Data from the YPG evaluation indicate that tires, which have an ultrasonic measurement less than forty percent of the equipment calibration point, fail more frequently and have a lower tire life expectancy than tires which have measurements greater than the forty percent calibration point. Despite favorable results, variability and anomalies of the YPG and RRAD evaluations' data warrent further investigation and control in a final Army evaluation at the Depot Activity at Ober-Ramstadt. With specific controls and TDM hardware modifications, the Ober-Ramstadt effort will provide documentation to determine the effectiveness of the TDM for pre and post retread tire inspection, to quantify the exact correlation between the digital ultrasonic tire reflection measurements and both tire casing quality and remaining expected tire life, and to identify the ultrasonic signal compensation or interpretation characteristics required for a military microprocessor based tire degradation monitor.

INTRODUCTION

The United States Government is the largest tire user in the country and the Army has the largest fleet within the Government. Under the centralized procurement system, the Army buys nearly all the tires for general purpose ground vehicles and the replacement tires for the Department of Defense. In each fiscal year (FY) the acquisition for Army totals in excess of 300,000 tires, both military and commercial types. This involves sums of approximately 7.4 million dollars for new tires and 7.2 million dollars for retreads. With regard to retreading, the Army retreads over 200,000 tires each year at a cost of about 50 percent of the cost of purchasing new tires. These statistics are used to illustrate and emphasize the importance that the Army as a user must place on the evaluation methods to measure reliability, durability, and safety, both for new tires and retreads.

PROGRAM JUSTIFICATION

There are some problems involved with retreading and the regulation on tire usage which justify the Army tire NDT program. In regards to Army tire usage, Army Regulation 750-36 mandates that at least 75% of replacement tires shall be retreaded tires. Field results have shown that the 75% figure is unrealistic because 24% of the tires are not retreadable due to damage from weather checking or ply separations. Of the remaining 76%, between four to eight percent will be rejected for various conditions such as sidewall damage, bead damage, too many required repairs etc. Therefore, the 75% figure is an idealized one and not obtainable. This premise is substantiated by the FY77 Army retread usage percentage of 69%.

Another retreading problem reported at the Fourth Symposium on Nondestructive Testing of Tires in May, 1978 relates to the low confidence shown by the military user regarding retreads. The military's lack of confidence in retreads has been substantiated during an Army evaluation of new vs retread tires at Yuma Proving Ground (YPG). The "NDCC Military Tire, New Vs Retread Test" (I) report summary contained the following information: "Failures of retread tires are significantly higher than for new tires. Carcass failures were four percent for new tires collectively and 27.6 percent for retreads. Road hazard failures were 14 percent for new tires and 16.6 percent for retreads. Combined, 18 percent of all new tires failed while 44.2 percent of all retreads failed." It must be pointed out that the YPG evaluation was an accelerated test with the tires operated in an extreme environment. Therefore, the ratio of retreaded tire failures to new tire failures (i.e. 2.5 to 1) becomes more relavent for tire life comparisons than the actual failure percentages. However, the casing failure comparisons still lend credance to the military users lack of confidence in retread tires. The NDCC report also documents the average mileage of the retread tires with casing failures as less than 50 percent of the tire mileage of the non-failed tire group. If the tires, which will fail, of the 69 percent of the total Army tire requirement met with retread tires could be identified and eliminated prior to retreading, tremendous savings could be realized and confidence in retread tires would be restored. However, only about 50 percent of the Army tire needs would then be met with retreads. This fact makes the 75 percent retread requirement imposed by AR 750-36 appear even more unrealistic.

As just eluded to in the previous statement, a large potential savings could be realized with a standard and effective nondestructive inspection system for evaluating tire casings prior to retreading or even before shipment to the retreading facilities. Remember that over 25 percent of the tires shipped to the retreading facilities at an average cost of over $220 per ton are found unsuitable for retreading. Of the remaining 69 percent of the Army tire requirement met with retreads, many of these fail prior to providing 50 percent service life. Both shipping costs and the retreading costs for these tires are partially lost due to the premature tire failures. The need for NDT tire inspection standards arises, therefore, not only because of the imposition of an unrealistic tire usage requirement and the lack of confidence in retreads, but for financial reasons as well.

The Army has evaluated various methods of nondestructive evaluation, such as x-ray, infrared, holography, and ultrasonics, and has concluded that ultrasonic tire inspection can solve many of the problems just presented. Through ultrasonic inspection, implementation of a low cost tire inspection equipment that is rugged, portable, simple to interpret and requiring a minimal of operator training appears realizable and able to be standardized. TARADCOM is at present testing an ultrasonic unit called the Tire Degradation Monitor (TDM) that measures the tire casing ultrasonic reflective signal strength during both pre and post retread tire inspection.

PROGRAM BACKGROUND

During the course of the Army program, tire degradation, a phenomenon which research has shown to be a fundamental mechanism of tire failures, was discovered. The first contact with tire degradation mechanism came during an investigation of moisture effects on tire retreadability. It was demonstrated that approximately 10 percent of nylon cord tires, which would absorb moisture into the ply area if directly exposed to water (from cuts or holes) had tire ultrasonic reflective signal differences from the 90 percent of tires which were not hygroscopic. Mechanical testing showed substandard cord and interply peel strengths for these 10 percent compared to the remaining 90 percent of the nylon tire population. In a subsequent program, during which 500 retread candidate tires were ultrasonically inspected, a sizable percentage (approximately 20 percent) of the tires demonstrated the same unusual ultrasonic characteristics. The ultrasonic reflective signal differences were fairly uniform around the circumference of the tire and thus seemed to represent a basic circumferential property of the tire, which was defined as tire degradation. Road testing of hundreds of military tires confirmed that indeed circumferential defects, tire degradation, can be correlated to ultimate tire failure and thus be used as a predictive tire inspection tool.

After these initial programs, the Army significantly curtailed its ultrasonic inspection program because of manpower and funding constraints. However, General American Research Division Inc. (GARD) continued on and developed the Tire Degradation Monitor (TDM) (Figure 1).

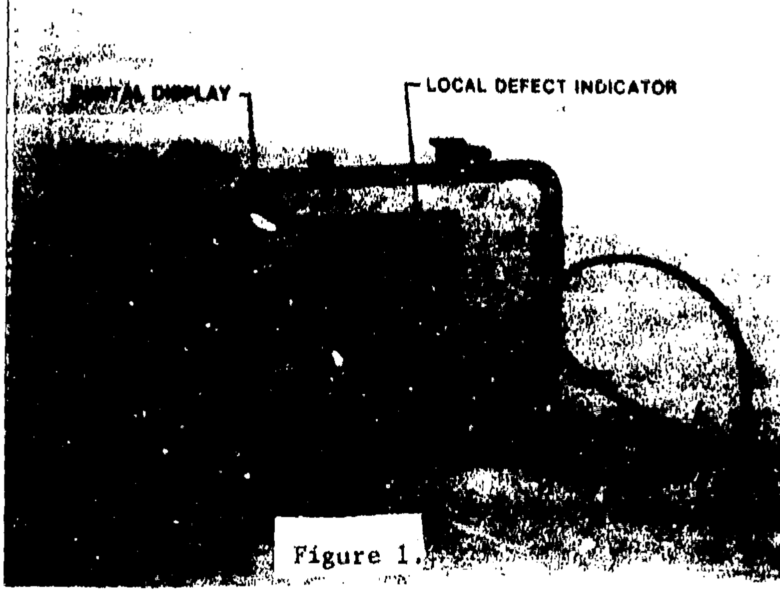

Figure 1.

The TDM, a portable instrument, measures degradation on a digital scale and can be used in conjunction with an oscilloscope to find a number of local types of defects. The unit consists of a transducer for both transmitting and receiving the ultrasonic signal, cabling, and electronics cabinet, which provides a digital display of the ultrasonic signal strength, red light indication of local defects such as separations or porosity and ultrasonic signal output to the oscilloscope.

FIELD RESULTS

For the past 24 months the Product Assurance Directorate, TARADCOM, has placed major emphasis on evaluating the commercially available tire degradation monitor (TDM). The efforts have been concentrated on a Red River Army Depot (RRAD) evaluation of the TDM and will now be directed towards an evaluation of the ultrasonic effectiveness in predicting remaining useful tire life at the Army Depot Activity at Ober-Ramstadt, Germany.

An evaluation plan for the Army Depot Activity at Ober-Ramstadt ultrasonic tire inspection program was prepared and coordinated with the Depot Activity. A preliminary checkout of the evaluation plan at RRAD was conducted, as just stated, as an evaluation in itself with extensive management control and data collection and analysis. TARADCOM report #12449 (II) documented the ultrasonic tire inspection data collected at RRAD with the commercially manufactured tire degradation monitor (TDM) and verified the existence of a direct correlation between the TDM ultrasonic tire measurements and the code H decision (i.e. the visual determination that the tire is unsuitable for retreading).

Before further discussion of the RRAD data on ultrasonic tire inspection, a brief description of the current visual inspection procedure is in order. Both in the field and at the retreading facility tires are inspected in accordance to TM9-2610-201-14 and are classified in accordance to a code system (i.e. code F for a repairable tire, code H for an unrepairable tire, etc.). At the retreading facility the inspection is performed with the tire mounted on a tire spreader. The inspection includes the identification of tire repair requirements, separations, extreme weatherchecking and numerous other tire tread, sidewall, bead and liner deficiencies. It is not intended that ultrasonic tire inspection eliminate the visual inspection but to supplement it.

Table 1 - INSPECTION RESULTS

Note: Total Number of Code H Tires Equals 349
Total Number of Retreaded Tires Equals 1140

TDM DIGITAL READING (N)	NO. OF CODE H TIRES W/READING ≤ N.	NO. OF RETREADED TIRES W/READINGS ≤ N	CORRECT TDM PREDICTION OF CODE H TIRES W/READINGS ≤ N
3	121	227	34.8
6	185	390	32.2

TDM DIGITAL READINGS	PERCENT CODE H IDENTIFIED	% OF CODE H TIRES W/DIGITAL READINGS > N	PERCENT OF TIRES RATED CODE H BY TDM %
3	34.8	20	38.7
6	53	17.7	49.6

The RRAD data (Table 1) showed that tire casings with low TDM measurements 0 to 40 percent of the TDM calibration point (in this case a TDM measurement of six) had a higher probability, 32.2 percent, of being visually classified code H, not suitable for retreading, than tires with readings greater than the 40 percent calibration point, 17.7 percent probability. The TDM, with accept/reject criteria set at the 40 percent calibration point, was able to identify 53 percent of the tires visually classified as code H.

During the course of the RRAD TDM evaluation, histograms (as shown in figures 2 and 3) and averages and standard deviations (Table 2) of the tire populations' (repairable or unrepairable) ultrasonic signals were maintained to assure control of the evaluation. Information depicted in figures 2 and 3 respectively gave overlay comparison of the ultrasonic inspection distribution of the code H1, weatherchecked tires, and code H2, tires with separations, to the ultrasonic inspection distribution obtained for the tires that were successfully retreaded. The histogram comparisons highlighted the difference in the ultrasonic signal strengths that were obtained from repairable and unrepairable tires.

Table 2 - STATISTICAL SUMMARY OF NON-"RED-LIGHT" INDICATING CASINGS

	AVERAGE μ	STD. DEVIATION σ	SAMPLE SIZE N
Code H1 - Weathercheck Damage	5.917±	4.540	(241)
Code H2 - Separation Damage	7.033±	4.953	(61)
Code accepted pre-retread	8.217±	4.992	(959)
Code accepted post-retread	9.414±	3.998	(995)

The RRAD TDM inspection results also supported a previous ultrasonic evaluation performed at YPG. Data from that evaluation indicated that tires which, again, had an ultrasonic measurement less than forty percent of the equipment calibration point, failed more frequently and had a lower tread life expectancy than tires which had measurements greater than the 40 percent calibration point. Although these two evaluations at YPG and RRAD provided positive results, uncertainties in remaining tire life prediction capability existed, and TDM hardware modifications required for the most effective military adaptation and application were identified.

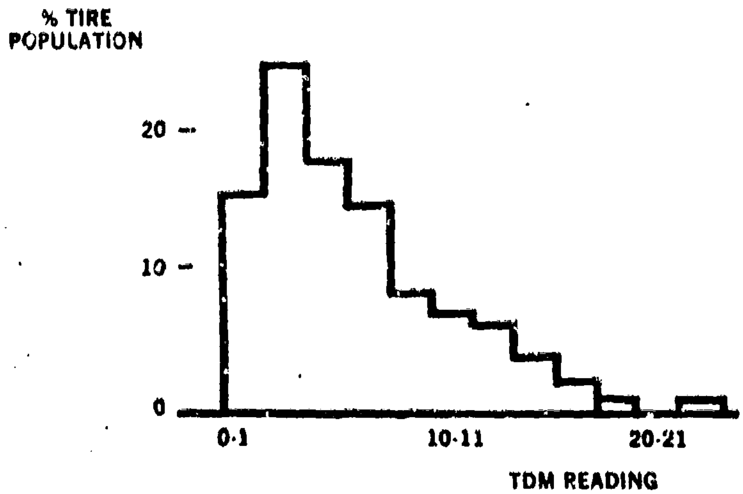

DISTRIBUTION OF TDM READINGS FOR CODE HI TIRES
DISTRIBUTION OF TDM READINGS FOR CODE ACCEPTABLE NON- "RED LIGHT" TIRES

FIGURE 2

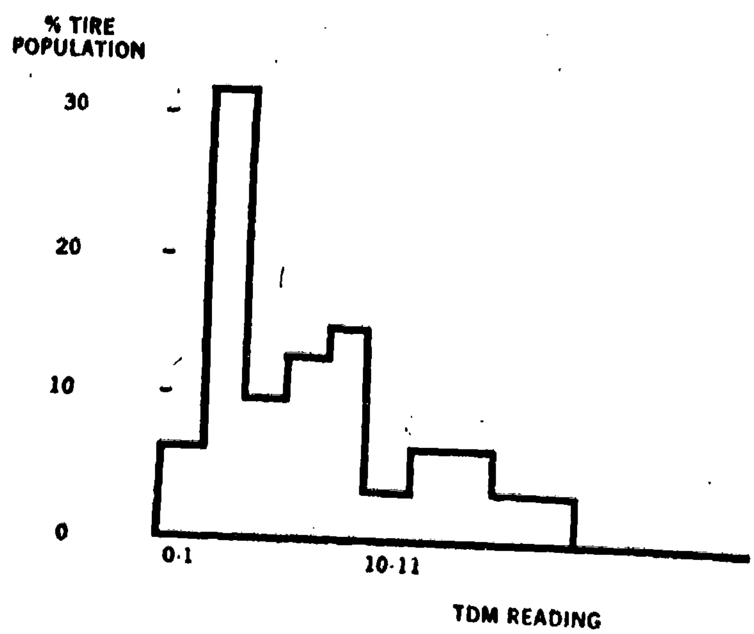

DISTRIBUTION OF TDM READING FOR CODE H2 TIRES
DISTRIBUTION OF TDM READINGS FOR CODE ACCEPTABLE NON- "RED LIGHT" TIRES

FIGURE 3

The RRAD evaluation results indicated that between approximately 38 to 49 percent of the tires turned in for retreading would have been rejected, designated code H, based on the combination of both ultrasonic and current tire spreader inspections. The visual tire spreader inspection code H designation percentage was approximately 24 percent. Therefore, for every 100 tires turned in for retreading an additional 14 to 25 tires would have been designated code H and would have been replaced by new assets. The imposition of this new assets requirement based on ultrasonic tire inspection appeared excessive with only the RRAD and YPG data as supporting information. However, what was not known from the data was the life expectancy of the additional 14 to 25 tires in a hundred that would have been rejected. If those tires failed prematurely or had low remaining useful life, then the ultrasonic inspection decision to reject them would have been justified. Tires from the RRAD evaluation were not followed through their field life, so their expected lives remained unknown. For a limited sample, 89 tires, from the YPG evaluation, 53 tires experienced either road hazard or casing failures. Of the 53 tires, 77 percent had ultrasonic measurements below 40 percent of the ultrasonic equipment calibration point.

The 77 percent correct failure prediction provides an initial guideline for the Ober-Ramstadt evaluation and will be closely monitored throughout the test. The determination of the expected remaining life of the tires with reflective ultrasonic signals of less than 40 percent of the TDM calibration point will also be made from data gathered from the Ober-Ramstadt evaluation because the tires will be monitored in the field until they fail or complete their service life.

The TARADCOM report #12449 on the RRAD evaluation also documents the requirement for a military adapted microprocessor based TDM. The first indicator of this requirement is pointed out in Table 2. The average ultrasonic signal, μ, for the post retread tire inspections is greater than that for the pre-retread inspection. By the theory of tire degradation it is assumed that the hot capping retread process should degrade the casing and a lower post retread inspection reading should be observed. This apparent data result anomoly requires further research to determine whether it represents a prognostic property of the retread failure mode or is due to a TDM hardware deficiency. Additionally, sources for ultrasonic tire reflective signal strength variations have been investigated and identified as:

(I) TDM calibration design limitation.

(II) Calibration standard blocks variations.

(III) Ultrasonic signal strength dependence on ambient temperature and on remaining tire tread rubber thickness, both of which change the tires attenuation of sound.

(IV) Tire type and construction effects on the ultrasonic signals.

It has also been determined from the RRAD evaluation that the TDM red light indication, by itself is <u>not</u> a valid indication of tire suitability for retreading. However, when used in conjunction with an oscilloscope, tire deficiencies (such as bondlines, separations, porosity, etc) can be identified. The interpretation of the signal patterns observed on the oscilloscope, as shown in figures 4 and 5, though, have proved too technical for the tire inspector. The interpretation task is made even more complex by the fact that the expected signal types will vary based on the type and construction of the tires. Typical signals from a steel belted radial tire are shown in figure 6. Clockwise from the upper left hand corner are the expected signals from a normal tire, a tire with a separation between the tread and first steel belt, a tire with a separation between the cord body and second steel belt and a tire with a separation between the two steel belts.

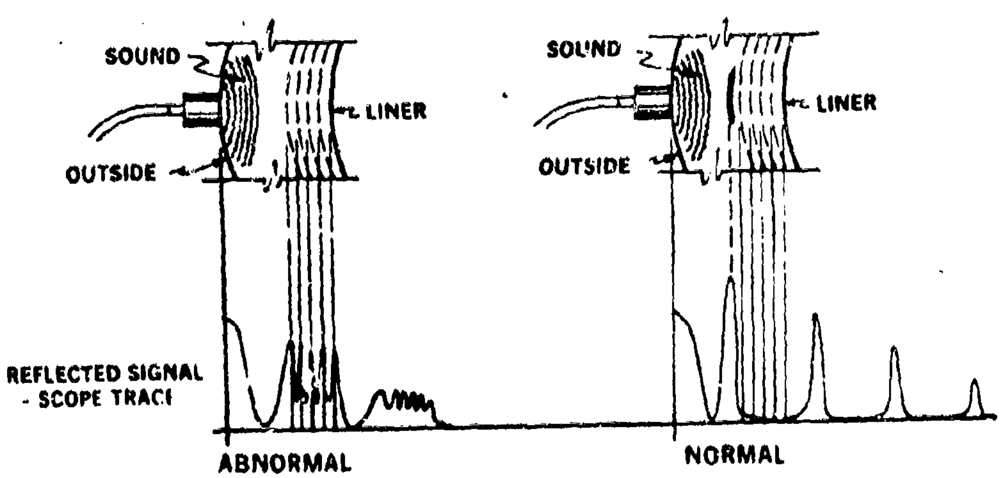

FIGURE 4 COMPARISON OF NORMAL TIRE ULTRASONIC SIGNATURE WITH INCORRECT TIRE — SEPARATION

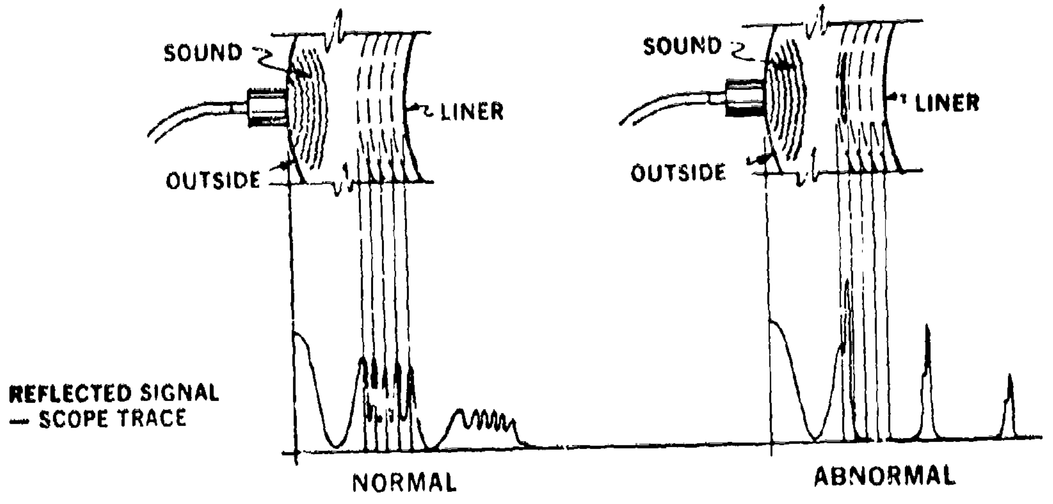

FIGURE 5 COMPARISON OF NORMAL TIRE ULTRASONIC SIGNATURE WITH INCORRECT TIRE — SEPARATION BETWEEN FIRST & SECOND PLIES

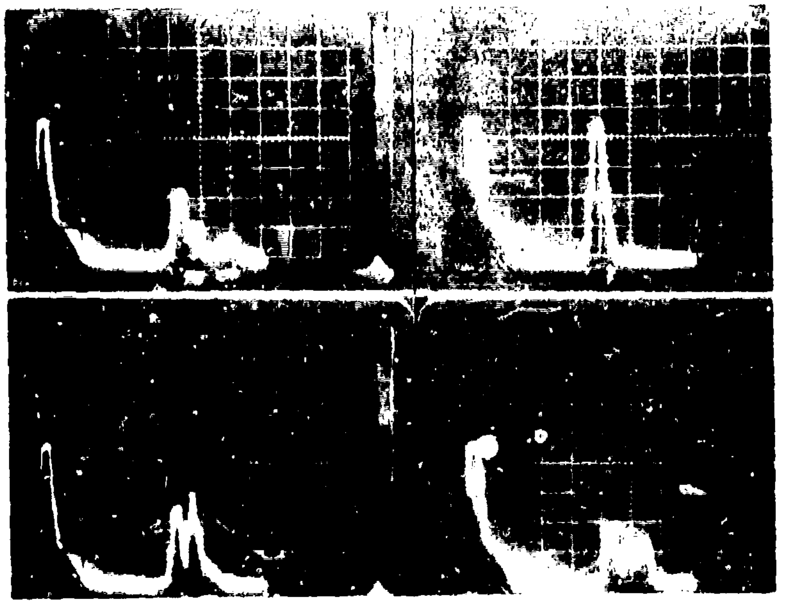

Figure 6.

As a result of the identification of these sources of tire inspection measurement variability and complexity of ultrasonic signal pattern interpretation, a new program has been proposed for FY's 81 and 82 to modify the TDM's. Besides being ruggedized for each major installations field utilization, the military adapted TDM's will be microprocessor based, self calibrating and preprogrammed to automatically compensate for ambient temperature and remaining tire tread depth. Operator dial settings to indicate tire type (textile or steel), relative size (passenger or truck) number of plys or belts, new or retread tire measurements and tire construction (bias ply, radial etc.) will also be provided to fully automate the interpretation of the ultrasonic tire reflection signal patterns. The data required to define the operational signal conditioning or interpretation characteristics will be collected during the Ober-Ramstadt tire inspection program.

The tire inspection evaluation at Ober-Ramstadt has been ongoing since June 1979. To date 246 of ultimately 1800 tires have been inspected, retreaded and fielded to Army units under a test agreement. Besides providing the inspection hardware ultrasonic signal compensation characteristics, the resultant data will be used to demonstrate the economics of ultrasonic tire inspection and to substantiate an ultrasonic tire inspection specification. Controls have been implemented and hardware modifications have been made to eliminate or monitor the data variability experienced at RRAD. The ambient air temperature will be recorded and remaining tread depth will be compensated for during the pre-retread tire inspections. The commercial Government owned TDM's (figure 7) have also been modified to provide one more significant digit for calibration measurements than is provided for TDM in-process tire inspection measurements (i.e. three significant digits as opposed to two significant digits). With the above controls and hardware modification the Ober-Ramstadt tire inspection evaluation will be successful and provide supporting documentation to determine the effectiveness of the TDM as both pre and post retread inspection equipment by quantifying the exact correlation between the digital ultrasonic tire reflection measurements and both tire casing quality and remaining expected tire life.

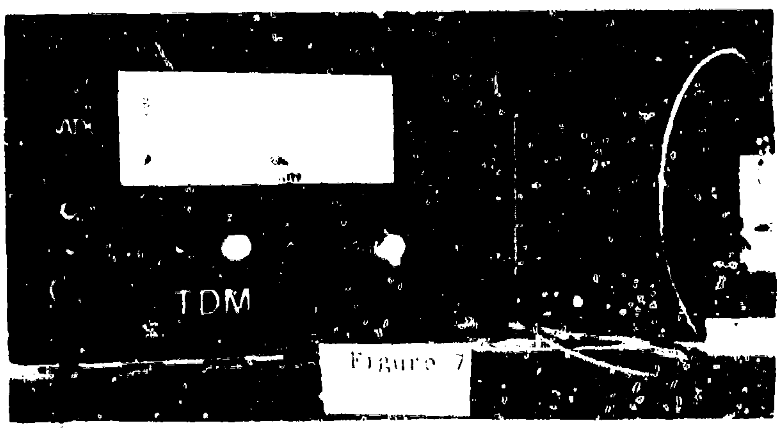

Figure 7

REFERENCES

I "NDCC Military Tire New vs Retread Test" Oct 1975, D. Gamache, C, Kedzior, P. Moore, B. Emerson, and J. Hubinsky.

II "Framework for Ultrasonic Inspection in the Army Tire Retread Process", June 1979, I. R. Kraska, T. A. Mathieson, and R. J. Watts.

III "Experience with TDM (Tire Degradation Monitor) in Commercial Application" May 23, 1978, Richard N. Johnson, 4th Symposium on Nondestructive Testing of Tires.

USING NDT METHODS TO INFLUENCE THE AIRCRAFT DESIGN PROCESS

William L. Andre
Staff Engineer
US Army Research and Technology Laboratories (AVRADCOM)
Ames Research Center
Moffett Field, CA 94035
AUTOVON 359-5578

ABSTRACT

The design of aircraft systems is heavily oriented toward providing high assurance that service life is achieved without the incurrence of failure. The cost of providing the reliability and integrity into a design to give the needed assurance is very high. Parts are designed to operate with many features that help provide the needed reliability. The high cost of aircraft systems drives the design considerations. In this paper, consideration is given to allowing NDT methods, as well as other monitoring techniques, to be evaluated on a competitive basis to determine how well a method can contribute to reducing the overall cost of a design. NDT methods, if considered at the design stage, can be evaluated to determine if component life can be extended through the use of such methods, or if a lower cost design is feasible.

If an NDT method can sufficiently contribute to reducing costs, then the aircraft item can be flown on-condition as opposed to simply establishing a TBO removal time. Formulas have been developed which can be used to identify cost curves for deciding the on-condition/TBO decision boundaries. The designer, if provided with the appropriate decision criterion, can elect to specify the use of a particular NDT method to enable functional design to be responsive to the NDT.

An example of the computational approach taken is discussed, and examples of how this applies to a design situation and a NDT method are presented.

USING NDT METHODS TO INFLUENCE THE AIRCRAFT DESIGN PROCESS

William L. Andre
Staff Engineer
US Army Research and Technology Laboratories (AVRADCOM)
Ames Research Center
Moffett Field, CA 94035

The design of aircraft systems is heavily oriented toward providing high assurance that service life is achieved without the incurrence of failure. The cost of providing the reliability and integrity into a design to give the needed assurance is very high. Parts are designed to operate with many features that help provide the needed reliability. The high cost of aircraft systems drives the design considerations. In this paper, consideration is given to allowing NDT methods, as well as other monitoring techniques, to be evaluated on a competitive basis to determine how well a method can contribute to reducing the overall cost of a design. NDT methods, if considered at the design stage, can be evaluated to determine if component life can be extended through the use of such methods, or if a lower cost design is feasible.

If an NDT method can sufficiently contribute to reducing costs, then the aircraft item can be flown on-condition as opposed to simply establishing a TBO removal time. Formulas have been developed which can be used to identify cost curves for deciding the on-condition/TBO decision boundaries. The designer, if provided with the appropriate decision criterion, can elect to specify the use of a particular NDT method to enable functional design to be responsive to the NDT.

An example of the computational approach taken is discussed, and examples of how this applies to a design situation and a NDT method are presented.

The use of NDT methods to inspect and diagnose is often considered the realm of maintenance. If the designer had some way to assess the design influence that various NDT methods offer then NDT would become a design issue. Most engineers will design to meet a set of specifications which usually hinge around functions and performance.

One interesting design consideration is that of allowing for on-condition maintenance and the impact this has on an aircraft for reliability and safety of flight. The objective of identifying a design approach which will minimize costs and still meet the specifications is of some concern.

The on-condition philsophy for aircraft requires that special attention be given to monitoring the condition of such items as structures, avionics, and power train.

In areas such as structures it is the NDT methodology that provides the capability to monitor the condition of the structure and assess structural integrity.

Until recently the establishing of TBO's (time between overhaul) or the safe life maintenance concept was used. This is a classical method for assuring that the necessary component reliability is achieved to preclude in-flight failures.

If a failure detection system is used to monitor the condition of components, it is possible to increase the service life of aircraft structures and components to achieve cost savings beyond the scope of a TBO concept. To the designer the function of condition monitoring can take several forms. Continuous monitoring and discrete or periodic monitoring are two different approaches which can be considered.

NDT methods can be used to provide the necessary capability for design decisions to be made in favor of reduced cost and improved maintenance.

Unless the NDT approach can be shown to reduce costs of ownership then the design influence will not be significant. The following discussion will identify an approach towards quantifying the cost impact of NDT methods used to provide the needed monitoring capability to assess aircraft condition.

The minimum cost TBO condition provides a good basis for comparison if NDT methods are to be used to help reduce costs. A TBO that will minimize the average cost per flight hour is preferred. This minimum average cost must be further reduced to replace the TBO concept with on-condition maintenance. The expression for minimum cost under the TBO concept can be used as a decision boundary for considering an on-condition maintenance concept where a detection system is used.

If R(t) denotes the life reliability function of a component, and a distinction is made between the cost of an unscheduled component renewal (e.g., one caused by an inflight failure) and the cost of a scheduled renewal or replacement where no failure has yet occurred, than an expression for the preferred TBO point can be obtained.

$$R'(T) \int_0^T R(t)dt = R(T) \left[\frac{X}{1 - X} + R(T)\right] \qquad (1)$$

where:

t = time or flight hours

$R(t)$ = component reliability

$R'(t)$ = first derivative with respect to t

T = TBO or renewal point

X = ratio of unscheduled to scheduled renewal cost

Equation (1) establishes the condition that must be satisfied if a TBO point, denoted by T, is to yield a minimum cost (Ref. 6).

There will be a solution to Eq. (1) if $X > 1$, such that when $T = T^*$, the cost per flight hour will be a minimum. The logical choice for a TBO time will be T^*.

The following model is useful for comparing the TBO and on-condition concepts. Let:

C_d = cost of detecting a failure (the NDT factor)

C_s = cost of a scheduled renewal

C_u = cost of an unscheduled renewal

μ_s = mean time to scheduled renewal

μ_u = mean time to unscheduled renewal

μ = average operating life of a component

For a TBO policy, the average cost per flight hour can be expressed as:

$$c_{TBO} = \frac{C_s}{\mu_s} + \frac{C_u}{\mu_u} \tag{2}$$

For an on-condition policy, the average cost per flight hour can be expressed as:

$$c_{on\text{-}condition} = \frac{C_d + C_s}{\mu} \tag{3}$$

Whenever it can be shown that on-condition costs are fewer than the costs of the TBO policy, then the on-condition policy can be justified, and the following expression can be used:

$$\frac{C_d + C_s}{\mu} < \frac{C_s}{\mu_s} + \frac{C_u}{\mu_u} \tag{4}$$

Then, if C_d can be shown not to exceed a certain value and to provide the detection or monitoring function, the on-condition policy is cost effective with respect to the best that a TBO policy can provide. The boundary on C_d can be assigned by substituting the appropriate expressions for μ, μ_u, μ_s into Eq. (4).

The resulting expression given by equation (5) provides a quantitative yardstick for relating the influence of an NDT method as represented by the term C_d in relation to the reliability properties and the maintenance costs associated with renewing the component or item under consideration.

The C_d term can be the results of performing periodic X-ray inspection, ultrasonic inspection etc.

$$\frac{C_d}{C_s} < \frac{\int_0^\infty R(t)dt}{\int_0^{T^*} R(t)dt}\left[R(T^*)(1 - X) + X\right] - 1 \tag{5}$$

Note that $X = \frac{C_u}{C_s}$

The curve boundary for Eq. (5) establishes the value of C_d that cannot be exceeded for a 100% detection level.

If, however, a detection probability less than 1 is achieved, then the C_d limit will be reduced in magnitude to compensate for the fact that sometimes the detection or monitoring system will not detect an incipient failure, thus reducing the cost effectiveness of the detection system. For a less than perfect detection system, Eq. (4) can be modified as follows to account for the reliability of the detection system:

$$\frac{C_d + R_d C_s + (1 - R_d)C_u}{\mu} < \frac{C_s}{\mu_s} + \frac{C_u}{\mu_u}$$

here R_d now expresses the detection probability. This can be considered to be more practical since an inspection procedure may not catch all the defects present or may only catch the most severe corrosion or largest cracks. Here again the NDT method and procedures will determine the degree to which a 100% detection capability can be achieved. If a designer is not aware of a NDT method or its capabilities, he cannot give it much consideration. On the other hand if preliminary design teams are provided with technical data or various inspection methods then the aircraft may be designed with a higher degree of awareness for NDT.

With the detection probability now a factor, equation (6) can also be converted as before.

By repeating the process used to get Eq. (5), the expression for C_d with imperfect detection becomes

$$\frac{C_d}{C_s} < \frac{\int_0^{\infty} R(t)dt}{\int_0^{T^*} R(t)dt}\left[R(T^*)(1 - X) + X\right] - \left[R_d + X(1 - R_d)\right] \qquad (7)$$

where:

R_d = reliability of the detection system

X = C_u/C_s cost ratio

The equations for perfect and less than perfect detection differ only by the R_d terms and can be related by the following simplified expression:

$$\left.\frac{C_d}{C_s}\right|_{\substack{R_d \\ \text{detection}}} \leq \left.\frac{C_d}{C_s}\right|_{\substack{100\% \\ \text{detection}}} - \left[R_d + X(1 - R_d) - 1\right] \qquad (8)$$

Periodic inspections in lieu of a continuous inspection capability will cause the R_d term to be less than one. But this can only have the advantage of reducing the total inspection cost. The tradeoff between detection probability and cost of detection can be addressed now in the overall setting.

A family of curves can be created to provide a decision mechanism to the designer for choosing one design approach over another influenced by NDT consideration.

Shown in Figure (1) is the on-condition versus TBO decision boundary, This can be used to determine whether or not an NDT method is justified.

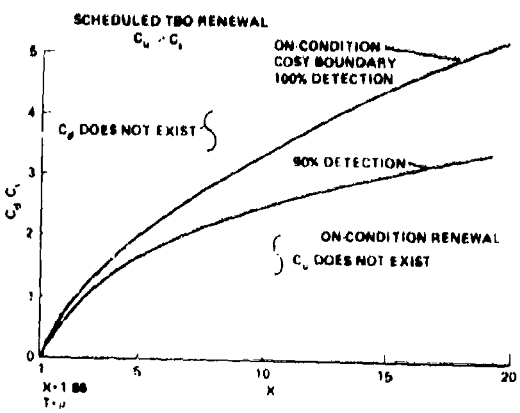

Figure (1) presents the results obtained when a reliability function is identified and the equations (5) and (7) are exercised. If a chosen design concept is found to exist above the desired detection boundary curve then the NDT method considered does not pay for itself or provide the needed inspection capability at an affordable cost. If on the other hand the design point falls below the cost boundary curve then the NDT concept will pay for itself and will be better than the lowest cost TBO policy available. The amount by which the design point falls below the decision boundary will represent the cost savings that will be achieved by using the chosen NDT or inspection method.

SUMMARY AND CONCLUSIONS

If on-condition design of fatigue-critical components is going to be an accepted practice required by contract for future U.S. Army helicopters, nondestructive testing and evaluation must become integral to the complete design development cycle. A clear correlation of NDT method indications with physical and mechanical properties must be established during material selection and component development. Structural design tradeoffs must include inspection complexity and frequency versus component inspectability as elements in the cost model. NDT reliability data must be gathered and reliability factors established so that component safe-life can be extended while maintaining consistent structural reliability of the aircraft system during its fleet-life cycle.

NONDESTRUCTIVE TESTING OF GRAPHITE REINFORCED ALUMINUM

Clifford W. Anderson
Code G53
Naval Surface Weapons Center
Dahlgren, Virginia 22448
(703) 663-8411, Autovon 249-8411

ABSTRACT

This paper highlights progress on an effort to evaluate nondestructive testing techniques for applicability towards the detection of material defects in graphite-reinforced aluminum. Techniques under evaluation include ultrasonics, eddy current, x-radiography, neutron radiography, dye penetrants and electrical resistance testing. Results obtained to date indicate that combinations of techniques will most likely be required to ensure detection of the full range of potential defects.

INTRODUCTION

Graphite reinforced aluminum is currently being evaluated by the Naval Surface Weapons Center for application in lightweight structures under a program funded by the Naval Sea Systems Command. In addition to material development, a simultaneous effort is being conducted to develop and evaluate nondestructive testing techniques for this metal matrix composite material.(1)

The material under investigation consists of Thornel 50 graphite fibers imbedded in a matrix of 201 aluminum. The fibers compose approximately 30% of the material volume. Fabrication of the material into its final shape begins by passing bundles of graphite fibers through a molten aluminum bath (Figure 1). The resulting product is a graphite/aluminum composite precursor wire approximately .040" in diameter (Figure 2). This wire is then cut into shorter lengths which are then placed side by side and diffusion bonded into panels (Figure 3). A typical panel has three plys and is about .110" thick. All plys are unidirectional in their fiber orientation. In addition, a thin skin, approximately .010" thick, is bonded to both surfaces of the panel to seal the material and prevent corrosion.

Fabrication of a structure from graphite/aluminum will require the fastening of panels to supporting members. Thus, welding techniques in addition to NDE methods for welds are also being evaluated.

Defective material can be produced at any stage of the manufacturing process from the fabrication of the precursor wire to the fastening of

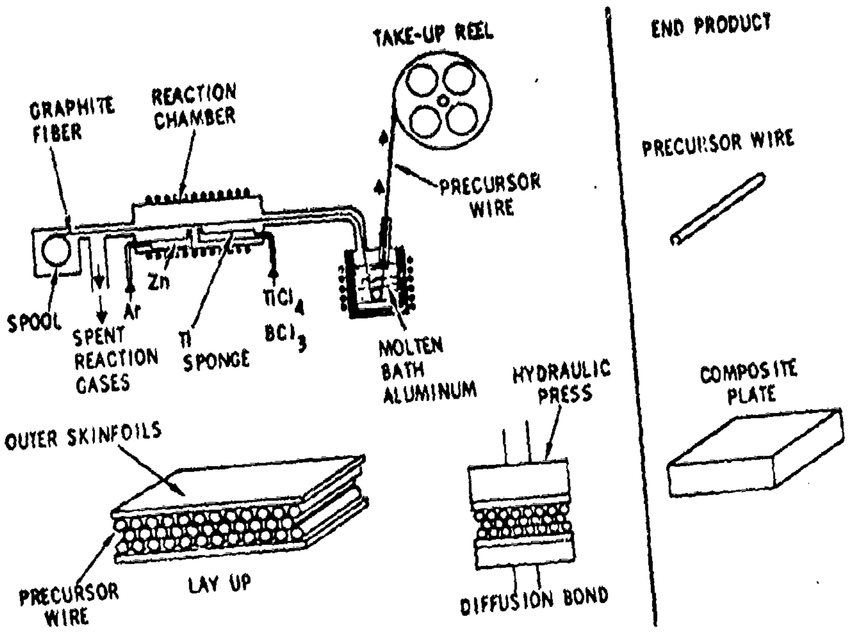

Figure 1. Graphite/Aluminum Fabrication Process

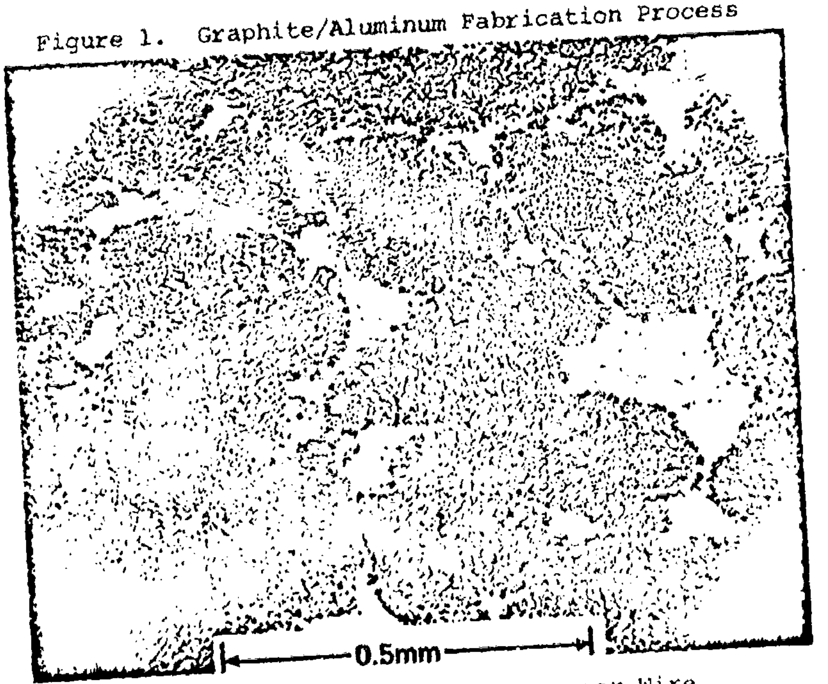

Figure 2. End View of Precursor Wire

Figure 3. Graphite/Aluminum Panel Cross Section

panels into a structure. In order to evaluate the capabilities of NDE methods, a series of intentionally flawed precursor wires, panels and welds were fabricated. These specimens were then subjected to a battery of NDE tests including ultrasonic, eddy current, x-radiography, neutron radiography, dye penetrant, and electrical resistance testing.

TESTING OF PRECURSOR WIRES

The primary cause for concern in the fabrication of precursor wires deals with the infiltration of aluminum into the fiber brindle. If proper wetting and thus total infiltration of the bundle is not achieved, the material properties of the wire and anything made from it will suffer. Several techniques to detect incomplete infiltration are being evaluated. These include eddy current, electrical resistance, radiographic and ultrasonic testing.

Surface roughness and diameter irregularities of the wire have been the major obstacles toward developing a reliable nondestructive test. This problem has been encountered with eddy current testing and was also noted with radiographic and electrical resistance testing. Both good and bad wires had been tested by all three techniques with excellent correlation of results. Dark regions on the radiographs indicating insufficient aluminum content matched the regions of low conductivity as measured by both eddy current and electrical resistance testing.

Unfortunately, radiography, eddy current, and electrical resistance testing are all sensitive to the amount of aluminum present in any given wire segment and not to its distribution across the wire diameter. Thus, it is possible for a non-infiltrated wire to have an excess of aluminum on its surface, and yet still register as "good" by eddy current, electrical resistance, and radiography testing. This was demonstrated to be the case by destructive testing of sample wires registering high electrical conductivity. The reliability of the above three techniques for testing wire is thus questionable at best.

Ultrasonic testing has given more encouraging results. Tests conducted by Dr. H. Frost at the Pennsylvania State University have demonstrated the feasibility of using an ultrasonic technique similar to that of Rasor, Harrigan, and Amateau[2] for detecting poorly infiltrated wire. The technique involved the sending and receiving of a pulse down a small segment of the wire being tested. High attenuation indicated bad wire. This technique was capable of properly classifying wires which had previously been incorrectly diagnosed by radiographic, eddy current and electrical resistance testing. In addition, Dr. Frost demonstrated that ultrasonic pulses could be transmitted and received in the wire by the use of contactless electromagnetic acoustic transducers (EMAT). This would facilitate the testing of rapidly moving continuous wire in a production environment.

TESTING OF PANELS

Several types of defects can occur in graphite/aluminum in panel form. These include interlaminar unbonds, cracks, surface foil unbonds, and intra-ply unbonds (between adjacent wires in the same ply). The detection of non-infiltrated wire may also be necessary depending on how successfully it can be screened out prior to panel fabrication.

As a basis for the evaluation of potential NDE methods, four panels containing intentional flaws were produced. The test panels measured 12" long x 6" wide x 0.11" thick. These panels contained interlaminar unbonds, surface foil unbonds, single and grouped non-infiltrated wires as well as a single twisted fiber. Figure 4 shows the placement of these defects in one of the four panels. It should be mentioned at this point that experience in fabricating such defects in this material is limited. Until the panels are sectioned at a later date, the nature of the defects will have to be inferred from nondestructive tests alone.

Ultrasonic testing of the test panels utilized the reflector plate C-scan method. This technique uses a smooth reflector placed on the opposite side of the test item from the inspection transducer. The round-trip attenuation of the ultrasonic pulses is monitored and recorded as the panel is scanned. Typically, an image is recorded by mapping areas for which the ultrasonic signal transmitted through the specimen exceeds a preselected threshold (Figure 5). This conventional C-scan approach can, under proper conditions, exhibit excellent spatial

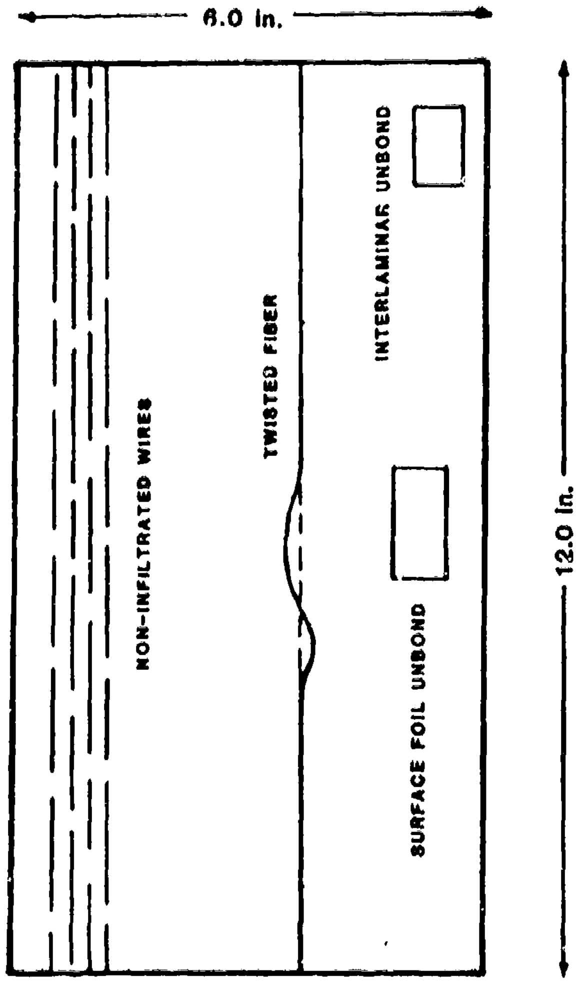

Figure 4. Placement of Intentional Defects in Panel 1

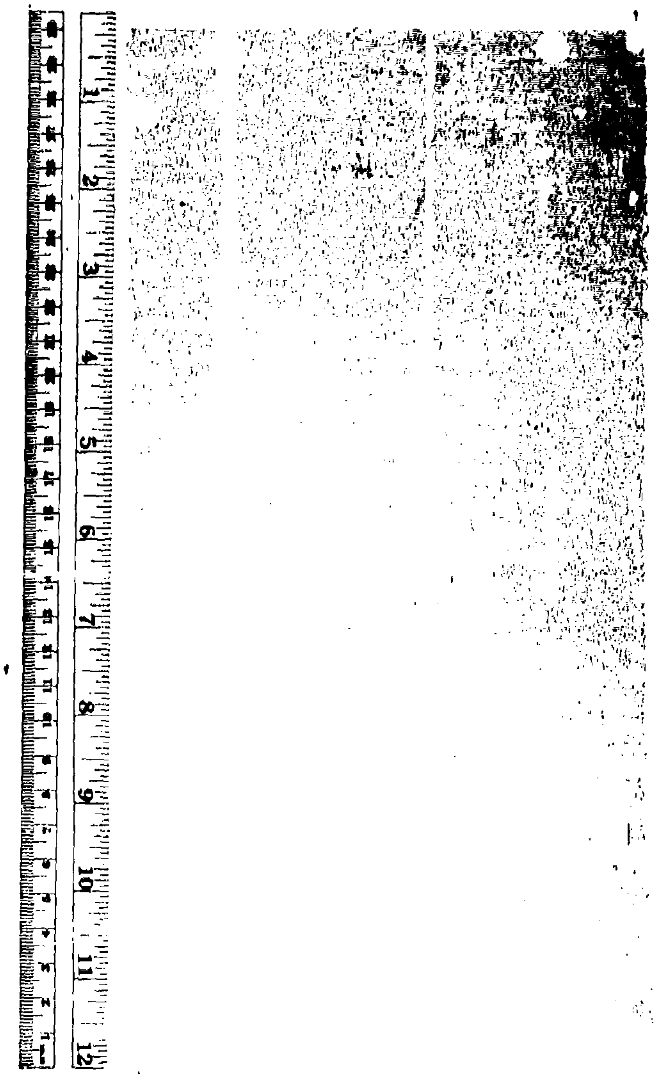

Figure 5. Conventional Ultrasonic C-Scan of Panel 1

resolution; but it does not sufficiently portray the total signal amplitude distribution for the panel. To overcome this difficulty, a modified ultrasonic C-scan was utilized in addition to the more conventional black and white recording technique.

A modified C-scan is made by connecting an X-Y recorder to the scanner so that the recording pen duplicates the motion of the scanner. The ultrasonic signal amplitude is then superimposed on either the X or the Y axis by means of a summing or differential amplifier. The resulting image displays signal amplitude as a function of position (Figure 6). One can now use the modified C-scan to evaluate the significance of indications appearing on the conventional C-scan. For instance, slowly varying fluctuations in the "background" attenuation can be distinguished from sudden changes caused by legitimate defects. This advantage is particularly important in the testing of composite materials where the baseline attenuation of acceptable material can vary significantly.

The ultrasonic scan recordings (Figures 5 and 6) both clearly reveal the twisted fiber indication and the non-infiltrated wire region as depicted in Figure 4. The interlaminar and surface foil unbonds do not appear on the scans, indicating that either they were not fabricated as intended or that the unbonds are too tightly closed to affect ultrasonic transmission. In spite of the lack of confirming ultrasonic results, it seems unlikely that any other technique besides ultrasonics would more readily detect unbonds or delaminations.

X-radiographic testing revealed the twisted fiber of panel 1 in addition to the grouped non-infiltrated wires (Figure 7). The attempted surface foil unbond also appears on the radiograph, but this is due to a bulge in the materials surface caused by the attempt to induce an artificial unbond. X-radiography was unable to reliably distinguish the presence of singular non-infiltrated wires in the other test panels.

Neutron radiography, however, readily identifies the presence of singular non-infiltrated wires within a panel. Unlike x-rays which are sensitive to the aluminum matrix, neutrons are mainly affected by the graphite fibers. Thus, the encouraging neutron radiographic results are at first somewhat puzzling since both infiltrated and non-infiltrated wires have equal amounts of graphite. A possible explanation for the neutron sensitivity to non-infiltrated wires may be that such wires collapse under the pressures of diffusion bonding, forming highly compact cores of graphite. Properly infiltrated wires cannot collapse into such compact concentrations of graphite, and thus are not imaged.

Eddy current scanning of the test panels was accomplished in much the same way as the modified ultrasonic C-scan. The recording pen was modulated with a voltage proportional to either the real or the imaginary component of the test probe impedance. An Automation Industries EM-3300 eddy current instrument was used in conjunction with a modified 450 series laboratory scanner (Figure 8). Precision position potentiometers were added to provide X and Y axis outputs, and a pivoting probe holder was constructed to allow the probe to maintain a constant lift-off.

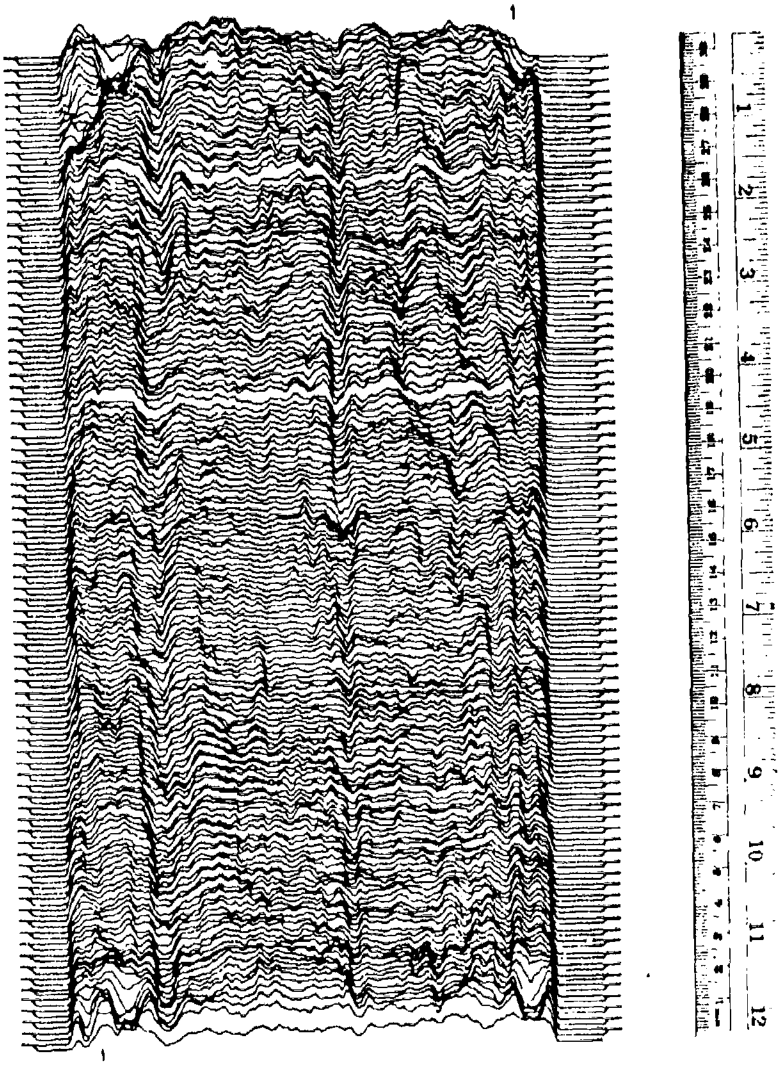

Figure 6. Modified Ultrasonic C-Scan of Panel 1

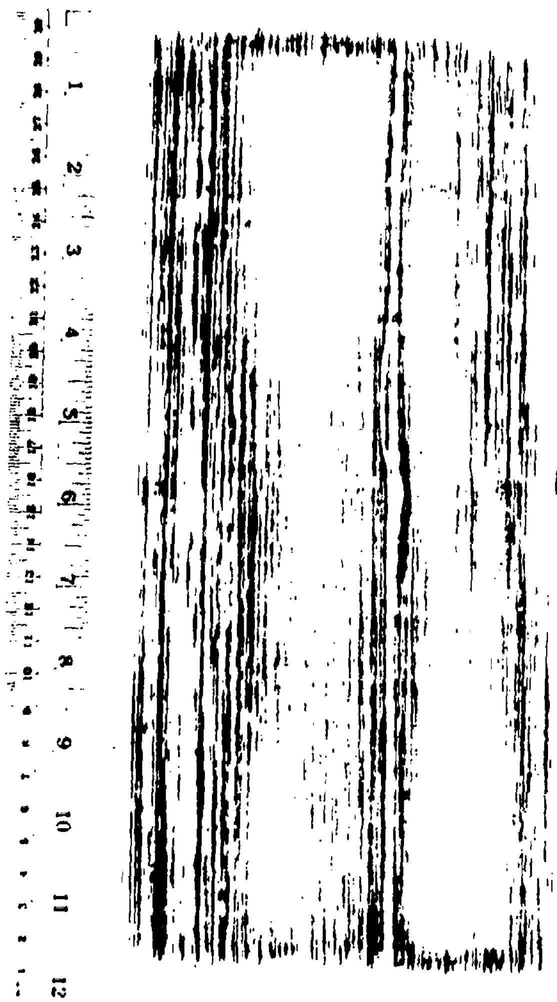

Figure 7. Contact Print Made from X-Radiograph of Panel 1

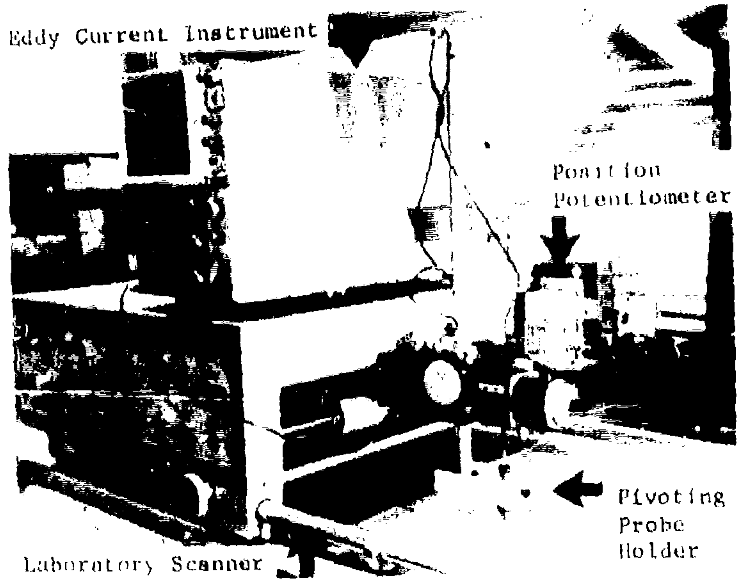

Figure 8. Eddy Current Scanning Apparatus

Since eddy current indications can often be difficult to interpret, an empirically derived model was developed to predict the test response for various defects. The model was developed by stacking thin sheets of material in such a manner as to simulate cracks of differing sizes at various depths below the surface. This is similar to the method described by Libby[3]. The results of the modeling exercise appear in Figure 9. The two variables considered are crack starting depth below the surface and crack size as measured perpendicular to the surface. This particular model is valid only at the test frequency of 10 KHz. The skin depth in graphite aluminum at this frequency is .070".

The imaginary component of the eddy current test coil impedance is plotted in Figure 10. The twisted fiber and non-infiltrated wires are both apparent. Note, however, that the indications for these two defects are in opposite directions. The twisted fiber appears to cause a localized increase in material conductivity whereas the non-infiltrated wires have the effect of decreasing conductivity. Unlike homogeneous materials, metal matrix composites can have both conductive and non-conductive defects depending on the localized ratio of fiber to matrix content. Thus the model in Figure 9 is only partially complete. When the defect indications for panel 1 are compared in phase and magnitude to the model in Figure 9, it becomes apparent that they are quite small. The non-infiltrated fiber region is equivalent to a crack less than .020" deep and starting at about .030" below the surface. The twisted

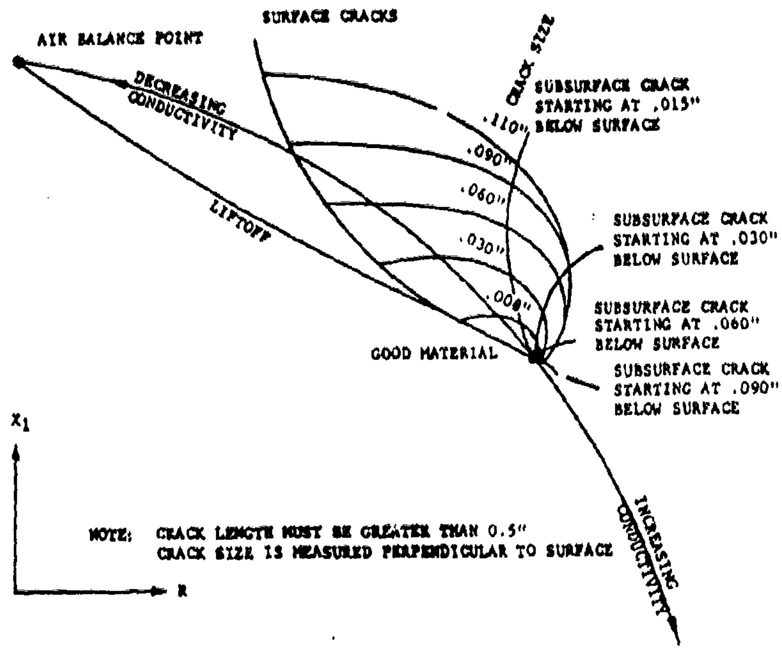

Figure 9. Graphite/Aluminum Eddy Current Model at 10 KHz

fiber indication is roughly equal in magnitude, but 180° out of phase.

Perhaps the greatest capability of eddy current testing lies in its ability to detect cracks as opposed to non-infiltrated wire regions. This is evidenced by the responses to simulated cracks in the model which dwarf the measured responses from non-infiltrated wires. By viewing the radiograph of panel 1 (Figure 7) one can easily appreciate how difficult crack detection would be by radiography. The cracks would align themselves with the fibers. Such cracks are most likely to occur in material forming and in-service operations as opposed to initial material fabrication. One might also reasonably conclude that the thin surface foil could prevent crack propagation to the surface.

At this point, ultrasonic shear wave detection of cracks in the composite has not been thoroughly explored. This may offer an alternative to eddy current testing provided that excessive attenuation is not a problem.

Yet another concern in the nondestructive evaluation of graphite/aluminum panels lies in the detection of potential corrosion sites. These include small pits in the surface foil as well as any other defect which could allow moisture to enter the material. Fortunately, conventional dye penetrant testing offers a straightforward and reliable solution to this problem.

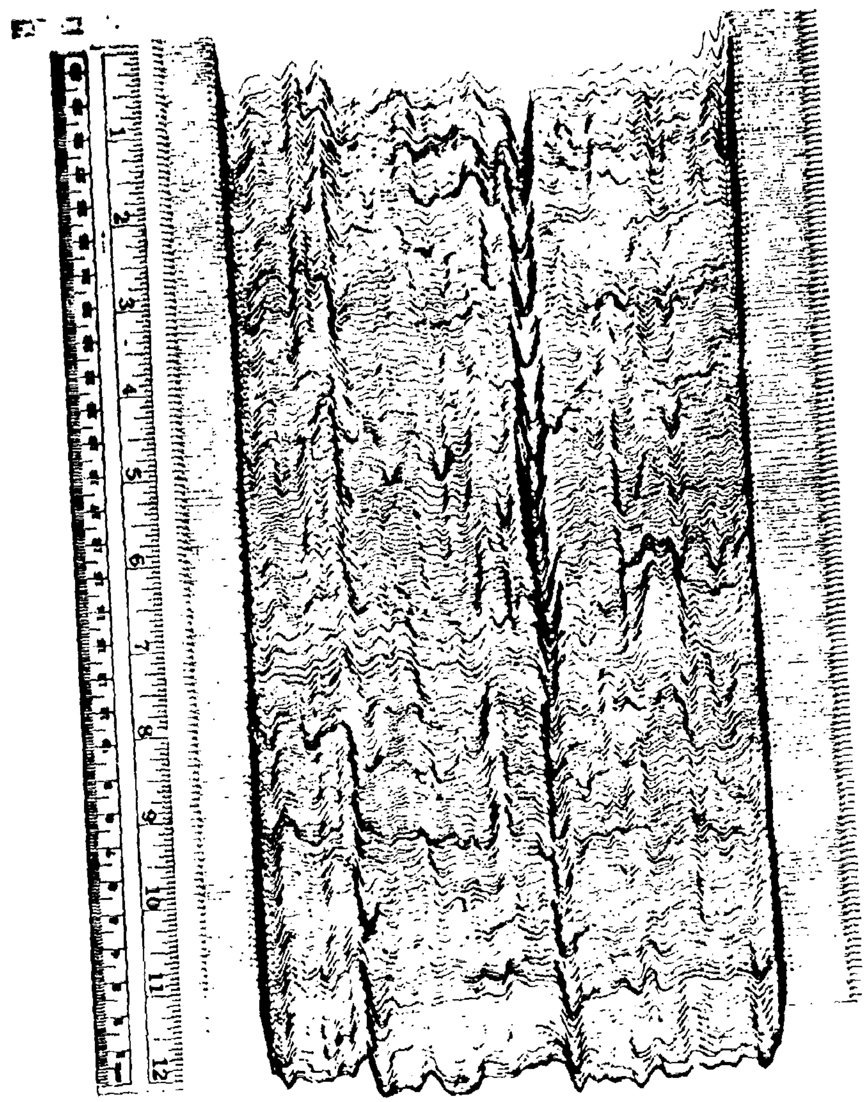

Figure 10. Eddy Current Scan of Panel 1
Showing Imaginary Impedance Component

TESTING OF SPOT WELDS

A series of electrical resistance and ultrasonic spot welds were fabricated to evaluate the mechanical properties of two welding techniques. Before the welds were destroyed, however, they were subjected to ultrasonic and radiographic evaluation. The radiographs clearly revealed several radial cracks in each of the electrical resistance welds. Ultrasonic testing was unable to detect the cracks due to their orientation in planes parallel to the ultrasonic beam. The advantage of the ultrasonic test was that it verified that fusion had occurred. This could not be achieved with radiography. Thus both ultrasonic and radiographic testing are required to assure both weld fusion and the absence of cracking. Eddy current testing has proved to be inconclusive to date due to irregular surface deformation of the welds.

SUMMARY

Efforts to develop and evaluate NDT methods for the testing of graphite/aluminum composite material indicate that a wide range of such methods is required to fully test the material. Ultrasonic testing with contactless EMAT devices appears to be the most promising technique for detecting non-infiltration of precursor wires prior to panel fabrication. Once the panel is fabricated, neutron radiography becomes the most reliable method tested to date for accomplishing this. Ultrasonics is the only technique tested which offers the possibility of detecting interlaminar unbonds or delaminations. Eddy current testing appears to be the optimum technique for crack detection in panels but possibly not in welds. Dye penetrant testing is the superior method for locating potential corrosion initiation sites. Finally, both ultrasonics and radiography are required to assure weld fusion without cracking.

ACKNOWLEDGEMENTS

The author wishes to acknowledge the assistance of D. Garrett and D. Polansky of the National Bureau of Standards for providing neutron and x-radiographs. Also appreciated are the efforts of J. M. Warren of NSWC/Dahlgren in modifying test hardware and G. V. Blessing of NSWC/White Oak for helpful guidance and discussions.

REFERENCES

1. C. W. Anderson and G. V. Blessing, Detection of Material Defects in Graphite Reinforced Aluminum, Naval Surface Weapons Center Technical Report NSWC TR 79-222, Sept 1979.
2. J. Rasor, W. C. Harrigan, and M. F. Amateau, A Non-Destructive Testing Technique for Quality Assurance of Aluminum Graphite Composite Wire, Aerospace Corporation Report No. TOR-0074 (9250-03)-1, December 31, 1973.

3. H. L. Libby, Introduction to Electromagnetic Nondestructive Test Methods, Wiley-Interscience, New York, 1971.

NONDESTRUCTIVE ACOUSTIC TECHNIQUES FOR
DETERMINING DEGRADATION OF TEXTILE MATERIALS

Vasant K. Devarakonda

Clothing, Equipment & Materials Engineering Laboratory
U.S. Army Natick Research & Development Command
Natick, MA 01760

ABSTRACT

Preliminary laboratory data presented at the 23rd Defense Conference on Nondestructive Testing showed an apparent relationship between resonant frequency and the level of degradation of textile materials which had a potential for a NDT technique. This paper deals with the investigation of that proposed technique and the use of sound velocity in a material as another means of measuring fabric degradation.

Samples of nylon rip-stop fabric commonly used in personnel parachutes were subjected to various levels of exposure to ultra-violet radiation. These exposed samples as well as the unexposed control sample were suspended under tension and forced to oscillate by mechanically impacting the fabric. The audio signal thus generated was picked up by a microphone placed in close proximity to the sample. The resulting amplitude vs. time decay curve was obtained as an oscilloscope trace from which the frequency was determined. The strength loss as a measure of degradation was obtained using the customary destructive methods and compared to the resonant frequency. It was found that the generated frequency is dependent on several variables including the vibrating length of the sample and the applied tension. The resonant frequency could not be defined as a function of the degree of degradation by the techniques used in this study. Plans for complete waveform analysis and the development of relationship between sonic velocity and elastic modulus are discussed.

BACKGROUND AND PURPOSE

There is a need for a reliable nondestructive method of assessing the degradation of mechanical properties of fabrics. When flexible structures such as fabrics are used as stress-bearing components in military items, it is necessary to monitor whether degradation has reached a point that will result in failure and cause loss of life or damage to equipment. Lack of such methods has resulted in the use of an estimated service life for these items, after which they are discarded. Such procedures undoubtedly result in the discarding of items with remaining useful life.

In the case of parachutes, for instance, considerable surveillance and destructive testing are necessary to provide data to guide the assignment of service life limits to maintain the reliability of the equipment on hand. A method for nondestructively testing all units of samplings at prescribed intervals would facilitate obtaining the full potential service life of such equipment and minimize replacement costs.

Use of natural resonance as a technique for determining the molecular reordering which occurs in the degradative process of textile materials was first proposed by John Hansen of NARADCOM at the 23rd Defense Conference on NDT.[1] Laboratory data developed by Hoffman and Davidson showed an apparent relationship between degradation and resonant frequency.[2] The material used for their study was an experimental 1.1-oz/yd^2 (37-g/m^2) nylon rip-stop fabric dyed with a shade of yellow that was found to accelerate the rate of UV degradation. Samples exposed in a weatherometer for 34 and 68 hours and a control were individually suspended under the same tension and impacted with the eraser head of a pencil. The vibration thus generated was picked up by a microphone and fed into an oscilloscope. The oscilloscope trace was used to calculate the induced frequency. This frequency showed a drop of 20 Hz from control to the 34-hour exposed state. However, the trend did not continue to the 68-hour exposed state. Instead, the generated frequency after the 68-hour exposure period increased 5 Hz over that of the 34-hour exposure. Based on these data, the possibility of a relationship between induced frequency and degradation was proposed.

The work reported here is an extension of Hoffman and Davidson's study and an introduction of a second technique which utilizes the sound velocity in materials as a means of measuring degradation.

RESONANT FREQUENCY METHOD

Materials

Two 1.1 oz/yd^2 (37-g/m^2) nylon rip-stop fabrics were used in this study. One sample was the standard olive green shade, while the other was dyed with Acid Yellow 129 and identified as yellow #3. Samples from both these fabrics were exposed in a Carbon Arc Weatherometer.

Apparatus

(1) Clamps used for tensioning by Hoffman and Davidson in their study.
(2) Instron tensile tester Model TT equipped with 3-inch (75-mm) wide air-activated clamps.
(3) Audio microphone
(4) Oscilloscope (Tektronix) with Polaroid camera attachment

Procedure

Both fabric samples were exposed to 24, 48, 100 and 300 hours of UV radiation in the Carbon Arc Weatherometer. The standard ravel strip method was used to determine breaking strengths of the control and the exposed samples.[3]

Frequency traces were made on the oscilloscope after impacting the sample with the eraser head of a pencil and the signal picked up by the microphone. The Instron was used to maintain a tension of 5.0 ± 0.1 lbs (22.0 ± 0.5 N). The original clamps were used to recreate the experimental setup.

All testing was done only in the warp direction of the fabric.

Results and Discussion

Breaking strength data are shown in Tables 1 and 2; and are plotted in Figures 1 and 2. The standard OG fabric showed a lower rate of degradation than the yellow #3 as evidenced from these data.

Table 1. Breaking Strength Data on Standard Nylon Rip-Stop Fabric

Condition	Breaking Strength in Warp, lbs (N)	Loss of Strength, %
Control	54.7 (243)	-
24-hr exposure	52.7 (235)	3.7
48-hr exposure	50.0 (222)	9.4
100-hr exposure	48.0 (214)	12.2
300-hr exposure	41.3 (184)	24.5

Table 2. Breaking Strength Data on Nylon Rip-Stop Fabric, Shade Yellow #3

Condition	Breaking Strength in Warp, lbs (N)	Loss of Strength, %
Control	47.0 (209)	-
24-hr exposure	42.7 (190)	9.4
48-hr exposure	39.0 (174)	17.0
115-hr exposure	19.5 (87)	58.5

Table 3 and Figure 3 show the frequencies of the standard OG fabric at the various levels of exposure using the Instron tester to maintain a constant tension. The standard 3-inch (75-mm) gage length used in the breaking strength test was selected for the frequency measurement. Although the actual breaking strength loss at 300-hour exposure is 25%, there was a drop in frequency of only 3 Hz. Since the fabric dyed with yellow #3 showed a higher rate of degradation as evidenced by the breaking strength, it was decided to use this fabric in an attempt to find a more definitive test.

Table 3. Frequencies in the Standard Nylon Rip-Stop Fabric on the Instron at the 3-inch (75-mm) Gage Length

Condition	Frequency, Hz
Control	248
24-hr exposure	247
48-hr exposure	247
100-hr exposure	245
300-hr exposure	245

Table 4 and Figure 4 show the frequencies obtained using the clamps from the original study placed 10 inches (250 mm) apart. This distance approximated that of the previous study. During this testing phase, a sensitivity of the frequency to the gage length was observed. Table 5 shows the frequencies on the control yellow #3 at various gage lengths and Figure 4 shows this relationship.

These data indicate that there is a direct relationship between the generated frequency and the gage length. Minor changes in gage length can cause large variations in frequency. There was no reference to a gage length effect in the earlier study.

Table 4. Frequencies in the Nylon Rip-Stop Fabric, Shade Yellow #3 with the Original Clamps at the 10-inch (250-mm) Gage

Condition	Frequency, Hz
Control	160
24-hr exposure	166
48-hr exposure	125
115-hr exposure	146

Table 5. Effect of Gage Length Using the Original Clamps on Yellow #3, Nylon Rip-Stop Control Fabric

Gage Length, in (mm)	Frequency, Hz
5 (125)	222
8 (200)	173
10 (250)	160
12 (300)	125
15 (375)	54

Additional testing was conducted with the objective of finding a more discriminating gage length using the Instron as a tensioning device. Data are shown in Table 6 and plotted in Figures 5 and 6.

Table 6. Effect of Gage Length Using Instron Clamps on Yellow #3, Rip-Stop Control and Exposed Fabrics

Gage Length, in (mm)	Frequency, Hz			
	Control	24-Hour Exposure	48-Hour Exposure	115-Hour Exposure
3 (75)	500	428	500	412
5 (125)	286	260	285	264
8 (200)	166	148	200	210
10 (250)	117	121	153	140
12 (300)	113	91	118	97

Once again, the gage length effect is evident from Figure 5. However, there is no pattern to the frequency vs. UV exposure relationship. There was an apparent lowering in the frequency at the first 24-hour exposure, but the trend did not continue, as did the data in the previous study. In some instances, the frequency in the sample with almost 60% loss in strength is higher than the control sample. The frequency of vibration as a function of loss in breaking strength is plotted in Figure 6 and shows no pattern. It is likely that other variables that are not considered in this study might be causing the apparent shifts in frequencies. The three values reported in the earlier study could also involve similar variations not related to degradation. Complete waveform analysis is planned to determine such characteristics as decay rates and spectral densities. The necessary apparatus to digitize and process the amplitude-time data is currently being procured.

DYNAMIC MODULUS METHOD

The use of sonic velocity in the investigations of fibers and films was proposed many years back and used in studies with filaments, paper and wood.[4, 5, 6, 7] Other studies utilizing this sonic technique showed its usefulness as a nondestructive method.[8, 9] There is a fundamental relationship between the speed of sound, the elastic modulus and the density of solid materials because sound itself is a mechanical application of a periodic strain. The velocity of sound generally increases with the modulus of the material. Sonic velocity C, elastic modulus E and density d are related by the expression

$$E = dC^2 \qquad (1)$$

Since the degradative process of textile materials effects the stress-strain relationship and thus the modulus, the determination of sonic velocity in a material could be used in the nondestructive estimation of the elastic modulus.

A device currently available known as the Dynamic Modulus Tester or the Pulse Propogation Tester is shown in Figure 7. This apparatus uses two piezoelectric ceramic crystal transducers with a natural frequency of 5 kHz. The sample to be tested is contacted by the transmit transducer and the receive transducer. Recurrent longitudinal mechanical pulses are transmitted through the sample and picked up by the receive transducer. The elapsed time is recorded on a strip chart as a function of the distance between the transducers from which the sonic velocity is obtained. Using equation (1) the elastic modulus can be calculated.

The control and laboratory exposed nylon samples used for the Resonant Frequency measurement are currently being tested on this device. If the results are favorable this study will be extended to determine if a degradation index could be developed as a criterion for establishing parachute serviceability.

CONCLUSIONS AND PLANNED ACTIONS

(1) Vibrating length is one of the critical variables that control the frequency of vibration of a sample of fabric held under tension.

(2) The resonant frequency could not be defined as a function of the degree of degradation by the techniques used in this study.

(3) Additional waveform analysis will be conducted to determine if there is any relationship between degradation and such parameters as decay rates and spectral densities.

(4) Studies on yarns and fabrics will also be conducted using the sonic velocity technique to relate degradation to elastic modulus.

REFERENCES

1. Hansen, J. V. E., "A Nondestructive Testing Approach to the Assessment of Degraded Textile/Fibrous Materials", Paper #30, 23rd Defense Conference on NDT.
2. Hoffman, B., and J. Davidson, "Determining Degree of Degradation of Nylon Rip-Stop Using Nondestructive Acoustic Techniques", Feasibility Study FCI-10-74; US Army Armament R&D Command, Frankford Arsenal, Philadelphia.
3. Test Method 5104, Strength and Elongation, Breaking of Woven Cloth; Ravel Strip Method; Federal Test Method Standard No. 191.
4. Ballou, J. and S. Silverman, "Sound Velocity Measurements" Text. Res. J. 14, 282-292 (1944).
5. Charch, W. H. and W. W. Moseley, "Structure-Property Relationships in Synthetic Fibers Part 1: Structure Revealed by Sonic Observations", Text. Res. J. 29, 525-535 (1959).
6. Chatterjee, P.K., "Sonic Pulse Propogation in Paperlike Structure" TAPPI 52 (4), 699-704, (1969).
7. Yiannos, P. N. and D. L. Taylor, "Dynamic Modulus of thin wood sections" TAPPI 50 (1), 40-47 (1967).
8. Craver, J. K. and D. L. Taylor, "Nondestructive Sonic Measurement of paper elasticity", TAPPI 48 (3), 142-147 (1965).
9. El-Shiek, Ali, "The Dynamic Modulus and Some other Properties of Viscose-Polyester Blends", Text. Res. J, 44, 343-351, 1974.

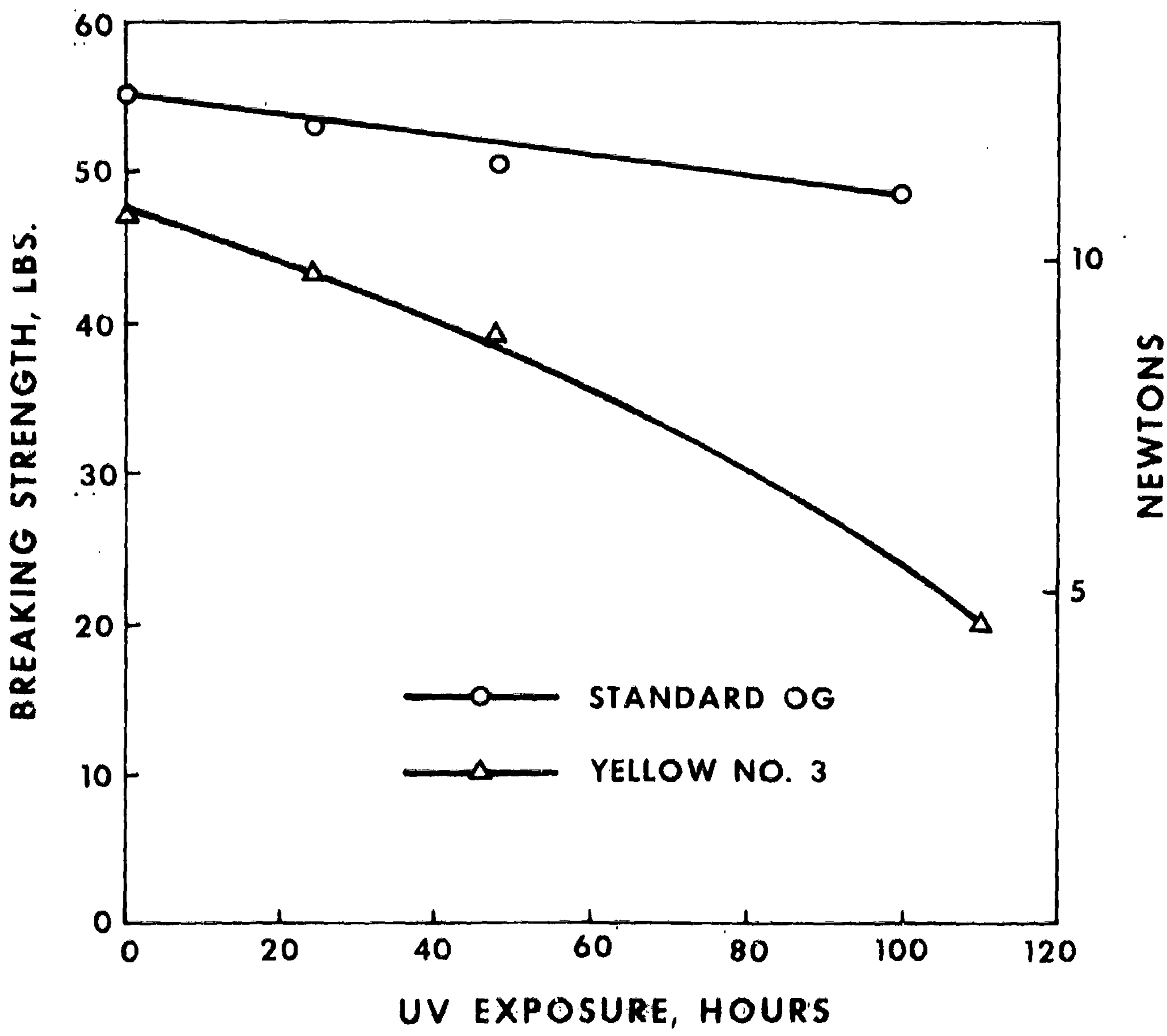

FIGURE 1. BREAKING STRENGTH VS. HOURS OF UV EXPOSURE.

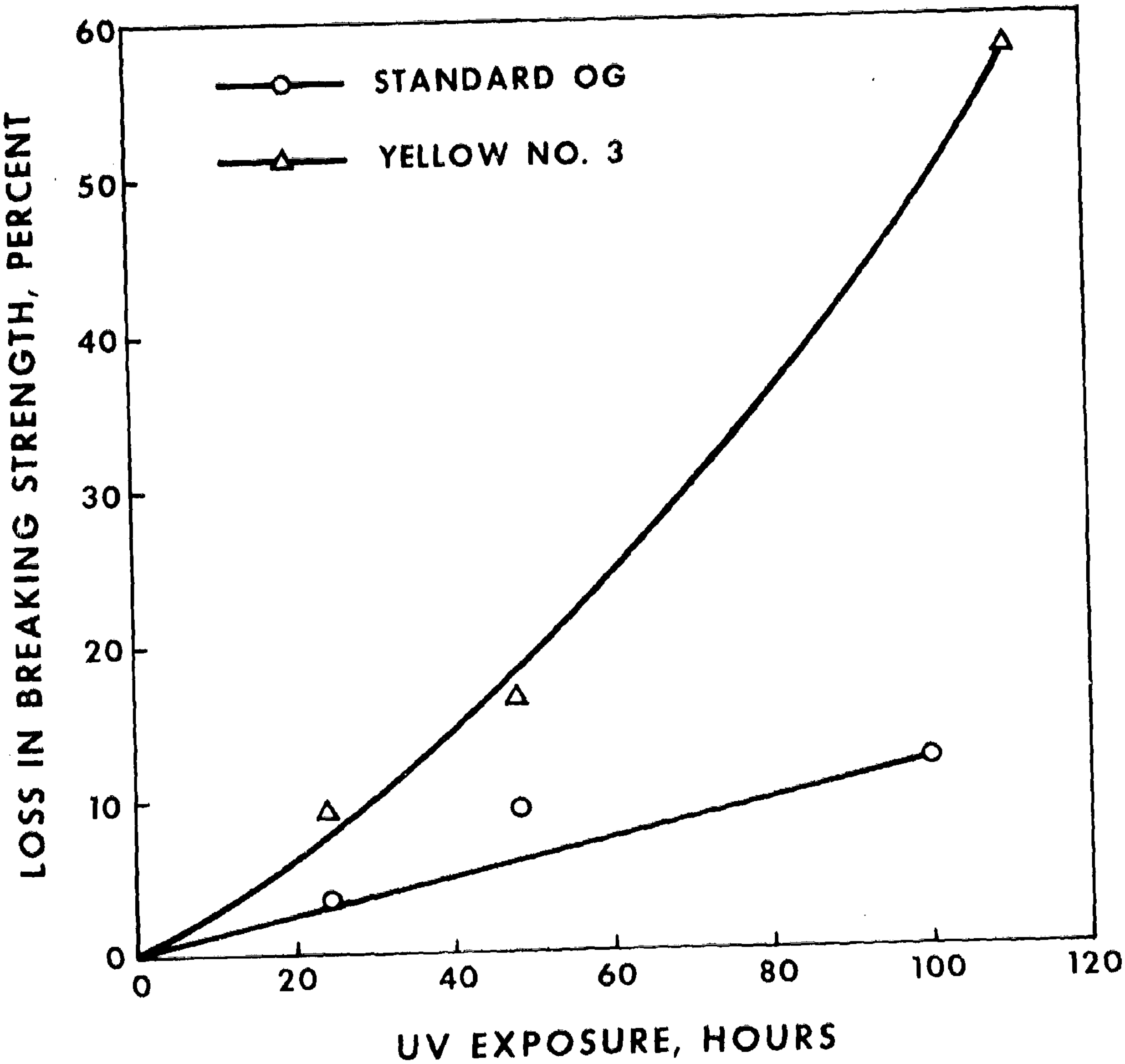

FIGURE 2. PERCENT LOSS IN BREAKING STRENGTH VS. HOURS OF UV EXPOSURE.

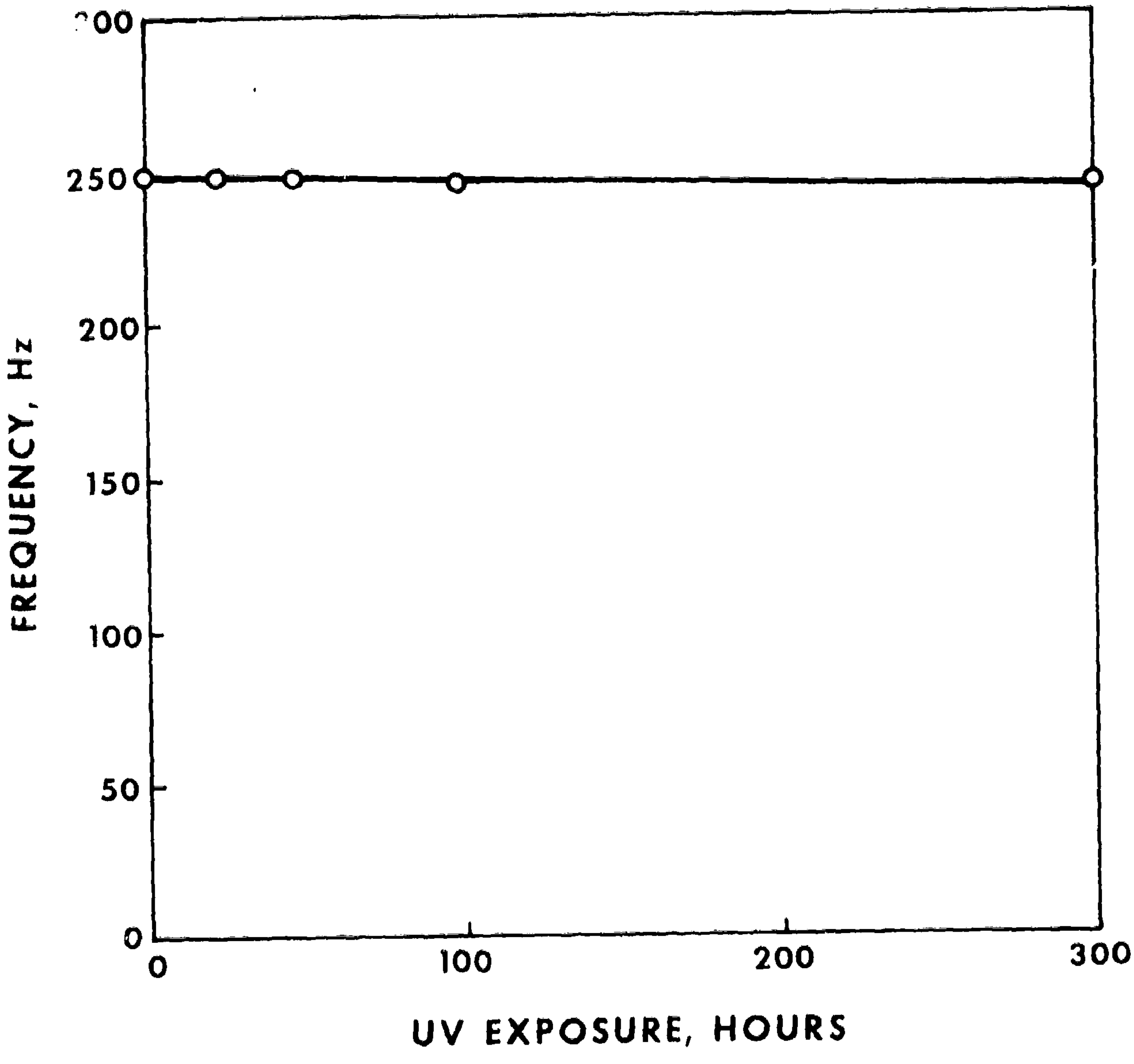

FIGURE 3. HOURS OF UV EXPOSURE VS. FREQUENCY GENERATED IN THE STANDARD OG FABRIC.

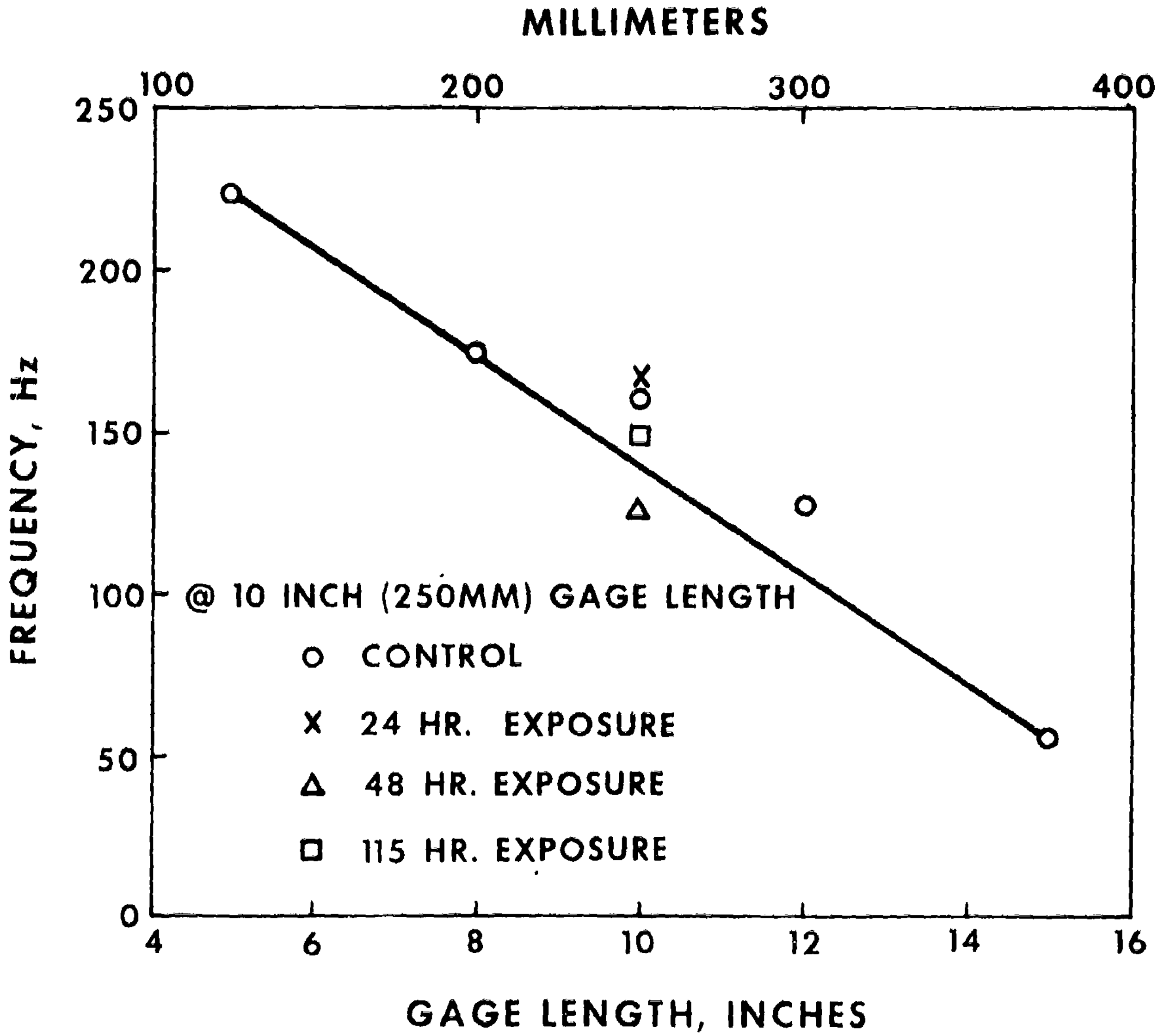

FIGURE 4. RELATIONSHIP BETWEEN GAGE LENGTH AND FREQUENCY GENERATED WITH THE ORIGINAL CLAMPS ON YELLOW #3 CONTROL FABRIC.

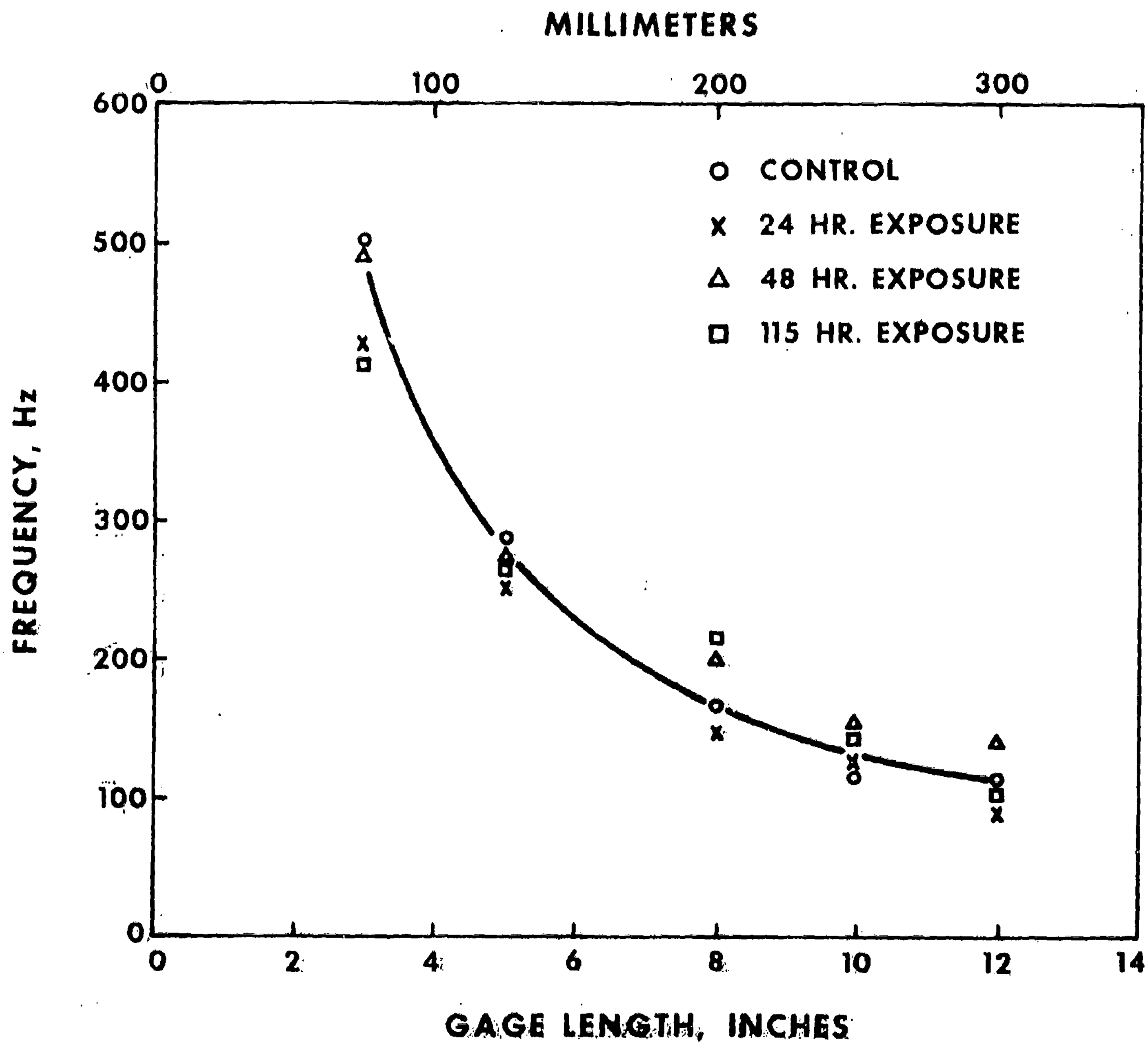

FIGURE 5. RELATIONSHIP BETWEEN GAGE LENGTH AND FREQUENCY GENERATED WITH INSTRON CLAMPS ON YELLOW #3 CONTROL AND EXPOSED FABRICS.

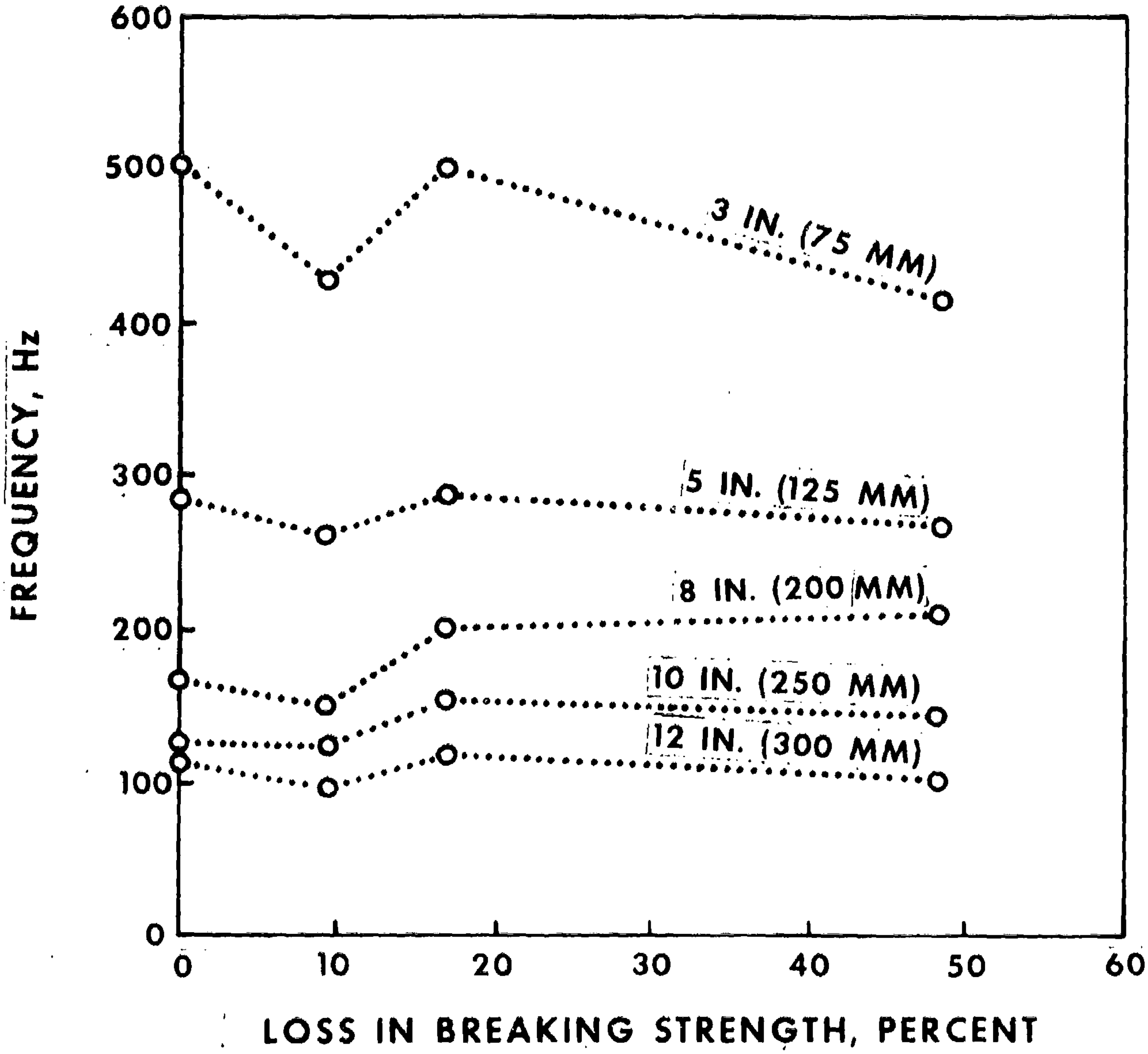

FIGURE 6. LOSS IN BREAKING STRENGTH VS. FREQUENCY AT VARIOUS GAGE LENGTHS, USING INSTRON CLAMPS ON YELLOW #3 FABRIC.

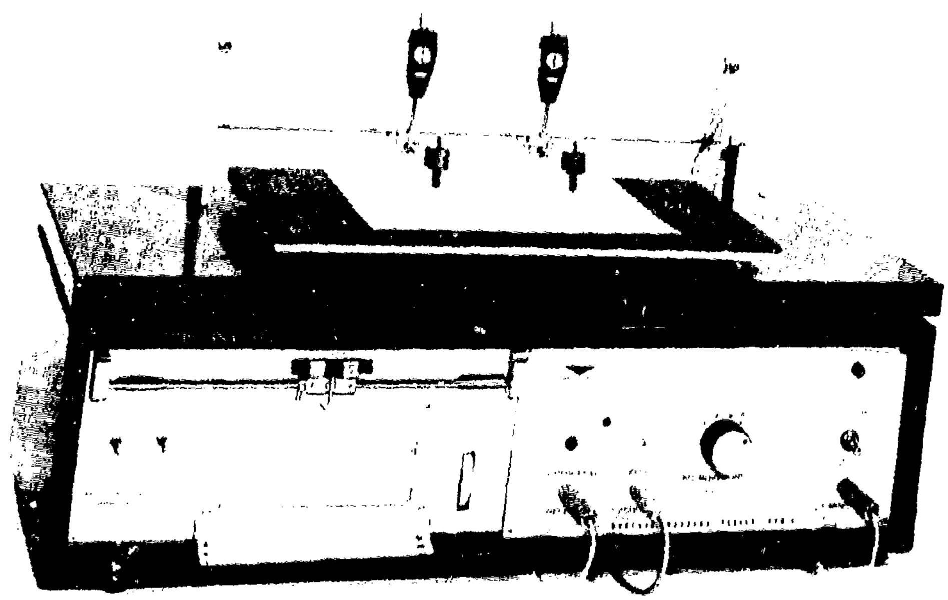

FIGURE 7. DYNAMIC MODULUS TESTER

TRACK PIN INDUCED STRESS

S. B. Catalano and S. T. Allen
Army Tank-Automotive Research and Development Command
DRDTA-RTAS
Warren, Michigan 48090
Autovon: 273-2712

ABSTRACT

Objectives of this study were: 1) Follow track pin residual stress history over the last few manufacturing steps (e.g., core hardening, induction hardening, straightening, grinding, and shot peening); 2) Examine the data for evidence of harmful levels/patterns of residual stress that may contribute to track pin failure. A total of 100 track pins were randomly selected from the last seven manufacturing steps. Residual stress measurements were made in longitudinal and hoop directions at 72 spots on each pin using automated x-ray diffraction equipment. Measurements were tabulated in terms of mean and standard deviation for each pin. Of particular interest to TARADCOM were: 1) The grinding operation induced hoop stresses 30 Ksi less compressive than longitudinal stresses induced at the same spots; 2) The 30 Ksi differences in directional stresses were not removed in the stress relief operation, and 3) It is possible to remove the 30 Ksi differences with good shot peening technique.

INTRODUCTION AND OBJECTIVE

Residual stresses are induced in components during heat treatment, machining, welding, casting and metal-working processes. These stresses can be of an undesirable nature, concentration, or level due to faulty processing or improper component design, adversely affecting functional performance and durability. High dynamic stresses in service superimposed upon existing residual stresses may exceed design load limits of the parts. X-ray diffraction is capable of measuring residual stresses nondestructively. Until recently, the method was time-consuming, required expert personnel to operate the equipment, and was limited to small parts. Time savings using automated equipment can be considerable while examining many points instead of just a few on a component. These large time savings have stimulated interest in measurement of residual stresses and has caused TARADCOM to investigate the effect of residual stresses on the serviceability of tank-automotive track components.

Track pin failures have been a problem which TARADCOM has historically investigated. Steps have been taken in the right direction in the past to alleviate this recurring problem. It was found that shot peened track pins last longer under fatigue testing than track pins that were not shot peened. Shot peening induces beneficial compressive residual stresses on the surface of the pin. This acts as a pre-stress which opposes tensile stresses, thereby allowing the pin to undergo larger applied tensile stresses as imposed in fatigue testing or in vehicular service. This should provide longer track pin life on the vehicle. To this date, track pin problems remain serious enough to warrant intensive study periodically by task force teams; these problems may be residual stress related. Residual stress data was not available at the time that the above mentioned fatigue life work was performed on shot peened track pins vs. track pins that had not been shot peened. Residual stress measurements were too time-consuming without automated x-ray diffraction equipment.

The work reported herein was motivated by the puzzling results of service type residual stress measurements obtained on track pins as requested on a recurring basis. Shot peening was the final step in manufacturing these pins. Shot peening should impart the same amount of compressive residual stress in all directions on a surface. However, some shot peened track pins submitted for analysis were found to be about 30,000 psi less compressive in the transverse (or hoop) direction than in the longitudinal direction of the pin; some invidivual hoop stress readings were found to be tensile. This anomaly provoked the desire to search for the cause. The objective of this work is twofold:

a. To follow track pin residual stress history over the last few processing steps, such as core hardening, induction hardening, straightening, grinding and shot peening.

b. To examine data for evidence of harmful levels or patterns of residual stress that may contribute to track pin failure.

APPROACH AND EQUIPMENT

A total of 100 T-142 track pins were randomly selected for this project from the last seven stages of manufacture at the manufacturer's plant. Figure 1 is a photograph of a T-142 track pin used in this study. T-142 track pins are 1¼ inches in diameter, 28 inches long and are made of 8650 H steel. M-60 tanks use approximately 360 T-142 track pins in each vehicle, depending on the model. The last seven stages of manufacture are core hardening, straightening, induction hardening, straightening again, centerless grinding, stress relief and shot peening. Ten pins were selected after the core hardening operation, ten after straightening, fifteen after induction hardening, twenty after straightening a second time, twenty after centerless grinding, fifteen after stress relief, and ten after shot peening as shown in Figure 2. In phase I of this work, residual stress measurements were made in both the longitudinal direction and the hoop

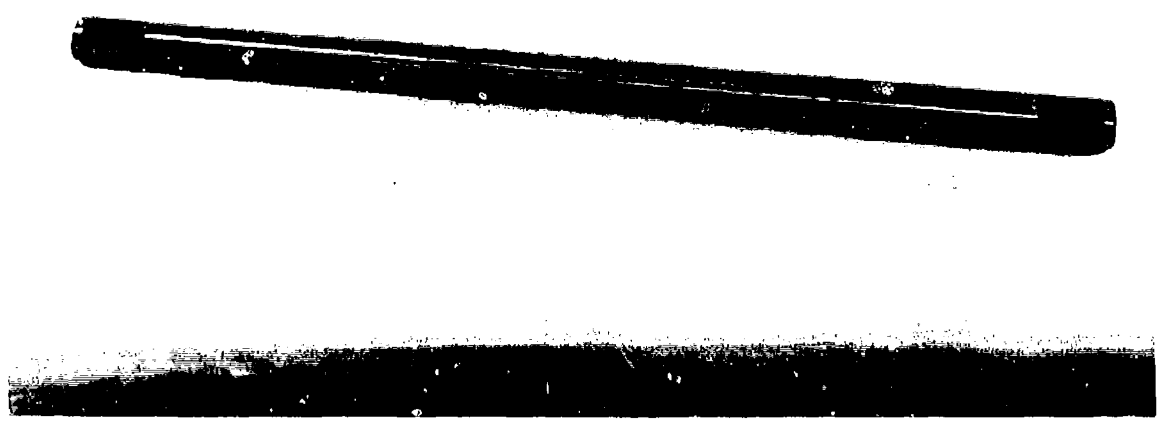

Figure 1. Photograph of a T-142 track pin used in Track Pin Induced Stress study

1. SELECT 100 TRACK PINS AT VARIOUS STAGES OF MANUFACTURE FROM MANUFACTURER'S PLANT.

SELECTION AS FOLLOWS:

CORE HARDENING
↓
STRAIGHTENING
↓
INDUCTION HARDENING
↓
STRAIGHTENING
↓
CENTERLESS GRINDING
↓
STRESS RELIEF
↓
SHOT PEENING

10 PINS
10 PINS
15 PINS
20 PINS
20 PINS
15 PINS
10 PINS

100 PINS TOTAL

2. MEASURE LONGITUDINAL AND HOOP STRESSES AT 72 SPOTS ON EACH PIN.

Fig 2 Test Procedure

direction at 72 spots on each pin. In phase II of this work, the pins were returned to the manufacturer; each pin was processed one stage further in the manufacturing process. Residual stress measurements were made in both the longitudinal and hoop directions at the same spots on these pins thereby providing increased data for statistical analysis purposes.

The equipment used in this project was an automatic stress analyzer manufactured by the American Analytical Corporation. This equipment is shown in Figure 3. It is x-ray diffraction equipment automated to measure residual stress using the method described in the SAE Technical Report No. 182. The automated equipment makes use of two x-ray tubes, two goniometers, four x-ray detectors used in pairs (each pair being coupled with a peak-seeking servomechanism), four x-ray activity meters, and electronic circuitry to calculate and display values of residual stress on a strip chart recorder. Residual stress is read directly from the strip chart recorder. The accuracy of the automatic stress analyzer is ± 5,000 psi as compared to ± 3,000 psi for conventional x-ray diffractometers. However, the automatic stress analyzer is anywhere from 10 to 100 times faster than the conventional x-ray diffractometer. Because of its greater accuracy, the conventional x-ray diffractometer is used as a check for calibration of the automatic stress analyzer.

On samples such as weldments, where the residual stress fluctuates rapidly, it is necessary to use a small size x-ray beam. The beam size is controlled by the size of collimator used; the automatic stress analyzer is equipped with three sizes: .030-inch, .045-inch and .060-inch. Either the 30-mil or the 45-mil collimator would be used on weldments. The 60-mil collimators were used in the present study.

RESULTS

The results of the residual stress measurements on each of the 100 track pins were tabulated in terms of mean and standard deviation of readings on each pin. The results obtained are shown in Figure 4. This chart is a tabulation of range of results obtained on the track pins selected for measurement at the seven stages of manufacture listed in the left column. The seven stages are:

a. Core Hardening: Core hardening is a salt bath, quench and temper operation yielding a Rockwell C hardness between 40 and 45.

b. Straightening: Straightening is required after core hardening because the pins are slightly warped by the core hardening operation. The straightening station is equipped with a dial indicator and a pneumatic press for bending the pin to remove the warp.

c. Induction Hardening: Induction hardening provides the case hardening. This is accomplished by passing the pin through an RF induction coil which heats only the outer shell of the pin. The pin is then water quenched as it emerges from the RF coil yielding a Rockwell C hardness between 55 and 60.

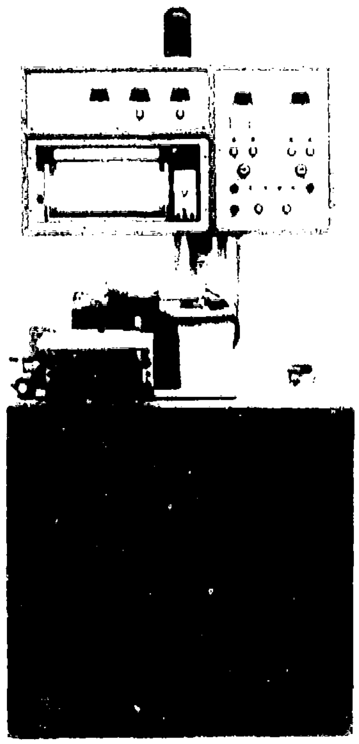

Figure 3. Automated x-ray diffraction unit for rapid measurement of residual stress.

RESULTS

	RANGE OF RESULTS							
	LONGITUDINAL STRESS				HOOP STRESS			
	MEAN		STD. DEV.		MEAN		STD. DEV.	
	HI	LOW	HI	LOW	HI	LOW	HI	LOW
1. AFTER CORE HARDENING	+15	-8	6	2	+18	-12	6	3
2. AFTER STRAIGHTENING	+15	+5	33	20	+10	-9	6	3
3. AFTER INDUCTION HARDENING	-60	-98	14	4	-90	-119	23	7
4. AFTER STRAIGHTENING	-59	-88	15	4	-87	-119	20	5
5. AFTER CENTERLESS GRINDING	-30	-64	20	6	-2	-38	15	4
6. AFTER STRESS RELIEF	-28	-40	16	7	+1	-9	10	5
7. AFTER SHOT PEENING	-48	-63	7	4	-51	-66	8	4

FIG. 4 RANGE OF RESULTS CHART

d. Straightening: Straightening is required again after the induction hardening step. This is done at the same station as was used for the first straightening operation.

e. Centerless Grinding: The pins are centerless ground to final size.

f. Stress Relief: In the stress relief operation, 16 skids containing 100 pins/skid are loaded into the stress relief furnace and are held at 350°F for three hours then removed from the furnace to air cool.

g. Shot Peening: Shot peening is similar to sand blasting; however, steel shot is used rather than sand. The shot dimples the surface slightly and creates a beneficial compressive residual stress on the surface.

A mean and standard deviation of readings obtained on each pin was determined for each pin. This was done for the longitudinal stresses and again for the hoop stresses. The data was grouped according to the seven processing steps under study. The highest and lowest means and standard deviations for each group were entered in Figure 4. In this order, the range of results can be reviewed rather conveniently. The entries are in units of Ksi (i.e., 10^3 psi) and are values of residual stress on the surface of the pin only. A positive sign indicates a tensile stress; a negative sign indicates a compressive stress. Instrument accuracy is $\pm$ 5 Ksi.

As the chart is reviewed, several things should be kept in mind for perspective and assessment purposes:

a. The values of residual stress are expected to change from one processing step to the next reflecting the processing or treatment received.

b. One does not know in advance what values of residual stress to expect as a result of processing steps 1 through 6 since this has not been studied before. Thus, one cannot categorically say the results found are good or bad.

c. One does know in advance that after shot peening, all of the readings should be compressive. One does not know, however, how highly compressive the readings should be. The track pin drawing calls for the shot peening to be performed according to specification MIL-S-13165B. It specifies shot peen intensity in terms other than residual stress.

d. The failure mode of track pins is known to be tensile. Areas on a final track pin that remain tensile or are only slightly compressive are definitely bad; these areas act as stress risers and promote crack initiation in those areas.

Characteristic results of the seven groups of track pins tested are as follows:

a. After core hardening, the pins are fairly stress-free in both longitudinal and hoop directions. This can be seen from the mean values listed ranging from $\pm$ 18 to -12. The standard deviations for this group ranged from 2 to 6, indicating a tight distribution of data.

b. After straightening: Longitudinal stresses are affected considerably by the straightening operation; hoop stresses are affected only slightly. Longitudinal stresses are found to be tensile on one side of the pin and compressive on the other. The large values of standard deviation reflect these large variations.

c. After induction hardening, the pins are difficult to measure and are highly compressive with a wide range of standard deviations. This is true for both the longitudinal and hoop directions.

d. After straightening: The straightening operation following induction hardening does not have much, if any, effect on the residual stress data in either the longitudinal or hoop directions.

e. After centerless grinding, the pins are easy to measure again. More significantly, the hoop stresses are now about 30 Ksi less compressive than the longitudinal stresses; in many instances, individual readings are tensile.

f. After stress relief, compressive residual stresses were lowered and the range of standard deviations lowered slightly reflecting a more uniform distribution of residual stresses. However, the hoop stresses were still about 30 Ksi less compressive than the longitudinal stresses and again many individual readings were tensile.

g. After shot peening, the 30 Ksi difference between the hoop stresses and longitudinal stresses disappeared and the range of standard deviations diminished. These two observations are indicators of good shot peening.

Data was taken at intersections of imaginary grid lines 1/2" x 1/2" located centrally on each track pin as shown in Figure 5. Individual data sheets as obtained from each track pin will not be presented here inasmuch as there were 380 data sheets involved. However, computer drawn histograms are presented for data taken from three pins that were typical of processing groups studied.

Pin 75 is typical of the pins processed up to and including centerless grinding. Figures 6a and 6b are histograms for data taken on pin 75 in the longitudinal and hoop directions respectively. Pin 85 is typical of the pins processed up to and including stress relief. Figures 7a and 7b are histograms for data taken on pin 85 in the longitudinal and hoop directions respectively. Pin 95 is typical of the pins processed up to and including shot peening. Figures 8a and 8b are histograms for data taken on pin 95 in the longitudinal and hoop directions respectively. The similarity between results on pins 75 and 85 should be noted. Both pins have no tensile readings in the longitudinal direction; both have tensile areas in the hoop direction. Pin 95 has no tensile readings in either direction. Similarly, data on pins processed up to but not including centerless grinding have no tensile readings in either direction.

DISCUSSION

It was stated earlier that some shot peened track pins measured

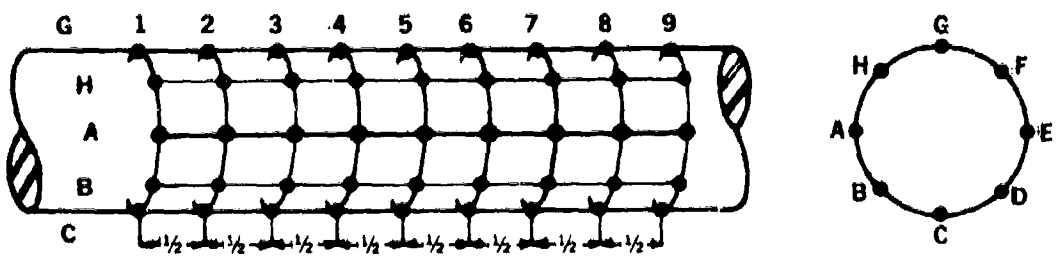

Fig. 5 Location of data points on central section of track pin

TRACK PIN 75 LONGITUDINAL STRESS

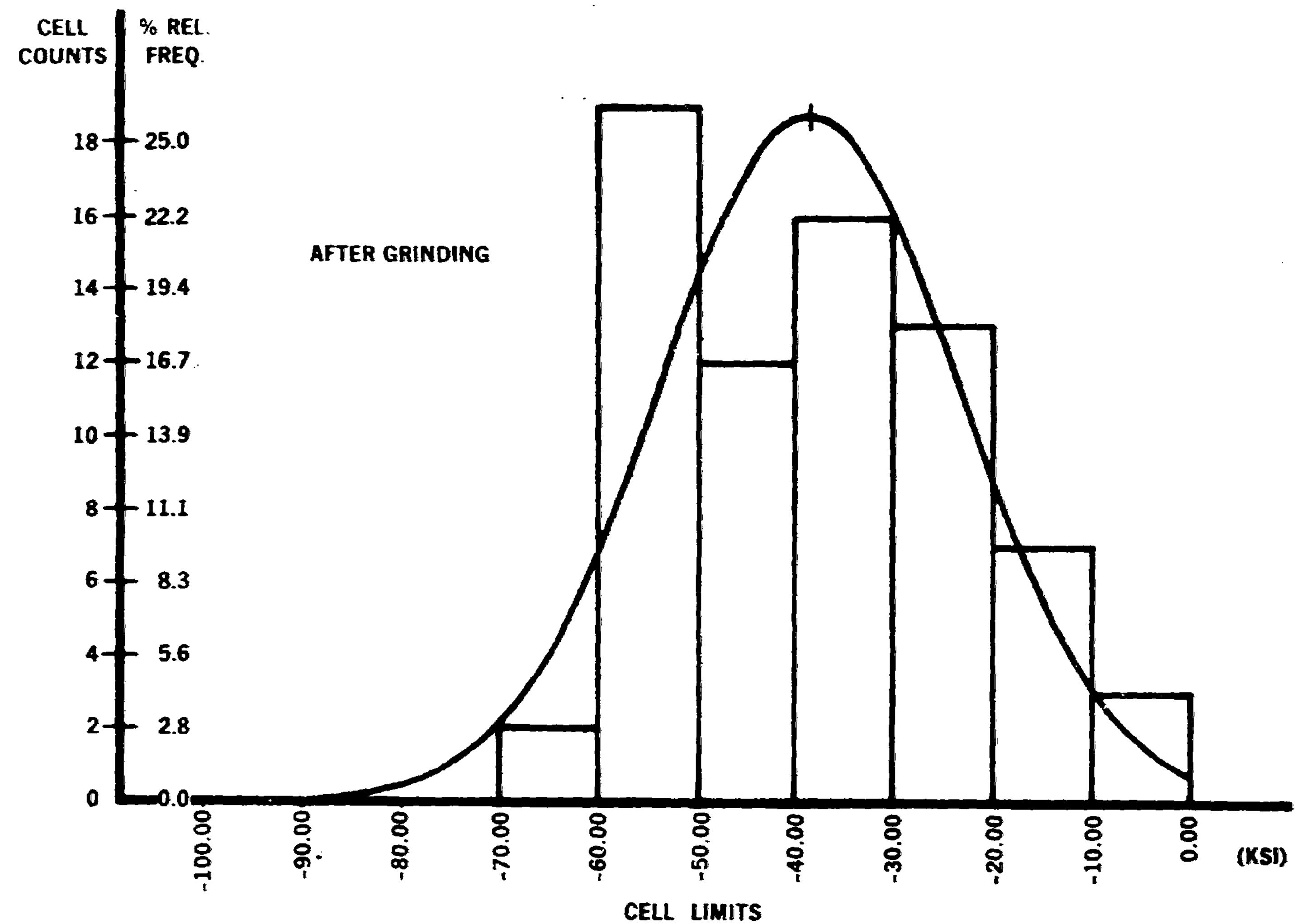

Fig. 6(a) Histogram for phase 1 data o. track pin no. 75 (longitudinal stress)

TRACK PIN 75 HOOP STRESS

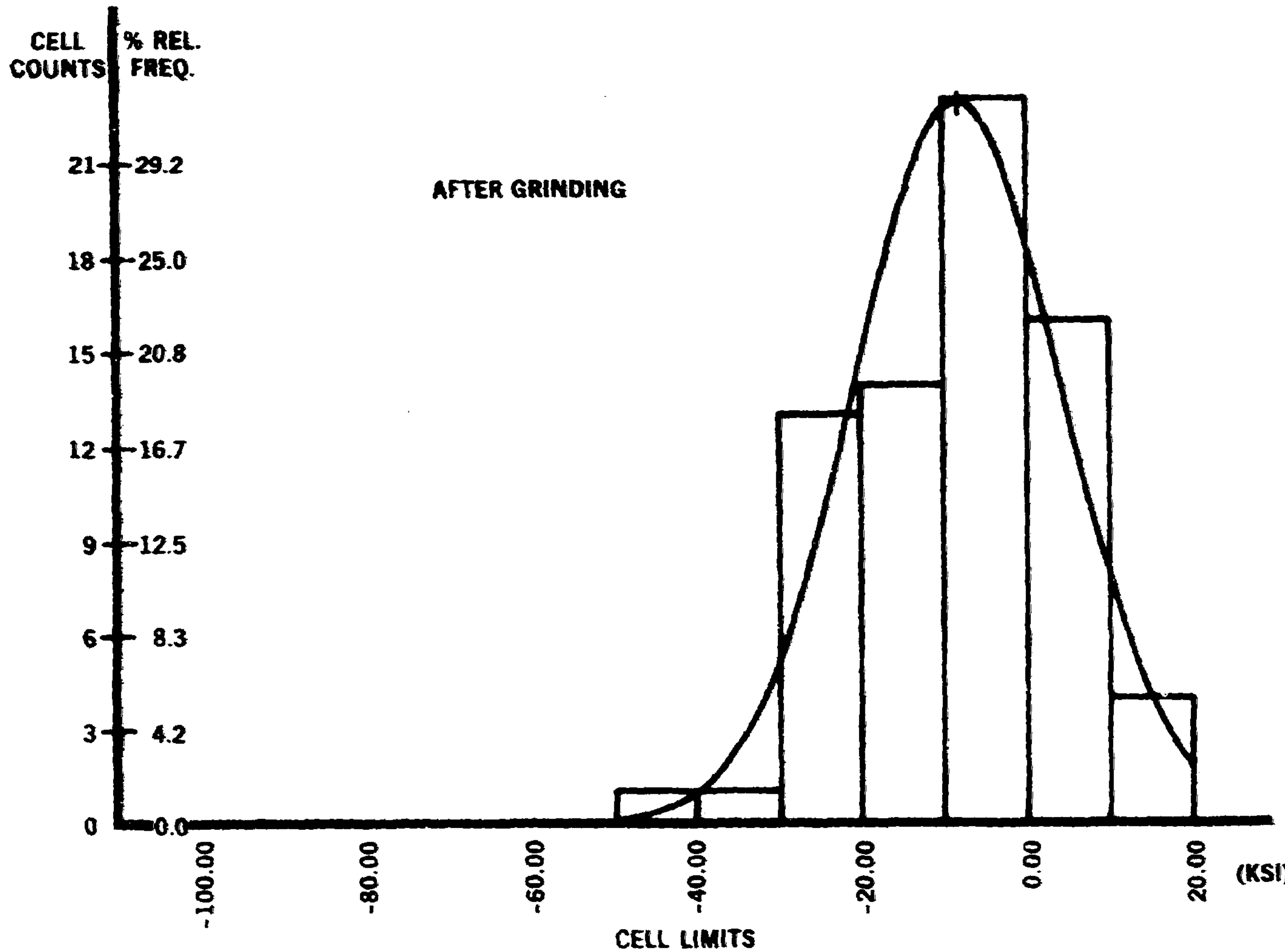

Fig. 6(b) Histogram for phase 1 data on track pin no. 75 (hoop stress)

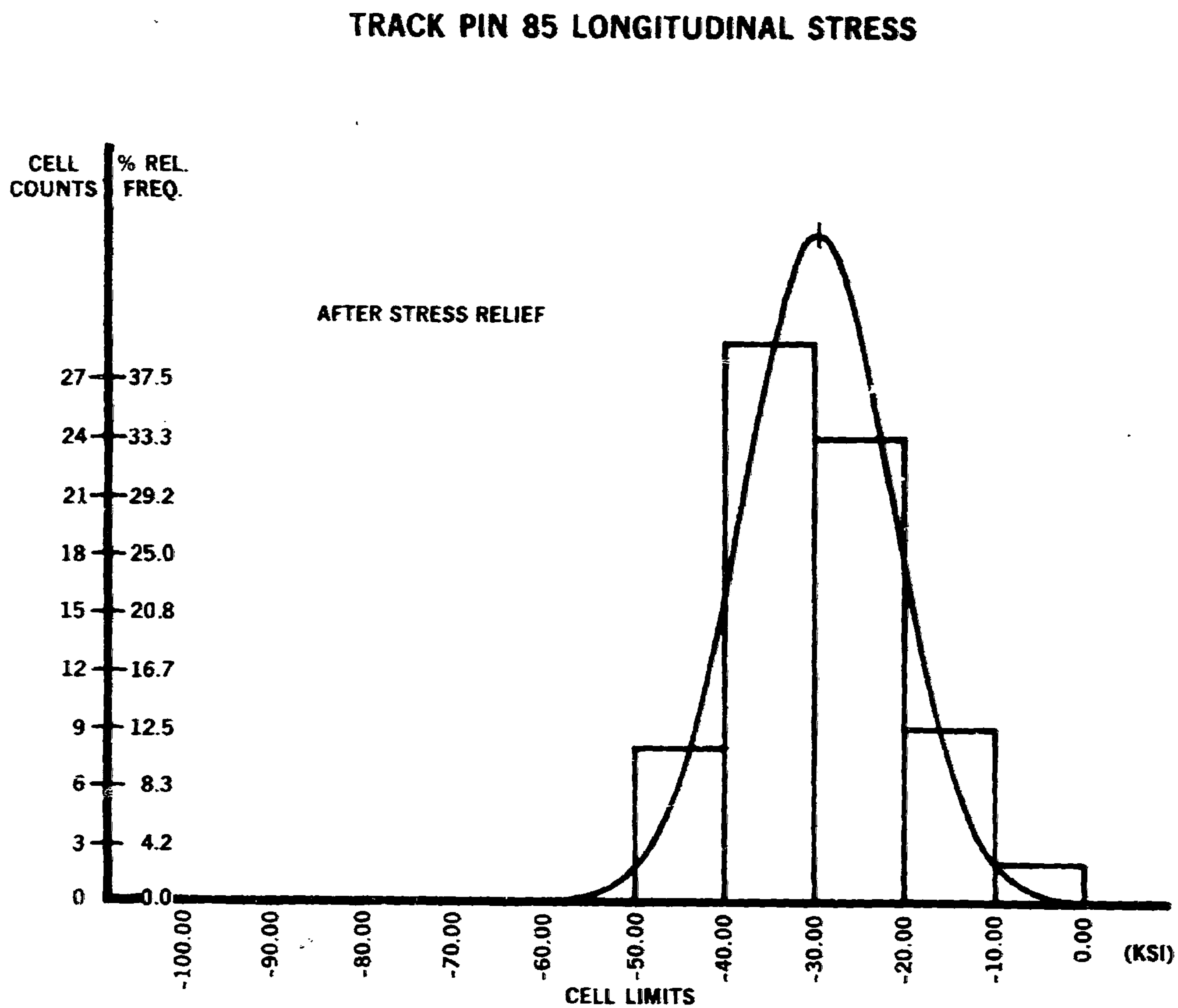

Fig. 7(a) Histogram for phase 1 data on track pin no. 85 (longitudinal stress)

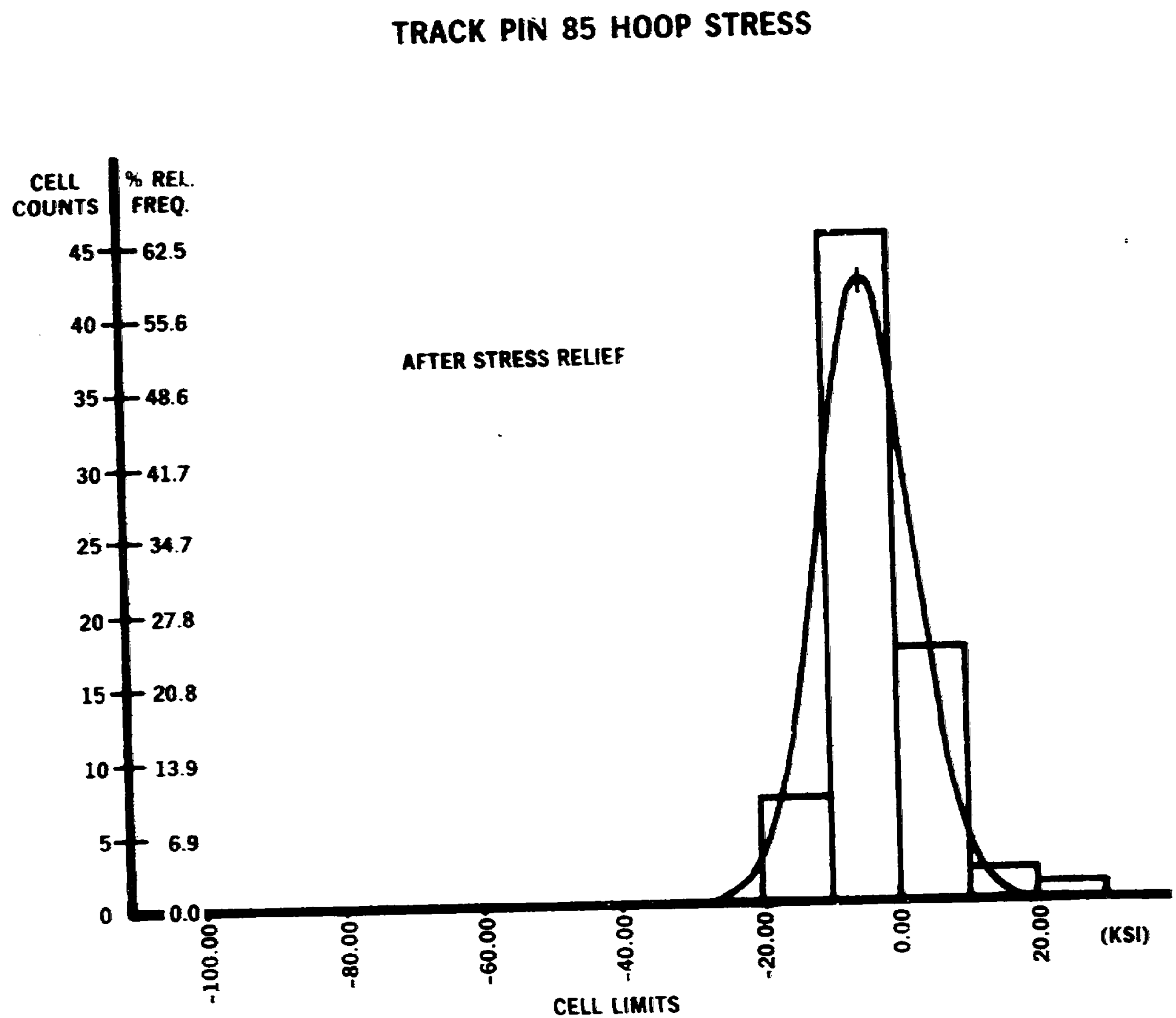

Fig. 7(b) Histogram for phase 1 data on track pin no. 85 (hoop stress)

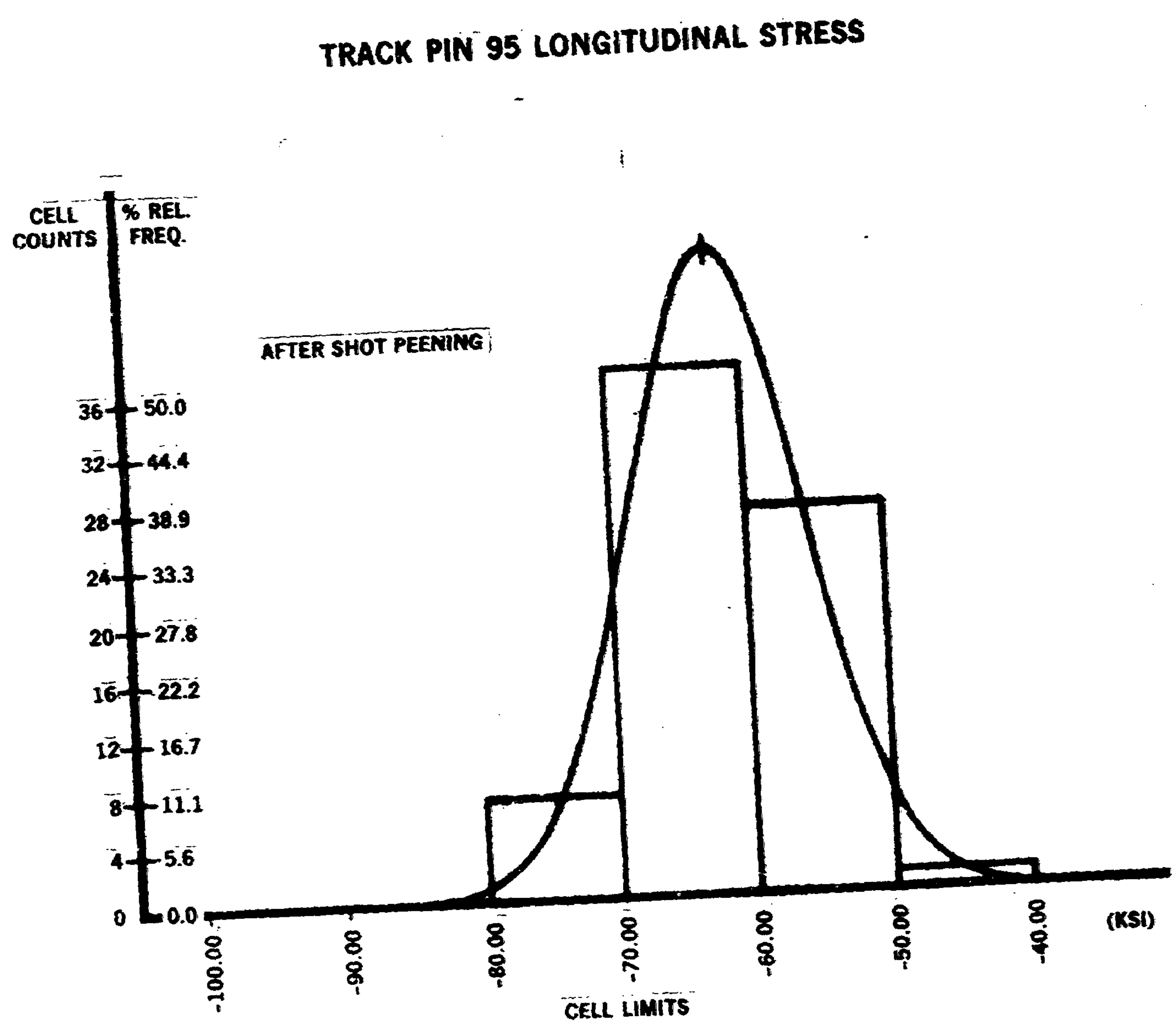

Fig. 8(a) Histogram for phase 1 data on track pin no. 95 (longitudinal stress)

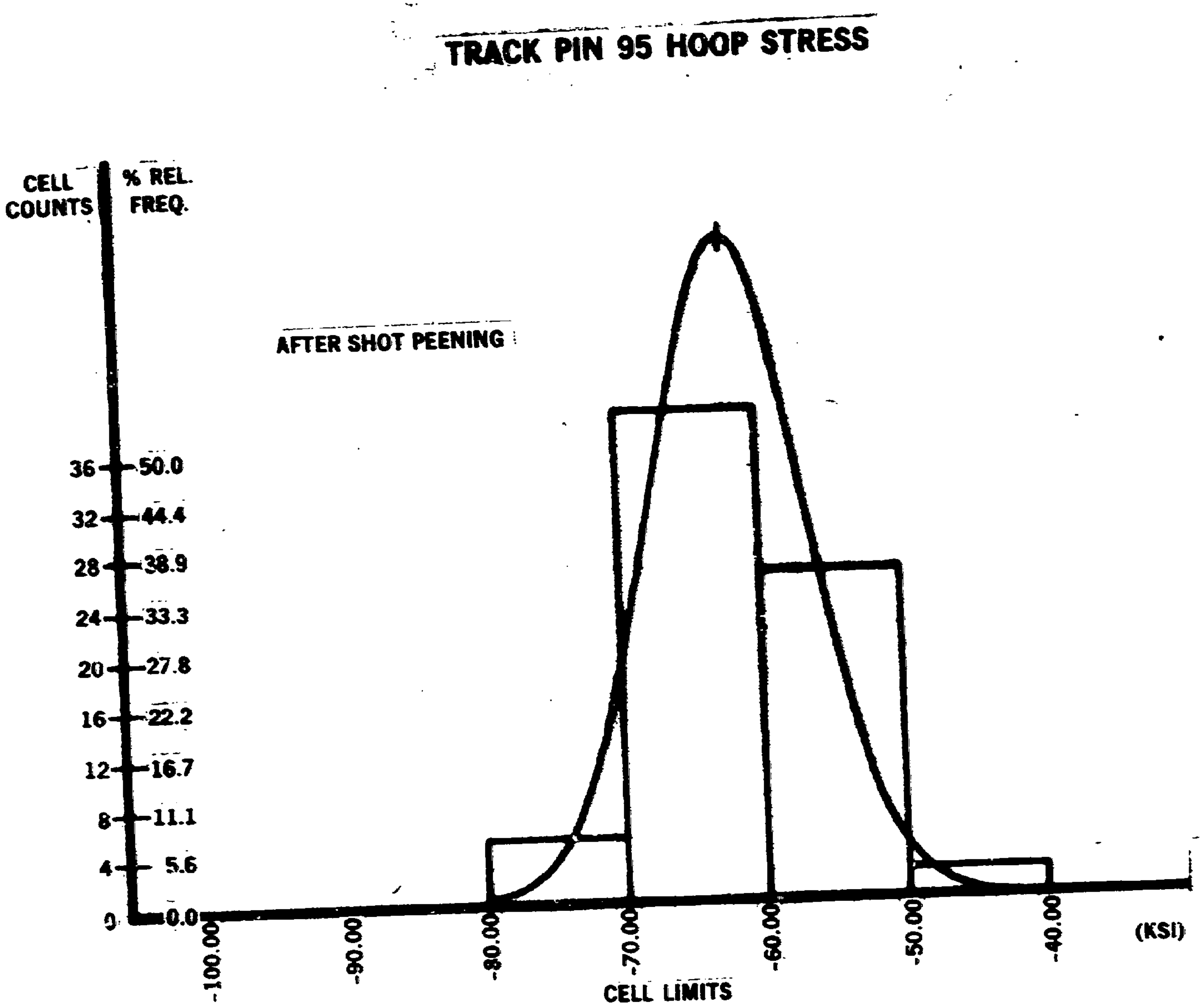

Fig. 8(b) Histogram for phase 1 data on track pin no. 95 (hoop stress)

prior to this study displayed hoop stresses 30 Ksi less compressive than the longitudinal stresses measured at the same point and that some of the individual hoop stress readings were actually tensile. Figure 4 showed the source of the 30 Ksi difference to be the centerless grinding step. The data showed that:

a. The 30 Ksi difference is generated in the centerless grinding operation.

b. The 30 Ksi difference is not removed in the stress relief operation.

c. It is possible to remove the 30 Ksi difference by shot peening.

This implies that if the shot peening is not adequate, some or all of the 30 Ksi difference remains and portions of the track pin are tensile in the hoop direction or nearly tensile. This is expected to be a serious factor in track pin failure. Implied also is that the stress relief step is of questionable value. The fact that the 30 Ksi difference is not removed in the stress relief operation raises questions about the need for the stress relief operation.

CONCLUSION

In view of the twofold objective of this work, first to measure residual stress levels on track pins after various manufacturing process steps and second to examine the data for potentially harmful levels or patterns of residual stress, conclusions to be made are as follows:

a. Some processing steps have large effects on residual stress level; other processing steps have little effect. The various residual stress levels observed after each step and the effects each step has on residual stress level was shown in Figure 4.

b. If shot peening is performed properly, the potentially harmful levels of hoop residual stresses as caused by the centerless grinding step and left remaining after the stress relief step are removed.

"FLAW DETECTION AND EVALUATION OF COMPOSITE CYLINDERS USING SPECKLE INTERFEROMETRY AND HOLOGRAPHY"

Terry Lee Vandiver
US Army Missile Command
GE&MS Directorate
Redstone Arsenal, AL 35809
Phone 205-876-5692
Autovon 746-5692

ABSTRACT

A nondestructive testing problem exists in defining what constitutes a flaw in fiber reinforced composite cylinders used for rocket motor cases and launch tubes. E-glass, S-glass, and Kevlar fiber composite cylinders were investigated. Several types of flaws were introduced into the cylinder walls. Laser speckle interferograms and holograms were made of the flawed composite cylinders using laser optics. Displacement data was obtained using an electromechanical single beam speckle interferometric analysis system which included a computer. Flaws, stress, strains, and material constants are easily obtained from the displacement data. A newly developed automated laser speckle interferometry displacement contour analyzer was also used to view the interferogram. The foremost advantage of these NDT techniques over such conventional methods as strain and dial gauges is that speckle interferometry allows the investigator to obtain "hands off" full field information.

LIST OF SYMBOLS

Symbol	Definition
D	Spacing Between Fringes
KE	Kinetic Energy
M	Free Fall Mass
S	Film Scale Factor
U	In-Plane Displacement
V	Terminal Velocity
f	Distance From Intefero-gram to Analyzer Screen
m	Fringe Order
n	Fringe Order At A Minima of Intensity At An Illumination Point

λ	Wavelength of Laser Light
X	Vertical Distance The Photodiode was Displaced From Central Bright

INTRODUCTION

An increasing demand for new materials has prompted the use of composites for such applications as rocket motor cases, launch tubes and aircraft tail sections. Filament-wrapped composite structures have merit because of the high strength to weight ratio and low cost of manufacture. With the increasing use of composites for structural applications there exists greater needs for flaw detection and evaluation. A need also exists for material elasticity constants to be used in the area of engineering design and structural analysis. Because of the nonhomogeneity of composite structures different techniques of analyzation must be used.

The twofold objective of developing valid and efficient techniques to detect flaws and determine some composite elasticity constants was investigated using optical processes to measure surface displacements. Some conventional methods of measuring surface strain and displacement utilize strain gauges, dial gauges and various other mechanical and electrical sensing devices. Such methods are highly accurate and sensitive; however, information is given over limited regions as discussed in Leendertz [1]. Therefore a full field view of the strain or displacement distribution requires a large number of measurements at different locations and is very time consuming. Speckle interferometry and holography are optical techniques which provide the investigator with sensitive noncontact methods of viewing displacements from the full field point of view.

TEST SPECIMEN PREPARATION AND FLAW TYPES

One hundred thirty-eight thin wall fiber reinforced composite cylinders were fabricated by a filament winding process where a continuous bundle of fibers is wetted with epoxy and wound onto a mandrel. Thirty structures made of E-glass were used in spot flaw evaluation and elasticity constant determination. Three groups of ten structures per group were prepared. Each group had a different helical wrap angle, either $\pm 30^{\circ}$, $\pm 45^{\circ}$, or $\pm 60^{\circ}$. Each group of ten structures consisted of six unflawed cylinders and four flawed cylinders. The simulated flaws in the cylinders were created by placing a 0.20-in. diameter by 0.003-in. thick disc of Teflon tape between two helical wraps of filaments located in the center of the wall of the hollow cylinder. Figure 1 shows the simulated spot flaws, wrap angle, and

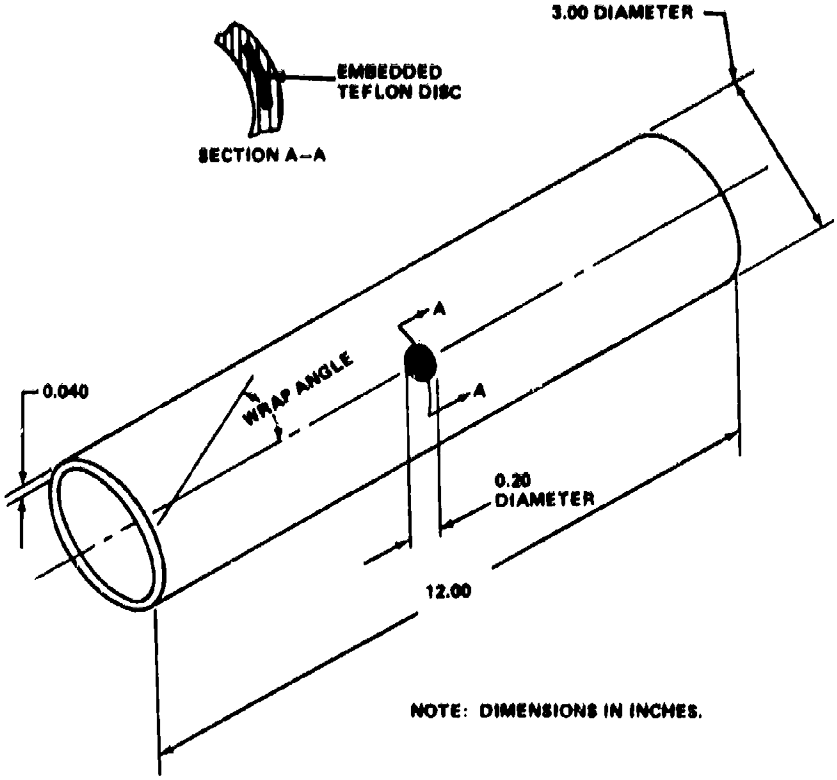

Figure 1. Composite Cylinder With Simulated Spot Flaw

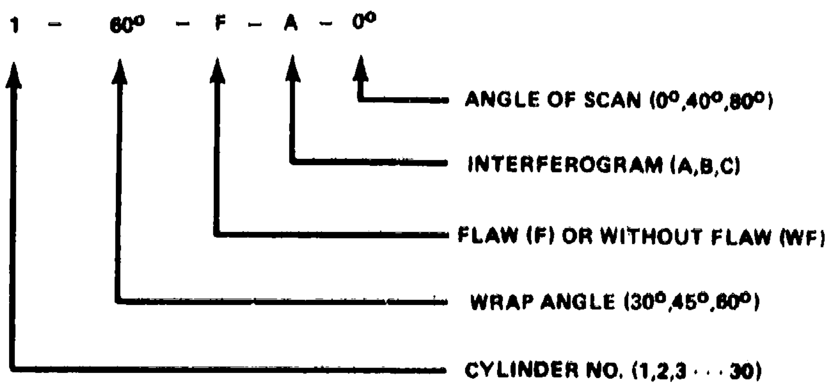

Figure 2. Test Cylinder Nomenclature Code

basic dimensions of the cylinders. The test nomenclature code was set up as shown in Figure 2 using test cylinder Number 1 as an example. The first three designations of the code were placed on each test specimen whereas all five designations were required to identify the interferogram scans. Figure 3 illustrates a typical interferogram showing scan lines representing angles of 40° separation.

One hundred eight structures were used in cut flaw and impact flaw evaluation. Three groups of thirty-six structures each were manufactured from E-glass, S-glass, and Kevlar rovings. The structures in each group consisted of ±45°, ±60° or ±70° wrap angles. The resin system for all the composite cylinders consisted of EPON 828, NMA hardener, and BDMA accelerator. The cut flaws were created by cutting an entire roving during the filament winding process. Compressive impact flaws were programmed into the outer cylinder wall by the fixture shown in Figure 4. The notches in the fixture allow a mass to be dropped from different heights, thus delivering different amounts of energy into the tube wall. The heat treated impacting darts had tip radii of 0.09-in., 0.13-in., 0.19-in., and 0.25-in. The test cylinder fits snugly onto a steel localizing bar so that the energy will be dissipated over a very small region of the tube, thus eliminating flexure considerations. The amount of kinetic energy applied to the cylinder wall can be calculated using

$$KE = \frac{1}{2} MV^2 \tag{1}$$

where KE = Kinetic Energy
M = Free Fall Mass
V = Terminal Velocity Of Mass At Impact

OPTICAL TEST SETUP AND PROCEDURE

When a diffuse surface is illuminated by the coherent radiation from a laser, a grainy speckle effect may be seen on the surface. This effect is because of multiple scattering points on the surface whose random phase distribution produces interference in a viewing plane. The test setup used to produce interferograms is shown in Figure 5. A Spectra Physics model 166 argon laser was used at an average power of 0.4 Watts. A double exposure photography technique was used to produce the interferogram on a 4-in. X 5-in. glass plate. One exposure was made with the test cylinder loaded with nitrogen gas and one with the cylinder unloaded. The load pressures ranged from 50 psig to 200 psig depending on the material and wrap angle of the composite cylinders. Three interferograms of each cylinder used for elasticity constant determination and spot flaw detection were made at 120° apart. Two interferograms of each cylinder used for cut flaw and impact flaw evaluation were made at 180° apart.

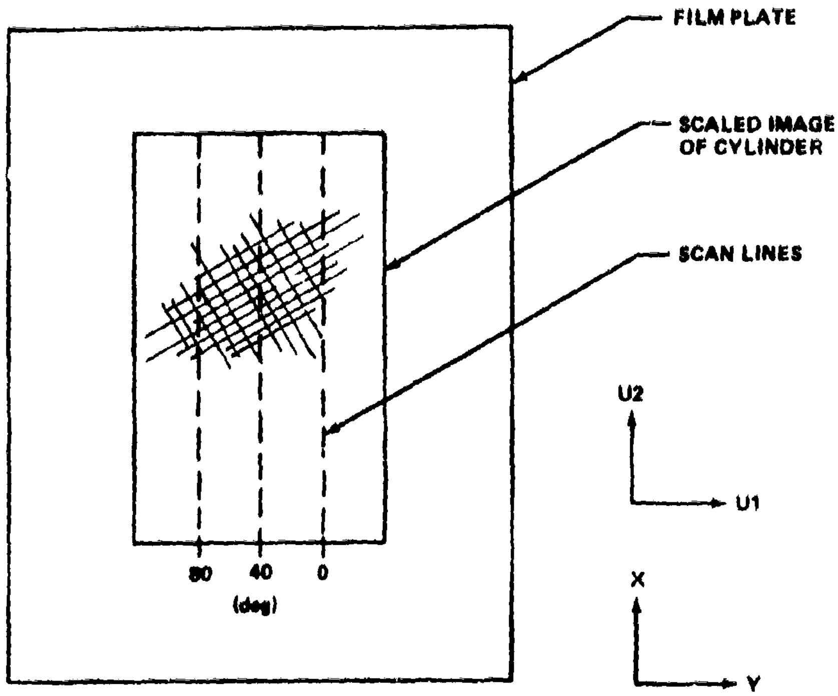

Figure 3. Interferogram Showing Scan Lines Representing Angles of 40° Separation

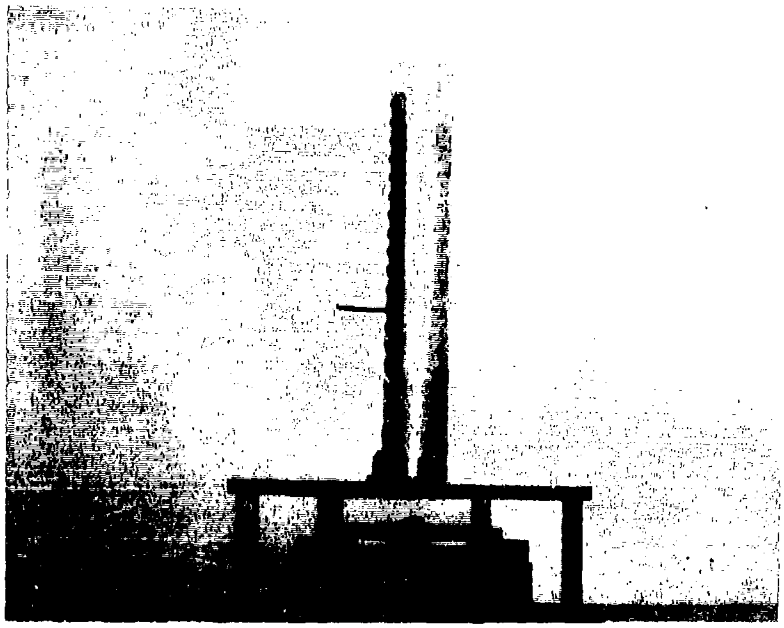

Figure 4. Impact Fixture

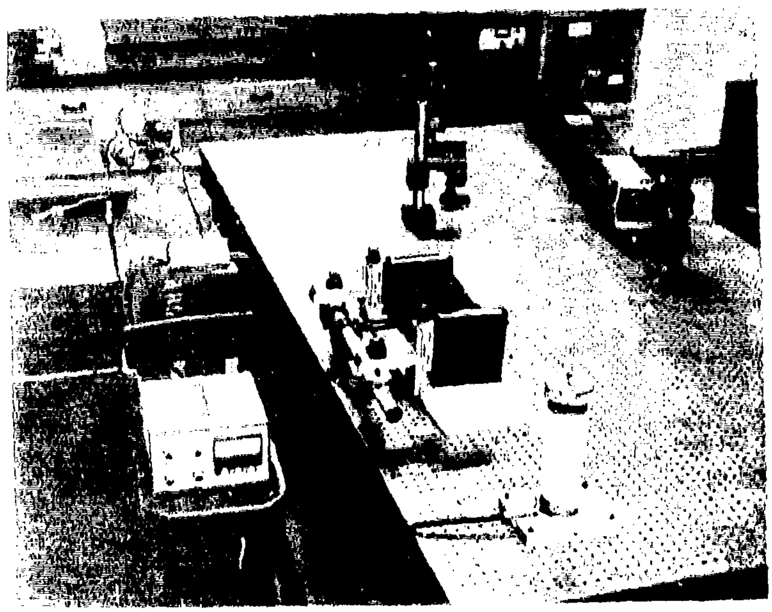

Figure 5. Test Arrangement For Speckle Interferometry

Holograms were made of the composite cylinders used for cut flaw and dynamic impact evaluation. The test setup used to produce the holograms is shown in Figure 6. A Spectra Physics Model 125 HeNe laser was used at an average power of 50 mW. A double exposure photography technique was used to prepare the holograms on 4-in. X 5-in. glass plates.

DATA ANALYSIS AND RESULTS

Three methods were utilized in the analysis of the interferograms: (1) point by point displacement determination, (2) contour mapping of the displacement field, and (3) full field interpretation. The point by point scanning of the interferograms was done by an electromechanical single beam interferometric analyzer system shown in Figure 7. The fringe spacing and angle of orientation were computer inputs. The displacement components in the circumferential and longitudinal directions were calculated from:

$$U = \frac{mfs\ \lambda}{D} \qquad (2)$$

where

- U = In-plane displacement at a point between loaded and unloaded model
- m = Fringe order
- λ = Wavelength of laser light used in data analysis
- f = Distance from interferogram to analyzer screen
- S = Film scale factor
- D = Spacing between fringes

The complete development of Equation (2) is presented in Mullinix [2].

Approximately twenty data points were taken along each of the 40° scan lines shown in Figure 3 for a total of 180 points per test cylinder. Figure 8 shows a plot of the displacement versus scan point for an 80° scan line. The stress-strain relationships as derived in Shaw and Smith [3] were used as a basis to develop the equations to calculate the composite modulus of elasticity and Poisson's ratio as shown in Table 1. Point by point displacements, strains, stresses, moduli of elasticity and Poisson's ratios are presented in completion in Vandiver [4].

The second technique of analyzing the interferograms used a new automated laser speckle interferometry displacement contour analyzer developed by Schaeffel [5]. Figure 9 shows the setup used to scan 5000 data points in four minutes. An off-axis optical photodetector was developed for generating displacement contour maps of bodies when

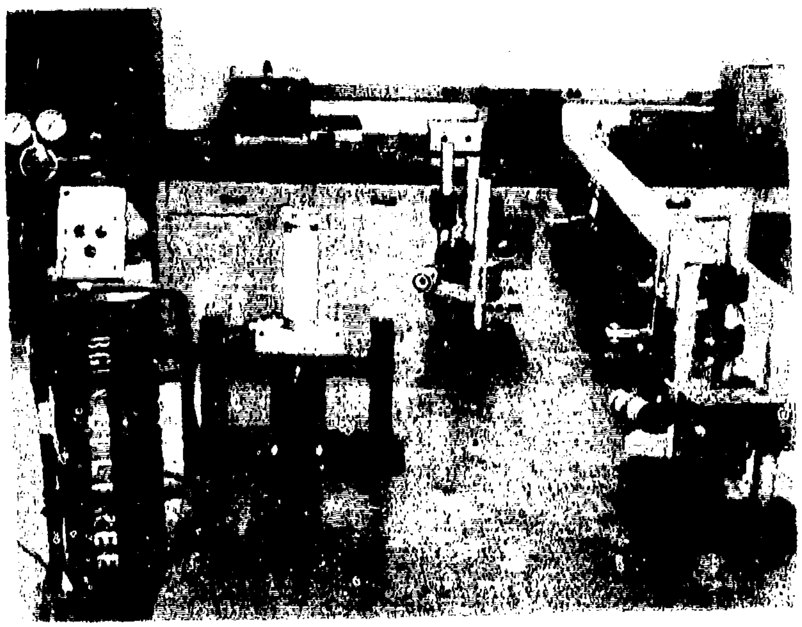

Figure 6. Test Arrangement For Holography

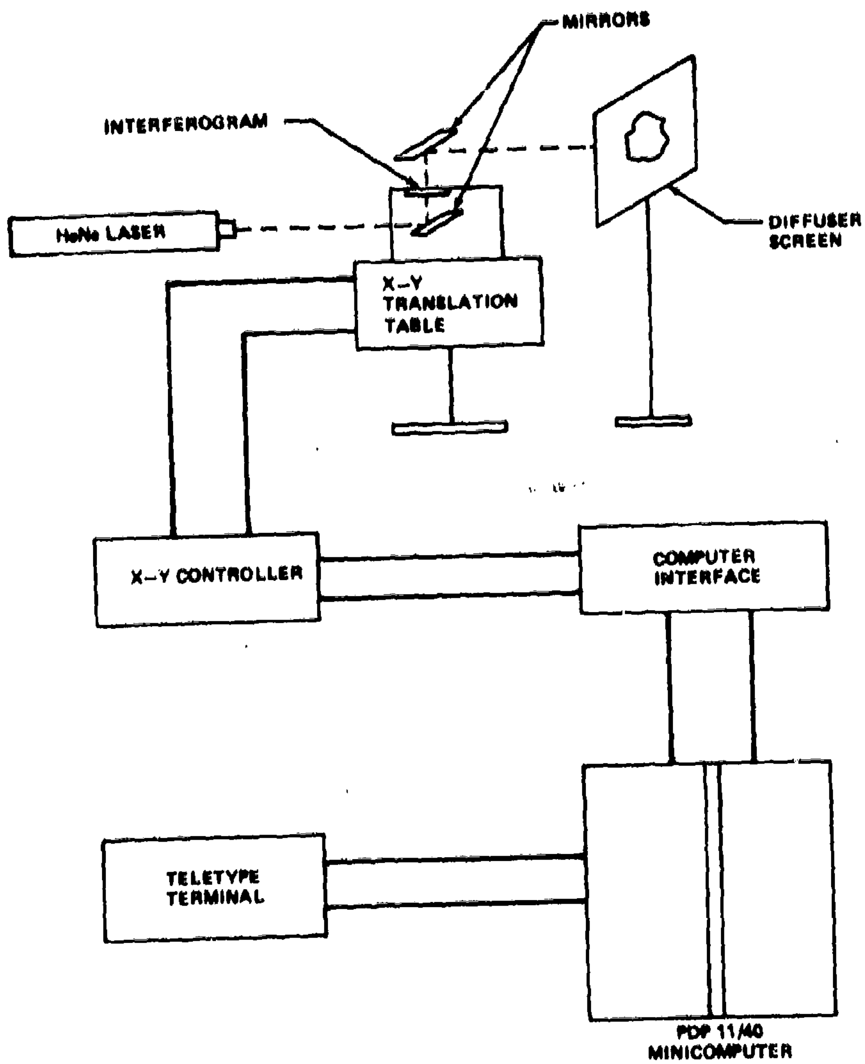

Figure 7. Electromechanical Single-Beam Speckle Interferometric Analyzer System

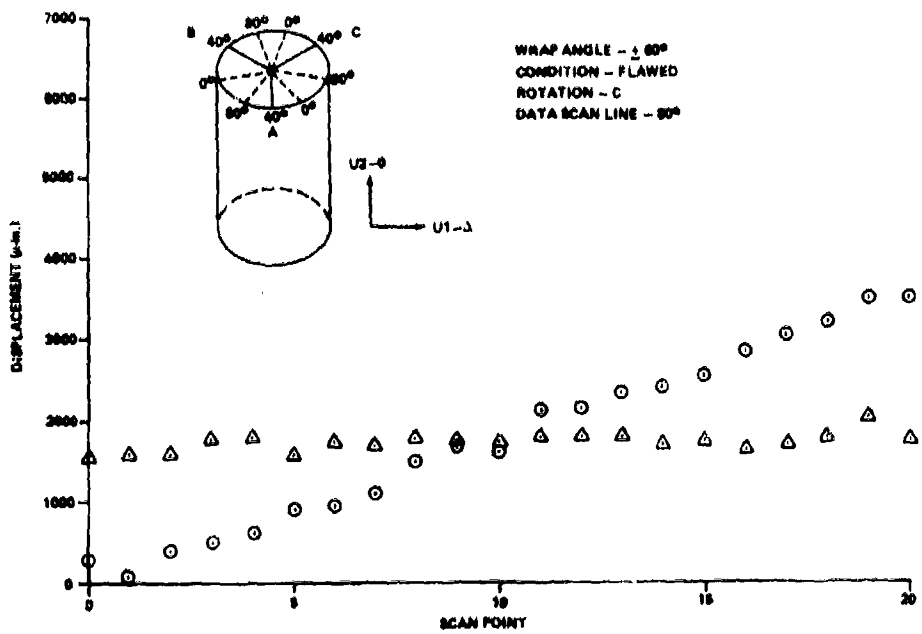

Figure 8. Displacement Versus Scan Point For Test (60°-F-C-80°)

Cylinder Tested	Poisson's Ratio	Composite Modulus Of Elasticity (Mpsi)
1-60°-F-A	0.503	7.67
-B	0.470	6.77
-C	0.471	6.35
2-60°-F-A	0.687	10.44
-B	0.647	9.82
-C	0.713	10.23
3-60°-F-A	0.362	7.35
-B	0.566	7.41
-C	0.558	7.80
4-60°-F-A	0.481	6.80
-B	0.631	8.96
-C	0.560	8.40
5-60°-WF-A	0.256	9.44
-B	0.500	8.72
-C	0.561	9.07
6-60°-WF-A	0.634	8.28
-B	0.494	7.00
-C	0.455	8.05
7-60°-WF-A	0.394	6.21
-B	0.476	6.87
-C	0.413	6.66
8-60°-WF-A	0.438	6.85
-B	0.436	6.39
-C	0.588	8.20
9-60°-WF-A	0.388	6.13
-B	0.356	5.90
-C	0.365	5.64
10-60°-WF-A	0.394	8.01
-B	0.397	7.70
-C	0.460	7.68

Table 1. Elasticity Constants For 60° Wrap Angle

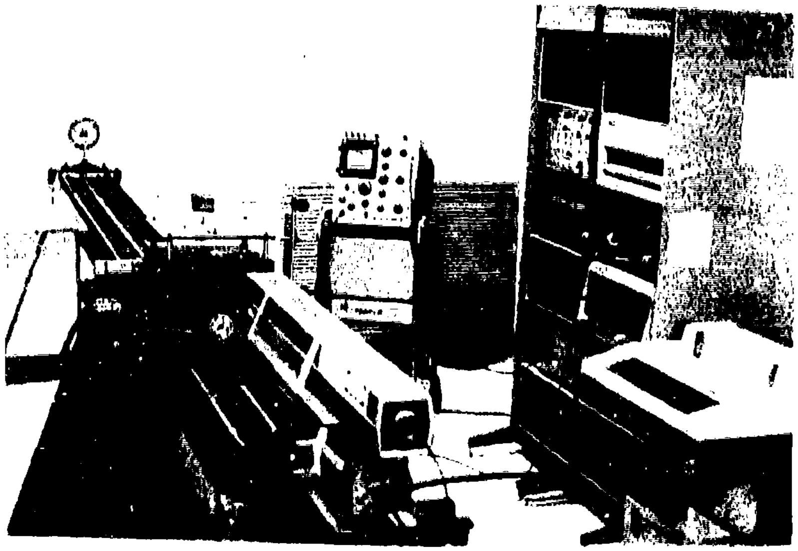

Figure 9. Setup For Automated Laser Speckle Interferometry Displacement Contour Analyzer System

deformed under load. An X-Y translation table which houses the interferogram moves in a raster fashion in front of a photodiode which in turn records the light intensity at each point. Contours of maxima and minima intensity were determined and printed in contour fashion on a decwriter. The contour maps represent loci of constant displacement on the body from which the interferogram was made. The direction of displacement is parallel to the axis formed from the central bright spot and the central axis of the photodiode and can be determined from:

$$U = n \left(\frac{Sf\lambda}{2X} \right) \tag{3}$$

where

U = displacement parallel to axis formed from central bright spot and central axis of photodiode
S = film scale factor
λ = wavelength of laser light used in data analysis
f = distance from interferogram to plane of viewing diode
X = vertical distance the photodiode was displaced from central bright
n = fringe order at a minima of intensity at an illumination point

A contour mapping of the unflawed side of a cylinder is shown in Figure 10 while the flawed side of the same cylinder is shown in Figure 11. Note the nonuniformity in the contours on the flawed side of the structure.

The third technique used in analyzing the interferogram was a full field interpretation around the flawed region. The whole field fringes are obtained by taking optically the Fourier transform of the amplitude function [6]. Figure 12 shows the optical setup used to record the data. This technique was mainly used as a visual tool to observe any large amounts of deformation around a flawed region. Figure 13 shows a full field photograph of the fringe pattern. In the center of the photograph one can see the very abrupt changes in deformation in the flawed region. The displacements can be obtained from the full field observations by equations developed in Wilson [6].

Full field reconstruction of holograms was also used as a technique to detect surface and subsurface flaws in the composite cylinders. The optical setup used is shown in Figure 14. When the processed film plate is illuminated by a coherent light source at the same reference beam angle used for making the hologram, a 3 dimensional image of the test object is produced as shown in Figure 15. One can easily detect the flawed region in the center of the cylinder by the abrupt changes

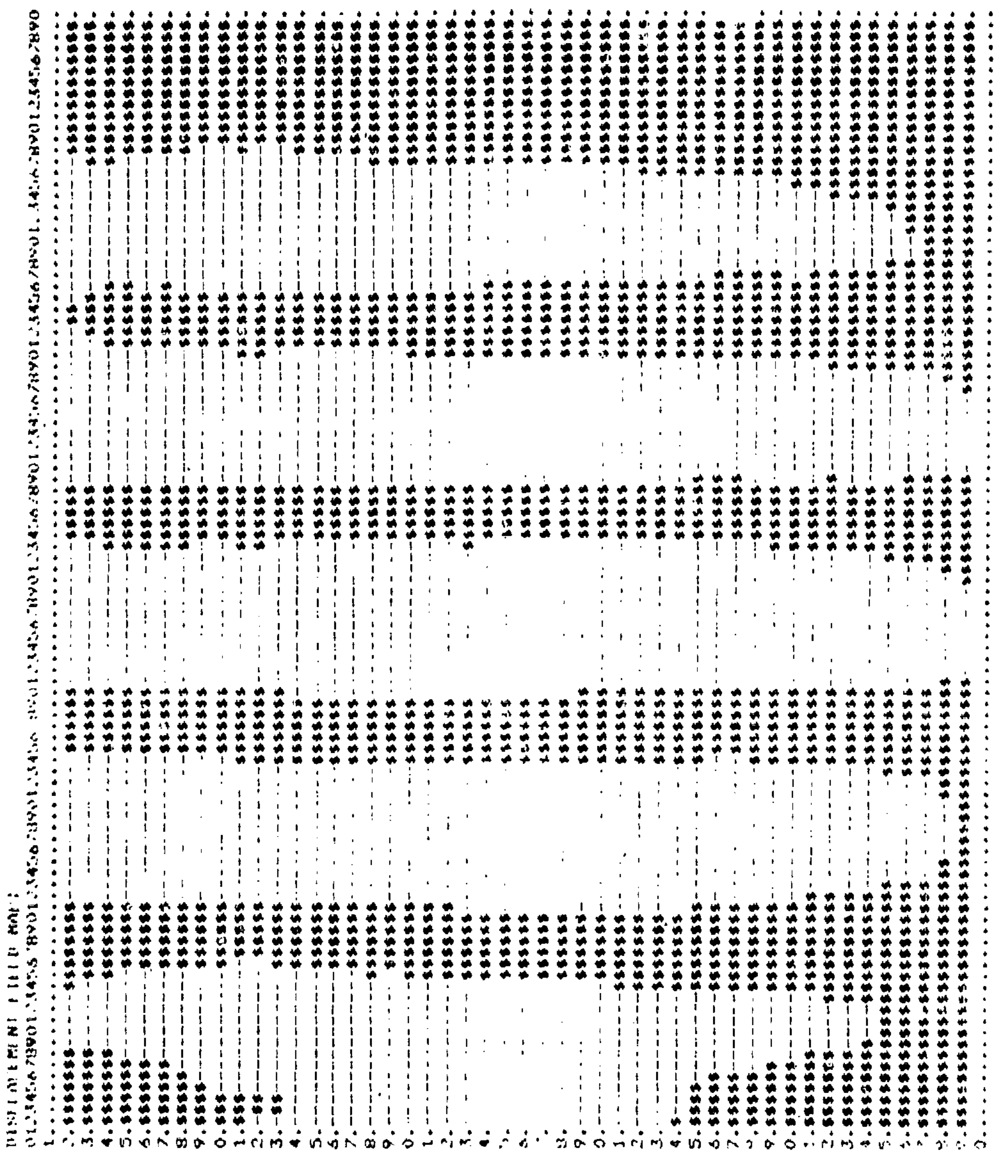

Figure 10. Displacement Contour Map Of Unflawed Side of Cylinder

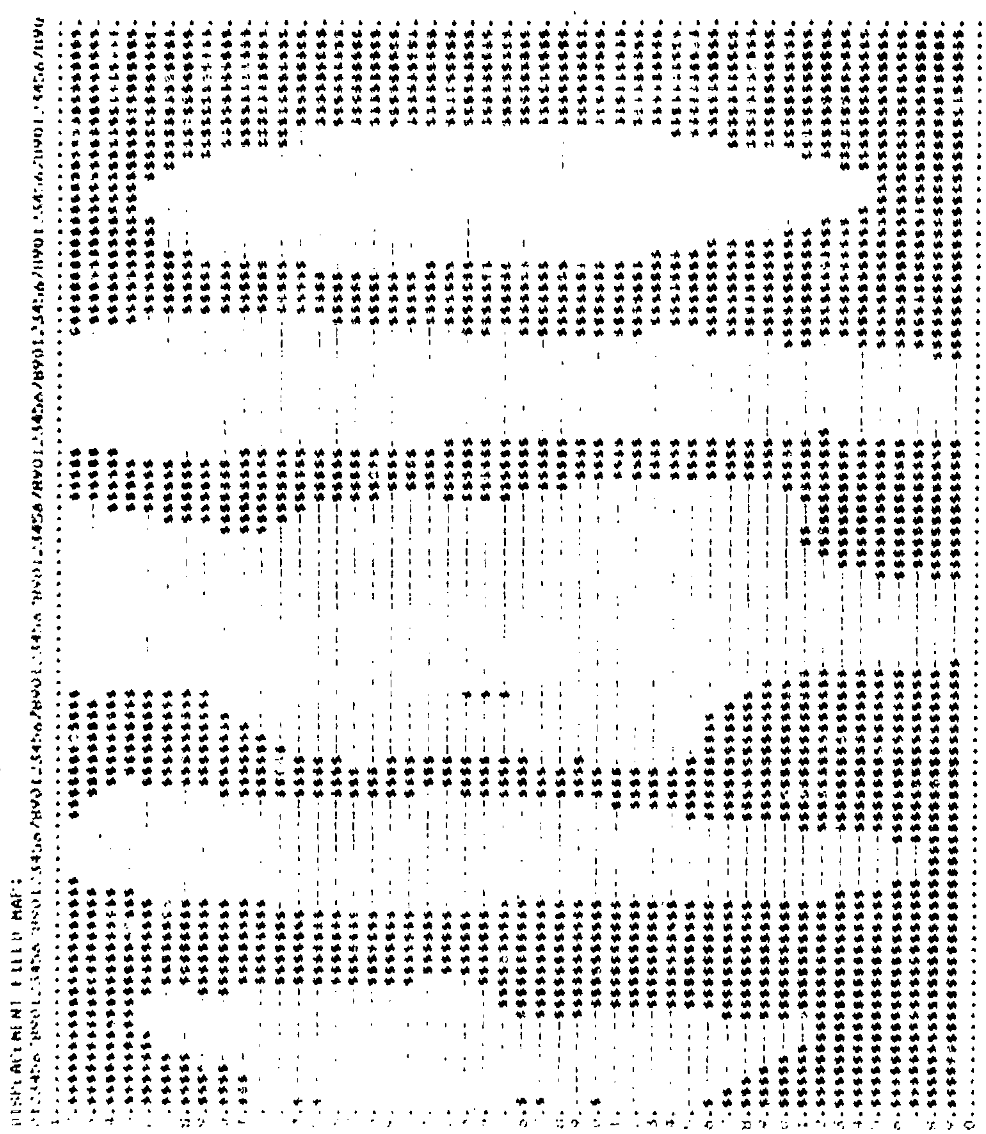

Figure 11. Displacement Contour Map Of Flawed Side Of Cylinder

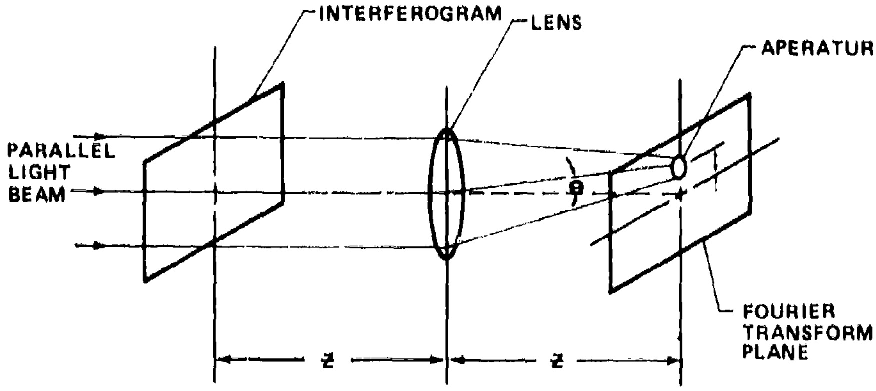

Figure 12. Full Field Reconstruction Of Interferograms

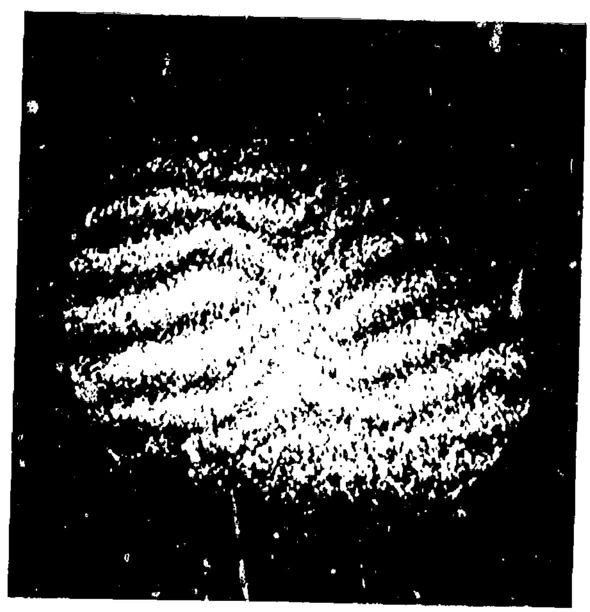

Figure 13. Fringe Pattern Of Full Field Reconstructed Interferogram

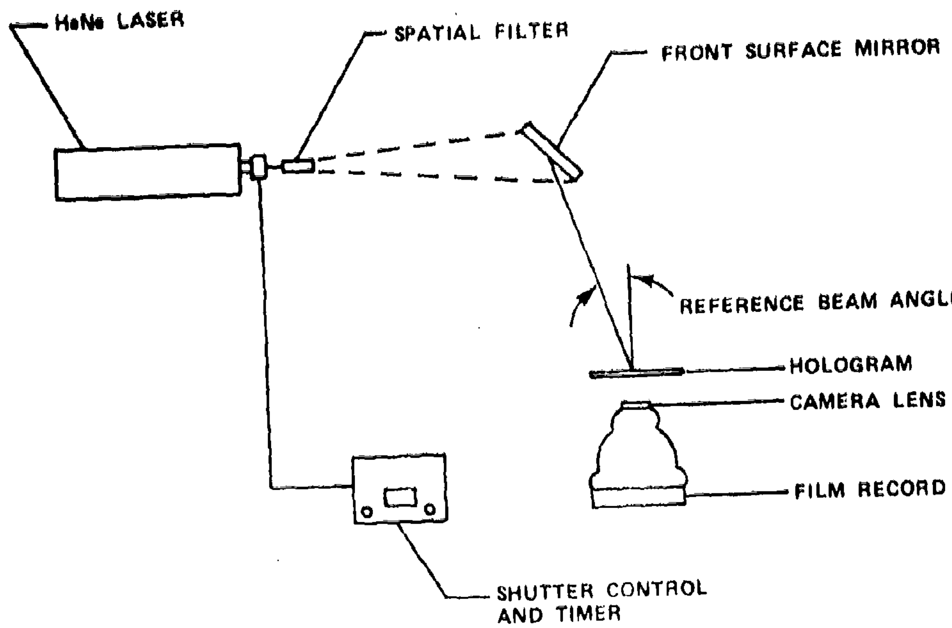

Figure 14. Full Field Reconstruction Of Holograms

Figure 15. Hologram Of Impact Flawed Composite Cylinder

in the slope of the fringe patterns. Out of plane as well as in plane displacements can be determined from the fringe patterns but this task was more concerned with visual detection than displacement data from the holograms.

Each of the composite cylinders was entered into a burst pressure testing program to determine the effects the different types of flaws had on the ultimate burst pressure of the structures. Figures 16 and 17 are plots of ultimate pressure versus wrap angle for impacted composite cylinders. The same plots were made using different energy levels. The results were correlated as to the amount of energy in the form of an impact the structure could withstand before significantly affecting the ultimate burst pressure.

SUMMARY AND CONCLUSIONS

One hundred thirty-eight composite cylinders were investigated using laser speckle interferometry and holography. Cut fiber, impact, and spot flaws were introduced into the walls of E-glass, S-glass, and Kevlar cylinders. Several optical techniques were used to determine surface displacements and detect flaws. The first technique described was a computer aided single beam interferometric analyzer system. This system produced very accurate displacement data which was used to determine the composite modulus of elasticity and Poisson's ratio as well as locating Teflon spot flaws.

The second NDT technique described was an automated laser speckle interferometry displacement contour analyzer. The foremost advantage of this system is the speed at which the data is collected. While operating at 20% of capacity, the system collected the data at the rate of 5000 data points in 4 minutes. The fringe contours which represent regions of constant displacement were observed for peculiar fringe behavior around the flawed regions.

The third technique used in both interferometry and holography was a full field reconstruction and interpretation of the fringe patterns. This technique was used on the cut flaw and impact flaw cylinders. The cut flaws could not be detected using any of the techniques described and had the same average ultimate burst pressure as unflawed cylinders; therefore, this type of damage was not defined as a flaw. However the impact flaws were easily detected using the full field reconstruction of interferometry and holography.

The optical techniques of flaw detection and displacement determination presented in this work are valid and efficient and could be used extensively in many areas of nondestructive testing. Flaws, stress, strains, and material elastic constants can easily be obtained from the data. The foremost advantage of these NDT techniques over such conventional methods as strain and dial gauges is that speckle

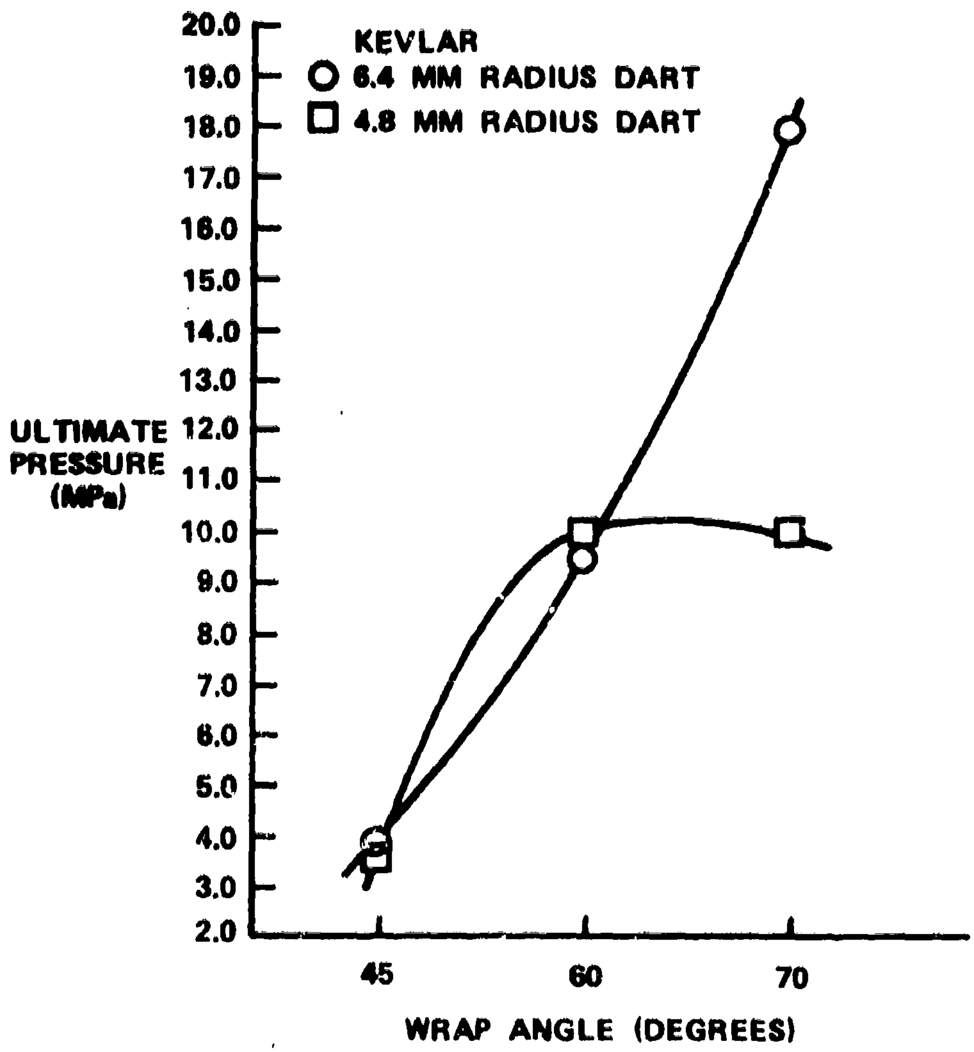

Figure 16. Ultimate Pressure Vs. Wrap Angle
(5.4 Joules Impact Energy)

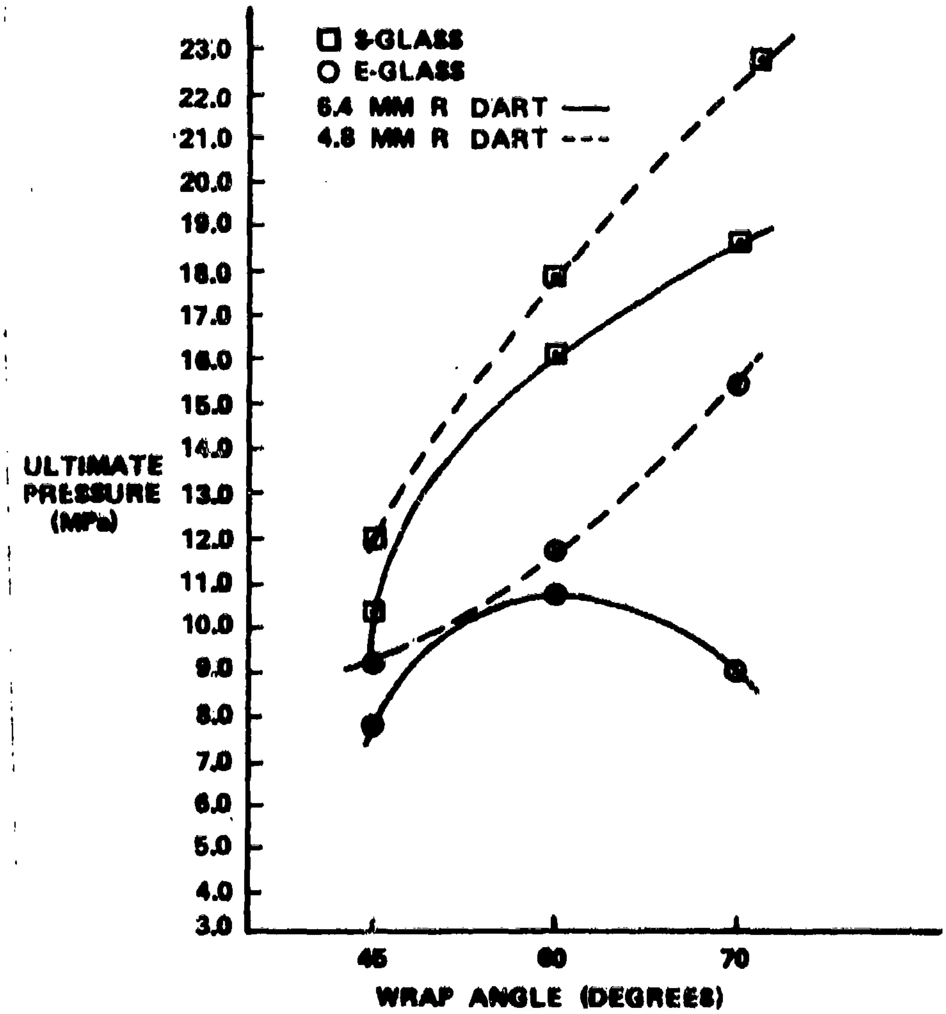

Figure 17. Ultimate Pressure Vs. Wrap Angle (7.2 Joules Impact Energy)

interferometry allows the investigator to obtain "hands off" full field information rather than combine data from many small regions.

REFERENCES

1. Leendertz, J., "Interferometric Displacement Measurement on Scattered Surfaces Utilizing Speckle Effect", Journal of Physics E, Volume 3; 1970.

2. Mullinix, B. R., Ranson, W. F., Swinson, W. F., and Cost, T. L., Quantification of Flaws in Fibered Composite Structures Using Interferometric Fringe Patterns, US Army Missile Command, Redstone Arsenal, Alabama, Technical Report RL-76-18, 20 April 1976.

3. Shaw, W. A. and Smith, F. S., Strength of Materials, Limited Distribution, 1968.

4. Vandiver, T. L., Determination of Elastic Constants For Flawed and Unflawed Composite Tubes Using Speckle Interferometry, US Army Missile Command, Redstone Arsenal, Alabama, Technical Report T-79-36, 8 March 1979.

5. Schaeffel, J. A., Automated Laser Speckle Interferometry Displacement Contour Analyzer, US Army Missile Command, Redstone Arsenal, Alabama, Technical Report T-79-71, 2 July 1979.

6. Wilson, T. F., "Determination of In-Plane Displacement Using Speckle Interferometry," Master of Science Thesis, Department of Mechanical Engineering, Auburn University, 7 June 1977.

MAGNETIC FIELD INTERACTIONS WITH MATERIALS DISCONTINUITIES

Patrick C. McEleney
Army Materials and Mechanics Research Center
DRXMR-MI
Watertown, Massachusetts 02172
AUTOVON 955-3444
Commercial 617/923-3444

ABSTRACT

Electromagnetic methods of nondestructive testing rely on the interaction of magnetic fields with material discontinuities to produce defect signals which contain information relevant to the physical characteristics of the discontinuity. A wide variety of NDT techniques are based on this type of interaction; Electromagnetics (Eddy Current), Magnetic Particles, and Fringe Flux (Magnetic Perturbation, Residual Field). Very little work has been done to model the phenomenon mathematically, and consequently most of the information in the defect signals related to the physical characteristics is lost.

The Army Research Office is sponsoring research to model the interaction of magnetic fields with material discontinuities using finite element analysis techniques. This work is conducted by Dr. William Lord at Colorado State University. This presentation will cover results to date, current activity and future directions of research activity.

Introduction

Precise information on the magnetic flux patterns is needed for the design of more effective test systems. The data provided by these models will provide a firm base for the design of more efficient test coils to help provide the information needed in the test signals. The instrumentation can be developed to evaluate the material meaningfully with knowledge of the behavior of leakage fields around defects. These refinements are vitally needed to tie in with fracture mechanics data.

At a recent "Workshop on Eddy Current Research and Development Requirements and Opportunities" sponsored by the Air Force Materials Laboratory, the need for modeling of probe/field interaction with flaws was cited as a high priority item by most task groups.

Technology Deficiencies noted by one task group were as follows:

a. Need to learn more about physics of ferromagnetic materials.

b. Need more accurate models of domains of ferromagnetic materials.

c. Need to extend existing models, computer programs from 2D to 3D.

d. Need to include nonlinear effects in analytical/numerical models.

e. Need to more accurately define electrical boundary conditions at flaws.

f. Currently lack general analytical tools for probe design.

This task group proposed specific programs, objectives, tasks as follows:

a. Determine electrical properties of cracks.

b. Study inverse problem.

c. Design probes for optimum detection of classes of flaws

d. Design probes for optimum detection of materials characteristics.

e. Develop models of real flaws, such as fatigue cracks.

f. Decide on "standard flaws" to validate modes.

g. Produce "standard flaws" on demand in laboratories.

h. Determine changes in electrical characteristics induced by stresses around crack tips.

i. Most work in Frequency Domain - how about Time Domain - 10 times resolution.

An important consideration in the area of nondestructive testing is the "problem of inversion" that is to obtain information concerning surface and subsurface conditions of a test object from the probe output signal. Solution of this "problem of inversion" is possible only with the development of viable mathematical models capable of predicting the interactions of many factors in the test object influencing the measured signal. In the case of eddy current methods of nondestructive testing, a change in the impedance of a search coil in the proximity of a material could be caused by several factors such as frequency of excitation, electrical conductivity and magnetic permeability of the material, geometry of the test object and search coil and discontinuties and inclusions in the material. In addition to these factors, the nonlinear magnetic characteristics of ferromagnetic materials and awkward defect boundaries have increased the complexity in the development of a broadly applicable mathematical model. For this reason, much of the existing literature associated with eddy current phenomena is concerned with making simplified assumptions so that, for a given eddy current situation, closed-form expressions can be obtained for the normalized impedance of the search coil.

In spite of the recent developments in automatic defect characterization associated with eddy current and leakage flux methods of nondestructive testing, the subject of electromagnetic methods of nondestructively testing ferromagnetic materials is characterized largely by empirical knowledge. An approach which does show promise of providing the basis of defect characterization schemes for active, residual and eddy current forms of nondestructive testing is the finite element analysis technique which was originally developed for the study of magnetic field in electrical machinery.

Availability of large digital computer, the proven capability of finite element methods of analysis to handle complicated boundaries and material nonlinearities and the ease with which a two-dimensional finite element computer code can be modified to handle three-dimensional field problems should make this numerical technique a promising tool for modeling eddy current NDT phenomena in ferromagnetic materials. In order to do this it will be necessary to modify the mesh structure to contain various defect shapes and to model the B/H characteristic for the material under test appropriately.

In order the develop defect characterization schemes for electromagnetic methods of nondestructive testing, a flexible mathematical model is needed to predict magnetic field/defect interactions under the constraints of nonlinear operating conditions and awkward boundary shapes. Although the dipole model predicts the <u>shape</u> of leakage field profiles around rectangular slots in ferromagnetic materials, the underlying linearizing assumptions associated with the technique prevent its use as the basis for defect characterization schemes.

Finite element analysis techniques have been applied with success to the prediction of magnetic fields in electrical machines. The work on this contract showed how they can be used to predict leakage fields around slots in ferromagnetic materials excited with a dc magnetization current. Certain assumptions have to be made with regard to the location of the zero vector potential boundary, discretization and B/H curve model, but on the whole, finite element techniques are sufficiently flexible and accurate to be applied to the defect characterization or "inverse" problem.

Modes of Field/Defect Interaction

The problem of modeling electromagnetic field/defect interactions in ferromagnetic materials is complicated not only by the nonlinear magnetization characteristic of the material and the awkward defect boundaries but also by the number of different phenomena utilized. Figure 1 shows the three major modes of field/defect interaction. In magnetic particle and magnetographic methods of nondestructive testing, the ferromagnetic specimen to be tested is initially magnetized with dc current. Residual leakage fields are set up around defects present in the specimen. The presence of such fields can be observed either directly using magnetic particles or indirectly by recording the leakage fields on magnetic tape. With reluctance and perturbation techniques, a constant dc magnetization current is used to set up active leakage fields around defects in the parts undergoing inspection, which can be detected using any flux sensitive transducer. Finally in eddy current testing, ac excitation is used to induce secondary currents and fields in the specimen. In this case, the presence of a defect causes changes in both induced currents and fields resulting in measurable impedance variations in the pick-up coil.

Differences in the residual, active and eddy phenomena are summarized in Figure 1 which shows the regions of the material's B-H characteristic over which the various phenomena occur.

The original effort in this work was to give details of a finite element model for predicting leakage fields around defects in ferromagnetic parts carrying dc magnetization current. It was felt that the finite element model could be used as the basis for developing defect characterization schemes for all electromagnetic methods of nondestructive testing, including active direct current, residual and alternating current methods of excitation.

1. A library of magnetic field profiles was developed for a variety of surface and subsurface defects in axially magnetized ferromagnetic bars.

2. The theoretical results were validated by monitoring the magnetic leakage field around actual defects using Hall plates (Figure 2).

3. Modeling techniques were extended to include residual forms of magnetization.

4. A feasibility study was made to examine the possibility of using the finite element analysis technique to model eddy current interactions with materials discontinuities.

5. All the computer algorithms needed to implement this program were developed. The initial results showed the flexibility of the technique.

In recent efforts, emphasis has been placed on further studies of the Russian dipole model including a computer simulation of the oblique slot equations and experimental measurement of the magnetic field within a slot in a ferromagnetic specimen. This work confirms that the underlying assumptions of the dipole model are invalid for active and residual leakage fields around defects. Also, initial studies have clearly shown that the computer code is extendable to eddy current phenomena, and the results obtained from simulating an ac current carrying conductor above a conducting slab agree very well with published analytical results (Figure 3).

The dipole studies did show that the assumption of a uniform "magnetic charge" density along the sides of a slot is invalid. Hall plate measurements made inside rectangular slots after removal of the excitation current clearly show a non-uniform distribution of magnetic field as would be expected if one considers the domain behavior of the material in the second quadrant of the B/H loop. This result has also been confirmed recently by workers at the Institut for Zerstorungsfreie Prufuerfahren, Saarbrucken who have attempted to refine the dipole model to include the effects of a non-uniform "magnetic charge" distribution. Even with this refinement, however, the dipole model cannot be readily extended to the study of realistic defect shapes as can the finite element model.

One criticism of this program was that the experimental verification of the theoretical results was made on electrical grade steel in which the magnetic properties are uniform and well known. This is not the case in the ferromagnetic materials of primary interest to the Army. In these materials, the magnetic properties are not well defined and are heterogeneous.

More accurate B/H data was gathered using a hysteresisgraph system for some of the steel specimens used in the past and many of Army samples acquired this year. With this data, the finite element simulations of selected active, residual and eddy current tests will be repeated and the results compared with experimental measurements. It is hoped that the B/H data obtained from the hysteresisgraph system will finally provide the kind of agreement between theory and practice needed to convince the NDT user that we, at last, have a viable modeling tool.

Future Work

Two additional research directions suggest themselves:

a. The results would be related to residual and active leakage fields around very narrow fatigue type cracks in ferromagnetic materials. In order to study this extension, an accurate x-y table and very small Hall probes would have to be obtained. This would allow a comparison to be made with our finite element model predictions.

b. At the recent workshop organized by AFML, the importance of analytical studies was emphasized in order to improve the eddy current testing art. If computer graphic equipment were available, the study of testing situations in both two and three-dimensions would contribute significantly to the modeling of eddy current phenomena. Already the 3D code needed for the solution of eddy current problems is being developed.

Potential Technological Applications

Electromagnetic methods of nondestructive testing have largely been characterized in the past by empirical models. As pressure has mounted during the last decade for improved evaluation, it has become increasingly clear that the old models of field/defect interactions are unsuitable for providing sound defect characterization schemes.

Finite element analysis techniques can be applied to the field/defect interaction problem. This project has shown that active, residual and eddy current phenomena can all be modeled if accurate B/H data is available for the materials under test. The major potential application of this work lies in the development of defect characterization schemes for automated electromagnetic NDT techniques.

Concluding Remarks

The final report on this contract will tie all of these electromagnetic NDT phenomena together via the finite element modeling. If this can indeed be accomplished, there is not doubt that the project will have contributed significantly to stimulating and advancing the state of the electromagnetic NDT art.

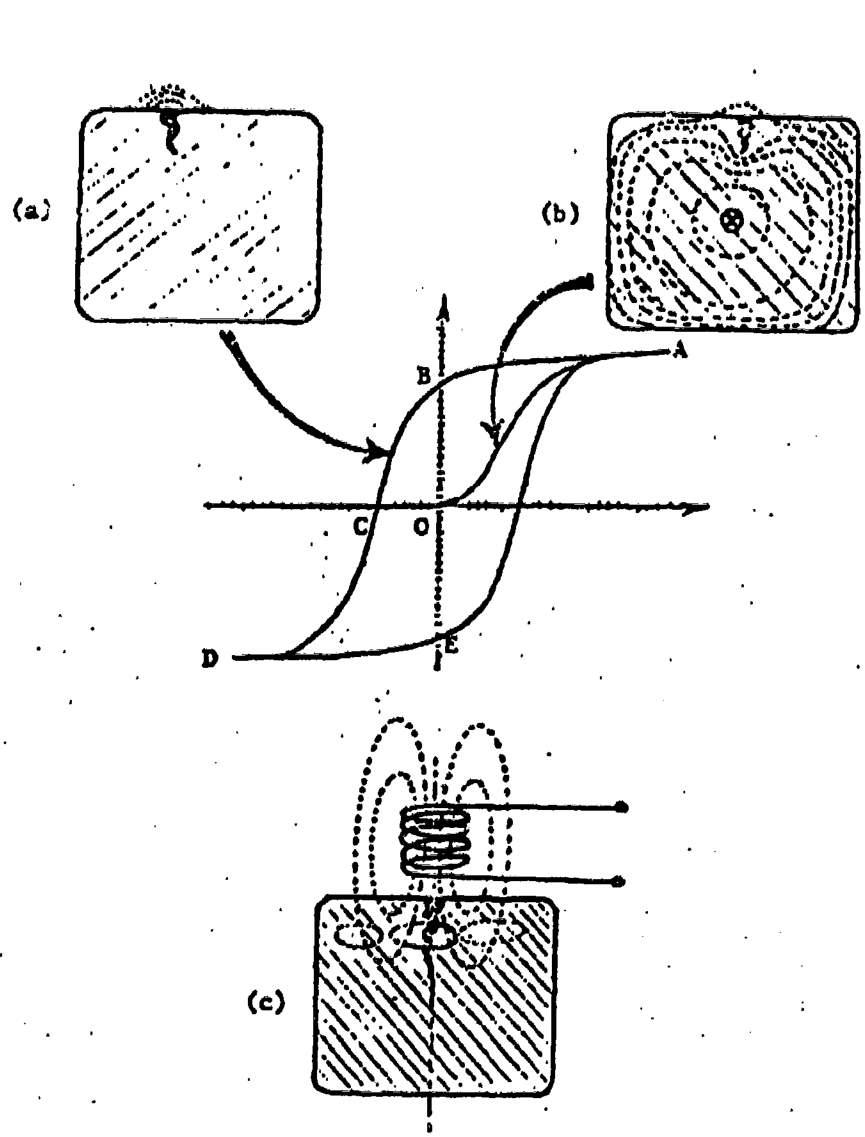

Electromagnetic phenomena utilized in detecting defects in ferromagnetic materials

a) Residual leakage field (region BC)
b) Active leakage field (region OA)
c) AC excitation (region ABCDEA)

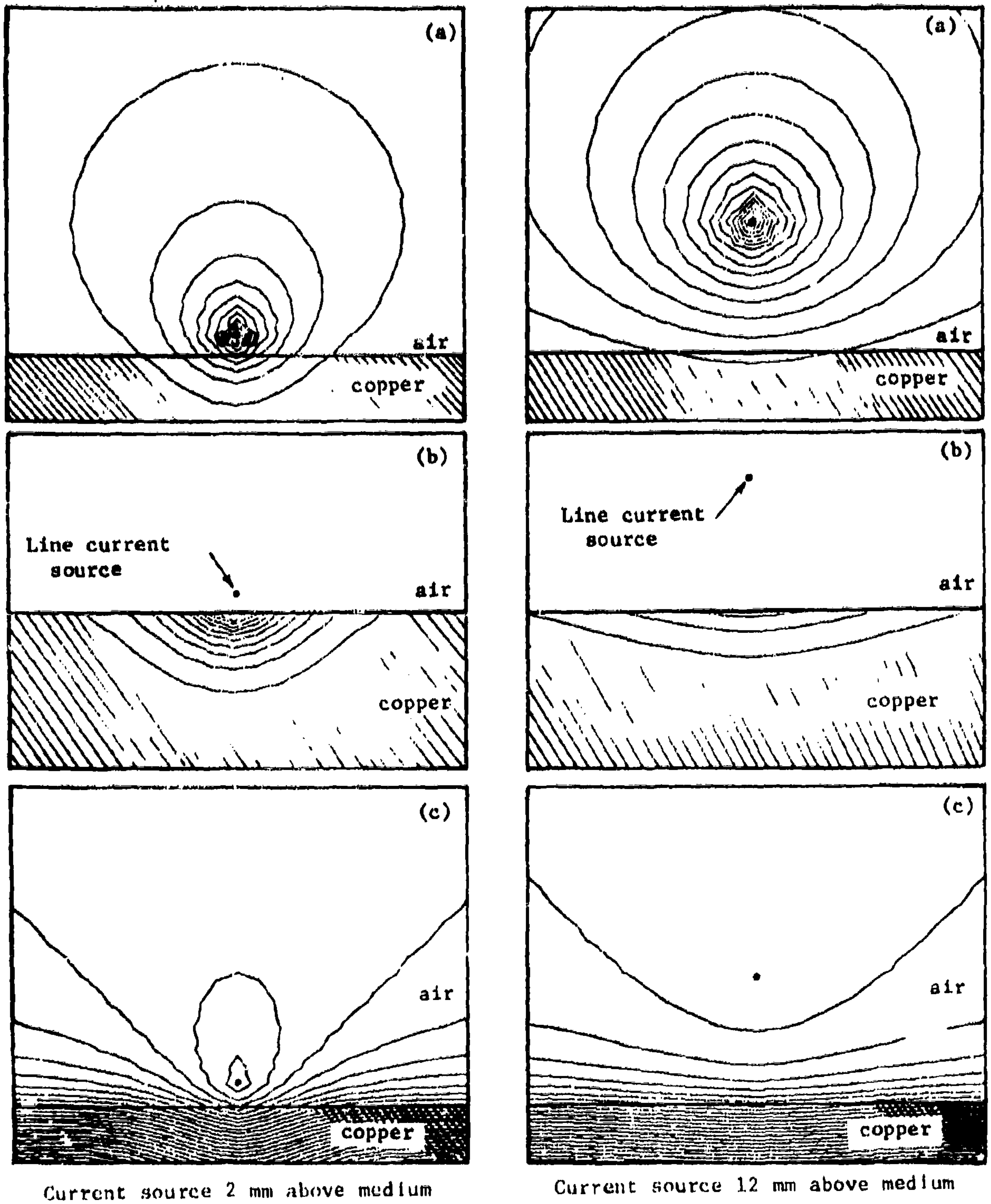

Contours of vector potential (a), eddy current density (b), and phase angle of vector potential with reference to excitation current (c).

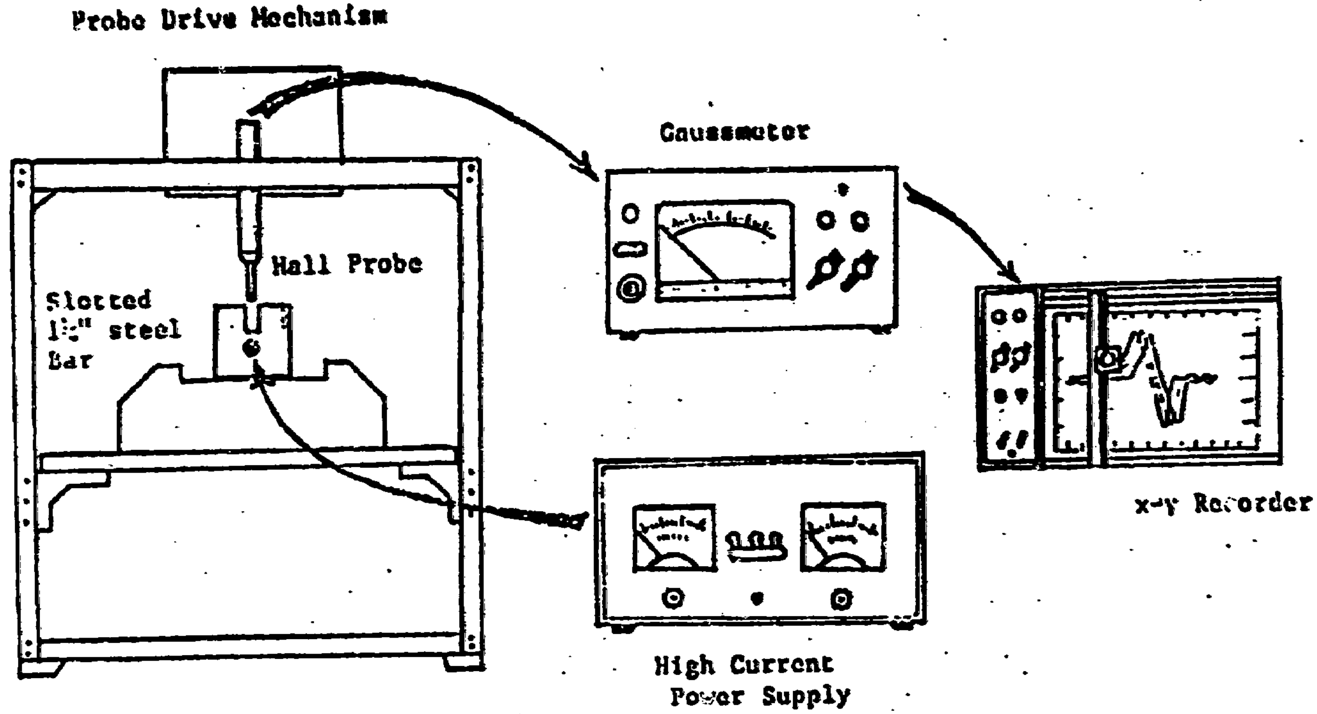

Experimental arrangement for the determination of residual and active leakage fields around rectangular slots in ferromagnetic bars.

A COMPARISON OF RESIDUAL STRESS MEASURING TECHNIQUES: THEIR STRENGTHS AND WEAKNESSES

Fred Witt
Fee M. Lee
Walter M. Rider

Materials and Manufacturing Technology Division
Fire Control and Small Caliber Weapon Systems Laboratory
U. S. Army Armament Research & Development Command
Dover, NJ 07801
Autovon: 880-6345

ABSTRACT

Ongoing in-house work concerning the measurement of residual stress in Army Materiel by both X-ray and strain gage mechanical relaxation methods is presented. The X-ray portion concerns itself with the problems associated with the calculation of stresses in highly textured samples while the strain gage portion describes effects produced by various mechanical methods to partially relieve the strain fields sensed by the active gage elements. Comparisons are also made of the errors introduced by considering the active element in the strain gage rosette as a point gage instead of one with finite length.

INTRODUCTION

This paper concerns itself with descriptions and methods used to circumvent some pitfalls encountered when standard X-ray and strain gage methods are indiscriminately used to perform residual stress measurements. As the name implies, residual stresses are those stresses which reside in the bulk of a material when the external forces acting on it are removed. One customarily excludes external forces such as gravity or thermal gradients. Since the body under consideration is in equilibrium, the force resultant equals zero. When the residual stresses are long range in nature; that is, are reasonably constant in magnitude, sign, and direction, and extend over distances comparable to many grain diameters, they are termed macrostresses. As such they are easily measured by mechanical methods employing dissection, layer removal, and careful hole-drilling procedures. Stresses of this type produce an X-ray line shift when the sample is rotated in the X-ray beam. When the residual stresses are short range in nature, and vary appreciably over distances comparable to the grain diameter, they are called microstresses. As such they can't be revealed by mechanical dissection methods; and may or may not produce an X-ray line shift, depending on the distances over which the microstresses exert their influence. When the stress acting distance is comparable to a micron or so, then X-ray line broadening and line shifts are observed. When this distance shrinks to approximately 1000 Å or less, X-ray line broadening persists, but line shifts are not removed.

Furthermore when the actual deformation mode produces extensive movement of material in a given direction, then complications arise which prohibit the use of here-to-fore commonly accepted X-ray approaches and computational formulas. In other words, the standard X-ray approach can produce erroneous results for cases where the specimens have been extensively rolled, drawn, stretched, compressed or bent. The standard X-ray methods do, however, produce reliable answers when the measurement is made on surfaces which have been machined, ground, or peened (Ref. 1). Here the mass movement is not predominantly one directional. A relatively unknown but straight forward way does exist, however, to correct for the deficiencies of the standard X-ray method when extensive amounts of uniaxial plastic metal flow has occurred. The method, put forth by Marion and Cohen (Ref. 2), will be described in a later section of this report. For the moment, however, consideration will be given to several problems the authors have encountered using some of the "handbook" approaches to determine the stress state of various specimens.

CIRCUMFERENTIAL STRESS BY LONGITUDINAL SLITTING

The stress condition of thin wall tubes is sometimes assessed by the method after Crampton (see fig. 1).

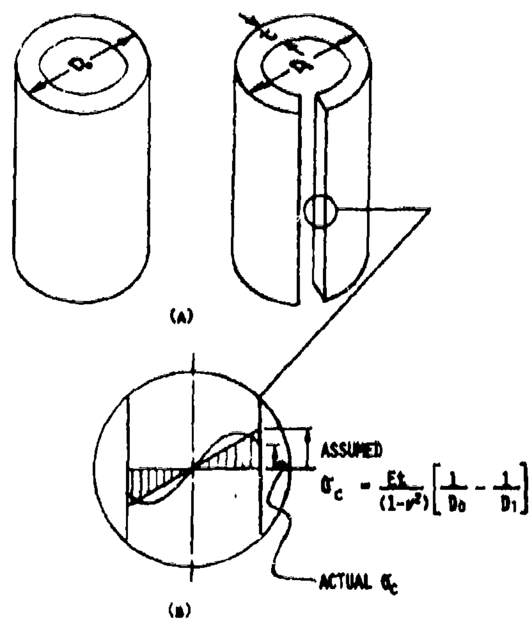

FIGURE 1. CRAMPTON'S METHOD FOR COMPUTING THE CIRCUMFERENTIAL STRESS IN THIN WALL TUBES.

Here one slits a tube along one element for its entire length, and makes use of the beam formula to compute the maximum circumferential stress. The method assumes that a condition of plane strain exists. In other words, the strain and curvature change in the longitudinal direction, is zero. According to Crampton, the circumferential stress on the outer fibers is given by,

$$\sigma_c = \frac{Et}{(1-\nu^2)}\left[\frac{1}{D_0} - \frac{1}{D_1}\right] \qquad (1)$$

Where E is Young's modulus, t is the wall thickness, ν is Poisson's ratio, D_0 is the mean diameter before slitting, and D_1 is the mean diameter after slitting. It can be seen from equation (1) that a tensile stress on the outside surface of the tube causes D_1 to be larger than D_0; while a compressive stress causes D_1 to be smaller than D_0.

It is possible to obtain some indication of the reasonableness of the computed Crampton result by noticing that the length of the thin wall tube does not enter into the formula. Consequently, after axial slicing, and the D_1 relaxation is noted, one can perform another cut, perpendicular to the cylinder axis, so two slit cylinders, each of length, $\ell/2$, can be obtained. The individual cylinders can be examined concerning their new D_1 values. If the new values differ considerably from the value produced by the first axial cut, then one can conclude that constant axial stress does not exist. The requirement that the stress varies linearly from inner wall to outer wall is illustrated in figure 1(b). Here, the shaded area represents the stress distribution according to the beam requirement. The sinusoidal type curve depicted therein might, however, be closer to the actual distribution. The point to be made here is that the use of slitting techniques provide at best a crude indication of the actual stress state in a given specimen. More accurate methods are described below.

BLIND HOLE DRILLING METHODS

It should be noted that residual stresses cannot be measured directly. This means that one must first determine the magnitude and algebraic sign of the strain that exists in a given sample under examination and then compute the residual stresses from the strain information. To obtain the strain information, the state of constraint of the material just beneath the strain gage is altered by removing a small amount of material adjacent to the gage. This is achieved by drilling a small hole in the center of a rosette, consisting of three linear gages (fig. 2), bonded to the base plug, and, connected to a digital strain indicator. The drilling operation relaxes the material at the edge of the hole, causes a local redistribution of the stress, which in-turn produces the strain change detected by the strain gages in the rosette.

It has been experimentally observed that the relaxed strains depend on the depth of the drilled hole. When the hole depth approximates the diameter, further drilling does not significantly change the strain gage readings; hence one normally takes as equilibrium surface strain values those obtained at a depth equal to the diameter of the drilled hole. Unless special precautions are taken when the hole is drilled, the strain gage readings will not only reflect the residual strains/stresses in the sample but will also reflect the strains produced by the hole drilling operation.

For a given state of stress, the strain gages sense relaxation signals which are proportional to the diameter of the drilled hole. It is desirable to obtain a strong signal by drilling a large hole. Care must be exercised, however, in selecting the drill size so that the cutting surface area is not too close to the gages and unduly perturb the true strain relaxation signal from the "drilling" operation. Holes of .159 cm (1/16 inch) diameter are normally used in practice, since they provide relatively strong and unperturbed relaxation signals.

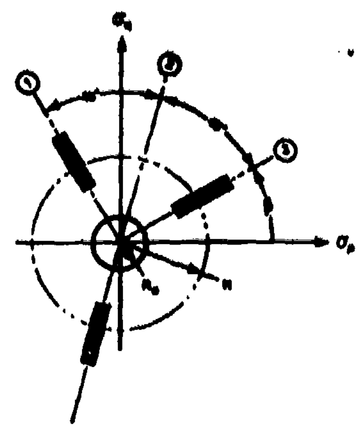

FIGURE 2. RELATIONSHIP BETWEEN THE LINEAR STRAIN GAGE ELEMENTS AND THE PRINCIPAL DIRECTIONS.

The radial distance from the center of the hole to the three linear elements, in the rosette, is critical because the strains are functions of the inverse second and inverse fourth powers of this radius. Therefore, one should use commercially available precision strain-gage rosettes and should not attempt to construct a "homemade" rosette by "gluing down" three linear gages because the formulas used to calculate the stress state assume that all three linear gages lie precisely on the same circle of radius R, and are symmetrically oriented with respect to each other; as shown in figure 2.

Hole Forming Methods

Various techniques have been described in the literature to produce the center hole in the strain gage rosette. These include the use of conventional drill bits, specially ground milling cutters, electric discharge machining and abrasive jet machining.

Bush and Kromer (Ref. 4) have investigated some problems associated with the use of various methods to produce the center hole. Their results for annealed steel are shown in figure 3. It can be seen, for conventional drill bits, that unpredictable errors, ranging from 60 $\mu\varepsilon$ to -70 $\mu\varepsilon$ can result. When these strain values are converted into stress, they amount to an error of $\pm$ 124.11 MPa ($\pm$ 18 ksi). For rotating cutters; there appears to be a fixed error ranging from $-30\,\mu\varepsilon$ to $-60\,\mu\varepsilon$.

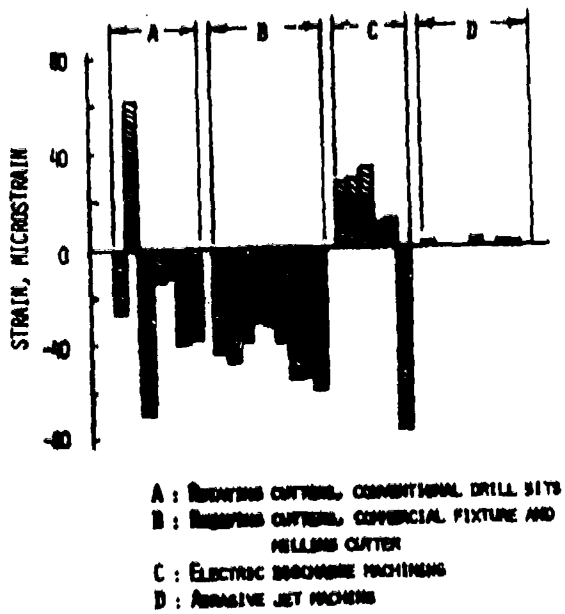

FIGURE 3. STRAIN EFFECTS CAUSED BY VARIOUS HOLE PRODUCING METHODS.

For electric discharge machining; the errors can range from $30\,\mu\varepsilon$ to $-80\,\mu\varepsilon$, depending on the hole diameter. The superiority of the abrasive jet machining method is obvious from the extremely low strain values of 2 or $3\,\mu\varepsilon$ shown in figure 3. This method will be described in more detail later. For now, consideration will be given to the equations normally used to convert the measured strains into computed stresses.

For the Blind Hole Method, the equations describing the principal stresses and their orientation with respect to the number three gage can be written in two different ways. These depend on whether or not one wishes to consider the linear gage element as a point gage (i.e. of infinitesimal length), or as one with a finite length, centered on the specimen, at the same location as the point gage. For the radially oriented point gage case, the principal stresses and their directions are given by (Ref. 3);

$$\sigma_p = \frac{\varepsilon_3(A + B\cos 2\beta) - \varepsilon_1(A - B\cos 2\beta)}{4AB\cos 2\beta}$$

$$\sigma_q = \frac{\varepsilon_1(A + B\cos 2\beta) - \varepsilon_3(A - B\cos 2\beta)}{4AB\cos 2\beta}$$

$$\beta = \frac{1}{2}\tan^{-1}\frac{(\varepsilon_3 - 2\varepsilon_2 + \varepsilon_1)}{(\varepsilon_3 - \varepsilon_1)}$$

where $$A = \frac{-(1+\nu)}{2Er^2} \qquad (2)$$

$$B = -\frac{(1+\nu)}{2E}\left[\left(\frac{4}{1+\nu}\right)\frac{1}{r^2} - \frac{3}{r^4}\right]$$

ε_1, ε_2 and ε_3 are the measured strains, E and ν are the elastic modulus and Poisson's ratio respectively and r is the ratio of the radius of the rosette to the radius of the drilled hole, R/R_o. The quantities σ_p and σ_q are the principal residual stress, while the angle β is measured from the number three gage element (see fig. 2). When the equations listed above are used, it should be realized that the strain gages are assumed to act as point gages, i.e. of zero gage length. For the finite length gage, the equations for the principal stresses become (Ref. 5):

$$\sigma_{p,q} = E\left[\frac{\varepsilon_1 + \varepsilon_3}{2S_1} \pm \frac{\varepsilon_1 - \varepsilon_3}{2S_2\cos 2\beta_1}\right]$$

where $$S_1 = (\nu - 1) + R_1 \text{ and } S_2 = -(\nu + 1) + R_2. \qquad (3)$$

Here $$R_1 = \frac{1}{(r_2 - r_1)}\int_{r_1}^{r_2}\left(\left(1 - \frac{a^2}{r^2}\right) - \nu\left(1 + \frac{a^2}{r^2}\right)\right)dr,$$

$$R_2 = \frac{1}{(r_2 - r_1)} \int_{r_1}^{r_2} \left(\left(1 - \frac{3a^4}{r^4} - \frac{4a^2}{r^2}\right) + \nu\left(1 + \frac{3a^4}{r^4}\right)\right) dr ,$$

where r_1 and r_2 are the inner and outer edge dimensions of the active gage element, respectively, and a is the radius of the drilled hole.

An attempt was made to compare the difference in the computed stress value when both equation 2 and equation 3 were used with the same input strain data. The results are given in Table 1 where it can be seen that the point gage equations (i.e. equations 2) produce numerical values for the residual stresses which are 10 to 20 percent higher than those produced by the finite length equations, (i.e. equations 3).

Abrasive Jet Method

In this method (see Fig. 4), a carefully controlled stream of gas, containing 50 micron aluminum oxide powder, is directed against the workpiece in a manner which chips away microscopic particles of the material to "drill" the nominal .159 cm (1/16 inch) diameter hole.

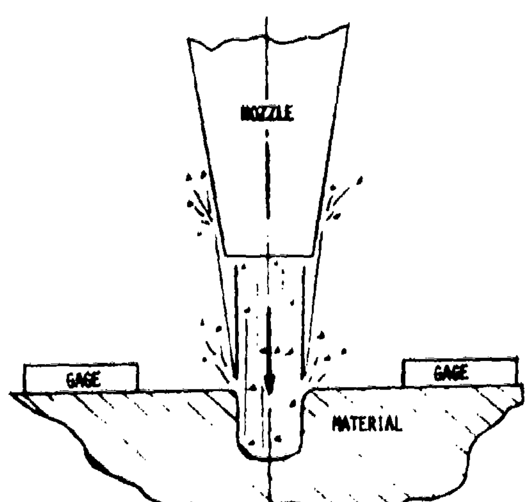

FIGURE 4. EXPERIMENTAL SETUP FOR ABRASIVE JET MACHINING.

As seen in figure 3, the method appears to be the most gentle one to produce the central hole. Special precautions must be taken however to insure that the walls are relatively "square" with the surface on which the rosette is bonded. It is also desirable to insure that the hole is accurately positioned at the center of the rosette. For the cases where the hole is off-center, the iterative method proposed by Sandifer and Bowie (Ref. 6) can be used to obtain corrected values for the stress. When the hole is centered to within a few thousandths of an inch, the iterative method is not needed. Under certain circumstances however, the formula used to compute the direction of the principal stress can be subject to large errors when small errors exist in the measured strain readings.

Indeterminacy of Beta

For an equal biaxial stress field the quantities ε_1, ε_2, and ε_3 are equal. When these values are inserted into the expression for β in equation 2 they produce a value for β of 0 degrees. When $\varepsilon_1 = \varepsilon_3 > \varepsilon_2$ then β approaches +45 degrees. When $\varepsilon_1 = \varepsilon_3 < \varepsilon_2$, then β approaches -45 degrees. In other words slight errors in the measurement of ε_2 can produce large errors in the computed value for β. The two points to be emphasized here are: (1) in an equal biaxial stress field the angle, β, describing the principal stress directions can fluctuate wildly; and (2) the algebraic sign and magnitude of the computed stress is not affected by this uncertainty in beta.

EFFECT OF THE CENTRAL HOLE ON THE MEASURED STRESS

It is well known from strain measurements and photoelastic experiments that geometrical discontinuities such as holes or notches act as stress raisers in plate material under tension. This multiplication of stress can be expressed in terms of a theoretical stress concentration factor K, given by the ratio of the maximum stress to the nominal stress on the net section. In other words, $K_t = \sigma max/\sigma nominal$. Both longitudinal and radial stresses are produced around a circular hole, in material subjected to a load. When a uniaxial stress is present and the hole is many diameters from the edge of the specimen, the radial, theta, and shear components of stress are given by the Kirsch (Ref. 7) equations, namely:

$$\sigma_{rr} = \frac{\sigma}{2}\left(1-\frac{a^2}{r^2}\right) + \frac{\sigma}{2}\left(1+\frac{3a^4}{r^4} - 4\frac{a^2}{r^2}\right)\cos 2\theta$$

$$\sigma_{\theta\theta} = \frac{\sigma}{2}\left(1+\frac{a^2}{r^2}\right) - \frac{\sigma}{2}\left(1+\frac{3a^4}{r^4}\right)\cos 2\theta \qquad (4)$$

$$\tau_{r\theta} = -\frac{\sigma}{2}\left(1 - \frac{3a^4}{r^4} + \frac{2a^2}{r^2}\right) \sin 2\theta$$

Here, σ is the uniform applied tensile stress far removed from the hole. The quantity, a, is the hole radius, while r is the location where the r, θ components of stress are desired. From the above equations, and inspection of Figure 5, it can be seen that the maximum stress occurs at points C and A, where r = a, and theta = 0° and 180°, respectively. Here $\sigma_{\theta\theta} = 3\sigma = \sigma$ max. In other words $K_t = 3$. It can also be seen that $\sigma_{\theta\theta} = -\sigma$ at points D and B when r = a and $\theta = 90^\circ$ and 270°, respectively. Hence, a tensile stress, far removed from the hole, produces at points B and D, a compressive stress of equal magnitude.

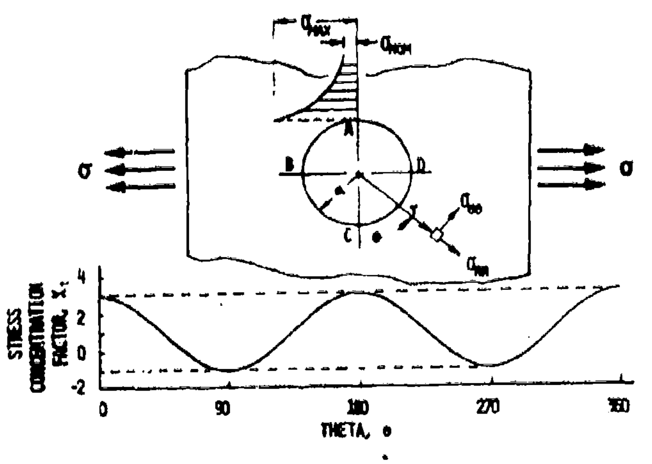

FIGURE 5. EFFECT OF THE STRESS CONCENTRATION FACTOR ON THE STATE OF STRESS IN A UNIAXIALLY STRESSED PLATE.

The net effect of the stress concentration factor is to produce plasticity at the edge of the drilled hole when the measured stress exceeds 1/3 of the yield stress for cases where the gages are positioned in a uniaxial field. When the gage is positioned in an equal biaxial field, plasticity occurs when the measured stress exceeds ½ of the yield stress. Beaney and Procter (Ref. 8) have shown, for the uniaxial case, that at stress values less than half yield, the errors are negligible while at full yield they have risen to 10 percent.

X-ray Measurement of Stress

In brief, the X-ray method measures the shift of the diffracted beam when the sample surface is rotated a known amount in the incident beam. From the measured peak shift one computes the change in the lattice spacing and attributes the shift to a residual macrostresses. In other words, the interplanar spacing change is used as a strain gage indicator to compute the biaxial stress residing on the outer surface of the sample. The mathematics describing the X-ray method is adequately described in section 2 of an SAE booklet (Ref. 9). Equation 31 of section 2 in (Ref. 9) shows that the stress is given by

$$\sigma = \frac{E}{(1+\nu)} \cdot \frac{1}{\sin^2\psi} \cdot \frac{\cot\theta}{2} \left(\frac{\pi}{180}\right) \left(2\theta_\perp - 2\theta\psi\right) \qquad (5)$$

where

E is the modulus of elasticity

ν is Poisson's ratio

ψ is the angle the sample normal was rotated in the X-ray beam

θ is the angle of incidence of the X-ray beam with the atomic planes

$2\theta_\perp$ is the angular position of the diffracted X-ray beam when the sample bisects the incident and diffracted X-ray beams

$2\theta_\psi$ is the position of the diffracted X-ray beam when the sample is rotated an additional ψ degrees about a vertical axis lying in the plane of the sample and perpendicular to the plane of the incident and diffracted X-ray beams.

There is some controversy in the literature concerning the appropriate values to use for Young's modulus and Poisson's ratio; however, the SAE paper (Ref. 9) gives a technique in section 6.4 for experimentally determining these quantities.

Equation 5 implies that the interplanar spacing, d, is linearly dependent on $\sin^2\psi$. From figure 6 it can be seen that a positive slope is produced by a tensile stress, a negative slope by a compressive stress, and a slope of zero by a residual stress of zero For highly textured samples, the interplanar spacing values oscillate above a least square line drawn through the experimental data points. It is found, experimentally, that the curve is above the mean straight line

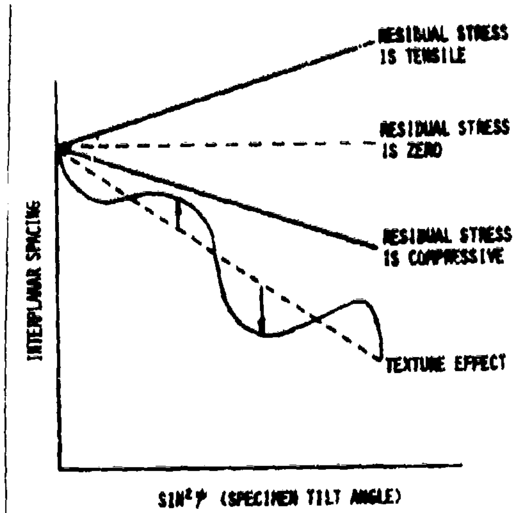

FIGURE 6. INTERPLANAR SPACING PLOT FOR DIFFERENT RESIDUAL STRESS STATES

for those orientations where the reflecting pole density is higher than the random level and below it, where it is lower than the random level. It is believed that the larger than expected values for the interplanar spacing results from stress relaxation by dynamic recovery.

In order to understand these findings we should first consider the shape of the modified stress-strain curve shown in Figure 7 and proposed by Cullity (Ref. 10 and 11), and Smith and Wood (Ref. 12). It should be noted that the positive abscissa describes the contraction of the (hkl) spacing when the stress direction is at right angles to the normal of the diffracting grains. Curve A-B-C, the total strain curve, consists of an elastic portion, A-B, and an elastic-plastic portion, B-C. In the elastic region, the strain measured by X-rays, called the lattice strain, and that measured by mechanical methods (i.e., total strain) are both proportional to the applied stress, and have the same slope. In other words, the lattice strain curve and the mechanically measured total strain curve are superimposed on each other along the path A-B. In addition, both curves return to zero when the applied stress is removed if the material has not been taken into the yield region. When the applied stresses exceed the elastic limit, the X-ray method presupposes that the lattice strain follows the line B-D. In practice, however, it deviates significantly from the line B-D and follows the curve B-E. As the applied stress is released the lattice strain curve follows the path E-F, and has the same slope as the path A-B.

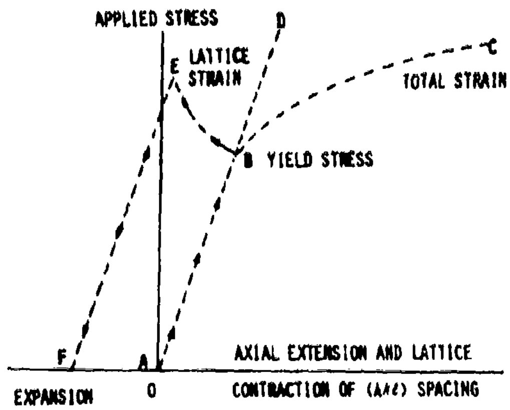

FIGURE 7. LATTICE AND TOTAL STRESS-STRAIN CURVE.

Thus, this result will produce a net mean compressive residual lattice strain which is represented by F-A, with large fluctuations from the mean being exhibited by individual diffracting crystallities. This net residual lattice strain produces an observed X-ray line shift which is interpreted by the X-ray stress formula as an indication of the presence of compressive macrostrain in the specimen. The picture becomes clearer when one considers the findings of other researchers (Ref. 13, 14, and 15) and also remembers that the X-ray diffraction signal arises predominantly from coherently diffracting domains which are centered in the subgrain interior regions.

Cullity proposes a rather new explanation for the anomalous computed residual stress values for uniaxially plastically elongated materials. He cites the work of Keh and Weissman (Ref. 16), Neurath and Waite (Ref. 17), and Morrill (Ref. 18) which indicate that, in uniaxially elongated metals, the subgrain walls remain in tension. Because the X-ray beam, predominately, "samples" the subgrain interior it can readily be seen that equation 5 is "preconditioned" to predict "overall" compressive stresses in the sample. The reverse prediction would occur if the subgrains were put into tension, by uniaxial compression.

Marion and Cohen (Ref. 2) have extended the work of Weidemann (Ref. 19) and have put forth the formula given below to describe the behavior of the interplanar spacing $d_{\phi,\psi}$ on $\sin^2\psi$. Here the nonlinear dependence of d on $\sin^2\psi$ is attributed to the relief of microstrains in subgrain interiors. The degree of relief depends on the orientation of the grain to the stressing system and to the texture developed during the plastic deformation process. The Marion-Cohen approach, separates the nonlinear and linear components of d by means of the expression:

$$d_{\phi,\psi} = (d_{max} - d_{\beta}) f(\alpha,\beta) + d_{\perp}\left(\frac{1+\nu}{E}\right)\sigma_{\phi}\sin^2\psi + d_{\beta} \quad (6)$$

The term d_{max} is the interplanar spacing in a region where the strain is fully relieved, while d_{β} corresponds to a region which has not been relieved. This means that the quantity (d_{max} - d_{β}) describes the range of interplanar spacings present in the sample. The distribution function $f(\alpha,\beta)$ describes the orientational dependence of d and is obtained from the observed integrated intensity of the diffraction peak at each ψ inclination. The distribution function is normalized to unity. Equation 6 is solved by measuring the interplanar spacing, $d_{\phi,\psi}$, and the normalized distribution function, $f(\alpha,\beta)$ as a function of $\sin^2\psi$, for six orientations of the sample. This overdetermined system of equations is solved by means of a least squares computation to yield the stress, σ_{ϕ}. The necessity of using equation 6 for a given sample is readily determined by plotting interplanar spacing measurements as a function of $\sin^2\psi$ for 5 or 6 orientations of the sample. If the plot is linear, then the standard formula shown in equation 5 can be used to compute the stress. When the plot oscillates, the more sophisticated Marion-Cohen expression must be used.

SUMMARY

A review was given of some problems encountered when dissection, strain gage, and X-ray methods are indiscriminately used to determine the stress state of specimens.

It was pointed out for thin walled tubes that the Crampton dissection method required a condition of plain strain in addition to a linear variation of the stress from the inside wall surface to the outside wall surface. Since the formula to compute the maximum circumferential stress was length independent, the condition of plain strain could be readily verified by cutting the slit tube, of length ℓ into two tubes of length $\ell/2$ whereby the new diameters could be compared with the diameter obtained from the slit tube of length ℓ.

For annealed steel, a comparison of various blind-hole drilling methods indicated that abrasive jet machining causes negligible error in contrast to other hole drilling methods which introduce errors rang- from +60 to -70$\mu\epsilon$. It was pointed out that the standard equations to convert strain readings to computed stresses assume that the strain gage is in reality a point gage (i.e. one of zero length). When the actual gage length is taken into account, the computed stresses can vary significantly. For cases where the strain gage is placed in an equal biaxial stress field, it was shown that small errors in the measurement of ϵ_2 can produce large fluctuations in the computed value for β.

The standard X-ray stress equations were reviewed and it was noted that a nonlinear plot of interplanar spacing versus $\sin^2 \psi$ identified those samples where the standard X-ray equations could not be used. The oscillating dependence of d on $\sin^2 \psi$ was attributed to the relief of microstrains during extensive plastic deformation and the production of a strong texture. The curve tended to lie above a mean straight line drawn through the data points for diffracting plane orientations where the pole density was higher than the random level and below it where it was lower than the random level. When measurements of the interplanar spacing were taken for six ψ tilts, the non-linear dependence of d could be separated from the linear component by using the Marion-Cohen formula.

REFERENCES

1. Cullity, B. D. "Some Problems in X-ray Stress Measurements," Advances in X-ray Analysis, Vol 20, Plenum Press, New York (1977), pp.259-271.

2. Marion, R. H. and Cohen, J. B. "Anomalies in Measurement of Residual Stress by X-ray Diffraction", Advances in X-ray Analysis, Vol. 18, Plenum Press, New York (1974), pp 466-501.

3. Measurements of Residual Stresses by the Blind Hole Drilling Method, Technical Data Bulletin T-403, 1977, Photolastic Inc.

4. Bush, A. J. and Kromer, F. J. "Simplification of the Hole-Drilling Method of Residual Stress Measurement", ISA Transactions, Vol. 12, No. 3, (1973), pp 249-259.

5. Milbradt, K. P. "Ring-Method Determination of Residual Stresses", Proc. Soc. Exptl. Stress Anal., Vol. 9, No.1 (1951), pp 63-74.

6. Sandifer, J. P. and Bowie, G. E. "Residual Stress by Blind-Hole Method with Off-Center Hole", Exp. Mech., 18, No. 5, (May 1978), pp 173-179.

7. Kirsch, G. "Die Theorie der Elastizitat und die Bedurfnisse der Festigkeitslehre", Zeitschrift des Vereines Deutscher Ingenievre, Vol. 42, (July 16, 1898), pp 797-807.

8. Beaney, E. M. and Procter, E. "A Critical Evaluation of the Centre Hole Technique for the Measurement of Residual Stresses", Strain, (Jan 1974), pp 7-14, 52.

9. Hilley, M. E., Larson, J. A., Jatczak, C. F., and Ricklefs, R. E., eds. "Residual Stress Measurements by X-ray Diffraction", SAE Report J 784a (1971), Available from SAE, Inc. 400 Commonwealth Drive, Warrendale, Pennsylvania 15096.

10. Cullity, B. D. "Residual Stress After Plastic Elongation and Magnetic Losses in Silicon Steel", Trans. Met. Soc., Vol. 227 (1963) pp. 356-358.

11. Cullity, B. D. "Sources of Error in X-ray Measurements of Residual Stress", JAP35 (1964) pp. 1915-1917.

12. Smith, S. I., Wood, W. A., "Internal Stress Created by Plastic Flow in Mild Steel, and Stress-Strain Curves for the Atomic Lattice of Higher Carbon Steels", Proc. Royal Society, Series A 182 (1944) pp. 404-415.

13. Greenough, G. B., Residual Lattice Strains in Plastically Deformed Metals. Nature 160 (1947) p. 258.

14. Greenough, G. B., "Residual Lattice Strains in Plastically Deformed Polycrystalline Metal Aggregates", Proc. Royal Society, Series A, 197 (1949) pp. 556-567.

15. Donachie, M. J., Norton, J. T., "Lattice Strains and X-ray Stress Measurement", Trans. Met. Society, AIME 221 (1961) pp. 962-967.

16. Darken, L. S., "Some Observations on Atoms and Imperfections", Trans. Quarterly Amer. Society Metals 54 (1961) pp. 559-642 (Fig. 30 by Keil and Weissman).

17. Neurath, P. W., Waite, R. E., "Elastic and Plastic Strains and Watt Losses in Grain-Oriented Three PCT Si-Fe", Trans. AIME 203 (1955) p. 480.

18. Morrill, W., Silicon Irons up to Date. Metals Progress 78 (1960) pp. 84-87.

19. Wiedemann, W. Ph.D. Thesis, Technische Hochschule, Auchen, Germany (1966)

Table 1. The Effect of Using Point Gage versus Finite Length Gage Equations in the Computation of the Residual Stress.

SAMPLE	ROSETTE	HOLE RADIUS mm (inch)	STRAIN με			RESIDUAL STRESS USING BLIND HOLE METHOD: POINT GAGE COMPUTATION σ_p MPa (KSI)	RESIDUAL STRESS USING BLIND HOLE METHOD: POINT GAGE COMPUTATION σ_q MPa (KSI)	RESIDUAL STRESS USING BLIND HOLE METHOD: FINITE LENGTH GAGE COMPUTATION σ_p MPa (KSI)	RESIDUAL STRESS USING BLIND HOLE METHOD: FINITE LENGTH GAGE COMPUTATION σ_q MPa (KSI)	β Degree
1	A*	0.81(0.032)	472	509	447	-252.4(-36.6)	-273.7(-39.7)	-206.9(-30.0)	-226.2(-32.8)	38
	B*	0.81(0.032)	327	313	436	-218.6(-31.7)	-184.8(-26.8)	-196.5(-28.5)	-163.4(-23.7)	26
2	A*	0.86(0.034)	357	423	498	-219.3(-31.8)	-193.1(-28.0)	-199.3(-28.9)	-174.4(-25.3)	2
	B*	0.81(0.032)	378	323	462	-246.8(-35.8)	-204.8(-29.7)	-224.8(-32.6)	-183.4(-26.6)	33
3	A*	0.81(0.032)	346	382	256	-143.4(-20.8)	-180.0(-26.1)	-128.2(-18.6)	-164.8(-23.9)	28
	B**	0.81(0.032)	434	319	518	-280.0(-39.3)	-209.6(-30.4)	-248.2(-36.0)	-187.5(-27.2)	38

*Hole was drilled by undercut end mill.

**Hole produced by abrasive machining.

PAPER NOT RECEIVED

PAPER NOT RECEIVED

PAPER NOT RECEIVED

PAPER NOT RECEIVED

28th DEFENSE CONFERENCE ON NONDESTRUCTIVE TESTING

LIST OF ATTENDEES

Robert L. ABNER
USAF/AFFTC/Edwards AFB 93523
6510 MSUG/MAFMFN/STOP 237
(805)277-2173 AV: 350-2173

Allan A. L. ABRAMS
Naval Weapons Station
Yorktown, VA 23691
(804)887-4707 AV: 953-4707

Paul R. AIGNER
452nd AREFW (AFRES)
March AFB, CA 92518
(714)655-3045 AV: 947-3045

Clifford W. ANDERSON
Code G-53 Naval Surface Weapons Ctr.
Dahlgren, VA 22448
(703)663-8411 AV: 249-8411

John J. ANTAL
AMMRC
Arsenal St.
Watertown, MA 02172
(617) 923-3454 AV: 955-3454

Douglas W. BALLARD
Dept. of Energy Agency
NDT Division 1551
Sandia Laboratories
Alburquerque, NM 87185
(505)264-3500 AV: 964-3500

Chris W. BARKE
North Dakota Air National Guard
P.O. Box 5536 State University Station
Fargo, ND 58105
(701)237-6030 Ext. 430 AV: 362-8430

Cal BATISTA
HMX-1 Maintenance Control
MCAF, MCB
Quantico, VA 22134
(703)640-2075 AV: 8-278-2075

Jess W. BAXTER
137th CAM Sq. Okla. Air Nat. Guard
P.O. Sta. 18 Will Rogers World Airport
Oklahoma City, OK 73169
(405)681-7551 Ext. 259 AV: 956-8259

T. E. BECKLUND
North Dakota Air National Guard
P.O. Box 5536 State University Station
Fargo, ND 58105
(701)237-6030 Ext. 400 AV: 362-8400

Howard W. BENNETT, Jr.
STEWS-TE-AE
WSMR, NM 88002
(505)678-5632 AV: 258-5632

Ronald E. BISHOP
174th TFW NYANG
Hancock Field, Syracuse, NY 13211
(315)458-5500 Ext. 3373 AV: 587-9373

William E. BLUM
182 Tactical Air Support Group/NDI
Greater Peoria Airport
Peoria, IL 61607
AV: 724-9230

James H. BONNEY, END-4
NAVPRO, Sikorsky Aircraft
Stratford, CT 06497

Maurice D. BOUCHER
157th Camron
Pease AFB, NH 03801
(603)436-0100 AV: 852-2491

Gregory M. BOWMAN
NERRA Box 50
FPO NY 09520
(NAPLES ITALY)
625-1110 Ext. 5342

Regenal W. BRAGG
USADA Ober Ramstadt APO NY 09175
06154-72-825/743

Bruce B. BROWN
Bonet Weapons Lab. Bldg. 115
Watervliet Arsenal, Watervliet, NY 12304
(518)266-4249 AV: 974-4249

B. J. BRUNTY
Weapons Quality Engineering Center
Naval Weapons Station
Concord, CA 94520
(415)671-5298 AV: 253-5298

AMS2 Dennis BRYANT
IM 2 Div. w/c 510
USS AMERICA CV66
FPO NY, NY 09501

Roy L. BUCKROP
ARRCOM DRSAR-QAE
Rock Island, IL 61201
(794)4851-272 AV: 793-4851-272

Morris L. BUDNICK
U.S. Army Natick Res. & Dev. Command
Kansas St., Natick, MA 01760
(617)653-1000 Ext. 2692 AV: 955-2692/2517

Samuel C. BULLARD
U.S. NAS Whiting Field
AIMD NDI Shop
Milton, FL 32570
(904)623-7620 AV: 868-7620

William G. BURGESS, Jr.
NAESULANT Bldg. S-3
NAS, Norfolk, VA 23511
(804)444-1224 AV: 690-1224/3530

Fred C. BURKE
GA A.N.G.
Dobbins AFB, Marietta, GA
(404)424-8811 Ext. 2164 AV: 925-2164

Jimmie D. BUSH
6585 Test Group (TKE)
Holloman AFB, NM 88330
(505)479-6511 AV: 349-2689

John E. CAMDEN
3037 Boulder Pk. Dr.
Nashville, TN 37214
AV: 446-6477

Harry A. CAPALDI
Air National Guard
2710 Eastern Blvd.
Blatimore, MD 21220
AV: 235-9236

James L. CAREY
Naval Weapons Station
Yorktown, VA 23691
(804)887-4707 AV: 953-4707

Sam B. CATALANO
DRDTA-RTAS, Army Tank-Automotive
R&D Command, Warren, MI 48090
(573)2712/3 AV: 273-2712

Richard CHAIT
USA AMMRC
Watertown, MA 02172
(617)923-3285 AV: 955-3285

Robert M. CHEATWOOD
SDSAN-DQ Anniston Army Depot
Anniston, AL 36201
AV: 694-6515

Michael G. CLARK
HMX-1, NDI Lab. MCAF, MCB,
Quantico, VA 22134
(703)640-2911 AV: 8-278-2-11

David A. CLAYTOR
507 TFG L13/MAF Tinker AFB,OK 73135
AV: 735-2664

Addison B. CLINGERMAN
PA Air National Guard
171 St ARW Greater Pittsburgh IAP
Pittsburgh, PA 16123

John T. CONROY
U.S. Army Aviation R&D Command
P.O. Box 209, ATTN: DRDAV-QP
St. Louis, MO 631-6
(343)263-1550 AV: 693-1550

Charles H. CRAIG
Air 5163B NAVAIRSYSCOM
Washington, D.C. 20361
(202)692-7540 AV: 22-7540/1

Phillip L. CREWS
Red River Army Depot
ATTN: SDSRR-QM, Texarkana, TX 75501
AV: 829-2371

Dennis E. CRIPPS
USAF, PSC Box 3188
McChord AFB, WA 98438
AV: 976-2946

Edward CRISCUOLO
Naval Surface Weapons Center
White Oak, Silver Spring, MD 20910
(202)394-1973 AV: 8-290-1973

Charles L. CUMBOW
Naval Air Test Center
Systems Engineering Test Directorate
GSS Branch, ATTN: SY55
Patuxent River, MD 20670
(301)863-4676 AV: 356-4676

Maurice J. CURTIS
Naval Weapons Center
China Lake, CA 93555
(714)939-2733/3292 AV: 245-2733/3292

Paul J. DANCE
CT. ANG.
Windsor Locks, CT 06096
AV: 636-276

Alfred H. DAVIDOFF
U.S. Army, ARRADCOM
Dover, NJ 07801
(201)328-2830

Luster DAVIS, Jr.
NADC Warminster
P.O. Box #7, Warminster, PA 18974
(441)2121-2630

James M. DEMING
NDI Tech. Alabama (ANG)
117 CAM/LGMFZ-B'ham MAP (ANG)
Birmingham, AL 35217
AV: 694-2302

Vasant K. DEVARAKONDA
U.S. Army Natick Research
& Development ATTN: DRDNA-VTF
Natick, MA 01760
(617)653-1000 Ext. 2549 AV: 955-2549

Roger L. DOORNBOS
NDI/SOAP Lab.
Luke AFB, AZ 85309
AV: 853-6191

John F. DORGAN
60 FMS/MAFF
Travis AFB, CA 94535
(707)438-2500 AV: 837-2500

Bruce W. EBERHARDT
HDQ 10AF Bergstrom AFB, TX
Austin, TX 78743
AV: 685-3995

Ed E. EDGERTON, Code 350A
Supervisor of Shipbuilding
U.S. Naval Station
San Diego, CA
AV: 258-1912

Benoni O. ELLIS
932 CAMS (AFRES)
Grisson AFB, IN 46971
(317)689-2536 AV: 928-2536

Lloyd N. EVANS
NAESULANT NAS, Norfolk, VA 23511
(444)1224/3662 AV: 690-1224/3662

George D. FARMER, Jr.
MERADCOM DRDME-VL
Fort Belvoir, VA 22060
(703)664-5820 AV: 354-5820/45126

B. J. FARRINGTON
U.S. Marines
Marine Corps Detachment
Chanute AFB, IL 68868
(271)495-2028 AV: 862-2028

Robert J. FEGAN, Code 912A1
Naval Air Engineering Center
Lakehurst, NJ 08733
(201)323-2595 or 2716 AV: 624-2595/2716

Leon A. FINNEGAN, Jr.
USAF 343 CRS
Elmendorf AFB, AK 99506
AV: 752-5404

Kenneth W. FIZER
NESO-341, NARF
Naval Air Station, Norfolk, VA 23511
(804)444-8811 AV: 690-8811

Daniel O. FOOTE
Bergstrom AFB, TX MAQ 924th TAG
AV: 385-4100/3501/3502

Melvin E. FOX
Letterkenny Army Depot ATTN: SDSLE-Q
Chambersburg, PA 17201
(717)263-6084 AV: 242-6084

Ronald L. FRAILER
NDT Section, Material Testing Dir.
APG, MD 21005
AV: 278-4417

Elvin L. FRITZ
NARF, Alameda, Code 341, Bldg. 44
Alameda, CA 94501
AV: 686-4559

Albert G. GALLO
Watervliet Arsenal
Watervliet, NY 12189
(518)266-5007 AV: 974-5007

Victor H. GEHMAN, Jr.
Code G53 NSWC/DL
Dahlgren, VA 22448
(703)663-8411 AV: 249-8411

Norman H. GEISEL
Naval Air Test Center, Systems
Engineering Test Directorate, GSS Branch
Patuxent River, MD 20670 ATTN: SY55
(301)863-4676 AV: 356-4676

J. W. GLATZ
Naval Air Propulsion Center
Box 7176, Trenton, NJ 08628
(609)882-1414 AV: 443-7224/5

Truman D. GLENN
Code 135, Bldg. 13
Charleston Naval Shipyard
Charleston, SC 29408
(803)743-4517 AV: 794-4517

James R. GORSUCH
317 FMS, Pope AFB, NC 28308
(919)394-2659 AV: 486-2659

James GRUGAN
(Code 035C) Naval Ship Systems
Engineering Station
Philadelphia, PA 19112
(215)755-3922 AV: 443-3922

Ronald S. HALE
Detachment 1 HqMiANG/MAAI
Selfridge ANGB, MI 48045
(313)466-5939 AV: 273-5939

Paul E. HALL
NAS Patuxent River, AIMD
Patuxent River, MD 20636
(301)863-3298 AV: 356-3714/3298

Ross E. HAMILTON
NARF Production Dept. Shop 93307
U.S. Naval Air Station
Pensacola, FL 32508
AV: 922-2632

James U. HANKINS
HMX-1, MCAF MCB, Quantico, VA 22134
AV: 278-2075

Walter HANSEN
SA-ALC/MMETP, Kelly AFB, TX 78241
(512)925-8735 AV: 945-8735

Stephen D. HART, Code 8431
Naval Research Laboratory
Washington, D.C. 20375
(202)767-3613 AV: 297-3613

Richard A. HERSAM
DARCOM HQS (DRCQA-E)
10001 Eisenhower Ave.
Alex., VA 22333
AV: 8-284-8916

Edward A. HOFF
Nondestructive Testing of
Metals School
32nd St Naval Station
San Diego, CA 92136

Ed C. HOLLAND
COMFAIRWESTPAC (Staff), Code 73.1
Box 3, FPO Seattle, WA 98767
(NAF ATSUGI, JAPAN)
AV: 228-3154/6567

William R. HOLLINGSWORTH, Code 34302
NARF, Noris, San Diego, CA 92135
AV: 951-6711

Wendell R. HONEA
940 AREFGp CAM Sq.
Mather AFB, CA 95655
(916) 364-3448

Gary J. HOOD
47th FMS/MAFF Laughlin AFB
Box 2805 Laughlin AFB, TX 78840
(512)298-5268 AV: 732-5268

Robert L. HUDDLESTON
STEAP-MT-G
Aberdeen Proving Ground, MD 21005
(301)278-3409 AV: 283-3409

Donald R. HUSEBY
AIMD, NAS Pensacola, FL 32506
AV: 942-2360

Fred IMMEN
U.S. Army Aviation R&D Command
(AVRADCOM)-RES & Technology Labs,
AMES Research Ctr, Moffett Fld., CA
(415)965-5581 AV: 359-5581

Frank J. JACKSON
SUPSHIP Seattle
Seattle, WA 98178
(206)527-3971 AV: 941-3971

Charles M. JOHNSON
U.S. Air Force 60 FMS/MAFF
Travis AFB, CA 94533
(707)438-5155 AV: 837-5155

Walton E. JOINER
DCASMA-BHAM
980 South 20th Street
Birmingham, AL 35205
(205)254-1414 AV: 340-1414

Gerald B. KATZ
Naval Ship Systems Engineering Sta.
Code 0538, Philadelphia, PA 19112
(215) 755-3587 AV: 443-3587

W. W. LAKE
USATSARCOM, DRSTS-MEA(2)
4300 Goodfellow Blvd.
St. Louis, MO 63120
(314)263-0396 AV: 693-0396

Glenn R. LANCASTER
920th W.R.G. Keesler AFB
2906 Pimlico Dr. Ocean Springs 39564

Roy E. LANGLEY
187th CAM Sqdn, Dannelly Field ANG Base,
Montgomery, AL 36105
AV: 485-9274/9296

Lars A. LARSON
AFPRO Det. 9 (Boeing)
P.O. Box 3707 M/S 63-53
Seattle, WA 98124
(206)655-8118

Robert H. LATIFF (CPT)
Dept. of Engineering, USMA
West Point, NY 10996
(914)938-4201 AV: 688-4360

Tom LEE
SM-ALC Physical Science Labs (MANC)
McClellan AFB, CA 95652
AV: 633-6987

Gilberto LEOS
Corpus Christi Army Depot
ATTN: SDSCC-QLE
NAS, Corpus Christi, TX 78419
(512)939-2598 AV: 861-2598

Walter M. LEWIS
104th T.F.G. Mass Air National
Guard, Barnes Muni. Airport
Westfield, MA 01085
(413)562-3691 Ext. 23 AV: 893-1470
Ext. 23

Edward W. LINKE
Naval Air Development Center
Warminster, PA 18974
AV: 441-3180

Warren T. LLOYD, Code 900
Naval Air Rework Facility
NAS, North Island
San Diego, CA 93125
(951)5988

Joe H. LOPEZ
1550th FMS/NDI Lab.
Kirkland AFB, NM 87716
AV: 964-8188

Alphonse J. LORANG
Coqmander, Naval Air Force
U.S. Pacific Fleet, ATTN: 7413
Box 1210
NAS North Island, San Diego, CA 92135
(714)437-6155 AV: 951-6155

Wa-lace T. LOVIN
COMFAIRMED, Box 2
FPO New York, NY 09521
(NAPLES ITALY)
AV: 625-4634

Danny LUCERO
NDI (SOAP) New Mexico
Air National Guard
P.O. Box 551
Albuquerque, NM 87103
(964)264-8188 AV: 964-0320

James E. LYMAN
Naval Plant Representative Office
Grumman Aerospace Corporation
Bethpage, NY 11714
(516)575-9360

Robert E. MATHERS, Code 343
Naval Air Rework Facility
NAS North Island, San Diego, CA 92135
(914)437-6711 AV: 951-6711

Ed MATZKANIN
U.S. Army Yuma Proving Ground
STEYP-MLS-P
Yuma, AZ 85364
(602)328-6745/6465 AV: 899-6745/6465/
6702

James P. MCCARVILL
USAF
Minneapolis, St. Paul Int'l Airport

Oscal Y. MCCLANNAN, Code 613)
Naval Air Rework Facility
NAS Norfolk, VA 23511
(804)444-8024/8056 AV: 690-8024/8056

Gwynn K. MCCONNELL
Naval Air Development Center
Warminster, PA 18974
(215)441-2543 AV: 441-2543

Patrick C. MCELENEY
U.S. Army Materials & Mechanics
Research Center
Watertown, MA 02172
(617)923-3444 AV: 955-3444

Bruce J. MCGREGOR
Naval Air Rework Facility
NAS Norfolk, VA 23511
(804)444-8607

Charles P. MERHIB
NDE Branch, AMMRC
Watertown, MA 02172
(617)923-3343 AV: 955-3343

Jessie L. MILEY
917 CAM AFR
Barksdale, LA
456-4185

John MITTLEMAN
Naval Coastal Systems Center
Panama City, FL 32407
(904)234-4388 AV: 436-4388

William C. MOFFAT
USAF
35th CRS/MACB/NDI
George AFB, CA 92392
(714)269-2494 AV: 353-2494

John F. MORAN
U.S. Army Natick Labs
Natick, MA 01867
(617)653-1000

Roger W. MORRISON
911th TAG NDI Lab
Greater Pittsburgh Intl Airport
Pittsburgh, PA
(412)264-5000 Ext. 203 AV: 277-8203

David M. MOSES
DMSSO Suite 1403
Two Skyline Place
5203 Leesburg Pike
Falls Church, VA 22041
(703)756-2343/5 AV: 289-2343/5

John J. MOZART
108TFW/LGFN
McGuire AFB, NJ 0864[illegible]
(609)724-3876 AV: 440-3876

Joseph H. MULHERIN
U.S. Army Armament R&D Command
Dover, NJ 07801
(201)328-5751 AV: 880-5751

Eli F. NICOSIA, Code 341
Materials Engineering Div.
Bldg. 741, NARF
NAS, Pensacola, FL 32508
(904)452-3551 AV: 922-3551

Elmer J. NALLS
MERADCOM StdzA Div. DRDME-DS
Fort Belvoir, VA 22060
(703)664-5728 AV: 354-5728

Delmer E. NORMAN
Naval Plant Office-Vought Corp.
P.O. Box 5907
Dallas, TX 75222
(214)266-3116

Paul S. OLDS
U.S. Navy Service School
Command Detachment
Chanute AFB, IL 61868
(217)495-2444/3375 AV: 862-2444/3375

Albert OLEVITCH
Air Force Materials Lab
Wright Patterson AFB, OH
(513)255-3691 AV: 785-3691

Joseph G. O'NEILL
438 MAW/MAFF/NDI
McGuire AFB, NJ 08046
(609)724-3271 AV: 440-3271

Milton S. ORYSH
Naval Ship Systems Engineering
Station, Naval Base, Code 035D
Philadelphia, PA 19112
(215)755-4168 AV: 443-4168/4144

Lowell P. OSBORNE
178th TFG/MAFFN, Municipal Airport
Springfield, OH 45501
(513)323-8653 AV: 346-2267

Bobby R. OSIER
U.S. Navy, NAS Miramar
San Diego, CA 92145
AV: 959-3578

Don R. PAYNE
U.S. Army Plant Rep Office
Be/DAVBE-E
P.O. Box 1605
Ft. Worth, TX 76101
(817)280-3220 AV: 885-3740

Larry G. PEACOCK
919th SOG MAF/NDI
Duke Field, Eglin AFB, FL 32542
(904)883-1423 AV: 872-1110

Ernest C. PETERS
120 LGMF/NDI-SOAP, Mont. ANG
Intl Airport
Great Falls, MT 59404
AV: 279-2264

James A. PHILLIPS
Hq. AFRES/LGMAS
Robins AFB, GA 31098
(912)926-5736 AV: 468-5736

William K. PHILLIPS
DCAS
P.O. Box 29300
DCASMA New Orleans, LA
(504)255-2506

Andrew E. PLANTE
U.S. Navy
NAS Cecil Field, FL
AV: 860-5465

Robert A. PODBIELSKI
109 Tagp. NYANG P.O. Box 938
Schenectady, NY 12301
(518)372-5621 AV: 974-9248

Daniel POLANSKY
National Bureau of Standards
Washington, D.C. 20234
(301)921-2201

William POLLAY
QA Code 4102
P.M.T.C. Pt. Mugu, CA 93042
(804)982-7816 AV: 351-7816

Daniel V. POPPEN
Naval Surface Weapons Center
Dahlgren, VA 22448
(703)663-8675 AV: 249-8675

John R. POWELL
Hq. Fourth Air Force (Reserve)
McClennan AFB, CA 95652
AV: 633-6081

David W. PRATT
NAVPBRO, P.O. Box 157
Magna, Utah 84044
(801)250-5911 Ext. 2-80

William C. PRICE
California Air National Guard
5425 E. McKinley
Fresno, CA 93727
(209)252-4041 AV: 949-9272

James M. QUIGLEY
Army Materials & Mechanics Research
Center
Watertown, MA 02172
(617)923-3563 AV: 955-3563

James W. REGAN
192 TFG/MAFF-N
Byrd Intl Airport, VA 23185
(804)222-8884, Ext. 346 AV 274-8346

Norman C. REID
AFPRO/QAX
Lockheed, GA Co.
Marietta, GA 30063
(404)424-2002

Richard A. RICHIE
148th CAMRON Minn. Air Natl Guard
Duluth Intl Airport, MN 55814
(218)727-8211 Ext. 666 AV: 825-2666

Daniel J. RODERICK
Army Materials & Mechanics
Research Center
Watertown, MA 02172
(617)923-3270 AV: 955-3270

Walter B. ROSE
Fairchild Republic Company
USAF Aerospace (AFPRO) A.F. Contract
Admin.
DET 44 Conklin Street
Farmingdale, NY 11735
(516)531-3232, 3131 AV: 994-9208

Gloria J. SANFORD
928th TAG O'Hare Intl Airport
Chicago, IL
(930)6336

Richard D. SANTANGELO
Naval Air Rework Facility
NAS Jacksonville, FL 32216
904)772-2164 AV: 942-2164

John A. SCHAEFFEL, Jr.
USAMICOM DRSMI-RLA(R&D)
Redstone Arseanl, AL 35809
AV: 746-5692

David J. SCHIELTZ
928th CAM USAFR O'Hare Intl Airport
Chicago, IL 60666
(694)3031 Ext. 6336 AV: 930-6336

Jimmie Q. SCHMIDT
Ballistic Research Lab
Interior Ballistics Div. APG, MD 21005
(301)278-4081

Alan L. SCOTT
Richards Gebanr AFB
Grandview, MO 64030
(816)348-2685 AV: 465-2685

Clifford B. SEELEY
Shore Intermediate Maintenance
Acty, Mayport, P.O. Box 228
Naval Station Mayport, FL 32228
(904)246-5133 AV: 960-5133

David G. SHERFICK
Naval Weapons Support Center
Crane, IN 47522
(812)854-1252 AV: 482-1478

G. J. SIMONE
Naval Plant Representative Office
c/o Grumman Aeorspace Corp.
Bethpage, NY 11714
(516)369-6518

Lloyd SIMONEAUX, Code 93307
Naval Air Rework Facility
NAS Pensacola, FL 32508

H. Gray SIMPSON
NARF, NESO Code 341
MCAS Cherry Point, NC 28533
(919)466-5249 AV: 582-5249

Clifford D. SMITH
NARF, Code 93300
NAS Pensacola, FL 32508
(904)452-3550/3240 AV: 922-3240

Lawrence E. SMITH
Q.A. Code 4102, D&E Dept.
P.M.T.C. Pt. Mugu, CA 93042
(805)982-7816 AV: 351-7816/7614

Donald L. SMITHLIN
62FMS/MAFF/NDI
McChord AFB, WA 98438
(976)2946

Larry SNOOK
U.S. Army Transportation School
Directorate of Training
Fort Eustis, VA 23604
(804)878-3868 AV: 927-5693

Larry E. SNYDER
Crane Army Ammunition Activitiy
Crane, IN 47522
(812)854-1264 AV: 482-1264

Wade H. SPRADLEY
NCOIC NDI Lab
22FMS/MAFFN
March AFB, CA 92508
AV: 947-4279

Michael L. STELLABOTTE
Code 606C, Naval Air Development
Center
Warminster, PA 18974
(215)441-2809 AV: 441-2809

Vernon C. STEWART
Physical Science Lab MANCMB
Robins AFB, GA 31098
AV: 468-2306

James L. STOKES (Dr.)
Naval Weapons Center (Code 3624)
China Lake, CA 93555
(714)939-3665 AV: 245-3665

Jim STOREY
Idaho Air National Guard
Boise Air Terminal, Boise ID 83702
(208)385-5383 AV: 941-5383

Terry E. SUMTER
3340 Tech Gng Gp/TTMM
Chanute AFB, IL 61868
(217)495-2444 AV: 862-2444/3375

Leroy R. TOFT
United States Air Force
41 Collins Rd. Jacksonville, AR 72076
AV: 731-6143

Curtis C. TRABUE
U.S. Army Missile Command
ATTN: DRSMI-EMN
Redstone Arsenal, AL 35809
AV: 746-3988

Elvis R. TRACY
142nd Combat Support Sq. ORE ANG
Portland Intl Airport, Portland, OR 97218
AV: 891-1711

Terry L. VANDIVER
U.S. Army Missile Command (DRSMI-TLA(R&D))
Redstone Arsenal, AL 35809
(205)876-5692 AV: 746-5692

Luther R. WALDROUP
AIMD
NAS Pensacola, FL 32508
(904)452-4666

James WASHINGTON
DCASMA-New Orleans
29300 Old Gentility Road
New Orleans, LA
AV: 255-2506

Robert J. WATTS
USA TARADCOM
ATTN: DRTTA-JA
Warren, MI 48090
(313)573-2849 AV: 273-2849

Mark H. WEINBERG
CDR U.S. Army ARRADCOM
ATTN: DRDAR-QAR-I
Bldg. 62, Dover, NJ 07801
(201)328-2550 AV: 880-2550

James E. WENDELL
U.S. Army Plant Rep. Office
Bell Helic[illegible]
P.O. Box 160[illegible]
Ft. Worth, TX 76101
(817)280-2388 AV: 885-3741

Eugene T. WHITEHEAD
U.S. Navy
NAS Cecil Field, FL (AIMD)
AV: 860-5465

Francis Lee WILLIAMS
Naval Air Rework Facility
NAS North Island, San Diego, CA 92135
AV: 951-6539

Virgil P. WILLIAMS
Naval Weapons Support Center
Crane, IN 47522
(812)854-1252 AV: 482-1478

Daniel J. WILSON (AMS1)
1M2 Div. W/C 510
USS AMERICA CV-66
FPO New York, NY 09501

Thomas D. WILSON
Aircraft Maintenance
4950TW/WPAFB, OH 45433
AV: 787-7781

Edward B. WINN
Tooele Army Depot
Tooele, Utah 84074
(801)833-2316 AV: 780-2316

Fred WITT
U.S. Army Armament Research
& Development Command
Dover, NJ 07801
(201)328-6345 AV: 880-6345

James T. WONG
U.S. Army Research & Technology Lab
AMES Research Center
Moffett Field, CA 94035
(415)965-5578 AV: 359-5578

Terrell H. WYATT
D/Maint. Eng. Div, Eng Proc Br
Corpus Christi Army Depot, NAS
Corpus Christi, TX 78419
(512)939-3513 AV: 861-3784

Robert D. WYCKOFF, Code 341
NARF, NESO, NAS Norfolk, VA 23511
(804)444-8811 AV: 690-8811

David B. WYMAN, Code 715
Naval Coastal Systems Center
Panama City, FL 32407
(904)284-4388 AV: 436-4388